

B cell receptor activation and effect of kinase inhibitors in CLL

Dr Talha Munir

Supervisors

Professor Peter Hillmen

Dr Gina Doody

**Section of Experimental Haematology
Leeds Institute of Cancer and Pathology**

&

**Haematological Malignancy Diagnostic Service
Leeds Teaching Hospitals NHS Trust**

ABSTRACT

i) BACKGROUND

Chronic lymphocytic leukaemia (CLL), the most common leukaemia in the western world, is a clinically and biologically heterogeneous disease. In the last 15 years, impressive improvements have been made in the treatment of CLL and chemo-immunotherapy has emerged as an excellent treatment for fit patients. Exceptions to this are sub-groups of CLL patients with TP53 deletion, fludarabine refractory CLL, early relapse following fludarabine based therapy and unfit patients. The B cell receptor pathway has been explored as a potential treatment target for B cell malignancies. Several cytosolic kinases are constitutively phosphorylated in B cell malignancies and inhibitors of these kinases are in development or approved for the treatment of B cell malignancies and autoimmune disorders. Ibrutinib (BTK inhibitor) and Idelalisib (PI3K- δ inhibitor) are the first-in-class of these subsets of drugs. These drugs have changed the treatment landscape of CLL. ICI-CLL trial was an endeavour to assess the clinical, immunophenotypic and biological responses to continuous ibrutinib monotherapy in treatment naïve (TN) and relapsed or refractory (RR) CLL patients.

ii) HYPOTHESIS

Assessment of B cell receptor (BCR) signalling with continuous ibrutinib will predict the depth of clinical and biological responses in both TN and RR cohorts.

iii) AIMS

To continuously evaluate BCR kinase activation in real-time in peripheral blood and bone marrow *in vivo* and *ex vivo* response to ibrutinib; Analysis of clinical response with BCR kinase response to ibrutinib to be evaluated in TN and RR cohorts.

iv) RESULTS

Ibrutinib monotherapy in TN and RR resulted in improved haematological, clinical and radiological responses in all assessable patients. Progression-free survival (PFS) was estimated at 90% for TN cohort and was estimated at 65% for RR cohort.

TN cohort had a deeper response than RR cohort in terms of BM clearance. The phosflow data confirmed the decline in steady-state and stimulated phosphorylation of BTK, SYK, ERK1/2 and AKT with continued ibrutinib therapy and this was consistent in both cohorts. Exploratory analysis was suggestive that declining steady-state and stimulated phosphorylation with IgM/IgD of assessed intracellular kinases correlated with the improving clinical response.

v) CONCLUSIONS

IciCLLe trial confirmed that ibrutinib is an effective treatment for patients with CLL. The clinical responses correlated with biological responses in both TN and RR CLL. The depth of biological response was reflective of improved depth of clinical response.

Table of Contents

CHAPTER 1:	12
Introduction and Aims	12
1.1 B LYMPHOCYTES	14
1.1.1 Introduction	14
1.1.2 Effector function of B lymphocytes- immunoglobulins.....	15
1.1.3 B lymphocyte development and mechanisms of self-tolerance.....	17
1.1.4 B lymphocyte activation and differentiation.....	18
1.1.5 Surface molecules of B lymphocytes.....	20
1.2 B CELL RECEPTOR STRUCTURE	21
1.2.1 The development and assembly of B cell antigen receptor	21
1.2.2 Structure of the B cell receptor	22
1.2.3 B cell receptor signalling.....	23
1.2.4 BCR signalling and receptor crosstalk	28
1.3 CHRONIC LYMPHOCYTIC LEUKEMIA	29
1.3.1 Introduction	29
1.3.2 Cell of origin.....	29
1.3.3 Diagnosis.....	31
1.3.4 Staging and prognostic scores	33
1.3.5 Treatment	34
1.3.6 Front-line CLL needing treatment	35
1.3.7 Relapsed refractory CLL needing treatment	36
1.3.8 Minimal residual disease	37
1.3.9 Flow cytometry in CLL.....	38
1.3.10 Proliferation markers.....	44
1.3.11 Molecular interactions in CLL microenvironment.....	45
1.3.12 Apoptosis and CLL.....	47
1.4 THE B CELL RECEPTOR IN CLL	49
1.4.1 B cell receptor signalling in CLL	50
1.4.2 Cytosolic kinases fundamental to CLL BCR signalling	51
1.5 B-CELL RECEPTOR ASSOCIATED INHIBITORS (BCRi)	56
1.5.1 BTK inhibitors.....	56
1.5.2 PI3K inhibitors.....	56
1.5.3 Ibrutinib	57
1.6 AIMS AND OBJECTIVES	58
CHAPTER 2:	60
Methods and Materials	60
2.1 PROTOCOL DEVELOPMENT	62
2.1.1 Phosflow	62
2.1.2 Calcium flux	64
2.1.3 Western blotting.....	64
2.2 ASSAY VALIDATION FOR DETECTION OF ACTIVE B CELL KINASES	65
2.2.1 Phosflow validation	65
2.2.2 Calcium flux	74
2.2.3 Western blotting.....	76
2.3 ICIcLLe TRIAL- METHODS	80

2.3.1 Trial design.....	80
2.3.2 Assessments	85
2.3.3 Outcomes.....	85
2.3.4 Statistical methods	85
2.4 PHOSFLOW IN ICICLLe TRIAL.....	85
CHAPTER 3: Clinical Results of ICICLLe trial; TN VS RR Patients	88
3.1 INTRODUCTION	89
3.2 TRIAL DESIGN	90
3.2.1 Patients.....	90
3.2.2 Assessments	90
3.2.3 Results	91
3.3 CONCLUSIONS.....	106
CHAPTER 4:.....	110
Results of ICICLLe trial Cellular Kinases; TN VS RR Patients	110
4.1 ASSESSMENT OF RESIDUAL KINASE ACTIVITY IN ICICLLe TRIAL.....	111
4.2 GENERAL METHODOLOGY	112
4.3 EFFECT OF IBRUTINIB TREATMENT ON STEADY-STATE KINASE PHOSPHORYLATION.....	112
4.4: EFFECT OF IBRUTINIB TREATMENT ON IGM/IGD STIMULATED KINASE PHOSPHORYLATION	116
4.4.1. IgM/IgD stimulated kinase phosphorylation in CLL cells as compared to T-cells for TN and RR cohorts should fall	117
4.4.2 IgM/IgD stimulated kinase phosphorylation in CLL cells as compared to unstimulated CLL cells for TN and RR cohorts should fall	121
4.4.3. IgM/IgD stimulated kinase phosphorylation in CLL cells as compared to baseline IgM/IgD stimulated kinase phosphorylation for TN and RR cohorts should fall.....	124
4.5 EFFECT OF IBRUTINIB TREATMENT ON EX VIVO EXPOSURE TO REPEATED DOSAGE.....	127
4.6 CONCLUSIONS	134
4.7 DISCUSSION	135
CHAPTER 5:.....	137
Does phosphorylation of kinases inform the degree of clinical response in patients treated with ibrutinib?.....	137
5.1 INTRODUCTION	138
5.2 CORRELATION OF PHOSFLOW RESPONSE WITH TREATMENT STATUS.....	139
5.3 CORRELATION OF PHOSFLOW WITH RADIOLOGICAL RESPONSE	141
5.4 CORRELATION OF PHOSFLOW WITH HAEMATOLOGICAL RESPONSE	144
5.5 CORRELATION OF PHOSFLOW WITH PERIPHERAL BLOOD LYMPHOCYTOSIS.....	147
5.6 CONCLUSIONS	150
CHAPTER 6:.....	152
CONCLUSION AND DISCUSSION	152
References:.....	160

LIST OF TABLES

Chapter 1

Table 1. 1 Immunoglobulin isotypes and functions(10)	16
Table 1. 2 Cell surface CD molecules expressed by B cells(40-42)	20
Table 1. 3 Scoring system for diagnosis of CLL(89)	31
Table 1. 4 Markers of poor prognosis in CLL(91-97).....	32
Table 1. 5 Responses with old regimen for CLL(99-102)	34
Table 1. 6 Antigens used in the diagnosis of CLL	39

Chapter 2

Table 2. 1 Mean fluorescence intensity (MFI) of various kinases with no stimulus and incubation with Ibrutinib for 60 minutes.....	71
Table 2. 2 Mean fluorescence intensity (MFI) of various kinases with no stimulus and stimulation with IgM (10µg/ml) and IgD (10µg/ml) for 2minutes.	72
Table 2. 3 Mean fluorescence intensity (MFI) of various kinases with no stimulus and stimulation of ibrutinib treated cells with IgM (10µg/ml) and IgD (10µg/ml) for 2 minutes..	73
Table 2. 4 Antibodies used in ICI CLL trial	86
Table 2. 5 Reagents used	86

Chapter 3

Table 3. 1 Baseline characteristics of TN and RR cohort of ICI CLL trial.....	91
Table 3. 2 Independent Samples test for comparisons of means between TN and RR group (Only statistically significant variables are shown in the table)	102
Table 3. 3 Best IWCLL response within first six months of therapy	105

Chapter 5

Table 5. 1 Correlation of phosflow response in TN and RR cohorts	139
Table 5. 2 Chi-Square tests analysis of significance of treatment status with phosflow analysis.....	141
Table 5. 3 Correlation of radiological response with phosflow response	142
Table 5. 4 Chi-Square tests analysis of significance of radiological response with phosflow response.....	144
Table 5. 5 Correlation of haematological response with phosflow response	145
Table 5. 6 Chi-Square tests analysis of significance of Haematological response with phosflow response	147
Table 5. 7 Correlation of peripheral blood lymphocytosis with phosflow response	148

Table 5. 8 Chi-Square tests analysis of significance of peripheral blood lymphocytosis with phosflow response.....	149
--	-----

LIST OF FIGURES

Chapter 1

Figure 1. 1 Antibody structure consisting of two heavy chain molecules coupled to two light chains. The Fab fragment contains the antigen recognition moiety and the Fc portion plays a role in determining functionality. Taken from (11).	16
Figure 1. 2 Proximal B cell receptor pathway. Red lines signify negative regulation. Blue lines suggest positive regulation.	24
Figure 1. 3 Distal B cell receptor signalling. Red lines signify negative regulation. Blue lines suggest positive regulation.	26
Figure 1. 4 MRD after CIT is a predictor of PFS and OS.	37
Figure 1. 5 DNA damage by chemo or radiotherapy activates p53 through the activation of ATM and other factors. p53 induces either cell cycle arrest or apoptosis through different targets. Various drugs like steroids, Alemtuzumab, lenolidamide, B cell receptor antagonists, Bcl2 inhibitors and MDM2 inhibitors bypass the p53 pathway.	49
Figure 1. 6 BTK domains with all known interacting serines/tyrosines.....	52
Figure 1. 7 Structure of Class 1A PI3 Kinases	53
Figure 1. 8 The domain structure of spleen tyrosine kinase (SYK) tyrosine residues shown to be sites of autophosphorylation.	56

Chapter 2

Figure 2. 1 Mononuclear cell (MNC) separation using Lymphoprep.....	63
Figure 2. 2 Diagrammatic representation of the quadrants for separation of T and B lymphocytes based on staining with antibodies to CD3 and CD19.	66
Figure 2. 3 The gate(P1) is placed on lymphocytes based on forward and side scatter. P1 is then divided into quadrants based on CD19 (Q4; B-cells) and CD3 (Q1; T-cells) expression. 67	67
Figure 2. 4 Histograms representing phosphorylation of Btk pY551 with no stimulus and anti-IgM at 2 and 10 minutes.....	67
Figure 2. 5 Histograms representing phosphorylation of Syk pY348 with no stimulus and anti-IgM at 2 and 10 minutes.....	68

Figure 2. 6 Histograms representing phosphorylation of MAPK-p38 pT180/Y182 with no stimulus and anti-IgM at 2 and 10 minutes	68
Figure 2. 7 Histograms representing phosphorylation of AKT pS473 with no stimulus and anti-IgM at 2 and 10 minutes.....	69
Figure 2. 8 Lymphocytes are gated based on SSC and FSC. A gate is further applied on CD19+ve B lymphocytes.	69
Figure 2. 9 Phosphorylation of Syk with no stimulus, anti-IgM or anti-IgD represented by overlay of histograms. Red line represents phosphorylation with no stimulus and blue dotted line denotes phosphorylation with anti-IgM or anti-IgD.....	70
Figure 2. 10 Phosphorylation of BTK, AKT, SYK and MAPK-p38 with no stimulus and after incubation with Ibrutinib. Red solid lines represent phosphorylation with no stimulus and dotted blue lines represent phosphorylation after incubation with Ibrutinib.....	71
Figure 2. 11 Phosphorylation of BTK, AKT, SYK and MAPK-p38 with no stimulus and stimulation with IgM (10µg/ml) and IgD (10µg/ml). Red solid lines represent phosphorylation with no stimulus and dotted blue lines represent phosphorylation after stimulation with IgM/IgD.....	72
Figure 2. 12 Phosphorylation of BTK, AKT, SYK and MAPK-p38 with no stimulus and stimulation of Ibrutinib (1µM) treated cells with IgM (10µg/ml) and IgD (10µg/ml). Red solid lines represent phosphorylation with no stimulus and dotted blue lines represent phosphorylation after stimulation with IgM/IgD.....	73
Figure 2. 13 Lymphocytes were gated based on FSC and SSC marked as P1. P2 and P3 populations are B and T lymphocytes, respectively. P4 and P5 show calcium flux in B and T lymphocytes, respectively, after stimulus.	74
Figure 2. 14 Lymphocytes were gated based on FSC and SSC marked as P1. P2 and P3 populations are B and T lymphocytes, respectively. P4 and P5 show calcium influx in B and T lymphocytes, respectively, after stimulus.	75
Figure 2. 15 Calcium flux in B cells after addition of ionomycin.....	76
Figure 2. 16 Actin detection in unstimulated and stimulated CLL sample at various time points.	77
Figure 2. 17 Phosphotyrosine detection in unstimulated and stimulated CLL sample at various time points.	77
Figure 2. 18 SYK phosphorylation in GM12828 cell line and primary CLL with anti-IgM.	78
Figure 2. 19 BTK phosphorylation in GM12828 cell line and primary CLL with anti-IgM.....	79
Figure 2. 20 CONSORT Diagram of IciCLLe trial	84

Chapter 3

Figure 3. 1 Baseline characteristics of treatment naïve (TN) and relapsed refractory (RR) cohorts: a) Age b) Haemoglobin c) Platelet count d) WBC count e) Neutrophil count f) Lymphocyte count g) β 2 microglobulin h) Bone marrow infiltration i) SPD of lymph nodes in cm j) Spleen size in cm. Median (central line), range (top and bottom bar) and interquartile

range (top and bottom end of box) of various baseline clinical parameters separated into treatment naïve and relapsed refractory group are shown in the plots.	93
Figure 3. 2 Baseline clinical staging, cytogenetics and IGHV status of TN and RR cohorts: a) Binet stage b) TP53 c) ATM d) Trisomy 12 e) 13 deletion f) IGHV mutation.	94
Figure 3. 3 Estimated marginal means for all patients (n=40) of (a) haemoglobin levels (b) platelet count (c) WBC count (d) neutrophil count (e) lymphocyte count (f) degree of bone marrow infiltration (g) SDP of lymph nodes and (h) spleen size. Error bars represent the 95% confidence interval.	96
Figure 3. 4 Independent sample median test for the indicated parameters in TN (n=20) and RR cohort (n=20). The median (central line), range (top and bottom bar) and interquartile range (top and bottom end of box) separated into TN and RR groups are shown in the plots.	100
Figure 3. 5 Independent sample median test for bone marrow infiltration and SDP of LN in TN (n=20) and RR cohort (n=20). The median (central line), range (top and bottom bar) and interquartile range (top and bottom end of box) separated into TN and RR groups are shown in the plots.	101
Figure 3. 6(a) Peripheral blood CLL count from baseline to 6 months of treatment in TN cohort (b) Peripheral blood CLL count from baseline to 6 months of treatment in RR cohort (c) Bone marrow response from baseline to 6 months of treatment in TN cohort (d) Bone marrow response from baseline to 6 months of treatment in RR cohort.	104
Figure 3. 7 Kaplan Meier Curve for Progression-Free Survival in TN and RR cohorts.	106

Chapter 4

Figure 4. 1 Estimated marginal means of kinase phosphorylation in peripheral blood samples during full course of ibrutinib treatment. MFI of phosphorylated versions of (A) BTK (B) SYK (C) ERK and (D) AKT in unstimulated CLL cells/ T cells.	113
Figure 4. 2 Estimated marginal means of kinase phosphorylation during ibrutinib treatment. (A) MFI of pBTK (pY551) in unstimulated CLL cells/ T cells from treatment naïve patients (TN) vs relapsed refractory (RR) in peripheral blood or (B) bone marrow; (C) MFI of pSYK in peripheral blood or (D) bone marrow; (E)MFI of pERK1/2 in peripheral blood or (F) bone marrow; and (G) MFI of pSYK in peripheral blood or (H) bone marrow.	115
Figure 4. 3 Estimated marginal means of kinase phosphorylation in peripheral blood samples following stimulation with anti-IgM/IgD for 2 min during full course of ibrutinib treatment. MFI of (A) pBTK (B) pSYK (C) pERK and (D) pAKT in stimulated CLL cells/ T cells.	118
Figure 4. 4 Estimated marginal means of kinase phosphorylation following stimulation with anti-IgM/IgD for 2 min. (A) MFI of pBTK (pY551) in stimulated CLL cells/ unstimulated CLL cells from treatment naïve patients (TN) vs relapsed refractory (RR) in peripheral blood or (B) bone marrow; (C) MFI of pSYK in peripheral blood or (D) bone marrow; (E)MFI of pERK1/2 in peripheral blood or (F) bone marrow; and (G) MFI of pAKT in peripheral blood or (H) bone marrow.	120
Figure 4. 5 Estimated marginal means of kinase phosphorylation following stimulation with anti-IgM/D for 2 min. (A) MFI of pBTK (pY551) in stimulated CLL cells/ unstimulated CLL cells from treatment naïve patients (TN) vs relapsed refractory (RR) in peripheral blood or (B)	

bone marrow; (C) MFI of pSYK in peripheral blood or (D) bone marrow; (E)MFI of pERK1/2 in peripheral blood or (F) bone marrow; and (G) MFI of pAKT in peripheral blood or (H) bone marrow.....123

Figure 4. 6 Estimated marginal means of kinase phosphorylation following stimulation with anti-IgM/D for x min. (A) MFI of pBTK (pY551) in stimulated CLL cells/ baseline unstimulated from treatment naïve patients (TN) vs relapsed refractory (RR) in peripheral blood or (B) bone marrow; (C) MFI of pSYK in peripheral blood or (D) bone marrow; (E)MFI of pERK1/2 in peripheral blood or (F) bone marrow; and (G) MFI of pAKT in peripheral blood or (H) bone marrow.....126

Figure 4. 7 Estimated marginal means of kinase phosphorylation following treatment with ibrutinib for 2 min. (A) MFI of pBTK (pY551) in stimulated CLL cells/ unstimulated CLL cells in peripheral blood or (B) bone marrow; (C) MFI of pSYK in peripheral blood or (D) bone marrow; (E)MFI of pERK1/2 in peripheral blood or (F) bone marrow; and (G) MFI of pAKT in peripheral blood or (H) bone marrow.128

Figure 4. 8 Estimated marginal means of kinase phosphorylation following treatment with ibrutinib for 2 min. (A) MFI of pBTK (pY551) in stimulated CLL cells/ baseline unstimulated from treatment naïve patients (TN) vs relapsed refractory (RR) in peripheral blood or (B) bone marrow; (C) MFI of pSYK in peripheral blood or (D) bone marrow; (E)MFI of pERK1/2 in peripheral blood or (F) bone marrow; and (G) MFI of pAKT in peripheral blood or (H) bone marrow.....130

Figure 4. 9 Estimated marginal means of kinase phosphorylation following a 30 min pre-treatment with 1 uM Ibrutinib or media followed by stimulation with anti-IgM/D for 2 min. (A) MFI of pBTK (pY551) in stimulated CLL cells/ ibrutinib treated stimulated CLL cells in peripheral blood or (B) bone marrow; (C) MFI of pSYK in peripheral blood or (D) bone marrow; (E)MFI of pERK1/2 in peripheral blood or (F) bone marrow; and (G) MFI of pAKT in peripheral blood or (H) bone marrow.132

Figure 4. 10 Estimated marginal means of kinase phosphorylation following a 30 min pre-treatment with 1 uM Ibrutinib or media followed by stimulation with anti-IgM/D for 2 min. (A) MFI of pBTK (pY551) in stimulated CLL cells/ ibrutinib treated stimulated CLL cells from treatment naïve patients (TN) vs relapsed refractory (RR) in peripheral blood or (B) bone marrow; (C) MFI of pSYK in peripheral blood or (D) bone marrow; (E)MFI of pERK1/2 in peripheral blood or (F) bone marrow; and (G) MFI of pAKT in peripheral blood or (H) bone marrow.....133

Chapter 5

Figure 5. 1 Bar charts showing the correlation of cohorts with phosflow response. The number of cases with complete response (CRPh) are shown in blue and partial response (PRPh) in red.140

Figure 5. 2 Bar charts showing the correlation of radiological response with phosflow response. The number of cases with complete response (CRPh) are shown in blue and partial response (PRPh) in red.143

Figure 5. 3 Bar charts showing the correlation of haematological response with phosflow response. The number of cases with complete response (CRPh) are shown in blue and partial response (PRPh) in red.146

Figure 5. 4 Bar charts showing the correlation of peripheral blood lymphocytosis with phosflow response. The number of cases with complete response (CRPh) are shown in blue and partial response (PRPh) in red.149

CHAPTER 1:

Introduction and Aims

CONTENTS OF THE CHAPTER:

1.1 B LYMPHOCYTES

1.2 B CELL RECEPTOR STRUCTURE

1.3 CHRONIC LYMPHOCYTIC LEUKEMIA

1.4 B CELL RECEPTOR IN CLL

1.5 B CELL RECEPTOR KINASE INHIBITORS

1.6 AIMS AND OBJECTIVES

1.1 B LYMPHOCYTES

1.1.1 Introduction

Immune responses can be classified as humoral or cellular immunity. Whilst cellular immunity is predominantly mediated by T lymphocytes, the humoral immunity is characterised by production of antibodies by B lymphocytes and their progeny, plasma cells. B (bursal or bone marrow-derived) lymphocytes can be defined as a population of cells that express clonally diverse surface immunoglobulin (Ig) receptor receptors identifying specific antigenic epitopes. These antibodies are involved in protection against infection but can also cause tissue injury in autoimmune conditions. B lymphocytes are also critical in contributing to cellular immunity and they have roles in T cell activation, effector and regulatory function.

Two main classes of B lymphocytes exist in mice and humans (1-4).

1. B1 Lymphocytes

2. B2 Lymphocytes which comprise of marginal zone (MZ) and follicular (FO) B cells

B1 lymphocytes are derived from progenitors in the foetal liver and persist as a self-renewing population during adulthood with minimal contribution from bone marrow (BM). B1 lymphocytes reside in pleural and peritoneal cavities in mice, and they produce polyreactive IgM antibodies against self-antigens and microbial antigens, but the responses are T cell independent. For example, B1 cells produce IgM antibodies against blood groups ABO system, IgM antibodies against oxidized LDLs in atherosclerosis as well as polyreactive IgA antibodies to help with mucosal immunity (5-8).

B2 lymphocytes develop from transitional 2 (T2) B cells that originate in the BM. MZ B-lymphocytes originate from transitional B cells after induction from NOTCH2 protein but reside in the marginal sinus of the spleen (4). These lymphocytes express a polyreactive B cell receptor (BCR), complement receptors CD21 and CD35 and the MHC class 1-like molecule C1d. MZ B lymphocytes like B1 lymphocytes can recognise T-independent carbohydrate and phospholipid antigens and produce IgM antibodies (4). Both B1 lymphocytes and MZ B lymphocytes express Toll-like receptors (TLR) and can respond via TLR ligands without depending on BCR activation. MZ B lymphocytes can also participate in

T cell-dependent pathways by generating high-affinity isotype switched antibodies and can interact with follicular dendritic cells (FDC) in the germinal centres (9).

Follicular (FO) B cells are the most common B lymphocytes which reside in the spleen and lymph nodes. The FO B lymphocytes originate from transitional B cells in the spleen and are generated by a pathway dependent on Bruton tyrosine kinase (BTK) induced by BCR-mediated signals (2). These cells produce high-affinity IgG antibodies with the help of T cells and the process of somatic hypermutation and are critical in establishing the humoral immune response.

1.1.2 Effector function of B lymphocytes- immunoglobulins

Immunoglobulin production is the principal function of B lymphocytes. Immunoglobulins are glycosylated protein molecules present on the surface of B cells called surface immunoglobulins which serves as antigen receptors (BCR), or are secreted into the extracellular space where they can bind and neutralise their target antigens (10). A single immunoglobulin molecule consists of two “heavy” and two “light” chains which are linked to each other by disulfide bonds (Figure 1.1). The N-terminus regions of the heavy and light chains collectively make up the antigen-binding site and the diversity to bind various antigen lies in this region (10).

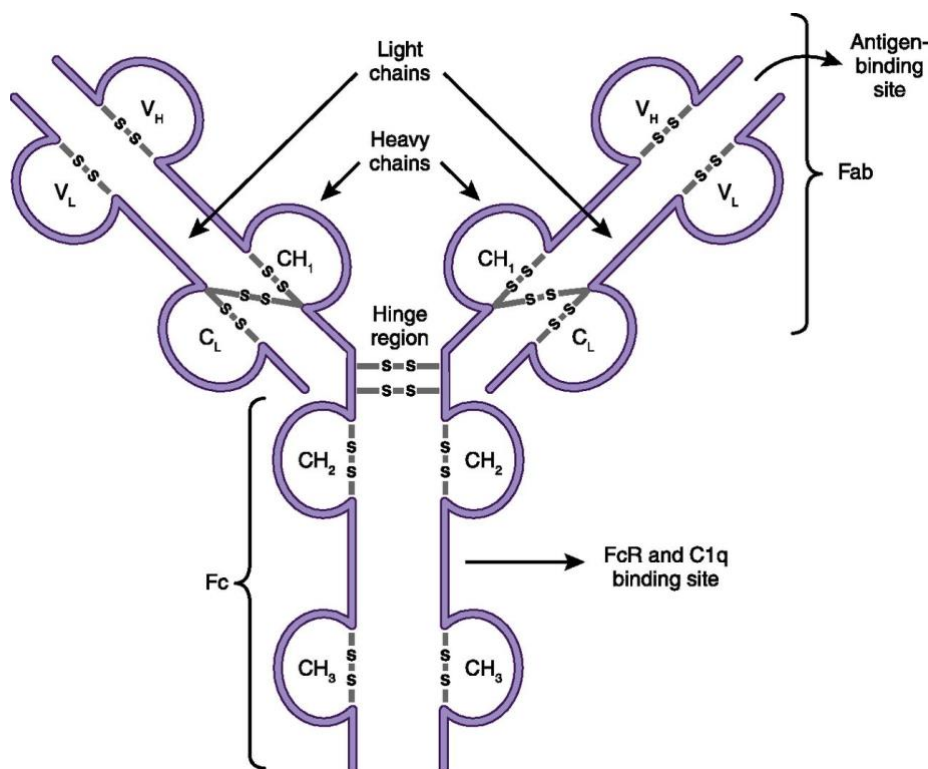


Figure 1.1 Antibody structure consisting of two heavy chain molecules coupled to two light chains. The Fab fragment contains the antigen recognition moiety, and the Fc portion plays a role in determining functionality. Taken from (11).

Five isotypes of antibodies named IgM, IgD, IgG, IgA, and IgE exist (Table 1.1). They are distinguished according to the C-terminus regions of the heavy chains, which are constant and therefore do not participate in antigen binding. Instead, these constant regions designated as Fc are important for the effector functions of antibodies, how antibodies eliminate pathogens or cause tissue injury. In addition, there are four subclasses or isotypes of IgG antibodies (IgG1, IgG2, IgG3, and IgG4). Immunoglobulins perform the following effector functions:

1. They neutralise their targets
2. They activate macrophages and other immune cells by binding to Fc receptors (FcRs) that recognise the constant regions of specific antibody classes
3. They activate the classic pathway of the complement system by binding to C1q (Table 3.1).

The effector mechanism is determined by heavy-chain isotype and the binding affinities of activating and inhibitory FcR on immune cells.

Table 1.1 Immunoglobulin isotypes and functions (10).

Characteristic	Immunoglobulin Isotype						
	IgM	IgG1	IgG2	IgG3	IgG4	IgA	IgE
Heavy chain	μ	γ_1	γ_2	γ_3	γ_4	α	ϵ
Molecular mass, kDa	970	146	146	165	146	160	188
Serum level (mean adult), mg/ml	1.5	9	3	1	0.5	2.1	5×10^{-5}
Half-life in serum, days	10	21	20	7	21	6	2
Polysaccharide antigens	++	+	+++	+/-	+/-	++	++

Protein antigens	+	++	+/-	++	++	+	+
Placental transfer	-	+++	+	++	-/+	-	-
Neutralization	+	++	++	++	++	++	-
Classic pathway of complement activation	++++	++	+	+++	-	-	-
Sensitization for killing by natural killer cells	-	-	++	-	++	-	-
Binding to macrophage and phagocyte Fc receptors	-	+	-	+	-/+	+	+
Binding to mast cells and basophils	-	+	-	+	-	-	+++

1.1.3 B lymphocyte development and mechanisms of self-tolerance

B lymphocytes develop from common lymphoid progenitors of haematopoietic stem cells, with a commitment to the B cell lineage being determined by the expression of paired box protein 5 (*Pax5*) (12). The maturation of a B cell progresses within the BM before the release of immature B cells into the circulation. Further completion of differentiation into mature B cells occurs within the spleen and lymph nodes. The maturation steps are intricate steps which involve the rearrangement of immunoglobulin heavy- and light-chain gene segments (variable V, diversity D, joining J) resulting in the transformation of pro-B to pre-B to immature B cells. The eventual culmination of this maturation is the expression of IgM mature B cell receptor on the B cell surface(13). There is a close interaction with of B cells with BM stromal cells (12). Immature B cells exit the BM to the spleen, where they differentiate into transitional 1 and 2 B cells. Maturation into MZ or FO B cells is usually guided by BCR signals, B cell-activating factor (BAFF), NOTCH2 and BTK (2, 4, 13). MZ B cells are retained in the spleen while FO B cells recirculate, populating various secondary lymphoid tissues including lymph nodes.

In the process of B cell development, the random rearrangement of immunoglobulin genes during B cell development results in the generation of a vast repertoire of BCRs. All this repertoire helps to recognise a variety of antigens. 75% of immature B cells in humans are

estimated to be self-reactive (14). Developing B cells undergo several selection processes in the BM and spleen that serve as checkpoints in purging autoreactive clones and establishing self-tolerance (13). The process of selection of immature B cells that occurs in the BM is called central tolerance and peripheral tolerance happens in the spleen to remove the autoreactive peripheral self-antigens.

Immature B cells within the BM modify their immunoglobulin repertoire by clonal deletion and receptor editing, and the latter mechanism contributes to the elimination of most self-reactive clones (20%–50%). Additional selection mechanisms occurring within the spleen remove the remaining autoreactive clones that recognise peripheral self-antigens: Transitional B cells with strong BCR signals undergo clonal deletion or attain a state of anergy, with shortened survival (15). The remaining self-reactive B lymphocytes are eliminated by CD4⁺ T cells *via* Fas receptor–Fas ligand and CD40–CD40L interactions. The T-regs and B-regs provide the additional mechanisms to ensure that the self-tolerance process is enhanced (16, 17). Failure of one or more of the self-tolerance checkpoints described is central to the development of autoimmune diseases.

1.1.4 B lymphocyte activation and differentiation

The activation and differentiation of B lymphocytes results in the formation of memory B cells, plasmablasts or plasma cells. The whole process is guided by the type of antigen, TLR signals, cytokines and co-stimulatory helper signals(18). For example, B1 and MZ B cells respond to polysaccharide or glycolipid antigens without the help of T cells and they can differentiate into IgM or isotype-switched short-lived plasmablasts and memory B cells in extrafollicular areas without entering the GC (19). MZ B cells interact with natural killer T cells, neutrophils, and DCs. The interactions provide cytokines such as BAFF, IL-21, IL-6, and IL-10 and costimulatory signals (CD40L) within the extrafollicular areas, facilitating limited somatic hypermutation and antibody diversification (19).

FO B lymphocytes are activated by the interaction of protein antigens with the BCR, and the helper signals derived from antigen specific CD4 T cells. On interaction with antigen, the BCR sets signals to initiate an essential gene expression programme and internalise the antigen. The endosome degrades the antigen into peptides which are linked to MHC-II molecules and then recycle to the cell surface, where interaction of MHC-II molecule with antigen-specific CD4 cells takes place (20). They take place within secondary lymphoid tissues guided by the

expression of chemokine receptors and corresponding ligands (21). Naive B cells expressing CXCR5 are retained in primary lymphoid follicles in lymph nodes by CXCL13 from FO DCs (21). After antigen recognition, B cells upregulate CCR7 and EBV-induced receptor to migrate adjacent to the T cell zone (referred to as T–B border), where they initiate interactions with early T follicular helper cells (Tfhs) (22, 23). The costimulatory ligands CD40 ligand and the cytokines IL-4, IL-21, and IFN- γ provide the T cell help to the B cell.

Activated B cells follow two routes from here on. A small number of activated B cells transform into extrafollicular plasmablasts and early memory B cells without entering the follicles. The other group of activated B cells upregulate *B cell lymphoma 6 (Bcl6)* return to the follicles (FO pathway). These activated B cells form GCs in collaboration with Tfhs and this interaction supports affinity maturation of immunoglobulin antigen–binding sites and immunoglobulin class switching (23, 24).

Somatic hypermutation (SHM) and class-switch recombination (CSR) happen in the GC. This important step is dependent on IL-21 and costimulatory signals derived from Tfh resulting in extensive B cell proliferation and induction of gene expression programmes. Both SHM and CSR need the expression of activation-induced cytidine deaminase (AID): SHM induces point mutations in the immunoglobulin gene segment that encodes for variable antibody-binding site whereas CSR switches the genes to develop the right isotype switch for the specific antigen without changing the antigen specificity (25-27).

After this complex interaction, the GC B cells with high-affinity antigen interaction are selected. They upregulate BCL2 family pro-survival factors to be incorporated into memory B cell or plasma cell pools (20, 28-30). The destiny of a GC B cell to enter the plasma cell pool is dependent on expression of transcription factors such as IRF-4, BLIMP1 and XBP1 induced by interaction with Tfh. This group of master regulators commit the differentiation into plasma cells after repression of Bcl6 (31, 32). Plasma cells home to the BM *via* CXCR4 supported by stromal cells secreting CXCL12 and cytokines such as IL-6 and APRIL. They produce antibodies maintaining serologic memory independent of further antigen exposure (18). Memory B cells recirculate in lymphoid tissues, where they can differentiate rapidly into plasmablasts (GC-dependent memory) or re-enter GCs upon antigen re-challenge

(extrafollicular and GC-dependent memory), resulting in further diversified secondary antibody responses (30, 33-37). Both memory B cells and plasma cells generate high-affinity immunoglobulin class-switched diversified antibodies. BAFF and APRIL are important cytokines required for survival of B cells during various stages from their initial development to terminal differentiation. BAFF and APRIL are produced by myeloid and stromal cells and bind to TACI and B cell maturation antigen, while BAFF also signals through B cell-activating factor-receptor (BAFF-R) (37, 38). BAFF is essential for survival and maturation of transitional B cells, sustains the GC reaction, and supports CSR (37, 39).

1.1.5 Surface molecules of B lymphocytes

The advent of monoclonal antibodies (mAb) has helped to ascertain the surface expression of various antigens. Most of the target antigens regulate B cell development and function to facilitate communication with the extracellular environment or provide a cellular context in which to interpret BCR signals. For example, CD79a (Ig α) and CD79b (Ig β) are noncovalently associated BCR complexes and their cytoplasmic domains contain highly conserved motifs for tyrosine phosphorylation and Src family docking that are essential for BCR signalling (40). CD19 is expressed by all B-lineage cells whereas CD20 is a mature B cell molecule that functions as membrane embedded calcium channel. CD21 is a C3d and EBV receptor which interacts with CD19 to generate a transmembrane signal. CD22 regulates follicular B cell survival and negatively regulates signalling. CD40 is ligand for CD154 expressed by T cells, whereas CD72 functions as a negative regular of signal transduction. CD24 is a GPI anchor protein but its exact function is unknown. These major B lymphocyte markers are shown in Table 1.2 below.

Table 1.2 Cell surface CD molecules expressed by B cells (40-42).

Name	Original names	Cellular reactivity	Structure
CD19	B4	Pan-B cell, FDCs	Ig superfamily
CD20	B1	Mature B cells	MS4A family
CD21	B2, HB-5	Mature B cells, FDCs	Complement receptor family
CD22	BL-CAM, Lyb-8	Mature B cells	Ig superfamily

CD23	FcεRII	Activated B cells, FDCs, others	C-type lectin
CD24	BA-1, HB6	Pan-B cell, granulocytes, epithelial cells	GPI anchored
CD40	Bp50	B cells, epithelial cells, FDCs, others	TNF receptor
CD72	Lyb-2	Pan-B cell	C-type lectin
CD79a, b	Igα, β	Surface Ig ⁺ B cells	Ig superfamily

1.2 B CELL RECEPTOR STRUCTURE

1.2.1 The development and assembly of B cell antigen receptor

B lymphocytes develop from the HSC in the bone marrow. The specialised microenvironment directs the development of lymphocyte progenitors from the HSCs. This is directed by the stromal cells in contact with HSCs in the bone marrow niche (43). There is gradual differentiation of HSC to multipotent progenitor cells and common lymphoid progenitors. The direction of differentiation is dependent on expression of IL-7 receptor on the progenitor cells which is triggered by FLT3 signalling along with activity of transcription factor PU.1 (31, 44-47). Other factors include Stem Cell Factor interacting with receptor tyrosine kinase c-Kit on progenitor cells, chemokine CXCL12 expression and thymic stromal lymphopoietin. The differentiation of lymphoid progenitor cell to pro-B cell is directed by B lineage specific transcription factors E2A and EBF induced by PU.1 and Ikaros (48). E2A and EBF induce proteins such as RAG-1 and RAG-2 of V(D)J recombinase required for immunoglobulin gene rearrangement. E2A and EBF also induce the transcription factor Pax5, which targets the gene for B cell co-receptor component CD19 as well as the gene for Igα which the signalling component for pre-B cell and B cell receptors. Pax5 induces expression of BLNK, which is an SH2-containing scaffold protein that is required for further development of the pro-B cell and for signalling from the mature B cell antigen receptor (12, 44, 46, 49-51). The B cell develops into early pro-B cell, late pro-B cell, large pre-B cell, small pre-B cell and mature B cell. The heavy chain locus rearranges first in early pro-B cells with rearrangement of D gene segment to JH gene segment. Successful VH to DJH rearrangement occurs in the late pro-B cell, which leads to expression of a complete immunoglobulin heavy

chain as a part of the pre-B cell receptor found mainly in the cytoplasm. The cell is then stimulated to form the large pre-B cell which proliferates. As soon as a productive heavy-chain gene rearrangement takes place, μ chains are expressed by the cell in a complex with two other chains, $\lambda 5$ and $VpreB$, which together make up a surrogate light chain and the whole complex is called pre-B cell receptor. The surrogate light chains are induced by transcription factors E2A and EBF. The invariant proteins $Ig\alpha$ and $Ig\beta$ are components of both the pre-B cell receptor and the B cell receptor complexes on the cell surface. $Ig\alpha$ and $Ig\beta$ transduce signals from these receptors by interacting with intracellular tyrosine kinases through their cytoplasmic tails. $Ig\alpha$ and $Ig\beta$ are expressed from the pro-B cell stage until the death of the cell or until its terminal differentiation. Formation of the pre-B cell receptor is an important checkpoint that mediates the transition between the pro-B cell and the pre-B cell. Pre-B cell receptors interact with each other to form dimers or oligomers that generate signals for transition from pro-B cell to pre-B cell such as sensitisation to IL-7. Pre-B cell receptor signalling requires the scaffold protein BLNK and non-receptor tyrosine kinase BTK. Deficiency in BLNK or mutation of BTK causes a block at the pro-B cell stage. As proliferation and division ceases, the cell is called small pre-B cell which is accompanied by cessation of surrogate light chain. Small pre-B cells re-express RAG proteins and this is followed by expression of light chain. The B cell now expresses IgM on the cell surface. With alternative RNA splicing, the mature B cells start to express IgD along with IgM (52).

The earliest B cell lineage surface markers are CD19 and CD45R. A pro-B cell is distinguished by expression of CD43, CD117 and the IL-7 receptor. A late pro-B cell starts to express CD24 and the IL-2 receptor α chain CD25. A pre-B cell is distinguished by expression of BP-1 and absence of expression of CD117 and IL-7 receptor.

1.2.2 Structure of the B cell receptor

The B cell receptor complex is made up of cell surface immunoglobulin with one each of the signalling proteins $Ig\alpha$ and $Ig\beta$ (52). The immunoglobulin recognises and binds antigen but cannot itself generate a signal. It is associated with antigen nonspecific signalling molecules $Ig\alpha$ (CD79a) and $Ig\beta$ (CD79b). $Ig\alpha$ and $Ig\beta$ are single-chain proteins composed of an extracellular immunoglobulin-like domain connected by a transmembrane domain to a cytoplasmic tail. Each has a single ITAM in their cytosolic tails that enables them to signal when the B cell receptor is ligated with antigen. The $Ig\alpha:Ig\beta$ dimer associates with the B cell

receptor through hydrophilic interactions. The complete B cell receptor is thought to be a complex of six chains—two identical light chains, two identical heavy chains, and one associated heterodimer of Ig α and Ig β .

The B cell co-receptor complex is a complex of cell surface proteins including CD19, CD21 and CD81. Antigen dependent signalling is enhanced if the B cell co-receptor is simultaneously bound by its ligand and clusters with the antigen receptor. CD21 is a receptor for the C3dg fragment of complement. This induces phosphorylation of the cytoplasmic tail of CD19 by B cell receptor-associated tyrosine kinases, which in turn leads to the binding of Src-family kinases such as Lyn, the augmentation of signalling through the B cell receptor itself, and the recruitment of PI3kinase. Recent evidence suggests that the tetraspanin CD81 functions in conjunction with CD19 to regulate the cytoskeleton association of the BCR during signal amplification (53).

1.2.3 B cell receptor signalling

In B cells, Src family protein tyrosine kinases Fyn, Blk, and Lyn are responsible for phosphorylation of the ITAMs (Figure 1.2) (54). These kinases associate with resting receptors via a low-affinity interaction with unphosphorylated ITAMs in Ig α and Ig β . After the receptors are cross-linked by a bound multivalent antigen, the receptor associated kinases are activated and phosphorylate the tyrosine residues in the ITAMs. B cells express the tyrosine kinase SYK, containing two SH2 domains, which is recruited to the doubly phosphorylated ITAM. Once SYK has been recruited to the receptor complex and activated, it phosphorylates the scaffold protein BLNK. The next step in the pathway is the activation of the key signalling protein phospholipase C- γ (PLC- γ) and recruitment to the membrane. First, PLC- γ is brought to the inner face of the plasma membrane by the binding of its PH domain to PIP3 that has been formed by the phosphorylation of PIP2 by PI3 kinase. It then binds to phosphorylated BLNK, where it can be activated by the membrane-associated tyrosine kinase BTK. BTK contain PH, SH2, and SH3 domains and are recruited to the plasma membrane by their PH domain, which interacts with PIP3 on the inner face of the membrane.

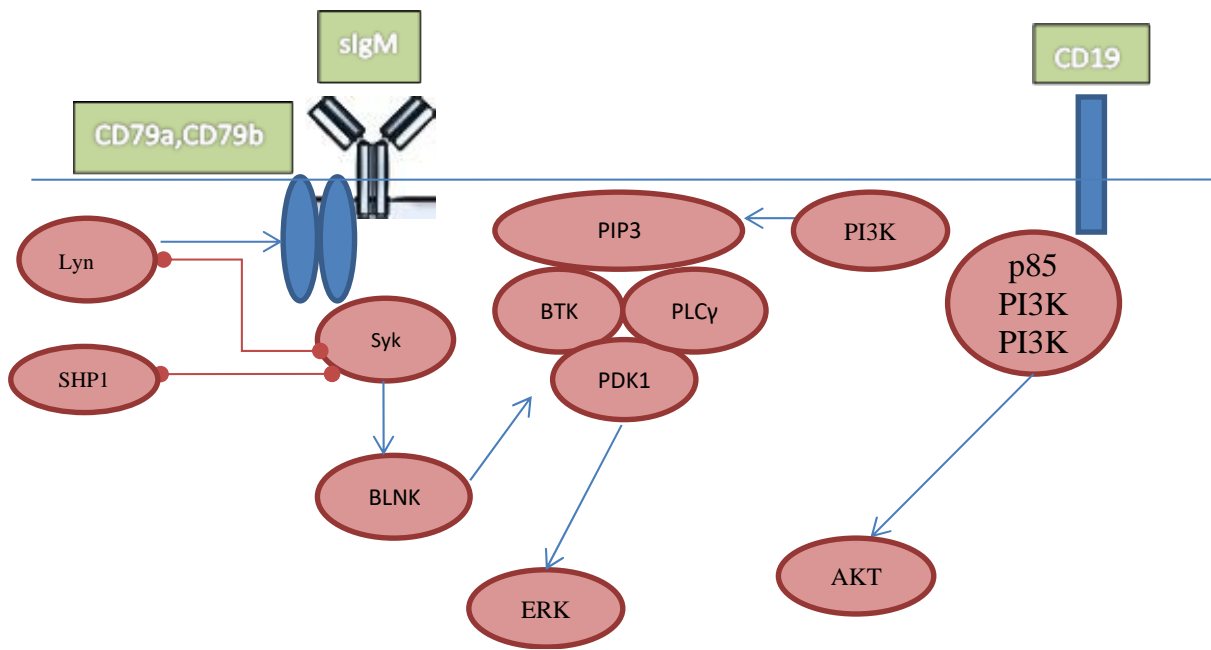


Figure 1.2 Proximal B cell receptor pathway. Red lines signify negative regulation. Blue lines suggest positive regulation.

PLC- γ can catalyse the breakdown of the membrane lipid PIP₂ to generate two products, the membrane lipid DAG and the diffusible second messenger IP₃ (54) (Figure 1.3). DAG is confined to the membrane but diffuses in the plane of the membrane and serves as a molecular target that recruits other signalling molecules to the membrane. IP₃ diffuses into the cytosol and binds to IP₃ receptors on the ER membrane. These receptors are Ca²⁺ channels, which open and release all the calcium stored in the ER into the cytosol. The consequent low levels of calcium in the ER then cause the transmembrane protein STIM1 to cluster within the ER membrane. STIM1 clustering triggers the opening of CRAC channels (calcium release-activated calcium channels) in the membrane, and they allow extracellular calcium to flow into the cell to activate further signalling pathways and to replenish ER calcium stores (55). The activation of PLC- γ marks a crucial step in B cell activation, because after this point the antigen signalling pathway splits into four distinct branches:

- The stimulation of Ca²⁺ entry
- The activation of Ras
- The activation of protein kinase C- β (PKC- β)
- The activation of AKT

Each of these pathways results in activation of different transcription factors. Increased cytosolic Ca²⁺ resulting from B cell receptor signalling causes the activation of a family of transcription factors called NFAT. NFAT is present in the cytosol of resting B cells and in the absence of activating signals, it is kept in the cytosol by phosphorylation by serine/threonine kinases, including glycogen synthase kinase 3 (GSK3) and casein kinase 2 (CK2) (56). This phosphorylation blocks entry of NFAT into the nucleus. The cytoplasmic Ca²⁺ binds a protein calmodulin and induces a conformational change in this protein which then binds to calcineurin, a protein phosphatase that acts on NFAT. Dephosphorylation of NFAT by calcineurin allows the nuclear localisation sequence to be recognised by nuclear transporters, and NFAT enters the nucleus. There it functions in turning on many of the genes crucial for B cell activation.

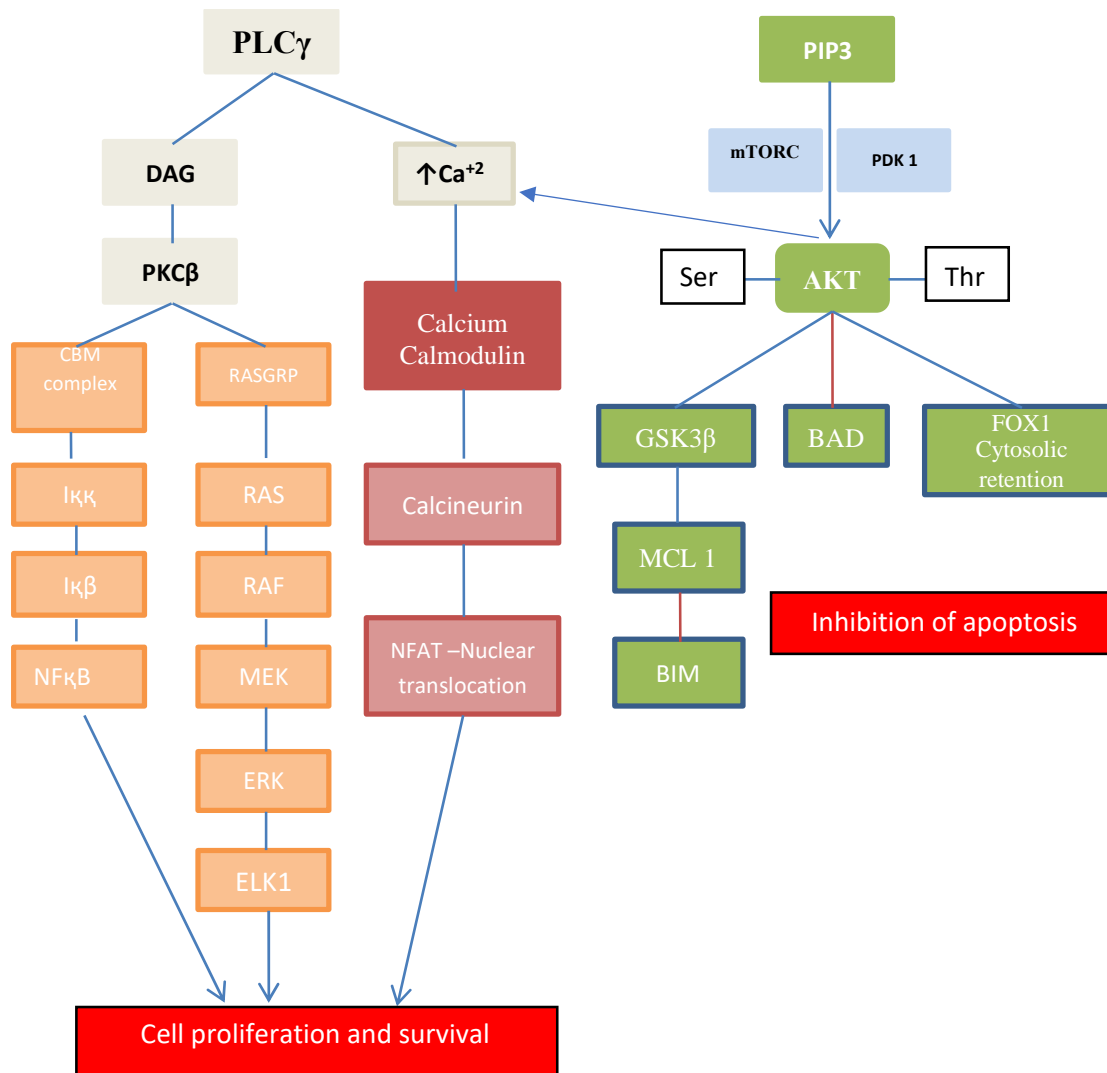


Figure 1.3 Distal B cell receptor signalling. Red lines signify negative regulation. Blue lines suggest positive regulation.

The DAG generated by PLC- γ diffuses in the plasma membrane and activates the protein RasGRP, which is a guanine-nucleotide exchange factor that specifically activates Ras. RasGRP contains a protein-interaction module called a CI domain that binds to DAG. Activated Ras then triggers a three-kinase relay that ends in the activation of a serine/threonine kinase known as a mitogen-activated protein kinase or MAP kinase (MAPK). In the case of antigen receptor signalling, the first member of the relay is a MAPK kinase kinase (MAP3K) called Raf. Raf then phosphorylates the next member of the series; a MAPK kinase (MAP2K) called MEK1. MEK1 then phosphorylates ERK (extracellular signal

related kinase) (57). Signalling by MAPK cascades is facilitated by specialised scaffold proteins that bind to all three kinases in a MAPK relay(58). The scaffold protein kinase suppressor of Ras (KSR) functions in the Raf/MEK1/ERK pathway. ERK acts indirectly to generate the transcription factor AP-1, which is a heterodimer composed of one monomer each from the Fos and Jun families of transcription factors. Active ERK phosphorylates the transcription factor ELK-1, which cooperates with a transcription factor called serum response factor to initiate transcription of the *FOS* gene. Fos protein then associates with Jun to form the AP-1 heterodimer, but this remains transcriptionally inactive until another MAPK called Jun kinase (JNK) phosphorylates Jun.

The third signalling pathway leading from PLC- γ results in the activation of PKC- β . The kinase activity of PKC- β initiates a series of steps that results in the activation of NF κ B. PKC- β phosphorylates the large membrane-localised scaffold protein CARMA1, causing it to oligomerise and form a multisubunit complex with other proteins such as MALT1 and BCL-10. MALT1 is stably associated with BCL-10 and becomes activated following its multimerization with CARD-containing MAGUK protein 1 (CARMA1) also known as CARD11 to form the CBM (CARMA1-, BCL-10- and MALT1-containing complex) (59). This complex recruit and activates TRAF-6. This protein then causes the activation of the NF κ B pathway.

NF κ B is the general name for a member of a family of homo- and heterodimeric transcription factors made up of the Rel family of proteins. The most common NF κ B activated in lymphocytes is a heterodimer of p50:p65Rel. The dimer is held in an inactive state in the cytoplasm by binding to an inhibitory protein called inhibitor of κ B (I κ B). TRAF-6 stimulates the degradation of I κ B by first activating the kinase TAK1, which activates a complex of serine kinases, I κ E kinase (I κ K). I κ K phosphorylates I κ B causing its ubiquitination, subsequent degradation and the consequent release and entry into the nucleus of active NF κ B (60). PKC- β can also activate JNK and might be able to activate the transcription factor AP-1 by this route.

Following the activation of the PI3K pathway, AKT is recruited to the plasma membrane, where it can be activated through the phosphorylation of Thr308 by PDK1 and of Ser473 by the mammalian target of rapamycin (mTOR) complex. Phosphorylated AKT enhances cell survival via the inactivation of BCL-2 antagonist of cell death (BAD) and the stabilisation of

myeloid cell leukaemia sequence 1 (MCL1). Moreover, it might promote B cell proliferation by disrupting the glycogen synthase kinase 3 β (GSK3 β)-dependent degradation of cyclin D3 and MYC. It causes cytosolic retention of FOXO1 which drives the expression of genes such as activation-induced cytidine deaminase that regulate B cell differentiation.

Some receptors that can inhibit B cell activation possess cytoplasmic motifs known as the immunoreceptor tyrosine-based inhibitory motif (ITIM). When the tyrosine in an ITIM is phosphorylated, it can recruit either of two inhibitory phosphatases, called SHP (SH2-containing phosphatase) and SHIP (SH2-containing inositol phosphatase), via their SH2 domains. SHP is a protein tyrosine phosphatase and removes phosphate groups added by tyrosine kinases to a variety of proteins. SHIP is an inositol phosphatase and removes the phosphate from PIP3 to give PIP2, thus reversing the recruitment of proteins such as TEC kinases and AKT to the cell membrane and thereby inhibiting signalling. These receptors include PD-1, CD22, BTLA and Fc γ RIIB-1. Lyn, the predominant Src kinase in B cells which activates ITAM on CD79a and CD79b and phosphorylates amino acids on CD19 also has a negative regulatory effect. It phosphorylates a regulatory tyrosine residue on SYK and ITIMs on the B cell co-receptor molecules Fc γ RIIB and CD22. Mutation of CD79a and CD79b or monophosphorylation of ITAM can cause development of different B cell malignancies or B cell anergy, respectively (54, 61).

1.2.4 BCR signalling and receptor crosstalk

The lymphoid microenvironment that might mediate crosstalk with BCR signalling to promote the activation of common downstream signalling pathways are ligands for the tumour necrosis factor (TNF) receptor superfamily receptors, ligands for TLRs, ligands for cytokine or chemokine receptors and ligands for adhesion molecules.

Signalling through the TNF receptor family member, BAFFR is the second homeostatic stimulus required for B cell propagation. BAFFR uses the BCR complex to promote follicular B cell survival in a SYK dependent manner (62).

B cells typically respond to antigens in the context of other factors such as cytokines and TLR ligands. Co-stimulation of B cells with IL-4, LPS or CD40 ligand (CD40L) can alter BCR signalling to adopt pathways that rely less on PI3K or NF- κ B signalling. These findings also

highlight the potential contribution of inflammatory mediators in promoting B cell malignancies particularly during chronic inflammation (63).

In lymphocytes, inside out signalling promotes an active conformation of integrins, which can then mediate anchorage-dependent growth and proliferation. These interactions are of importance for the activation of germinal centre B cells, the cells of origin for most B cell malignancies. As PI3K and the SYK–BTK–PLC γ 2 axis are required for BCR-induced integrin binding, the striking efficacy of PI3K, SYK and BTK inhibitors in ongoing clinical trials for B cell malignancies such as could also result from the control of integrin signalling (64, 65).

1.3 CHRONIC LYMPHOCYTIC LEUKEMIA

1.3.1 Introduction

Chronic lymphocytic leukaemia (CLL) is characterised by accumulation of abnormal monoclonal B-lymphocytes in the blood, bone marrow and lymphoid tissue (66). It is the commonest leukaemia in the western world with an estimated 3880 new CLL cases diagnosed in UK every year with 41% case above the age of 75 years, and a male-to-female ratio of 1.8:1 (67). The median age at diagnosis of CLL patient is 70 years (65-74) with median age at death of 81 years (68). The disease is both biologically and clinically heterogeneous. CLL can present clinically in a spectrum of ways ranging from totally asymptomatic to a picture of variety of symptoms such as fatigue, night sweats, infections, autoimmune complications, hepatosplenomegaly and lymphadenopathy (69-73). Patients with an indolent form of CLL survive more than 10 years after diagnosis, on average, and often do not require immediate treatment, while patients with an aggressive form of CLL have an average survival of 2 years despite several lines of treatment. Overall survival (OS) of patients with CLL at 5 years ranges from about 20% among very high-risk patients to more than 90% in those with less-aggressive genetic risk features (66, 74).

1.3.2 Cell of origin

Possible consensus concerning the precise cell of origin of CLL has been reached (75). It is unclear whether CLL cells are derived from a single or multiple normal B cell types (76). Haematopoietic stem cells (HSCs) from CLL patients can engraft efficiently in immunodeficient mice and cause clonal B cell lymphoproliferations *in vivo* suggesting that

genetic alteration happens early on (77). The various approaches taken to decipher the cell of origin include morphological assessment, immunophenotyping and more sophisticated techniques including molecular and epigenetic profiling. Typical CLL cells have a normal-shaped nucleus with clumped chromatin surrounded by a thin ring of cytoplasm. These morphologic features are very similar to those of transitional/naïve mature resting B cells but differ from memory-B cells (78). Immunophenotyping of CLL cells suggest that these cells almost always express IgM, IgD, CD5, CD23 along with increased expression of co-stimulatory molecules including CD38, CD69, CD40 and CD39. This led to hypothesis that the origin of CLL cells must be derived from antigen experienced B lymphocytes as the CLL cells also express CD27 (79, 80). CD5 expression on CLL cells inhibit BCR signalling and maintain self-tolerance (81). Studies have identified human CD5+ B cells that co-express CD27 and this was thought to be the normal counterpart of CLL cells (75, 82).

Based on molecular data, IGHV mutational status of CLL divided the CLL into two distinct types of CLL which has clinical significance as well. This also suggested that the cell of origin is different; Mutated CLL (M-CLL) originating from post-germinal centre (GC) memory B cell and unmutated CLL (UM-CLL) originating from pre-GC naïve B cells (76, 83). The earliest transcriptome analysis of both normal B cell and CLL cells revealed a homogeneous gene expression profile (GEP) for both M-CLL and U-CLL and suggested a strong link to memory B cells (84). This analysis was disputed by another GEP study which suggested that the UM-CLL originates from unmutated CD5+ CD27- B cells, whereas the origin of M-CLL is CD5+CD27+ post GC memory B cells (75). Both populations display similar GEP suggesting that CD5+ CD27+ B cells originated from CD5+ CD27- B cells that have undergone GC reaction. Again, microRNA expression of CLL cells resembles antigen-experienced cells (85). Epigenetic studies looking at the methylation of genomic DNA in CLL and normal B cells suggest naïve B cells as normal counterpart of UM-CLL and memory B cells as normal counterpart to UM-CLL (86). Another proposed hypothesis based on an epigenome study suggests that heterogeneity in CLL is likely due to continued maturation of normal development of memory B cells (87). The role of autonomous BCR signalling is intriguing but is shown to happen in both M-CLL and UM-CLL. It is possible that antigen-dependent and autonomous signalling results in CLL proliferation and these signalling events may operate at various

stages of development (88). In short, cell of origin is still a matter of debate though considerable progress has been made in this field.

1.3.3 Diagnosis

The diagnosis of CLL requires the presence of $\geq 5 \times 10^9/L$ B lymphocytes in the peripheral blood, sustained for at least 3 months. The clonality of these B lymphocytes needs to be confirmed by demonstrating immunoglobulin light chain restriction using flow cytometry.

The diagnosis of CLL is established by the combination of clinical features, full blood count, examination of blood film, bone marrow aspirate, bone marrow trephine and lymph node biopsy in some cases. Patients with $< 5 \times 10^9/L$ circulating CLL-type cells may be diagnosed with small lymphocytic leukaemia if they also present with either lymphadenopathy, organomegaly or extramedullary disease; or with monoclonal B cell lymphocytosis (MBL) if they do not (66).

The diagnosis of CLL is predominantly confirmed by immunophenotyping using flow cytometric methods which can be performed on the peripheral blood or bone marrow aspirate. CLL scoring system is used to establish the diagnosis of CLL (Table 1.3).

Table 1.3 Scoring system for diagnosis of CLL(89).

Marker	Marker Intensity	Score	Marker intensity	Score
slg	Weak	1	Strong	0
CD5	+	1	–	0
CD23	+	1	–	0
CD22/79b	Weak	1	Strong	0
FMC	–	1	+	0

92% of CLL cases score 4 or 5, 6% score 3 and 2% score 1 or 2. Most other chronic B cell lymphomas and leukaemia score 1 or 2, but a minority score 3.

IWCLL diagnostic criteria suggests that CLL cells co-express the surface antigen CD5 together with the B cell antigens CD19, CD20, and CD23. The levels of surface immunoglobulin, CD20, and CD79b are characteristically low compared with those found on normal B cells (89-91). Each clone of leukaemia cells is restricted to expression of either κ or λ immunoglobulin light chains (90). A panel of CD19, CD5, CD20, CD23, κ , and λ is usually sufficient to establish the diagnosis according to a recent harmonisation project (92). In borderline cases, markers such as CD43, CD79b, CD81, CD200, CD10, or ROR1 may help to refine the diagnosis (92).

The clinical course of CLL is heterogeneous and various prognostic markers have been established. These include clinical features, serum markers, immunophenotypic features, chromosomal abnormalities detected by FISH analysis and molecular markers (Table 1.4).

Table 1.4 Markers of poor prognosis in CLL(93-99)

Clinical Features	Serum markers	Surface Phenotype	Chromosomal abnormalities	Molecular subtype
<ul style="list-style-type: none"> - Advanced Rai or Binet stage - Atypical morphology - Male - CLL doubling time < 12 months - Fludarabine resistance - Diffuse marrow histology 	<ul style="list-style-type: none"> - High β_2 microglobulin - High LDH - Raised Soluble CD23 - Raised soluble thymidine kinase - Raised TNF-α 	<ul style="list-style-type: none"> - CD38 - ZAP70 - High surface IgM - High surface FMC - High surface CD13 - High surface CD11b - High CD49d 	<ul style="list-style-type: none"> - Del 11q22-q23 - Del 17p13 - TP53 mutation - Trisomy 12 	-Unmutated IGHV

1.3.4 Staging and prognostic scores

There are 2 widely accepted staging systems for use in both patient care and clinical trials:

1. Rai staging system (Modified Rai staging) (93)
2. Binet staging system (94)

The modified Rai classification defines low-risk disease as occurring in patients who have lymphocytosis with leukaemia cells in the blood and/or marrow (formerly considered Rai stage 0). Patients with peripheral blood lymphocytosis, enlarged lymph nodes in any site, and splenomegaly and/or hepatomegaly (lymph nodes being palpable or not) are defined as having intermediate-risk disease (formerly considered Rai stage I or II). High-risk disease includes patients with disease-related anaemia (formerly stage III) or thrombocytopenia (formerly stage IV).

The Binet staging system is based on the number of involved lymphoid areas, as defined by the presence of enlarged lymph nodes ≥ 1 cm in diameter or organomegaly, and on whether there is anaemia or thrombocytopenia.

Stage A. Hb ≥ 10 g/dL and platelets $\geq 100 \times 10^9/L$ and up to 2 of these areas involved.

Stage B. Hb ≥ 10 g/dL and platelets $\geq 100 \times 10^9/L$ and 3 or more of the lymphoid areas involved.

Stage C. Hb < 10 g/dL and/or a platelet count $< 100 \times 10^9/L$.

Following the identification of new prognostic parameters, several prognostic scores and stratification systems have been proposed based on multivariate analyses to extract the most significant independent prognostic information. These models are very useful to identify high-risk patient populations for experimental protocols, but also those patients with a very good prognosis even at advanced stages. The CLL international prognostic index (CLL-IPI) consists of a weighed score that includes the clinical stage, age, *IGHV* mutational status, serum β_2 -microglobulin, and the presence of del(17p) and/or *TP53* mutations

(100). The value of prognostic markers or scores might change with the application of novel therapies.

1.3.5 Treatment

In most cases, CLL remains an incurable disease and the goals of therapy are to improve quality of life and to prolong survival. Treatment of CLL depends on the clinical stage and need for treatment. Previous studies have shown that early treatment with chemotherapeutic agents does not translate into a survival advantage in patients with early-stage CLL.

The treatment of CLL has evolved over number of years. Early therapeutic regimens included alkylating agents such as Chlorambucil monotherapy (C) and nucleoside analogues such as Fludarabine (F) and Cladribine monotherapy. Subsequently, combination therapy with Fludarabine and cyclophosphamide (FC) has been used to achieve better response rates but there was no benefit in terms of overall survival (Table 1.5).

Table 1.5 Responses with old regimen for CLL (101-104).

Reference	Treatment	Patients	CR (%)	PR (%)	PFS (mo)	OS
InterGroup	Fludarabine	170	20	43	25	66mo
	Chlorambucil	181	4	33	14	56mo
UK LRF CLL 4 Study	Fludarabine	181	15	65	10% at 5yr	52% at 5yr
	Chlorambucil	366	7	65	10% at 5yr	59% at 5yr
	FC	182	38	57	36% at 5yr	54% at 5yr
German CLL group	Fludarabine	164	7	76	20	80.7% 3yr
	FC	164	24	70	48	80.3% 3yr
GCLLSG CLL8	FC	409	22	58	33	62.3% 5yr
	FCR	408	44	46	57	69.4% 5yr

However, there are number of new drugs which have changed the landscape of management of CLL in both front-line and relapsed-refractory CLL in the last decade.

1.3.6 Front-line CLL needing treatment

The first breakthrough in management of CLL was the introduction of anti-CD20 monoclonal antibody rituximab to the chemotherapy backbone of FC. The German CLL8 trial had shown that adding Rituximab (Anti-CD20 monoclonal antibody) to chemotherapy (Fludarabine and cyclophosphamide) improved the overall response rate (ORR), complete remission (CR), progression-free survival (PFS) and overall survival (OS) in previously untreated fit patients (105). Alongside that, minimal residual disease (MRD) negativity after treatment has emerged as an important prognostic marker in terms of disease progression and this was confirmed in other landmark studies (106). Data from the German CLL 10 trial showed that FCR was more efficacious than Bendamustine with rituximab (BR), but the main benefit was evident in patients aged less than 65 years (107). In unfit patients, type 2 anti-CD20 monoclonal antibody Obinutuzumab in combination with Chlorambucil (CO) improved progression-free survival (PFS) as compared to Chlorambucil monotherapy (108). However, it was clear that patients with TP53 deletion or mutation do not benefit from chemo-immunotherapy as compared to TP53 wild type patients (109).

The next breakthrough in the treatment of CLL was the introduction of B cell receptor inhibitors and BCL-2 antagonists which were initially developed in the management of relapsed refractory CLL. These molecules have been incorporated into the management of frontline CLL with success. Continuous therapy with first-in-class BTK inhibitor ibrutinib alone or in combination with anti-CD20 antibodies has improved PFS as compared to fixed duration CIT in the form of FCR, BR, CO or Chlorambucil in phase III randomised control trials (110-113). ECOG 1912 suggested that ibrutinib in combination with rituximab may improve overall survival (OS) as compared to FCR (113). The ELEVATE study compared 2nd generation BTKi acalabrutinib alone or in combination with obinutuzumab in comparison to CO and showed a PFS improvement in favour of acalabrutinib containing arms (114). Subgroup analysis of three out of four trials using BTKi failed to demonstrate a significant benefit of continuous BTKi therapy as compared to fixed-duration CIT in patients with mutated IGHV disease (110, 111, 113). Fixed duration 12 months therapy using BCL-2 inhibitor Venetoclax in combination with obinutuzumab was compared to fixed duration 12 months of CO in phase 3 randomised CLL14 trial which recruited patients with comorbidities. There was a clear PFS but no OS advantage in favour of Venetoclax with

obinutuzumab. The benefit was clear in a sub-group analysis, but the advantage was significant in IGHV mutated group (115).

For TP3 aberration CLL, CIT is not recommended due to inferior outcomes. BCRi in the form of ibrutinib or idelalisib with rituximab are both effective but BTKi are preferred due to better side effect profiles (74). Fixed duration Venetoclax with Obinutuzumab is another option but a subgroup analysis of the CLL14 trial has also demonstrated less efficacy of venetoclax plus obinutuzumab in *TP53* mutation or del(17p), though the difference was much less than in the CIT arm (115).

1.3.7 Relapsed refractory CLL needing treatment

The treatment of relapsed refractory CLL has seen several changes but now is dependent on the treatment used in front-line setting. CIT in the form of BR and FCR have been used in this setting with limited success (116, 117). RESONATE was the first phase 3 randomised controlled trial which led to ibrutinib being approved as the first BTKi for treatment for relapsed refractory CLL (118). Addition of ibrutinib to BR was compared to BR in the HELIOS study which has shown a PFS and OS advantage in favour of the ibrutinib containing arm (119). Similarly, idelalisib, a first-in-class PI3K inhibitor in combination with rituximab was superior to rituximab only arm in terms of PFS based on Gilead 116/117 study (120). Similarly, idelalisib in combination with BR was compared to BR only in phase 3 randomised Gilead 115 trial and again showed PFS superiority in favour of the idelalisib containing arm (121). Duvelisib is a PI3K- $\gamma\delta$ inhibitor which has shown PFS advantage as compared to Ofatumumab in the DUO study (122). However, there were autoimmune and infectious complications related to PI3Ki which led to high drug discontinuation rates due to toxicity. ASCEND trial is the first trial to provide head-to-head comparison between 2nd generation BTK inhibitor, Acalabrutinib and PI3K inhibitor, idelalisib with rituximab or BR (123). There was a clear PFS advantage in favour of the acalabrutinib arm. Head-to-head trials comparing various BTKi are on-going and are due to report soon.

Fixed duration Venetoclax given for 24 months in combination with rituximab given for 6 months is compared to BR in phase 3 randomised controlled trial MURANO. This showed a clear PFS and OS advantage in favour of Venetoclax with rituximab arm. Sub-group analysis has shown that participants achieving MRD-negativity to the threshold of $<10^{-4}$ have longer

PFS (124). Continuous Venetoclax monotherapy has been effective in relapsed TP53 aberrated CLL and patients relapsing after BCRi in phase 2 studies (125). Lastly, real world data suggests that BTKi are effective in patients relapsing on Venetoclax treatment (126). Autologous stem cell transplantation (autoSCT) is not useful in CLL (127). Allogeneic stem cell transplantation (alloSCT) should be considered in patients refractory to CIT with *TP53* mutation or del(17p), but fully responsive to novel inhibitor therapy (128-132). Patients with Richter's transformation in remission after therapy and clonally related to CLL should be offered alloSCT (74). Treatment with chimeric antigen receptor T (CAR-T) cells or bi-specific T cell engager (BiTE) antibodies within clinical trials could be an alternative to alloSCT for all three groups (74).

1.3.8 Minimal residual disease

Combination chemoimmunotherapy has enabled clinicians to achieve much better overall response rates in the treatment of CLL. There has been increasing interest in the assessment of minimal residual disease (MRD) in the management of CLL. It has been shown that patients achieving MRD negativity have longer progression free survival (PFS) and overall survival (OS) (Figure 1.4) and MRD negativity was shown to be an independent prognostic marker in German CLL trial (103, 133, 134).

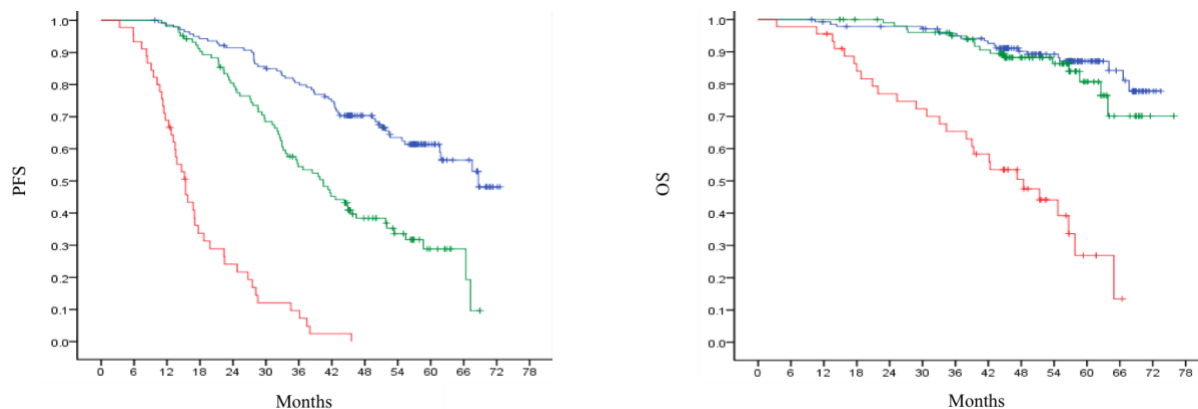


Figure 1.4 MRD after CIT is a predictor of PFS and OS.

Diagnosing disease at the MRD level is also challenging. The sample is usually taken three months after the end of treatment.

Current methods include:

- **4 Colour flow cytometry:** using a combination of CD5/CD19 with CD20/CD38, CD81/CD22, and CD79b/CD43: Detects 1 CLL cell in 10,000 leukocytes (10^{-4}) (135).
- **Allele specific oligonucleotide PCR:** Detects 1 CLL cell in 10,000 leukocytes (10^{-4}) (136).
- **High-throughput sequencing:** Detection limit is 10^{-5} to 10^{-6} .

Issues will be related to cost, validation and reliability (137).

Minimal residual disease would be important in future treatment algorithms as it clearly has a prognostic value. However, its role is still not clear in the era of B cell receptor antagonists which cause peripheral lymphocytosis, and it might not be possible to achieve MRD negativity with these drugs. On the other hand, MRD-negativity is achievable with BCL-2 antagonists such as Venetoclax with or without immunotherapy (115).

1.3.9 Flow cytometry in CLL

Immunophenotyping using flow cytometry has helped in the diagnosis of CLL and in differentiating it from other B cell disorders. There are various markers on CLL cells that help to ascertain the diagnosis. CLL cells co-express the T cell antigen CD5 and B cell surface antigens CD19, CD20, and CD23. The levels of surface immunoglobulin, CD20, and CD79b are characteristically low compared with those found on normal B cells (92). Each clone of leukaemia cells is restricted to expression of either kappa or lambda immunoglobulin light chains. Variations of the intensity of expression of these markers may exist. Surface immunoglobulin was initially used as a marker of B cell lineage. Since then, several markers have been identified that have substantially aided in studying the biology of the disease (Table 1.6).

Table 1.6 Antigens used in the diagnosis of CLL.

Antigen	Cell function	Presence in CLL and clinical implication	Reference
CD20	Act as a calcium channel and plays a role in B cell activation, proliferation and differentiation.	Dim. Target for monoclonal antibody, rituximab, in treatment of CLL	(138)
CD19	Assembles with BCR complex to decrease the threshold for antigen receptor dependent stimulation	Positive. Preclinical data on monoclonal antibody against CD19 in CLL (XmAb5574)	(139-141)
CD5	Regulates intracellular signal strength induced by antigen receptors in both T and B cells	Positive.	(141, 142)
CD79b	Signal transmitting unit of BCR complex	Weak or negative. Preclinical data on antibody drug conjugate (anti-79b-vc-MMAE)	(141, 143)
CD43	Implicated in the regulation of cell adhesion, activation and survival	Positive.	(144-146)
CD81	CD19/CD21/CD81 complex enables B-lymphocytes to respond to low concentration of antigens and induces homotypic cellular aggregation	Positive.	(92)
CD52	In presence of antibody, it is a good target for complement action and activates cell proliferation in T cells, but function in the absence of antibody is unknown	Positive. Target for monoclonal antibody, Alemtuzumab, in treatment of CLL	(147)
CD200	Interaction with its receptor CD200R sends inhibitory signal to	Positive. Preclinical data on CD200 blocking	(148, 149)

	macrophages. In T cells it alters the cytokine profile from Th1 to Th2 and it suppresses the antitumor immunity	antibodies enhancing the tumour specific immunity	
CD23	Acts as a low affinity receptor for IgE	Positive. Phase 1/2 clinical data on anti-CD23 (Lumiliximab) antibody in combination with chemotherapy	(150-153)
CD22	Acts as B cell associated adhesion protein and regulates B cell activation	Negative or positive. Phase 1/2 clinical data on anti-CD22 (Epratuzumab) antibody treatment	(140, 154-156)
CD25	Part of IL2 receptor	Positive. Phase 2 clinical data on antibody conjugated with diphtheria toxin (denileukindiftitox)	(157)
CD10	Metalloendopeptidase that cleaves small peptides like angiotensins, bradykinin, enkephalins and oxytoxin. It also controls neutrophil chemotaxis and inflammation	Negative.	(92, 158)
CD38	Serves as an ectoenzyme those catalyses the synthesis and hydrolysis of cyclic ADP-ribose which is a calcium mobilizing agent. This helps in transmembrane signalling thereby affecting differentiation and proliferation of various immunoregulatory cells.	Positive or negative. Prognostic marker in CLL	(159-161)

CD103	Presence on T regulatory cells helps these cells to adhere to epithelial cells on which its ligand, E-cadherin, is present.	Negative.	(162, 163)
CD11c	CD11c/Cd18 complex is a $\beta 2$ integrin expressed in granulocytes, monocytes NK cells and dendritic cells. Helps in cell adhesion and B cell activation	Weak.	(164-166)
FMC7	An epitope on CD20 molecule whose expression is sensitive to the level of membrane cholesterol	Negative or weak.	(97)
CD79a	Signal transmitting unit of BCR complex	Positive.	(167)

CD20: CD20 spans the cell membrane four times and is constitutively phosphorylated but not glycosylated. Long N and C terminal ends are located within the cytoplasm and only a minor portion of molecule is expressed on the cell surface. The gene locus is at 11q13 near CD5 gene (138). CD20 is expressed on B cells after the expression of CD19 and CD22 at the pre-B cell stage. It is strongly expressed in germinal centre B cells and then declines at the end of B cell differentiation. It is not expressed on plasma cells and there is a weak expression on CLL cells. CD20 functions as a Ca^{2+} channel and can induce a proliferative signal in B-lymphocytes. This is a crucial molecule in terms of treatment for CLL (168).

CD19: This pan-B cell marker is also dim on CLL cells. The extracellular regions contain two C-2 Ig-like domains. The cytoplasmic region contains nine tyrosines. CD19 interacts with CD21 through extracellular and transmembrane regions, with CD81 through extracellular region only and with surface IgM through the first 17 amino acids of cytoplasmic region. The gene locus is on 16p11.2. CD19 is the earliest recognisable marker of B cells and is retained throughout B cell differentiation but may be downregulated in plasma cells. It is also expressed on follicular DC(169). CD19 amplifies B cell activation and is itself phosphorylated after BCR engagement (140). CD19 recruits tyrosine kinases in a stepwise manner and its

large cytoplasmic region act as a scaffolding protein linking several signalling molecules. It lowers the threshold of antigen required for B cell stimulation several fold.

CD79b,CD79a: In contrast to other B cell diseases, the extracellular epitopes of CD79b and CD79a are either expressed at a low density or absent. Although early reports suggested that most CLL cases were CD79b negative, a monoclonal antibody has shown that CD79b is expressed weakly in most CLL cases (92). CD79a and CD79b form a disulfide linked heterodimer which is noncovalently associated with membrane Ig (mIg) on B cells. The cytoplasmic regions of both proteins have an ITAM which links them to signalling molecules. The gene locus for CD79a is 19q13.2 and for CD79b is 17q23. Both molecules are restricted to B lymphocytes, first appearing on the surface of pro-B cell and persist throughout the stages of B cell differentiation. They are both crucial for B cell differentiation and absence of either of them causes B cell arrest at pro-B cell stage. This heterodimer plays a key role in expression of BCR, antigen internalisation and signalling. Mutations of CD79b have been identified in CLL and may contribute to poor expression of CD79b (170).

CD22: It is a member of the sialic acid-binding immunoglobulin superfamily lectin, which binds sialic acid. There are two isoforms, CD22 β and CD22 α . The cytoplasmic regions contain six Tyr residues, two of which conform to an ITAM configuration and the other four forms potential ITIMs. ITIMs phosphorylation leads to association with SH2-containing phosphatases SHP-1, SHP-2 or SHIP (inositol phosphatases). The gene for CD22 is present on 19q13.1. Cytoplasmic CD22 expression is present in pro-B and pre-B cells. It is a marker for B cell commitment. Cell surface expression is seen in mature stages, and it disappears on B cell activation. CD22 is an adhesion molecule and possesses lectin activity. On BCR regulation, Src kinases Lyn and Syk phosphorylate ITIMs on CD22 which phosphorylate SHP-1/2 and SHIP. CD22 is masked on resting B cells. Release from this masking is required for CD22 to bind to its ligands and exert the negative regulatory function on B cell activation. CD22 is under-expressed in CLL (156).

CD5: CD5 antigen is positive in the majority of CLL cells. It is a pan T cell marker and NK- cell marker. CD5 is also present in some B cells and these are usually found in mantle cells of secondary lymphoid follicles (142). Some normal B cells express the CD5 marker in peripheral blood. CD5+ B cells are increased in rheumatoid arthritis. CD5+ B cells have been

implicated in producing autoantibodies. The CD5 gene is present on 11q13 close to the CD20 gene. The extracellular region contains three scavenger receptor cysteine-rich domains and cytoplasmic region contain multiple Ser/Thr and Tyr residues. Tyr 429 is critical for inhibitory function mediated by CD5 and is independent of an ITIM motif.

CD154: CLL cells express the CD40 ligand, CD154. CD154 is a member of the TNF superfamily. It forms a trimer and binds to three CD40 molecules. The gene is present on Xq26. It is usually expressed on activated CD4⁺ and CD8⁺ T cells, monocytes, basophils, mast cells, eosinophils and activated DCs. CD40/154 interactions drive germinal centre formation, B cell proliferation, differentiation and Ig isotype switching. This interaction helps APC functions, T cell priming and differentiation, activation of NK cells and stimulation of cytokine production from monocytes (169). CD40L is constitutively expressed in malignant B cells.

CD23: CD23 is an immunophenotypic hallmark of CLL. CD23 is expressed on B-lymphocytes especially when associated with IgD, follicular DCs specifically those in the light zone of the germinal centres, transiently on some T cells in allergic individuals, Langerhans cell, monocytes, platelets, NK cells, CLL and EBV-transformed B cells (171). CD23 is a 45-kDa transmembrane glycoprotein that functions as a low affinity receptor for IgE. It also binds to CD21 and to the α -chain of β_2 integrin. Soluble CD23 enhances IgE synthesis (151). It acts as an adhesion molecule by its ability to promote T-B cell interactions and in B-lymphocytes when it interacts with its ligand CD21. It is expressed at low levels in normal B cells, but upon activation, high expression is seen on B cells, and yet, it is characteristically expressed in CLL in which the neoplastic lymphocytes are believed to be dormant. CD23 exists in two isoforms (172). The CD23a promoter is only stimulated by IL-4 but the promoter of CD23b is stimulated by IL-4 and other stimuli. CD23a is expressed in B cells only whereas CD23b is expressed by other cells (150, 151). CD23 is cleaved by an unknown metalloprotease releasing a soluble form sCD23. Overexpression of CD23 in CLL is due to a deregulation of Notch 2 signalling. sCD23 is elevated in CLL and may have a prognostic significance because its levels reflect tumour mass (153).

CD27: CD27 is a member of the TNFR superfamily. It is expressed on CD4⁺ and CD8⁺ T cells, early B cell progenitors, memory B cells, CLL B cells and a subpopulation of NK cells.

CD27/CD70 interaction contributes to T and B cell activation and regulates the CD4+ and CD8+ T cell pool at sites of immune responses. CD27 is expressed on normal plasma cells. All CLL cells are CD27+, which is typically a marker of the memory B cells. Most normal memory B cells have *IGHV* gene mutation, but a small fraction does not though this is disputed (173-175). The presence of CD27 on CLL cells as well as the presence of both *IGHV* mutated and unmutated CD27+ memory cells support the idea that CLL cells may have evolved from memory B cells.

1.3.10 Proliferation markers

CLL cells show specific changes in membrane protein expression during various stages of the cell cycle. Various markers have been established to divide the resting and proliferating fractions of CLL. Expression of proteins CD39, CD86, CD95 and CD23 are uniformly increased during cell cycle but only CD23 was thought to be associated with proliferation in CLL (176). CD24 modulates B cell activation responses by promoting antigen dependent proliferation of B cells and prevents their terminal differentiation into antibody-forming cells. Its expression was only down-regulated when CLL cells entered S-phase.

Three markers require special attention and are of independent prognostic significance in CLL: CD38, CD49d and ZAP70.

CD38: CD38 is a 45 kDa non-lineage restricted type II transmembrane protein. CD38 expression in haematopoietic cells is discontinuous. Uncommitted stem cells are CD38⁻ but committed CD34⁺ cells are CD38⁺. B cell progenitors are CD38⁺ but circulating naïve B cells are CD38⁻. Centroblasts and centrocytes retain the expression of CD38 but it is lost in memory B cells. Plasma cells strongly express CD38. It is also expressed in early T cell precursors, myeloid precursors, monocytes, NK cells, erythroid progenitors and platelets.

It is an important prognostic marker in CLL (159, 161, 177). It was initially developed as a surrogate marker for *IGHV* mutational status. CD38 positivity was associated with unmutated group which carries worse prognosis. However, CD38 was established as an independent prognostic factor. The percentage of cells within a CLL clone expressing CD38 is an indicator of the level of cellular activation of the clone. There is a lot of variation in reporting of CD38 positive cells. The cut-off at which a CLL clone becomes CD38 positive or

negative ranges from 7-30% and that creates an issue regarding the relevance of prognostic significance of bimodal expression of CD38 in a CLL clone.

CD49d: CD49d is an α -integrin subunit ($\alpha 4$) that can pair with CD29 (the $\beta 1$ subunit) to form a complete integrin ($\alpha 4\beta 1$) that binds fibronectin and VCAM-1. Like other integrins, $\alpha 4\beta 1$ is involved in anchoring cells to tissues and can be the first step in cell migration. CD49d and CD38 are often expressed on CLL B cells (164). A large macromolecular complex comprising CD49d, CD38, CD44v, and MMP-9 has been identified on U-CLL clones. Higher levels ($\geq 30\%$) of CD49d have been correlated with shorter survival times.

ZAP-70: ZAP-70 is another molecule, which is used as a surrogate marker for *IGHV* mutation. ZAP-70 is a member of the SYK-ZAP-70 protein tyrosine kinase family, which is normally expressed in T cells and natural killer cells. It has a critical role in the initiation of T cell signalling. Intracellular expression of the ZAP-70 protein above a certain threshold of cells by immunofluorescence and flow cytometry of $\geq 20\%$ has proven to be an important indicator of time to treatment and survival in CLL. ZAP-70 levels are an independent marker of clinical outcome (178-181).

1.3.11 Molecular interactions in CLL microenvironment

Tissue microenvironments are important for CLL cell survival and proliferation. CLL cells interaction with stromal cells is maintained by chemokine receptors and adhesion molecules expressed on CLL cells.

1.3.11.1 CXCR4-CXCL12 axis:

The CXCR4 chemokine receptor (CD184) is expressed at high levels on the surface of peripheral blood CLL cells and mediates homing of CLL cells underneath nurse-like cells (NLCs) or bone marrow stem cells (BMSCs), a process known as pseudoemperipoiesis. CXCR4 surface expression is regulated by its ligand CXCL12 via receptor endocytosis. This characteristic can be used to distinguish tissue (lymphatic and BM derived) from blood CLL cells, which express low or high CXCR4 levels, respectively (182, 183). Proliferating Ki-67⁺ CLL cells from BM and lymphatic tissue display significantly lower levels of CXCR4 and CXCR5 than non-proliferating CLL cells.

1.3.11.2 CXCR5-CXCL13 axis:

CXCR5 (CD185) is the receptor for the chemokine CXCL13, which regulates lymphocyte homing and positioning within lymph follicles. CLL cells express elevated levels of CXCR5 and stimulation with CXCL13 induces activation via G proteins, PI3Ks, and p44/42 MAPK, resulting in actin polymerization, CXCR5 endocytosis, and chemotaxis (182).

1.3.11.3 Cell surface adhesion molecules:

Another interesting group of molecules studied in CLL is cell surface adhesion molecules. Several markers including integrins, selectins, homing receptors, as well as the serum levels of some of these molecules has been studied. Adhesion molecule expression is heterogeneous in CLL as described below.

Low LFA-1 (CD18/CD11a) and CD54 (ICAM-1), high L-selectin and CD44 (HCAM), and variable CD11c characterise CLL (165). Expression of CD11c/CD18, CD31, CD48 and CD58 are significantly lower in CLL cases with 11q23 deletions (164). Elevated levels of expression of CD11a, CD18, CD29, and CD11c on the surface of the leukemic cells were found in cases with splenomegaly and LFA-1 is expressed in patients with predominant lymphadenopathy. Serum levels of intercellular adhesion molecule 1 (CD54) are significantly elevated in CLL patients compared with healthy subjects (184). It correlates with tumour burden and hepatosplenomegaly in the advanced clinical stage of CLL. Similarly, CLL cells invariably express one or more isoforms of the lymphocyte homing receptor CD44 and of the CD62L (L-selectin), which is different from that of related low-grade B cell disorders and strong expression of these also correlate with poor prognosis in CLL (164). Strong expression of CD36, a thrombospondin receptor, correlates with diffuse pattern of bone marrow involvement and poor prognosis (185). Compared to other non-Hodgkin lymphomas (NHL), β -integrins are generally under-expressed.

1.3.11.4 Other interactions:

Integrins, particularly VLA-4 integrins (CD49d), expressed on the surface of CLL cells interact with ligands on the stromal cells (VCAM-1 and fibronectin) (164). NLCs also express the TNF family members BAFF and APRIL, providing survival signals to CLL cells via corresponding receptors (BCMA, TACI, and BAFF-R) (186). CD38 expression allows CLL cells to interact with CD31 expressed by stromal and NLCs (159). Ligation of CD38 activates ZAP-70 and

downstream survival pathways. BCR stimulation and co-culture with NLCs also induces CLL cells to secrete chemokines (CCL3, CCL4, and CCL22) for the recruitment of immune cells (T cells and monocytes) for cognate interactions(187). CD154+ T cells are preferentially found in CLL-proliferation centres and can interact with CLL cells via CD40 (169).

1.3.12 Apoptosis and CLL

Apoptosis removes aged and damaged cells from a healthy multicellular organism, and the balance between cell survival and cell death, as maintained by apoptosis, is critical for normal development and homeostasis of multicellular organisms. The apoptotic pathways include the extrinsic pathway and the intrinsic pathway.

Apoptosis is carried out by proteases called caspases, which are synthesised initially as pro-caspases. There are two classes of caspases involved in the apoptotic pathway. Initiator caspases promote apoptosis by cleaving and activating other caspases, and the effector caspases initiate the cellular changes associated with apoptosis. The extrinsic pathway uses caspase 8 and caspase 10, whereas the intrinsic pathway uses caspase 9 (188). Both pathways use caspases 3, 6, and 7 as effector caspases (188, 189). The effector caspases cleave a variety of proteins that are critical for cellular integrity and activate enzymes that promote the death of the cell.

1.3.12.1 Extrinsic pathway:

This route uses the death receptors to induce apoptosis. Death receptors are part of TNF superfamily and carry a cytoplasmic death domain. Death receptors in immune system include FAS (CD95) and TNFR-I, a receptor for TNF- α . Loss of function mutations in Fas lead to the increased survival of lymphocytes and are one cause of the disease autoimmune lymphoproliferative syndrome (ALPS). On binding to the ligand, the death domain of FAS binds to FADD which has a death domain and death effector domain. The death effector domain activates initiator pro-caspases 8 and 10. The TNFR-I pathways uses TRADD as binding molecule to FADD which then recruits initiator pro-caspases. The initiator caspases activate effector caspases which induces apoptosis.

1.3.12.2 Intrinsic Pathway:

In this alternative form of apoptosis, the critical step is the release of cytochrome c from mitochondria, which triggers the activation of caspases. In the cytoplasm, cytochrome c

binds to a protein called Apaf-1, stimulating its oligomerisation. The Apaf-1 oligomer then recruits an initiator caspase, pro-caspase 9. Aggregation of caspase 9 stimulates the activation of effector caspases as in the death receptor pathways.

The intrinsic apoptotic pathway includes Bcl-2 family proteins which are important regulators of the intrinsic apoptosis pathway and were first identified in follicular lymphoma where the t(14;18) chromosomal translocation results in significant overexpression of Bcl-2 in B cells.

The Bcl-2 family of genes encodes a family of closely related proteins that possess either pro-apoptotic or anti-apoptotic activity and share up to 4 Bcl-2 homology (BH) domains. The anti-apoptotic family members (Bcl-XL, Bcl-2, Bcl-w, A1, and Mcl-1) are characterised by 4 BH domains that are designated BH1 through BH4. The pro-apoptotic proteins can be further subdivided into multidomain proteins (Bax, Bak) and the BH3-only proteins (Bad, Bim, Noxa, Puma) (190). The interplay between these 3 groups of proteins serves as the gateway to the intrinsic apoptosis pathway. The multidomain pro-apoptotic proteins Bax and Bak are direct mediators of apoptosis and are absolutely required for the initiation of the mitochondrial apoptosis pathway. Anti-apoptotic Bcl-2 family proteins (e.g., Bcl-2 and Bcl-XL) inhibit cytochrome C release by blocking Bax/Bak activation. The ratio of pro-apoptotic to anti-apoptotic proteins is associated with the outcome of cell survival or programmed cell death. In contrast to other known oncogenes, Bcl-2 does not stimulate cellular proliferation, but rather inhibits programmed cell death by protecting cells from a wide variety of pro-apoptotic stimuli, including cytokine withdrawal, irradiation, cytotoxic drugs, heat, and deregulated oncogenes (191, 192).

Resistance to apoptosis is a hallmark of CLL. Overexpression of anti-apoptotic Bcl-2 family members is associated with tumour initiation and disease progression. Hence, Bcl-2 is a compelling target for CLL therapy.

p53: p53 is a tumour suppressor transcription factor which regulates cellular pathways such as DNA repair, apoptosis, angiogenesis and senescence (Figure 1.5). In normal unstressed cells, the level of p53 is kept low due to binding of protein such as MDM2 that promote p53 degradation via the ubiquitin/proteasome pathway (193). After genotoxic or

non-genotoxic stress, the p53 level is increased by inhibition of interaction with MDM2 and other inhibitors. Also, a series of modulators increase p53 transcriptional activity.

p53 deletion/mutation is the most important prognostic factor which confers resistance to chemotherapy (194, 195). *TP53* gene is located on short arm of chromosome 17 at band 13, and it plays an integral role inducing apoptosis or cell cycle arrest in cells whose DNA is damaged by either chemotherapy or radiation. In CLL, functional dysregulation of p53 can occur directly due to deletion or mutation on the 17p chromosome or indirectly due to defects in the regulatory genes, e.g., the *ATM* gene located in the chromosomal region 11q23.

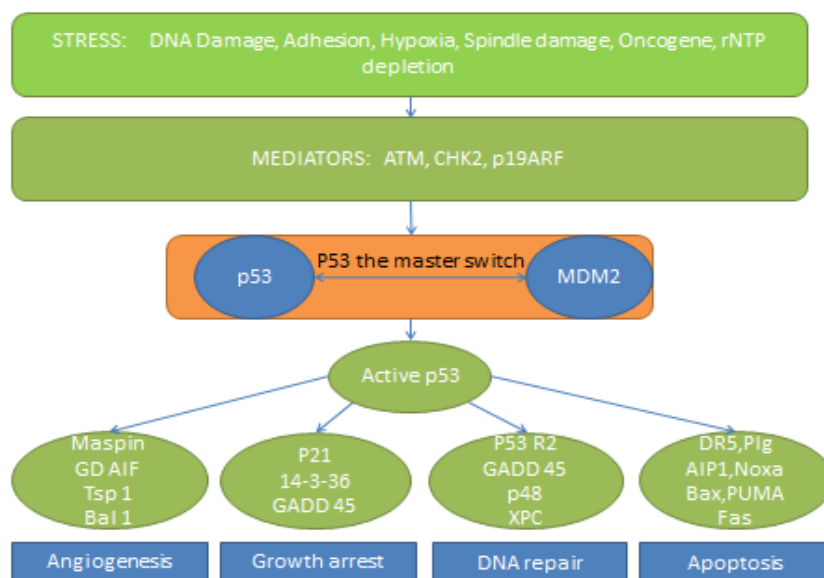


Figure 1.5 DNA damage by chemo or radiotherapy activates p53 through the activation of ATM and other factors. p53 induces either cell cycle arrest or apoptosis through different targets. Various drugs like steroids, Alemtuzumab, lenolidamide, B cell receptor antagonists, Bcl2 inhibitors and MDM2 inhibitors bypass the p53 pathway.

1.4 THE B CELL RECEPTOR IN CLL

Low expression of the BCR is a hallmark of the CLL lymphocyte and is unique to CLL among mature B cell malignancies. The mechanisms accounting for poor expression of the BCR in CLL are not currently known. There is very low expression of surface IgM and CD79b on the surface of CLL cell in most cases (61, 196). However, mRNA transcription and intracellular synthesis of BCR components appear to be normal.

The structure of the BCR strongly influences progression of the disease. Based on the degree of somatic hypermutation within the BCR antigen-binding site, CLL patients can be classified as unmutated if they have 98% or more homology with the germline sequence; Mutated if they have less than 98% sequence homology(197, 198). Mutated CLL (M-CLL) is typically associated with slower disease progression and better overall survival (OS), whereas unmutated CLL (U-CLL) progresses faster, resulting in a shorter time to treatment and shorter survival (96, 197). Secondly, 30% of CLL patients express a skewed Ig repertoire called “stereotyped” receptors(196, 199-201). Thirdly, the BCR signalling pathway is the activated in the lymph node microenvironment resulting in formation of proliferation centres or pseudofollicles (202).

BCR engagement in CLL cells remains controversial (203), with support for both tonic- and antigen-induced BCR activation. CLL cells are in state of reversible anergy which is characterised by constitutive phosphorylation of MEK and ERK in the absence of AKT being phosphorylated (204). The concept of antigen-induced BCR activation is also based on the fact that nearly 30% of both M-CLL and UM-CLL present a highly restricted and biased repertoire of immunoglobulin genes called “stereotyped receptors” such as heavy usage of IGHV -1-69, IGHV 3-7, IGHV 3-21 and IGHV 4-34 (83, 196, 205-207). The presence of these stereotyped receptors led to the concept that the antigens stimulating these receptors may be restricted and suggests that antigen engagement may be responsible for the pathogenesis of CLL (208). However, UM-CLL BCRs are reactive to multiple self-antigens, predominantly cytoskeletal proteins (non-muscle myosin heavy chain 2A, filamin B, colifin-1), DNA, lipopolysaccharides, apoptotic cells, insulin, and oxidized low-density lipoproteins (209-212). Another example would be autonomous signalling in the form of epitopes in the BCR CDR-3 of heavy chain (88, 213). Foreign antigens have shown to stimulate CLL cells with specific BCRs. For example, BCRs with IGHV1-69 or IGHV3-21 interact with the cytomegalovirus-derived super-antigen pUL32 and mutated CLL with BCRs expressing IGHV3-07 interacting with $\beta(1,6)$ -glucan (214, 215).

1.4.1 B cell receptor signalling in CLL

The responsiveness of CLL cells to stimuli is varied. For example, BCR signalling in CLL is dependent on the surface expression of IgM and IgD. Responsive to stimulation to IgM is

much higher in U-CLL. M-CLL shows features of anergised CLL cells resulting from prolonged antigen activation, including reduced IgM levels, baseline activation of calcium signalling, constitutive ERK phosphorylation (204, 216-218). IgD signalling can be induced in all CLL samples with significant differences between M-CLL and U-CLL. Markers associated with active BCR signalling, such as zeta chain-associated protein kinase 70kDa (ZAP-70) expression and increased expression of the T cell-attracting chemokines CCL3 and CCL4, are strong predictors of CLL progression and time to treatment (187). Thus, CLL cells appear to depend on continuous and intermittent BCR signalling that drives cell survival and expansion.

1.4.2 Cytosolic kinases fundamental to CLL BCR signalling

1.4.2.1 Bruton's tyrosine kinase (BTK)

BTK is a non-receptor tyrosine kinase belonging to the Tec family of kinases. B cells express the Tec kinases, BTK and Tec. BTK is critical for B cell development, differentiation and signalling (219). The *BTK* gene consists of 19 exons and spans 37.5kb on the X chromosome. Loss of function mutations of *BTK* gene in humans causes X-linked agammaglobulinemia, the result of which is absence of circulating B-lymphocytes (220). The patient has an inability to mount any humoral immune response and the disease manifests itself with recurrent bacterial and enteroviral infections. Similar spontaneous mutation in mice causes a milder X-linked immunodeficiency.

BTK is present in B lymphocytes but not in plasma cells (220). In primary B lymphocytes, BTK is almost always non-phosphorylated. BTK is required for differentiation of pro-B cell to pre-B cell. BTK deficiency also causes abnormalities in platelets, macrophages and osteoclasts (219).

The BTK protein comprises several domains, which includes a PH, Tec homology, SH3, SH2 and SH1 (Kinase) domain (Figure 1.6). Each domain can bind to various proteins to direct intracellular signalling. It is metalloprotein requiring Zn^{+2} for optimal activity and stability. Mutation affecting zinc binding at the Tec homology domain leads to an extremely unstable protein.

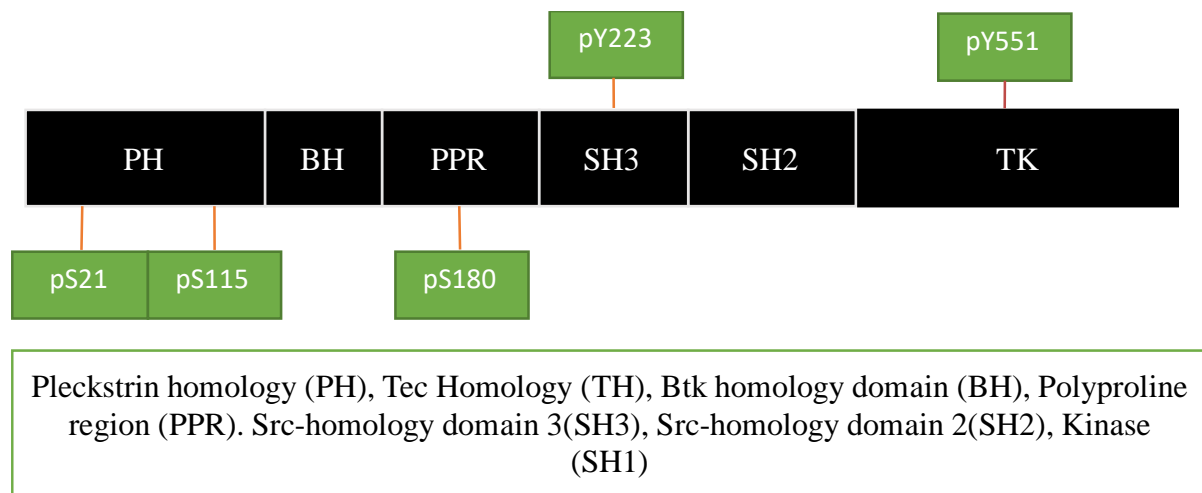


Figure 1.6 BTK domains with all known interacting serines/tyrosines.

BTK is activated by post-translational modification as well as subcellular localisation. The cytosolic BTK is translocated to the plasma membrane after B cell receptor engagement and subsequent activation of P13kinase leading to generation of PIP3. BTK via its PH domain binds to PIP3 and gets phosphorylated at tyrosine Y551 in the kinase domain by the Src family kinase Lyn. This is followed by autophosphorylation of tyrosine at Y223 in the SH3 domain. BTK along with BLNK phosphorylates phospholipase C γ 2 which causes the activation of further downstream pathways.

BTK also interacts with the members of the TLR family and key proteins from TLR signalling pathways such myeloid differentiating protein (MYD88), MYD88 adaptor like protein (Mal) and interleukin-1 receptor (IL-1R) associated kinase (IRAK-1) (221).

A small amount of BTK can be detected in the nucleus suggesting that it is a nucleocytoplasmic shuttling protein (222). Some mutations in the *BTK* gene cause the BTK to be nuclear in position (219). PKC β negatively regulates BTK whereas PKC θ activates BTK. IBTK, and caveolin inhibit the kinase domain of BTK and hence negatively regulate BTK. Phosphorylation of S21 and S115 in the PH domain leads to the recruitment of the protein phosphatase Pin1, which attenuates the signalling activity of BTK.

BTK interacts with multiple transcription factors including NF- κ B, Bright and STAT5A (223-225). Both NF- κ B subunits p50 and p65 bind to the BTK promotor hence increasing BTK expression. Thus, BTK can positively regulate its own promotor via NF- κ B signalling.

1.4.2.2 Class 1 PI3 Kinases

Class 1 PIKs are present in all cell types. Class 1 PI3Ks use phosphatidylinositol-4,5bisphosphate (PtdIns(4,5)P₂) as their substrate (226). It is divided into two groups.

Class 1A: It exists in a combination of catalytic (p110 α , p110 β , p110 δ) and regulatory subunit (p85). The catalytic subunit has a PI3K core consisting of a C2 domain, helical domain and a catalytic domain. This is attached to a Ras-binding domain and p85-binding domain. p110 δ is highly enriched in leukocytes.

The regulatory subunit (p85) has a p85 core consisting of two SH2 domains and p110-binding domain (Figure 1.7). It is attached to BH domain and SH3 domain. The p85 domain serves three functions: stabilisation, inactivation of kinase activity in the basal state and recruitment of pTyr residues in receptor and adaptor molecules.

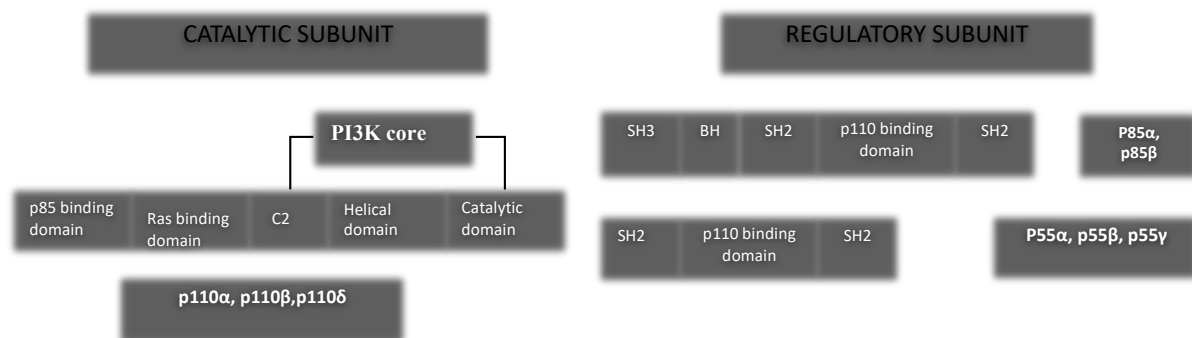


Figure 1.7 Structure of Class 1A PI3 Kinases

Class 1B: It consists of a catalytic domain (p110 γ) and regulatory subunit (p101 and p87). p101 and p87 lack SH2 domains, do not have homology to other proteins and have no identifiable domain. p110 γ is highly enriched in leukocytes.

Class 2 PI3K: This class uses PtdIns as a substrate. They lack regulatory subunits but have amino and carboxy-terminal extensions to the PI3K core structure, which can mediate protein-protein interactions.

Class 3 PI3K: Class 3 PI3K has one catalytic member, Vps34, which uses PtdIns as substrates and binds Vps15.

Multiple signalling inputs can activate the PI3 Kinases. All p110 subunits have a Ras-Binding domain. Ras activates p110 α and p110 γ while TC21 (Ras family member) activates p110 δ . Other signalling inputs include other small GTPases such as RAB5, Rac, Rho and Cdc42. G-protein coupled receptors (GPCRs) can activate PI3 kinases directly through the allosteric activation of heterotrimeric G proteins or indirectly via tyrosine kinases and Ras.

Class 1 PI3 Kinases generate PtdIns(3,4,5)P₃ lipids, which are quickly converted by phosphatases to PtdIns(4,5)P₂ and PtdIns(3,4)P₂. These lipids coordinate the localisation and function of multiple effector proteins, which bind the lipid through their PH domain. These include Ser/Thr and Tyr protein kinase such as AKT and BTK, adaptor proteins such as GAB2 and regulators of small GTPases such as GAPs and GEFs (227).

1.4.2.3 AKT (Protein kinase B)

In mammals, there are three isoforms of AKT. All three isoforms share a high degree of amino acid identity and are composed of three functionally distinct regions: N-terminal PH domain, a central catalytic domain, and a C-terminal hydrophobic motif. Together, these regions encompass a phosphoprotein of approximately 56 kDa. The N-terminal PH domain is common to numerous signalling proteins and provides a lipid binding module to direct PKB to PI3K generated phosphoinositides PIP₃ and PIP₂. PTEN catalyses the dephosphorylation of PIP₃ and PIP₂ at the D3 position, thus reducing the pool of lipids capable of binding with PKB. The phosphatase SHIP catalyses the dephosphorylation of PIP₃ to generate PIP₂, also depleting lipids capable of recruiting PKB to the plasma membrane. The hydrophobic motif (HM) found in PKB provides a docking site for the upstream activating kinase, PDK1. PI3K-generated PIP₃ and PIP₂ also recruits PDK1 to the plasma membrane. PKB undergoes HM phosphorylation by the Ser473 kinase or by autophosphorylation. The HM of PKB stabilises and activates PDK1 which then phosphorylates PKB on Thr308. The HM of PKB associates with and stabilises its kinase domain, which then phosphorylates cytosolic and nuclear targets (228).

1.4.2.4 Spleen Tyrosine Kinase (SYK)

SYK is a 72 kDa non-receptor tyrosine kinase that contains two SRC homology 2 (SH2) domains and a kinase domain and is most highly expressed by haematopoietic cells (Figure 1.8). Mammals also express a SYK homologue, ZAP70, which is mostly restricted to T cells and natural killer (NK) cells. The SYK signalling pathway is present in classical immunoreceptors of the adaptive immune response and glycoprotein VI (GPVI), a collagen receptor expressed by platelets. SYK is required for several functions of innate immune cells and for certain non-immune functions, such as bone resorption by osteoclasts. SYK has also been shown to mediate signalling by classes of receptors, including integrins and C-type lectins that do not contain conventional ITAMs (229).

SYK interacts with several molecules such as VAV family members, PLC γ isoforms, the regulatory subunits of phosphoinositide 3-kinases (PI3Ks), SLP76 and BLNK. These molecules form the proximal signalosome and trigger downstream processes including Ca²⁺ and protein kinase C (PKC) signalling, RAS homologue (RHO) family and protein tyrosine kinase 2 (PYK2) -mediated cytoskeletal rearrangement, reactive oxygen species (ROS) production and phagocytosis, PI3K mediated Tec family and AKT signalling pathways, as well as transcriptional regulation through the RAS-ERK and NFAT pathways. Ligation of classical immunoreceptors also triggers pro-inflammatory transcriptional programmes through activation of NF- κ B. The action of SYK is often counteracted by phosphatases such as SHP1, and it is the balance of SYK and SHP1 activities that determines the ultimate signalling output. The expression of SYK is also negatively regulated by the E3 ubiquitin ligase CBL leading to ubiquitylation and degradation of SYK.

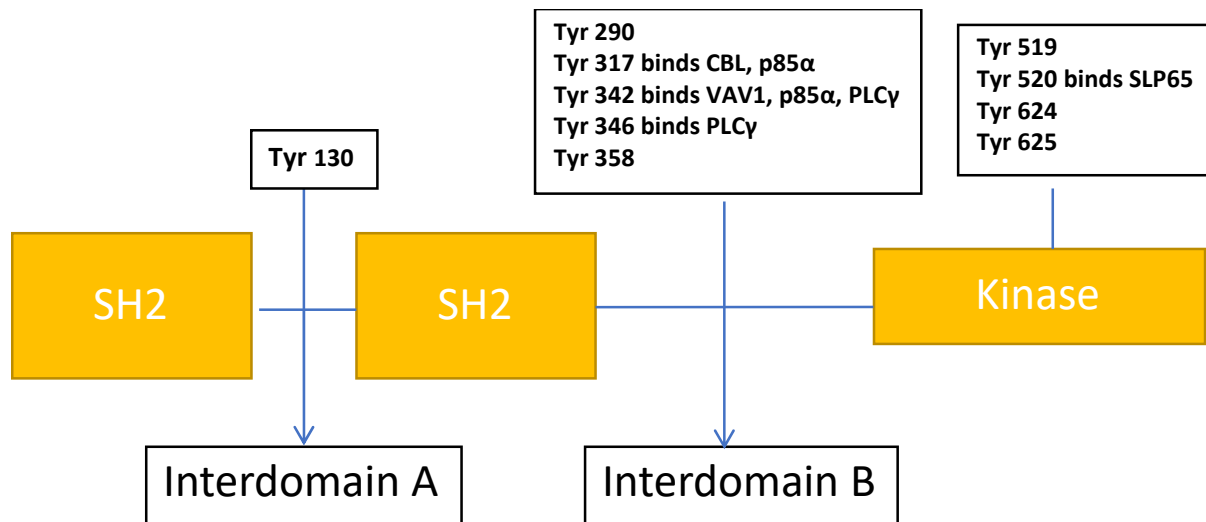


Figure 1.8 The domain structure of spleen tyrosine kinase (SYK) tyrosine residues shown to be sites of autophosphorylation.

1.5 B-CELL RECEPTOR ASSOCIATED INHIBITORS (BCRi)

In the last few years, many B cell receptor inhibitors affecting different kinases involved in B cell receptor signalling have been developed. The two main classes of BCR antagonists are as below:

1.5.1 BTK inhibitors

There are two main types of BTKi in development.

1.5.1.1 Covalent irreversible BTKi:

- Ibrutinib
- Acalabrutinib
- Zanubrutinib
- Tirabrutinib

1.5.1.2 Non-covalent reversible BTKi:

- Pirtobrutinib (LOXO-305)
- ARQ-531

1.5.2 PI3K inhibitors

PI3K inhibitors are differentiated by the ability to inhibit various isoforms of PI3K subunits.

- Idelalisib
- Duvelisib
- Umbralisib
- Copanlisib

In short, the BCR-i have revolutionised the treatment of CLL and multiple inhibitors are in clinical trials in variety of diseases. For the purpose of thesis, characteristics of ibrutinib are explained below:

1.5.3 Ibrutinib

Ibrutinib binds covalently to a cysteine residue (Cys-481) near the BTK active site and inhibits the enzymatic activity of purified BTK with a half maximal inhibitory concentration (IC₅₀) of 0.5 nM. Covalent binding to Cys-481 results in irreversible inhibition of BTK. Because ibrutinib binds irreversibly and covalently to BTK, the enzyme is permanently inhibited. There is only one site (Cys481) for drug binding, a one-to-one stoichiometric concentration of ibrutinib is needed. Hence, a concentration of the drug that occupies >95% of the BTK molecules in CLL lymphocytes is considered ideal. Such measurements are achieved using BTK occupancy assays and were performed in the context of early phase I and II studies. BTK occupancy was achieved 4 hours post-dose at a dose of 2.5 mg/kg/day of ibrutinib in the phase I study in relapsed/refractory B cell malignancies (230).

At a signalling level, ibrutinib binding inhibits activity of BTK, autophosphorylation of the enzyme, and abrogates activation of downstream survival pathways (PI3K, ERK, NF-κB), inducing modest apoptosis and inhibiting activation-induced proliferation of CLL cells *in vitro*. Other kinases that are potentially inhibited by ibrutinib include ITK, EGFR, BLK, HER2, HER4, BMX, and JAK3. All these kinases have a modifiable cysteine residue homologous to Cys-481 in BTK, and thus have the potential to be irreversibly modified by ibrutinib. The effective half-life of ibrutinib following oral dosing is only 1.5 to 3.3 hours (231, 232).

Ibrutinib inhibits human BCR activation (IC₅₀ <10 nM) in B cells but does not affect T cell receptor activation (233). Ibrutinib fully inhibits degranulation following stimulation at the high-affinity Immunoglobulin E (IgE) receptor (234). In monocytes and macrophages, ibrutinib inhibits the secretion of pro-inflammatory cytokines following stimulation at the Fc-gamma receptors (FcγR) by immune complexes (235). Consistent with the proposed

function of BTK in platelets, ibrutinib inhibits shear-force and collagen-induced platelet aggregation *in vitro* (IC50 = 10-100nM)(236).

1.5.3.1 Treatment related lymphocytosis

The blockade of the BCR signalling pathway by B cell receptor antagonists in CLL results in three major effects: 1) direct induction of apoptosis, 2) inhibition of cell homing and migration to chemokines and with subsequent adhesion to cellular substrates, and 3) inhibition of proliferation. Administration of these drugs to patients with CLL has been associated with mobilisation of tumour cells from the tissue to peripheral blood. This effect begins in some cases within hours of the first administration and typically reaches peak magnitude within the first 3 months of treatment. Coincident with the treatment-related lymphocytosis is a rapid and substantial decrease in lymph node and spleen size often observed with or without an improvement in haematological parameters and symptomatic improvement of disease-related symptoms (232). The drug blocks the interaction of CLL cells with tissue homing chemokines (CXCL12, CXCL13, CCL19), possibly through blockade of BCR-induced activation of lymphocyte cytosolic protein 1 (LCP1) (237) and restoration of the balance between expression levels of the homing receptors CCR7 and CXCR4 and the S1P receptor 1 (S1P1). While an efflux of tumour cells from the tissue compartments into the blood has been conclusively shown (238), mathematical models have estimated the fraction of the tissue CLL cells redistributed into the blood during ibrutinib therapy to be $23.3\% \pm 17\%$ of the total tissue disease burden, arguing that the reduction of tissue disease burden is due more to CLL cell death and less to egress from nodal compartments (239). While the lymphocytosis resolves within 8 months in most patients, it may last for over a year in some patients. Importantly, this persistent lymphocytosis does not represent disease progression or clonal evolution, and these patients do not have inferior PFS (240).

1.6 AIMS AND OBJECTIVES

Inhibitors of BCR signalling have shown great promise in the treatment of CLL, but the optimum dosing and combinations need refinement to achieve deeper remissions and may be different for certain groups of patients. The primary aim of this study is to analyse the impact of continuous inhibition of BCR signalling with the BTK inhibitor ibrutinib in the setting of a single-arm multi-centre feasibility study. The central hypothesis is that the

degree of residual BCR signalling in CLL cells will predict outcome. To test this, the following will be performed:

- Evaluate protocols for assessing kinase activation status to be used on real-time samples from patient blood and bone marrow samples
- Analyse the effect of ibrutinib on disease progression over a 12-month period using parameters such as blood cell count and measurements of secondary lymphoid organs
- Analyse the effect of ibrutinib on kinase activation status in CLL cells longitudinally in either the steady-state or following *ex vivo* activation
- Analyse and compare the effects between treatment-naïve and relapsed refractory cohorts

CHAPTER 2:

Methods and Materials

CONTENTS OF THE CHAPTER:

2.1 Protocol development

2.2 Assay Validation for Detection of Active B Cell kinases

2.3 IciCLLe trial- Methods

2.4 IciCLLe trial- Use of Phosflow

2.1 PROTOCOL DEVELOPMENT

2.1.1 Phosflow

2.1.1.1 Patient and control groups

All samples were taken from the patients with confirmed diagnosis of CLL according to the guidelines established by the National Cancer Institute-sponsored working group (NCI-WG). The samples were taken from patients who have not received treatment, received treatment more than 6 months ago or are undergoing treatment with B-cell receptor antagonist. The samples were anonymised, and no patient identifiable information was used. The samples were collected from the patients diagnosed with CLL attending the clinic at St James's University hospital, Leeds, UK. Control samples were taken for some experiments from healthy donors. Positive and negative control specimens were taken from GM12828 cell line (EBV transformed lymphoblastoid cell line) and HeLa cell line (epidermal cell line), respectively, for Western blot analysis. All research was performed in accordance with local ethical guidelines and the appropriate approval is in place.

2.1.1.2 Red cell lysis

Leucocytes were isolated by incubating whole blood with a 4-fold excess of ammonium chloride (8.6 g/l in distilled water) or BD Pharm lysis buffer for 10 min at 37°C to lyse red cells. Samples were centrifuged at 800 x g for 10 minutes and cells were washed twice in FACS Flow (BDIS) containing 0.3% bovine serum albumin (BSA). Alternatively, cells were washed in Phosphate Buffered Saline (PBS) or Hank's Balanced Salt Solution (HBSS).

2.1.1.3 Isolation of mononuclear cells (MNC) using Lymphoprep

Blood was collected in EDTA containing tubes. Blood was diluted by adding an equal amount of 0.9% sterile sodium chloride (NaCl) solution. The diluted blood was then layered over half the volume of lymphoprep in a centrifuge tube. The tube was then centrifuged at 800 x g for 20min at room temperature in a swing-out rotor. If the blood is stored for more than 2 hours, the centrifugation time was increased to 30min. Mononuclear cells form a distinct band at the sample medium interface. The cells were removed from the interface using a pasture pipette without removing the upper layer.

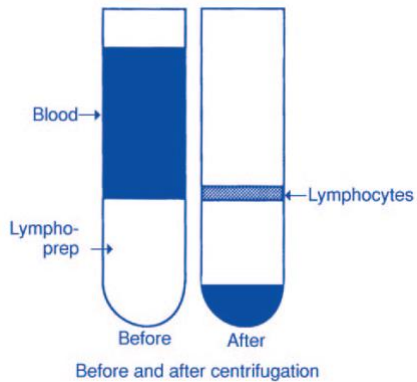


Figure 2.1 Mononuclear cell (MNC) separation using Lymphoprep

The harvested fraction was diluted with medium to reduce the density of the solution and the cells were pelleted by centrifugation for 10 min at 250 x g. Cells were counted using an automated cell counter (Sysmex KX-21N).

2.1.1.4 Phosflow experiments:

Following red cell lysis, 1×10^6 leukocytes were used per experiment. The cells were incubated with extracellular antibodies for 20 minutes. These included antibodies to CD3, CD19, CD5 and CD20 conjugated to various fluoro-chromes. Combinations of extracellular antibodies were used to distinguish the CLL cells and T cells. The cells were washed with PBS/HBSS twice. Ibrutinib was added next to the cells in following concentrations: 1-10 μM . The cells were then incubated at 37°C for 30 minutes followed by stimulation with F(ab')_2 anti-IgM (10 $\mu\text{g/ml}$) or anti-IgD (10 $\mu\text{g/ml}$) at 37°C. The cells were lysed by using BD Phosflow lysis buffer (1X) at different time points. The time points used were 0, 1, 2, 5 and 30 minutes in variety of conditions. The treated cells were well mixed by vortexing and then stored at 37°C for 10-12 minutes. The samples were centrifuged at 600 x g for 6 minutes and decanted. BD Perm wash buffer (1X) was added to each sample and incubated for another 10-12 minutes. The cells were then washed twice with 1ml of BD Perm wash buffer. The next step was to add intracellular phosflow antibodies at a concentration titrated in additional experiments. Antibodies to BTK pY551, SYK pY348, MAPK-p38 T180/Y182, ERK1/2 pT204/pY204, AKT pS473, AKT pT308, ZAP 70 pY319/SYK pY352 were used tagged to various fluoro-chromes (Purchased from BD Biosciences). The samples were then incubated for 60

minutes at room temperature in the dark. The cells were washed again with 3mls of BD Perm wash buffer once. Cells were re-suspended in 200 μ L of BD Permwash buffer and acquisition on a BD Fortessa flow cytometer was carried out using standard procedures. Phosphorylation of various kinases was assessed in each experiment and the results were assessed based on the changes in MFI using Diva software and FlowJo software.

2.1.2 Calcium flux

Whole blood was lysed by using ammonium chloride or BD pharm lysis buffer. Alternatively, the MNCs were collected after Lymphoprep separation. 5×10^5 leukocytes were required per sample. The cells were initially incubated with extracellular antibodies i.e., CD3 and CD19 for 20 minutes. 1×10^6 cells were suspended in 1ml of HBSS⁺⁺ (HBSS supplemented with 1mM of CaCl₂, 1mM of MgCl₂, 1% FCS). 50 μ g of Fluo-3 and Fura Red dyes (Calcium indicator dyes purchased from Invitrogen) were suspended in 50 μ l of DMSO. 3 μ L of Fluo-3 and 0.75 μ L of Fura Red were mixed by repeated pipetting and added to 1×10^6 leukocytes suspended in 1ml of HBSS⁺⁺. The cells were kept at 37°C in dark for 30 minutes. The cells were then centrifuged at 500 x g for 3 minutes, and medium was discarded. The sample was washed with 1ml of HBSS⁺⁺ and then re-suspended in 1ml of HBSS⁺⁺. This was split into 500 μ L for each condition. For drug experiments, the cells were kept with ibrutinib (1-10 μ M) at 37°C for 30 minutes. The sample acquired on flow cytometer (BD Fortessa) for 1-minute background followed by stimulation (e.g., anti IGD/IGM/IGG 10 μ g/ml) and acquisition for another 4 minutes. A control sample and ionomycin stimulated sample was run in parallel. The data was interpreted using the FloJo software.

2.1.3 Western blotting

2.1.3.1 Cell lysates

Samples were obtained after red blood cell lysis or Lymphoprep separation. 5×10^6 cells were taken for each time point. The cells were washed with PBS twice and a pellet was made by centrifuging the cells at 800 x g for 5 minutes. The cells were re-suspended in PBS and were divided into unstimulated and stimulated groups (anti-IgM/IgD 20 μ g/ml). Unstimulated cells were transferred to NP40 lysis buffer (1% Nonidet P-40, 50 mM Tris pH 7.4, 80 mM KCl, 10 mM EDTA) with freshly added protease inhibitors and kept on ice. The stimulated samples at each time point were transferred to NP40 lysis buffer and kept on ice. The samples were then spun in a centrifuge at 13,000rpm at 4°C for 10 minutes. The supernatant was then

transferred to a new tube. Sample buffer (4% SDS, 20% glycerol, 0.004% bromophenol blue, 0.125 M Tris HCl) with 2-Mercaptoethanol was added and lysates were then stored at -20°C. The lysates were boiled for 5 minutes before loading them on the gel.

2.1.3.2 SDS-PAGE and Western blotting

SDS-PAGE resolving and stacking gels were prepared using a Bio-Rad Protean II electrophoresis cell. Pre-stained molecular weight marker (Precision Plus, Bio-Rad) was included on each SDS-PAGE gel. The lysates were boiled for 5 minutes and approximately 3×10^5 cell equivalents of lysate were added to each well. Electric current was applied for 60 minutes at 50mA to separate the proteins according to molecular weight. Proteins were then transferred to nitrocellulose membrane using Western transfer buffer (25 mM Tris, 192 mM Glycine, 20% methanol) at 100V for 1hr at 4°C or overnight at 20V at 4°C. The membrane was then blocked with 1% BSA in Tris Buffered Saline containing 0.1% Tween (TBS-T) or 1% non-fat dry Milk/TBS-T for 1hour. The membrane was then incubated with primary antibody (dilution specified according to manufacturer) for 1hour at room temperature on a rocking platform. Membrane was then washed three times with TBS-T and then incubated with secondary antibody (dilution 1:20000) conjugated to horseradish peroxidase (all secondary antibodies purchased from Jackson Immunoresearch) on a rocking platform for 30 to 60 minutes at room temperature. The membrane was washed with TBS-T three times and then developed with a chemiluminescent substrate (SuperSignal West Pico ECL, Pierce). The membrane was then exposed to film to determine the presence of antibody binding.

2.2 ASSAY VALIDATION FOR DETECTION OF ACTIVE B CELL KINASES

2.2.1 Phosflow validation

Although CLL cells have down modulated surface immunoglobulin, the kinase pathways downstream of B-cell receptor remain intact and are required for persistence of the neoplastic clones. Furthermore, many of the signalling components have a restricted expression pattern, and thus targeting these pathways represent an attractive clinical strategy for treating CLL. The drug ibrutinib is an irreversible inhibitor of the B cell kinase BTK. To determine the effect of ibrutinib on the signalling and survival of CLL cells, patient samples were evaluated for changes in phosphorylation patterns in key regulatory

pathways. The samples were taken from patients with established diagnosis of chronic lymphocytic leukaemia. Samples were then assessed within the first 4 hours, 24 hours and 48 hours to assess the level of phosphorylation. PBS was used as a buffer to simulate in vivo conditions.

As a first means of evaluating phosphorylation levels, a flow cytometry-based assay was employed using antibodies that recognise specific phosphorylated residues. Lymphocytes were gated initially based on the Side scatter and Forward scatter characteristics. T and B lymphocytes were separated into quadrants based on CD3 and CD19 expression as represented in Figures 2.1 and 2.2. Phosphorylation of various kinases was established with no stimulus, IgM (10µg/ml) and IgD (10µg/ml) at various time points. Included in the analysis were antibodies used to detect:

- BTK pY551
- SYK pY348
- MAPK-p38 pT180/pY182
- AKT pS473
- AKT pT308
- ERK1/2 pT202/pY204

The phosphorylation was also assessed with the addition of BTK inhibitor ibrutinib prior to stimulation.

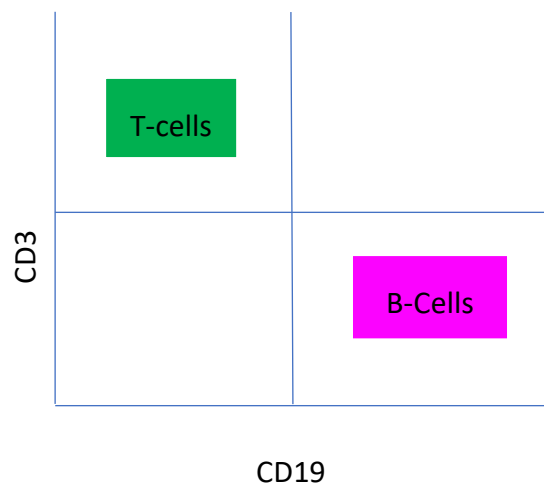


Figure 2.2 Diagrammatic representation of the quadrants for separation of T and B lymphocytes based on staining with antibodies to CD3 and CD19.

The following experiments show the various layouts in assessment of phosphorylation of intracellular kinases using BD FACS Diva software.

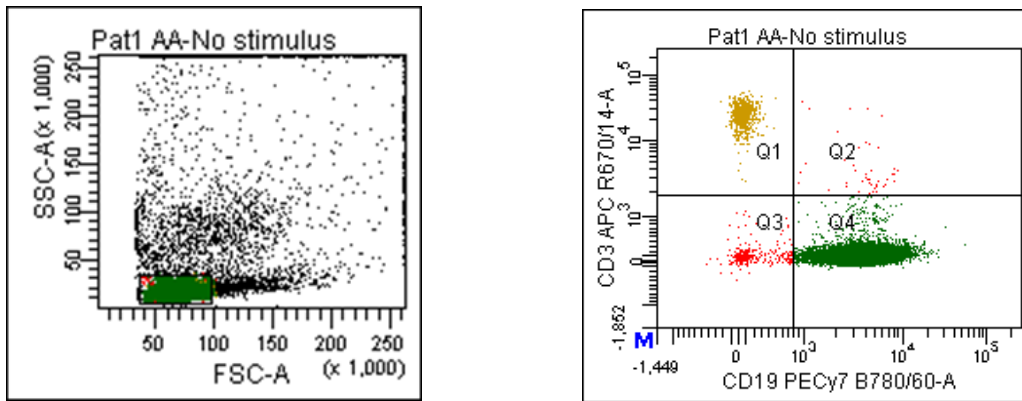


Figure 2.3 The gate(P1) is placed on lymphocytes based on forward and side scatter. P1 is then divided into quadrants based on CD19 (Q4; B-cells) and CD3 (Q1; T-cells) expression.

The phosphorylation on individual kinases was then established using the mean fluorescence intensity (MFI) and comparison at various time points. Figure 2.4 depicts the results from one CLL patient. In this example stimulation with anti-IgM resulted in an increase of BTK phosphorylation on Y551, the target of LYN kinase by two minutes with a shift from an MFI of 103 in the unstimulated state to 198. The response is maintained at 10 minutes, but with some loss of phosphorylation. One can also observe that the entire B cell population is shifted and thus all cells appear to be responding equally well to the stimulus.

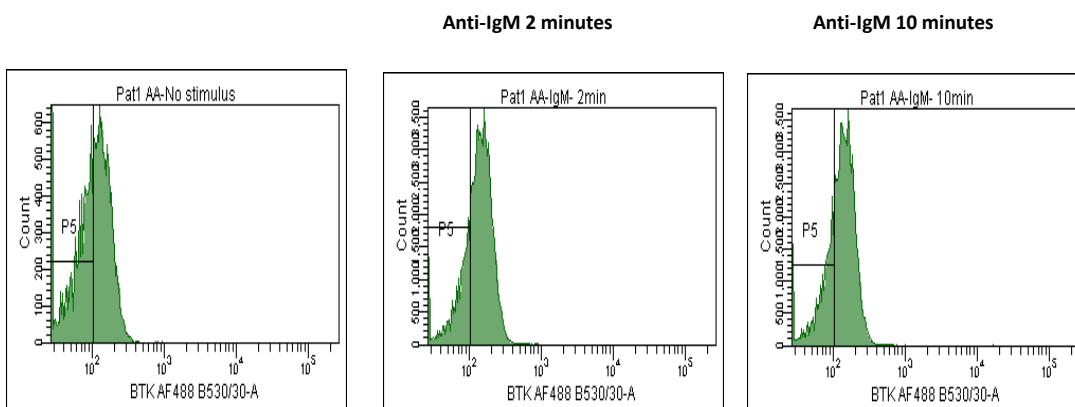


Figure 2.4 Histograms representing phosphorylation of Btk pY551 with no stimulus and anti-IgM at 2 and 10 minutes.

Figure 2.5 represents the results of increase in phosphorylation of SYK kinase on Y348 on stimulation with anti-IgM from the same sample. The effect has persisted at 2 and 10 minutes suggesting a sustained response to anti-IgM.

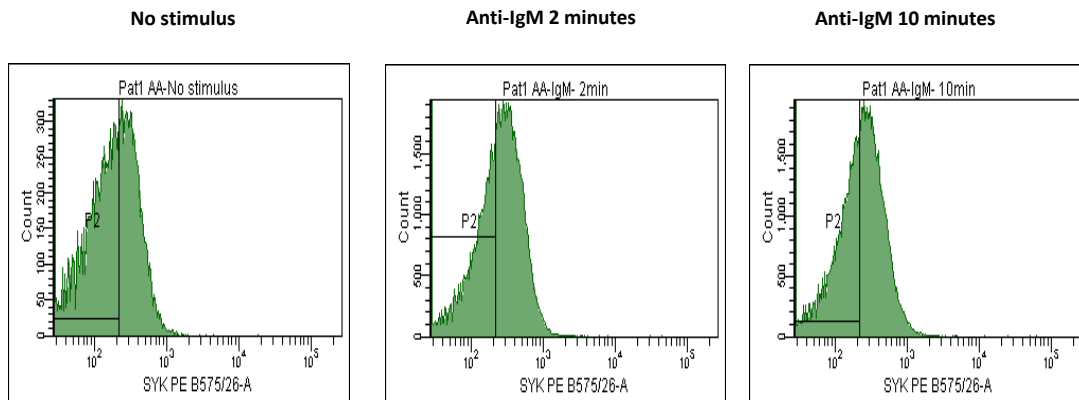


Figure 2.5 Histograms representing phosphorylation of Syk pY348 with no stimulus and anti-IgM at 2 and 10 minutes.

Figure 2.6 shows the level of phosphorylation of MAPK-p38 in response to anti-IgM. There is an increase in phosphorylation of MAPK-p38 at 2 and 10 minutes in response to anti-IgM suggesting a continued response to the stimulus.

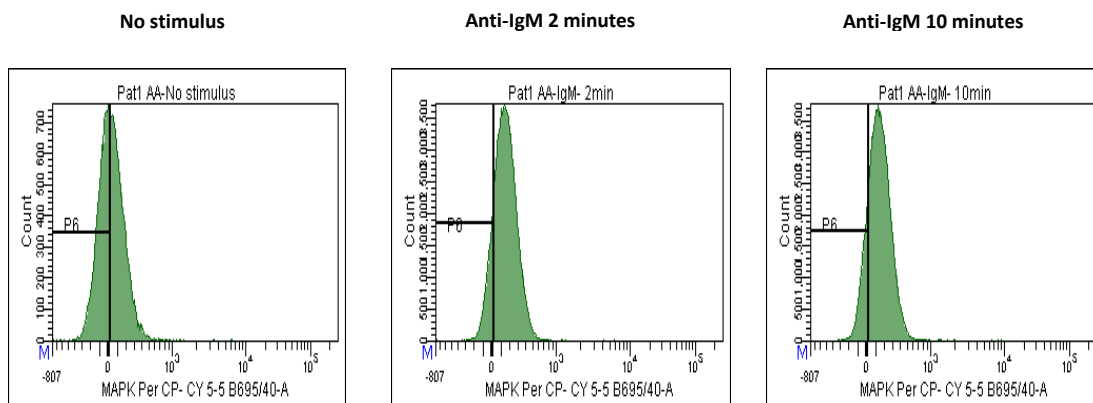


Figure 2.6 Histograms representing phosphorylation of MAPK-p38 pT180/Y182 with no stimulus and anti-IgM at 2 and 10 minutes.

Figure 2.7 shows the phosphorylation of AKT S473 in response to anti-IgM stimulation. There is slight increase in phosphorylation at 2 minutes and this effect is lost at 10 minutes.

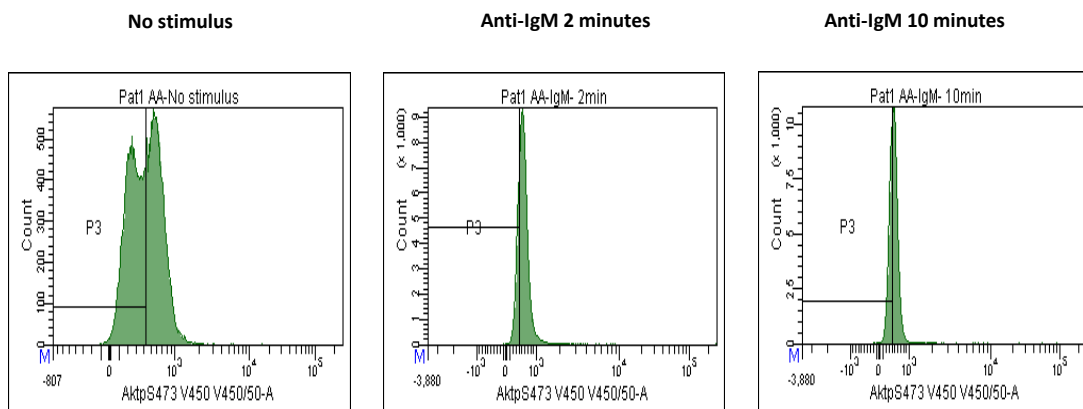


Figure 2.7 Histograms representing phosphorylation of AKT pS473 with no stimulus and anti-IgM at 2 and 10 minutes.

The phosphorylation can also be displayed by overlaying histograms to assess the pattern of stimulation, however FACS Diva software is unable to perform this function. Therefore, the analysis was repeated with FlowJo software which considers the number of events in each experiment and is able to overlay the histograms for various conditions. Moreover, the effect of stimulation with anti-IgM versus anti-IgD was also evaluated. An example for one of these experiments using FlowJo software is shown below in Figure 2.8.

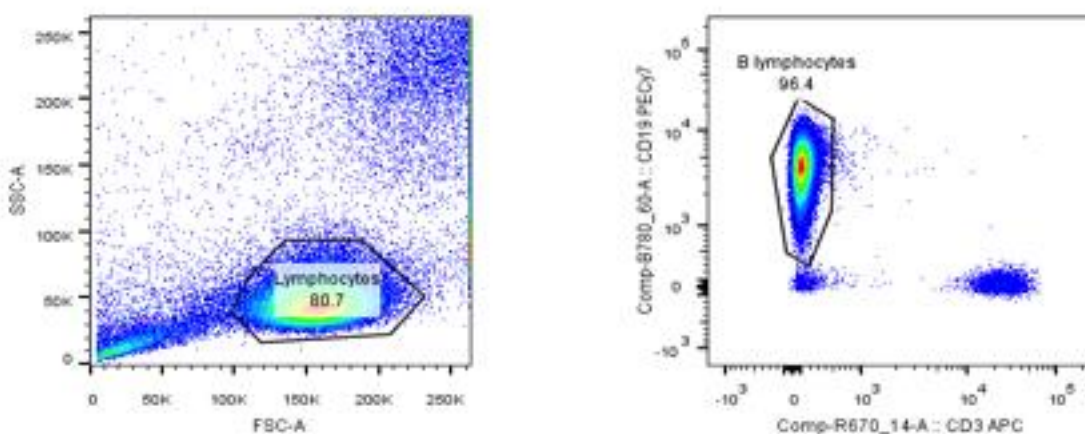


Figure 2.8 Lymphocytes are gated based on SSC and FSC. A gate is further applied on CD19+ve B lymphocytes.

Figure 2.9 illustrates the overlay of histograms representing the phosphorylation of SYK pY348 with no stimulus and anti-IgM stimulation at 1 minute. The MFI has increased from 166 to 219 in response to anti-IgM stimulation. In this example, the change due to IgD stimulation is greater, with an increase in MFI from 166 to 262.

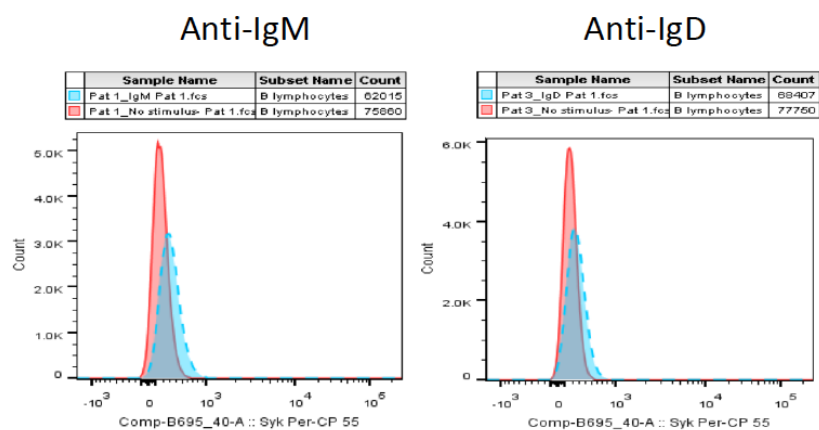


Figure 2.9 Phosphorylation of Syk with no stimulus, anti-IgM or anti-IgD represented by overlay of histograms. Red line represents phosphorylation with no stimulus and blue dotted line denotes phosphorylation with anti-IgM or anti-IgD.

Having established the staining conditions required to see a change in phosphorylation levels, the effect of ibrutinib was evaluated. Samples were pre-incubated for 1 hour with or without the drug at 37°C and then stimulated. The representative experiment in Figure 2.10 to 5.12 shows the phosphorylation of various kinases with no stimulus, incubation of sample with ibrutinib (1µM), addition of IgM and IgD with or without ibrutinib (1µM). The results show inhibition of phosphorylation of BTK, SYK and AKT on incubation of sample with ibrutinib. However, there was increased level of phosphorylation of MAPK-p38. There was phosphorylation of SYK, AKT 473 and MAPK-p38 with IgM/IgD stimulation which was abrogated with addition of ibrutinib.

Figure 2.10 shows the phosphorylation of BTK, AKT, SYK and MAPK-p38 at baseline with no stimulus and after incubation with ibrutinib (1µM) at 37°C for 60 minutes. There is reduction in phosphorylation of BTK, AKT and SYK with addition of ibrutinib but there is an increase in phosphorylation of MAPK-p38. MFI changes are shown in attached Table 2.1.

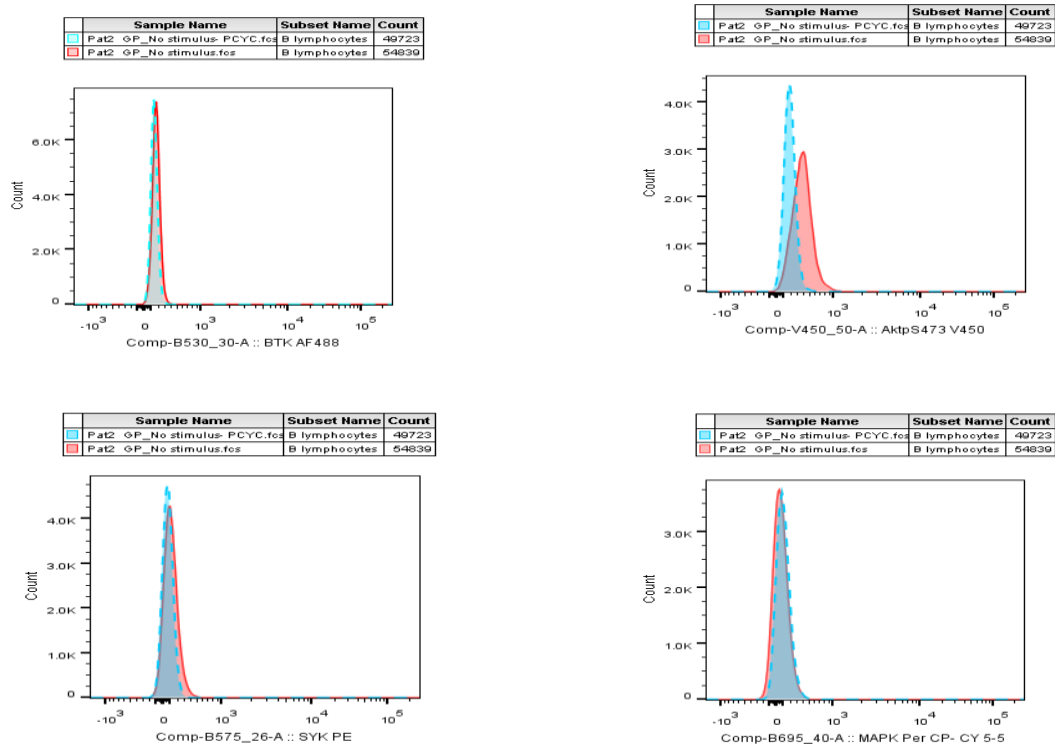


Figure 2.10 Phosphorylation of BTK, AKT, SYK and MAPK-p38 with no stimulus and after incubation with Ibrutinib. Red solid lines represent phosphorylation with no stimulus and dotted blue lines represent phosphorylation after incubation with Ibrutinib.

Table 2.1 Mean fluorescence intensity (MFI) of various kinases with no stimulus and incubation with Ibrutinib for 60 minutes.

Condition	BTK	AKT	SYK	MAPK
No stimulus	175	407	95	44
No stimulus+ Ibrutinib	141	193	53	86

Figure 2.11 below depicts the increase in phosphorylation of BTK, AKT, SYK and MAPK-p38 in response to IgM and IgD stimulation. The changes in MFI are shown in the attached table 2.2.

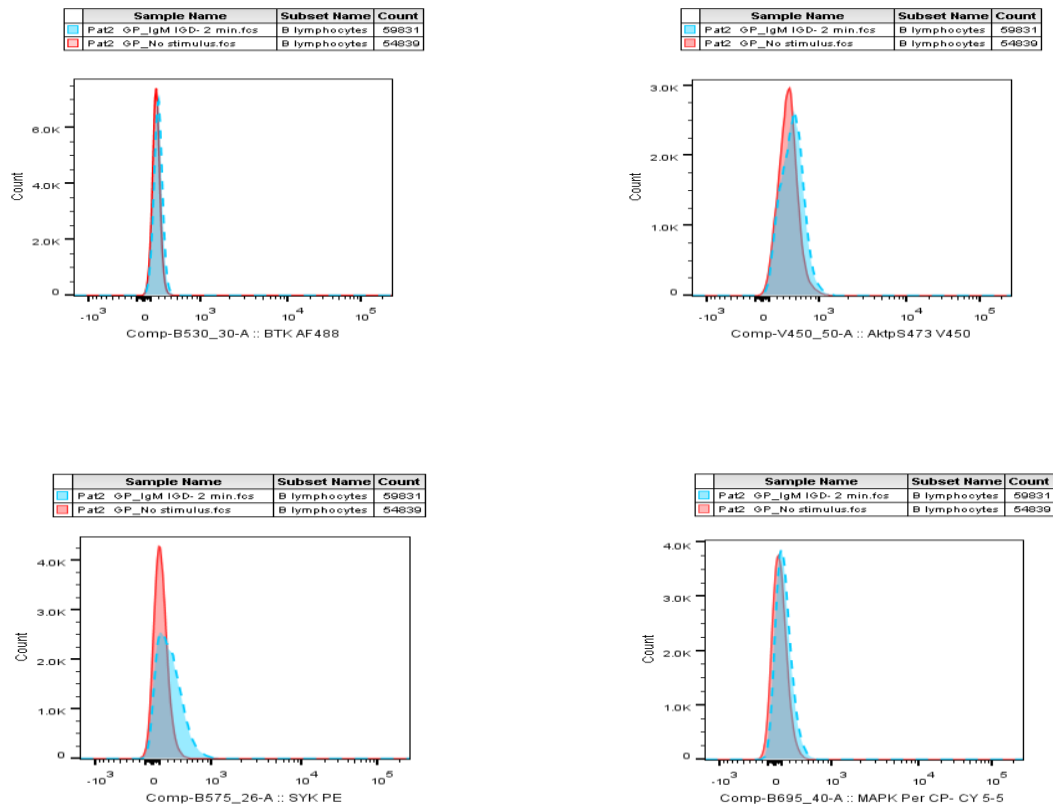


Figure 2.11 Phosphorylation of BTK, AKT, SYK and MAPK-p38 with no stimulus and stimulation with IgM (10 μ g/ml) and IgD (10 μ g/ml). Red solid lines represent phosphorylation with no stimulus and dotted blue lines represent phosphorylation after stimulation with IgM/IgD.

Table 2.2 Mean fluorescence intensity (MFI) of various kinases with no stimulus and stimulation with IgM (10 μ g/ml) and IgD (10 μ g/ml) for 2minutes.

Condition	BTK	AKT	SYK	MAPK
No stimulus	175	407	95	44
IgM and IgD- 2minutes	211	492	220	107

Following figure 2.12 shows the overlay of histograms of phosphorylation of BTK, AKT, SYK and MAPK-p38 with no stimulus and after the sample was incubated with ibrutinib (1 μ M) for 60 minutes and then stimulated with IgM and IgD. Ibrutinib abrogated the

phosphorylation of kinases induced by IgM and IgD except MAPK-p38. The MFI for kinases is shown in attached Table 2.3.

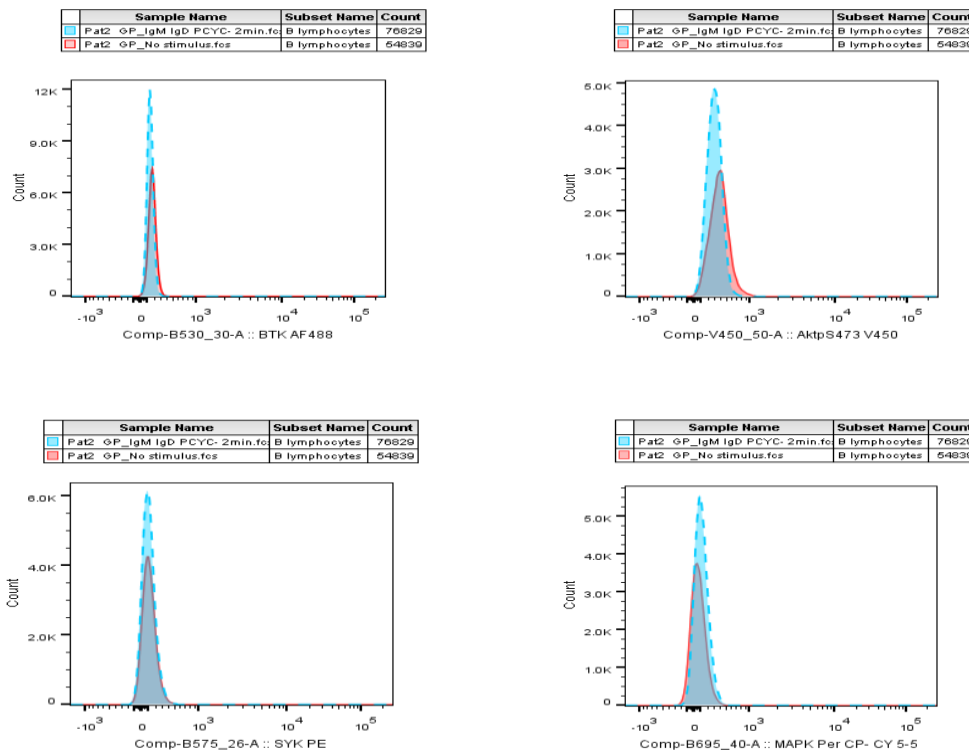


Figure 2.12 Phosphorylation of BTK, AKT, SYK and MAPK-p38 with no stimulus and stimulation of ibrutinib (1 μ M) treated cells with IgM (10 μ g/ml) and IgD (10 μ g/ml). Red solid lines represent phosphorylation with no stimulus and dotted blue lines represent phosphorylation after stimulation with IgM/IgD.

Table 2.3 Mean fluorescence intensity (MFI) of various kinases with no stimulus and stimulation of ibrutinib treated cells with IgM (10 μ g/ml) and IgD (10 μ g/ml) for 2 minutes.

Condition	Btk	Akt	Syk	MAPK
No stimulus	175	407	95	44
Ibrutinib + IgM and IgD- 2minutes	140	323	90	97

In conclusion, the Phosflow experiments were optimised for various combinations of intracellular phosphorylated proteins and extracellular antibodies. The experiments performed thus far focussed on the response of CLL cells, but additional surface markers can be employed to establish the phosphorylation in various subsets of B lymphocytes such as

CLL cells, normal B lymphocytes and memory B cells. This will allow a detailed dissection of the effect of therapeutic agents on the different B cell populations present in patients.

2.2.2 Calcium flux

In addition to the phosphorylation status of key signalling components, the release of intracellular Ca^{2+} represents an essential component of BCR-triggered events. Ca^{2+} flux provides a rapid measure of the extent of stimulation and can be readily monitored using Ca^{2+} binding dyes in a flow cytometric assay. To perform this analysis, lymphocytes were collected using lymphoprep and tagged with extracellular antibodies. Fluo-3 and Fura Red were added to the sample and stored at 37°C before acquisition. The sample was assessed for calcium flux before and after addition of stimulus. The ratio of Fluo-3 to Fura Red was assessed using FACS Diva software.

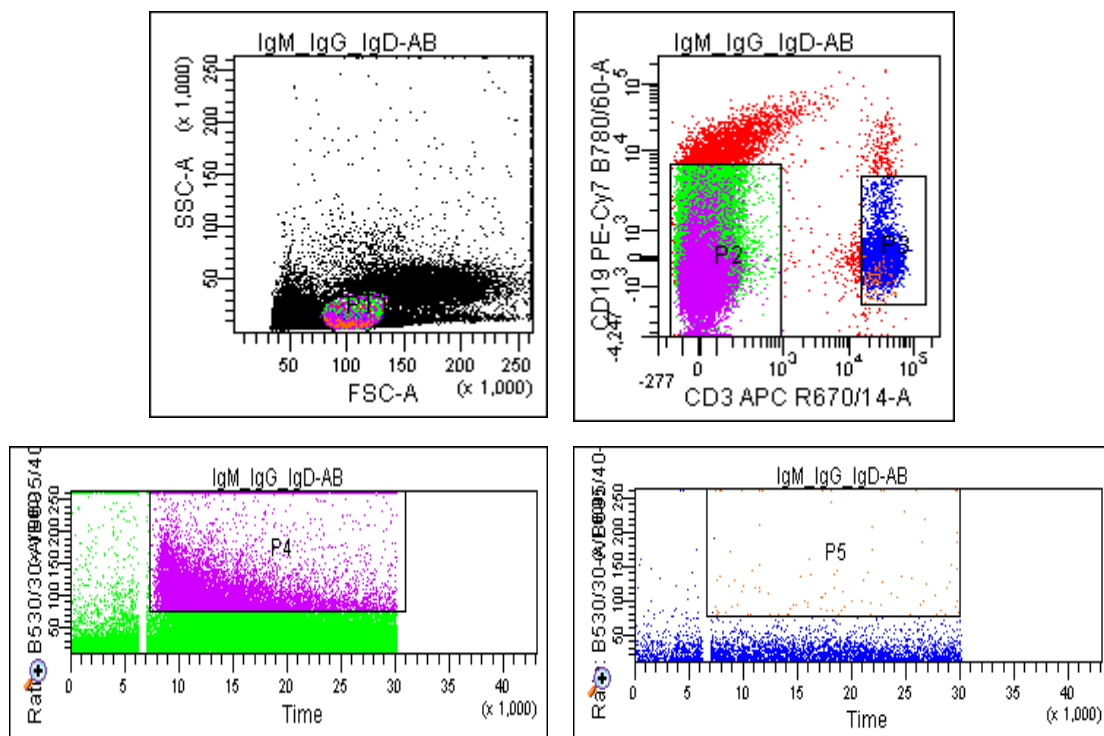


Figure 2.13 Lymphocytes were gated based on FSC and SSC marked as P1. P2 and P3 populations are B and T lymphocytes, respectively. P4 and P5 show calcium flux in B and T lymphocytes, respectively, after stimulus.

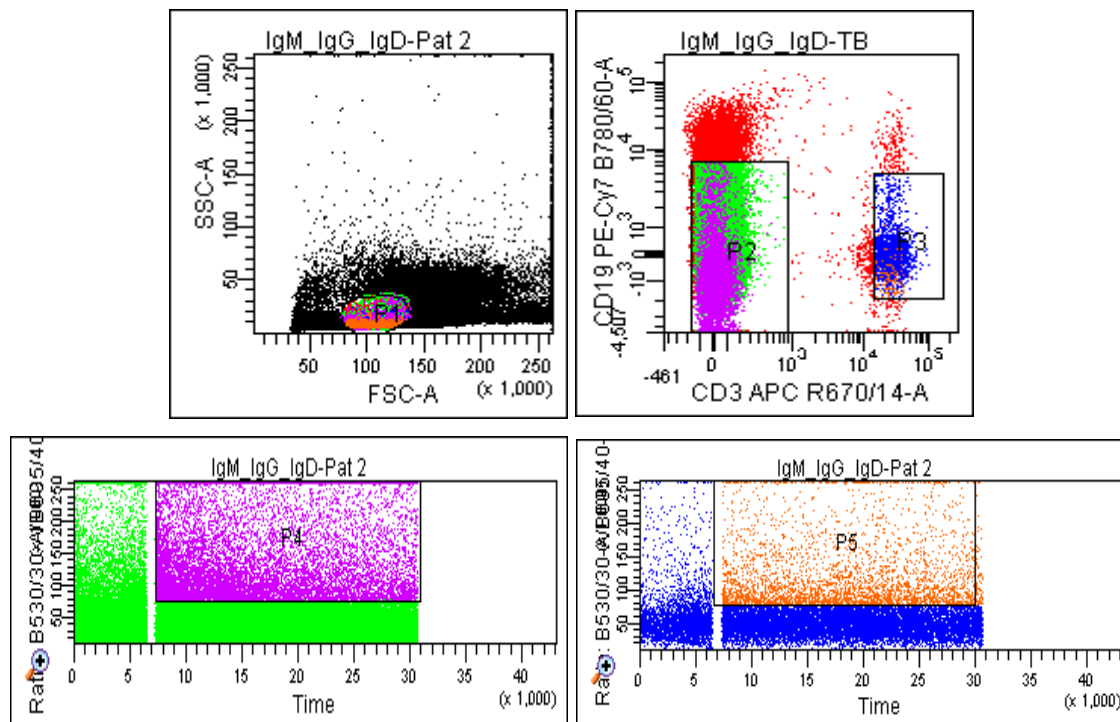


Figure 2.14 Lymphocytes were gated based on FSC and SSC marked as P1. P2 and P3 populations are B and T lymphocytes, respectively. P4 and P5 show calcium influx in B and T lymphocytes, respectively, after stimulus.

The experiments depicted in Figures 2.13 and 2.14 show the increase in calcium flux in B lymphocytes from two CLL patients on stimulation with a polyclonal antibody mixture against IgM/IgD/IgG. The T lymphocytes did not show any increase in flux, but the B cells did respond. There was an initial surge in cells showing flux followed by a plateau in response. The level of flux in the cells correlated with the IgM and IgD expression on the CLL cells. In subsequent experiments, the calcium flux has been assessed with individual stimulus such as IgM and IgD with similar responses. The responses can also be assessed after addition of B-cell receptor antagonists. The data in Figure 2.15 shows flux with ionomycin which is used as a positive control in these experiments.

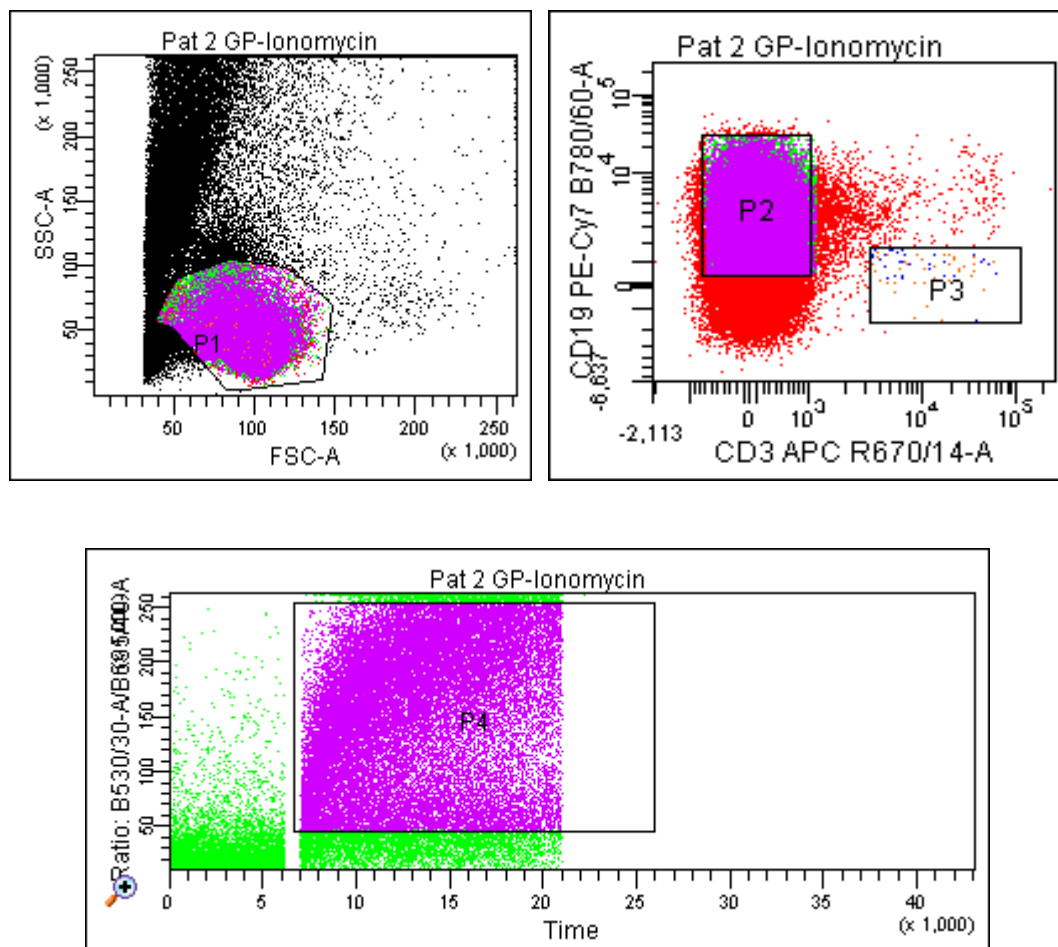


Figure 2.15 Calcium flux in B cells after addition of ionomycin.

2.2.3 Western blotting

While phosphorylation can be monitored with flow cytometry, the gold standard for assessment of changes in protein status is Western blotting. To corroborate the results obtained with phosflow, additional samples were evaluated for the presence of phosphorylated proteins using whole cell lysates run on SDS-PAGE, transferred to nitrocellulose and immunoblotted with specific antibodies. The lysates were made from fresh CLL cells and the GM12828 lymphoblastoid B cell line. 1%Milk/TBS-T was used as a blocking buffer for detection of phosphorylated kinases. 1%BSA/TBS-T was used as blocking buffer for actin detection. Figure 2.16 shows an example of an actin blot, confirming equivalent amounts of protein were present in each sample loaded. Figure 2.17 shows total phosphotyrosine containing proteins in CLL cells that had been stimulated with anti-IgM for the indicated times. In this experiment, there was a weak induction of phosphorylation of

some proteins in the molecular weight range of 70-80 kDa and strong induction of a phosphoprotein of approximately 25 kDa. This pattern was observed within 2 minutes of stimulation and persisted for the time course of the experiment. The level dropped at the 5 minutes time point, but this may have been due to loading. The identity of these proteins has not been ascertained.

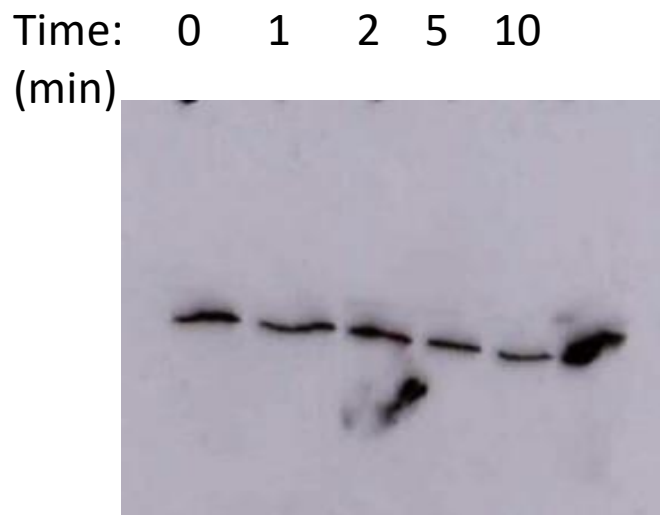


Figure 2.16 Actin detection in unstimulated and stimulated CLL sample at various time points.

Time: 0 2 5 10 (min)

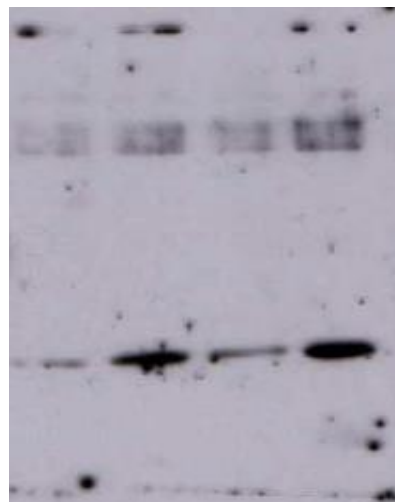


Figure 2.17 Phosphotyrosine detection in unstimulated and stimulated CLL sample at various time points.

Figure 2.18 shows an example of SYK phosphorylation in GM12828 cell line and primary CLL with anti-IgM at different time points. A weak protein band around the molecular weight of 70kDa is visible in GM12828 cell line and there appears to be strong induction of phosphorylation with anti-IgM at 1 minute. There does not appear to be any expression of phosphorylated SYK protein in this CLL sample

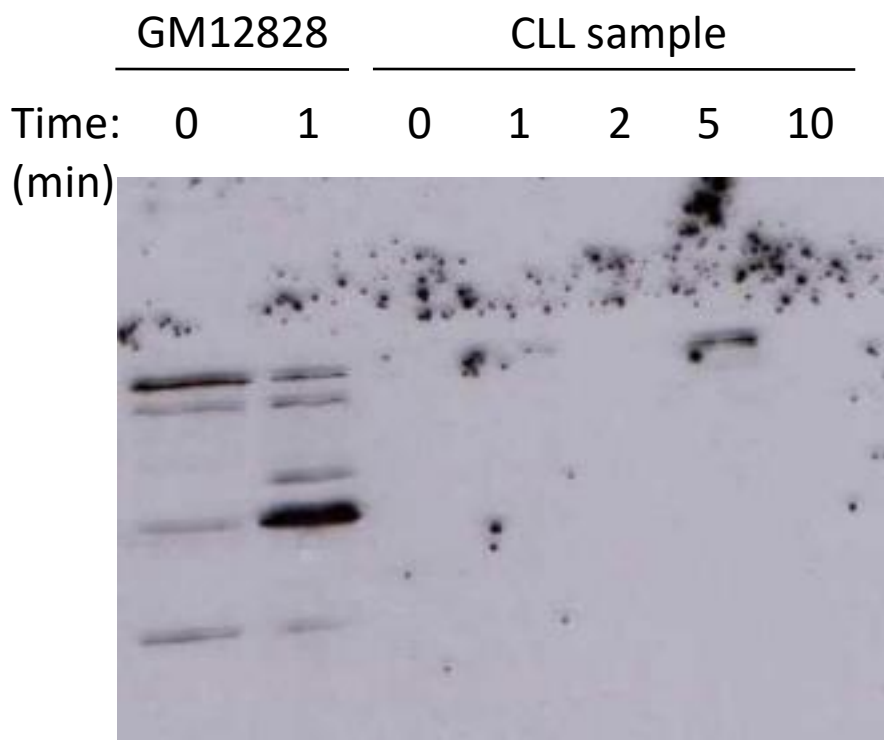


Figure 2.18 SYK phosphorylation in GM12828 cell line and primary CLL with anti-IgM.

Figure 2.19 shows the expression of total BTK in the GM12828 cell line and primary CLL cells. There is a strong expression of total BTK in GM12828 cell line with or without stimulus. The primary CLL cells do not show any expression of BTK. Another protein is detected around 25kDa in GM12828 cells.

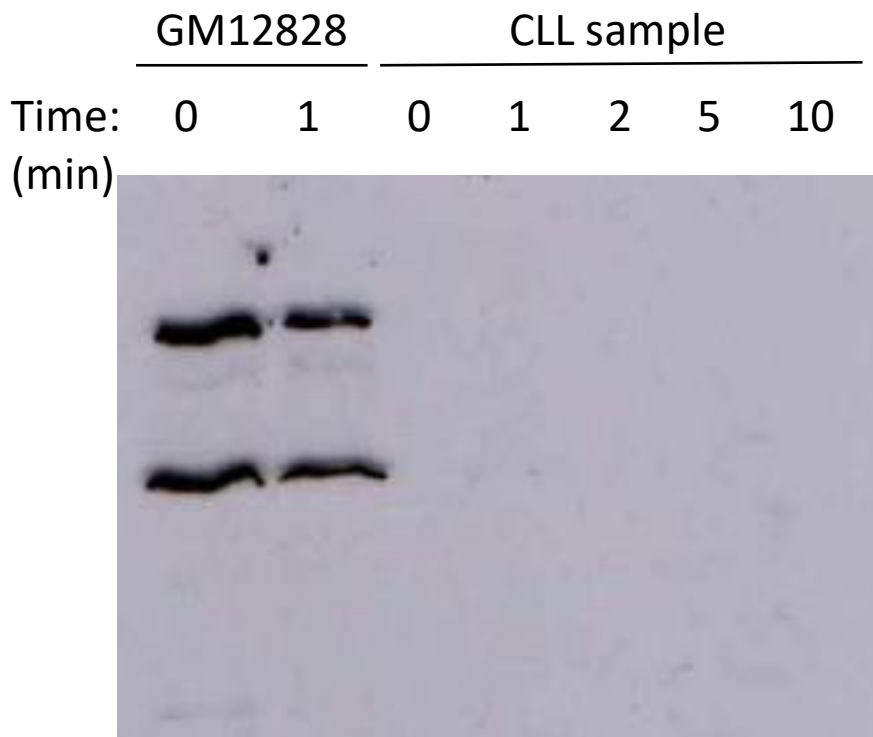


Figure 2.19 BTK phosphorylation in GM12828 cell line and primary CLL with anti-IgM.

To conclude, the detection of active intracellular kinases with Western blotting has been successful in lymphoblastoid B-cell line GM12828 but inconsistent in primary CLL cells. The results presented here suggest that the conditions (i.e., blocking buffers and antibody concentrations) used for detecting the various proteins of interest were appropriate and that the problem was more likely to reside in the preparation of the CLL samples. While the actin and total phosphotyrosine blots appeared to detect proteins as expected, subsequent evaluation of individual kinases was inconclusive.

2.3 IciCLLe TRIAL- METHODS

2.3.1 Trial design

The IciCLLe trial was designed as a single-arm, multi-centre feasibility study of ibrutinib in two cohorts: (A) TN CLL patients requiring therapy according to IWCLL criteria; and (B) RR CLL patients. All patients received continuous oral therapy with ibrutinib (420mg once daily (OD)) from registration until disease progression. Response to treatment was scrutinised at specified time-points in the trial. It recruited 40 patients from nine specialist haematology centres in the United Kingdom. The sample size was selected in order to adequately determine the trial's biological endpoints balanced with available laboratory resource for the required analysis.

An independent Data Monitoring Committee (DMC) was established to review the safety of the study on a six-monthly basis. The clinical trial was approved by all relevant institutional ethical committees and regulatory review bodies and was performed in accordance with local ethical guidelines. The study was undertaken in accordance with Good Clinical Practice and the Declaration of Helsinki. The trial was included on appropriate trial registers (ISRCTN12695354 and EudraCT Number 2012-003608-11).

2.3.1.1 Patients

40 patients were recruited to the study, and all gave written informed consent prior to entry; cohort A comprised 20 TN patients, cohort B 20 RR patients. The inclusion and exclusion criteria of the trial are mentioned below:

2.3.1.2 Inclusion Criteria

Cohort (A): Treatment naïve (20 patients)

- Progressive Stage A, Stage B or Stage C CLL
- CLL requiring therapy by the IWCLL criteria
- (ECOG performance status) of 0, 1, or 2
- Life expectancy of at least 6 months
- Age ≥ 18
- Prepared to undergo the stipulated investigations within the trial (including bone marrow examinations)
- Able to give informed consent

- Adequate hepatic function, defined as serum aspartate transaminase (AST) or alanine transaminase (ALT) $<2.5 \times \text{ULN}$, and total bilirubin $\leq 1.5 \times \text{ULN}$ unless due to Gilbert's syndrome
- Adequate renal function, defined as estimated creatinine clearance $\geq 30 \text{ ml/min}$ using the Cockcroft-Gault equation

Cohort (B): Relapsed/refractory (20 patients)

B-CLL requiring therapy according to the IWCLL guidelines

- The leukaemia cells should co-express CD19, CD5, and CD23 and each clone should have restricted to expression of either kappa or lambda immunoglobulin light chains.
- The levels of surface immunoglobulin, CD20, and CD79b should be low. If there is atypically strong surface immunoglobulin, CD20, or CD79b expression, or other atypical features, it may not be possible to perform the MRD monitoring required to evaluate the primary endpoint.

Refractory/relapsed CLL defined as any of the following:

- Failure to achieve a response (CR or PR by IWCLL Criteria) to a purine analogue alone or in combination with chemotherapy, or:
- Relapse within 6 months of responding to a purine analogue alone or in combination with chemotherapy, or:
- Relapse at any time after fludarabine, cyclophosphamide and rituximab (FCR) or bendamustine plus rituximab, or:
- Patients with CLL with deletion of chromosome 17p who have failed at least one previous therapy.
- ECOG PS of 0, 1, or 2
- Life expectancy of at least 6 months
- Prepared to undergo the stipulated investigations within the trial (including bone marrow examinations)
- Age ≥ 18
- Able to give informed consent
- Ability to comply with study protocol procedures

- Adequate hepatic function, defined as serum aspartate transaminase (AST) or alanine transaminase (ALT) $<2.5 \times \text{ULN}$, and total bilirubin $\leq 1.5 \times \text{ULN}$ unless due to Gilbert's syndrome
- Adequate renal function, defined as estimated creatinine clearance $\geq 30 \text{ mL/min}$ using the Cockcroft-Gault equation
- Minimum platelet count of $\geq 50 \times 10^9/\text{L}$ and ANC $\geq 1.0 \times 10^9/\text{L}$

2.3.1.3 Exclusion Criteria

All patients

- Unwilling to undergo the protocol assessments including the bone marrow examinations
- Active infection (at the time of registration), history of chronic or recurrent infection
- Other severe, concurrent (particularly cardiac or pulmonary) diseases or mental disorders that could interfere with their ability to participate in the study
- Use of prior investigational agents within 6 weeks
- Pregnancy or lactation
- Unwilling to use appropriate contraception during and for 18 months following treatment
- Central nervous system (CNS) involvement with CLL
- Mantle cell lymphoma
- Known HIV positive
- Patients with active Hepatitis B disease
- Active secondary malignancy excluding basal cell carcinoma
- Currently active, clinically significant hepatic impairment Child-Pugh class B or C according to the Child Pugh classification
- Persisting severe pancytopenia (neutrophils $<1.0 \times 10^9/\text{L}$) or transfusion dependent anaemia unless due to direct marrow infiltration by CLL (to be confirmed via bone marrow biopsy)
- Active haemolysis (not controlled with Prednisolone at 20 mg or less)
- Patients requiring or who have received anticoagulation treatment with warfarin or vitamin K antagonists within one week of the first dose of ibrutinib
- Patients requiring concomitant use of strong CYP3A4/5 inhibitors
- Patients with evidence or history of transformation and/or PLL

- Major surgery within 4 weeks prior to registration
- Currently active, clinically significant cardiovascular disease, such as uncontrolled arrhythmia or Class 3 or 4 congestive heart failure or a history of myocardial infarction, unstable angina, or acute coronary syndrome within 6 months prior to registration
- History of stroke or intracranial haemorrhage within 6 months prior to registration
- History of severe allergic or anaphylactic reactions to humanised or murine monoclonal antibodies. Known sensitivity or allergy to murine products.
- Vaccination with a live vaccine a minimum of 28 days prior to registration.
- Patients with Progressive Multifocal Leukoencephalopathy (PML).
- No known allergy to obinutuzumab or excipients

CONSORT 2010 Flow Diagram

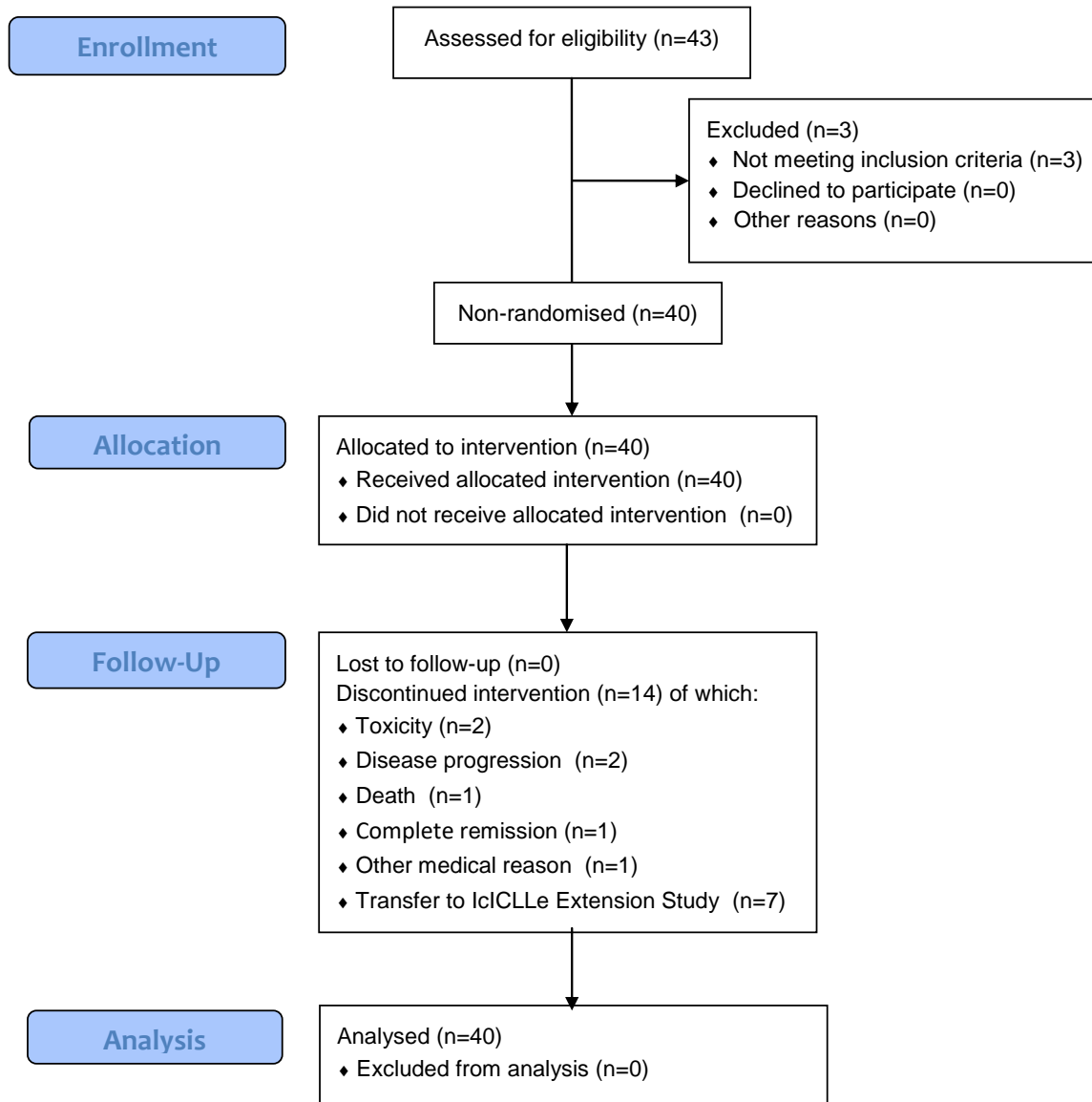


Figure 2.20 CONSORT Diagram of IciCLLe trial

2.3.2 Assessments

Response to treatment was assessed according to the as per updated 2008 IWCLL guidelines(66). MRD was assessed by highly sensitive multiparameter flow cytometry with a level of detection below 1 CLL cell in 10000 leukocytes (135). Peripheral blood (PB) and bone marrow (BM) were taken at screening, and 1 & 6 months with additional PB at 0h (baseline), 4h, 24h, 7 & 14 days, and 2, 9, & 12 months. Levels of phosphorylated BTK pY551/SYK pY348/AKT S473/ERK1/2 were analysed *in vitro* via phosflow at these time-points. Clinical assessments were performed at the protocol-specified time-points above and 6-monthly thereafter. Adverse Events (AEs) were assessed from day 1 of treatment and at follow-up visits according to the NCI Common Terminology Criteria for Adverse Events (version 4). All AEs and Serious Adverse Events (SAEs) were recorded until 30 days after end of therapy.

2.3.3 Outcomes

The objective of ICIcLLe was to investigate the mechanism of action of ibrutinib and the biological response to ibrutinib. The primary outcome was the proportion of patients achieving MRD-negative remission by IWCLL criteria (depletion of CLL below 0.01% in the PB and BM) within 6 months of trial treatment. The clinical secondary outcomes included overall response rate (ORR), PFS at 1- and 2-years, OS at 1- and 5-years, and safety of ibrutinib. The biological secondary endpoints included CLL cell levels in PB and BM, proliferation index (Ki67) of CLL cells in PB and BM, and changes in expression of protocol specified CLL cell surface markers during treatment.

2.3.4 Statistical methods

Outcomes are analysed by descriptive statistics only. Analysis was conducted using R v3.3.1 with the dplyr, survival, and SPSS packages (241-244). Confidence intervals for binary variables are calculated using Wilson's method. Data were frozen in May 2021 after being validated using pre-specified checks. No missing values have been imputed.

2.4 PHOSFLOW IN ICIcLLe TRIAL

A panel of markers was assessed on peripheral blood (PB) and bone marrow (BM) taken at screening, 1 & 6m. PB was also taken at baseline, 4 & 24h, 7 & 14d, & 2, 9 & 12m.

Phosphorylation of SYK pY348, BTK pY551, ERK1/2, AKT S473 was assessed in 4 conditions:

unstimulated +/- ibrutinib and stimulated with IgM/ IgD +/- ibrutinib at each time point. 1×10^6 leukocytes were tagged to extracellular antibodies (CD3/CD19) conjugated to fluorochromes. Ibrutinib (1uM) was added to the cells (30min, 37°C followed by anti-IgM/IgD stimulation (10ug/ml)). The BD phosflow protocol was followed to lyse/fix/permeate the CLL cells. Antibodies to BTK pY551, SYK pY348, ERK1/2 pT204/pY204, AKT pS473 were used tagged to fluorochromes (from BD Biosciences). Cells were acquired on a BD Fortessa flow cytometer.

Table 2.4 Antibodies used in IciCLLe trial

Antigen	Conjugate	Clone/Animal	Volume	Manufacturer
CD3	APC	HIT3a	5µl	BD Bioscience
CD19	PE-Cy7	SJ25C1	1µl	BD Bioscience
BTK (pY551)	AF488	24a/BTK (Y551)	5 µl	BD Bioscience
AKT (pS473)	V450	M89-61	2.5 µl	BD Bioscience
SYK (pY348)	PE	J1-223.371	5 µl	BD Bioscience
ERK1/2	PE-Cy7	20A	5 µl	BD Bioscience

Table 2.5 Reagents used

Ammonium Chloride	Sigma-Aldrich	8.6g/l in distilled water
FACS flow	BD Biosciences	
Bovine Serum Albumin	Sigma Aldrich	0.3% in FACSflow
Phosphate buffered solution 1X	Gibco	1.0588236mM Potassium Phosphate monobasic (KH ₂ PO ₄) 155.17241mM Sodium Chloride (NaCl)

		2.966418 Sodium Phosphate dibasic (Na ₂ HPO ₄ -7H ₂ O)
Goat F(ab') ₂ anti-IgM	Stratech	
Goat F(ab') anti-human-IgD	Cambridge Biosciences	Dialysis into 0.01sodium phosphate, 0.25M NaCL, pH 7.6
Lyse/Fix Buffer 5X	BD Biosciences	Aqueous buffered solution containing formaldehyde and proprietary ingredients
Perm Buffer IV 10×	BD Biosciences	
BD Pharm lysis buffer 10X	BD Biosciences	Ammonium chloride based lysing reagent

CHAPTER 3: Clinical Results of IcICLE trial; TN VS RR Patients

3.1 INTRODUCTION

Ibrutinib shows great promise in improving outcomes in patients with CLL and is now approved by the FDA and the EMA for treatment of relapsed or refractory (RR) and treatment-naïve (TN) CLL patients based on compelling data from Resonate-1 and Resonate-2 trials (118, 245). Resonate-1 trial was a phase 3 randomised controlled trial that randomised RR CLL patients to either receive ibrutinib in experimental arm or Ofatumumab as standard therapy. Patients relapsing in Ofatumumab arm were allowed to cross-over to receive ibrutinib. The six-year follow-up of the trial confirmed improved progression-free survival (PFS) in favour of ibrutinib. Similarly, Resonate-2 was a phase 3 randomised control trial comparing Ibrutinib to Chlorambucil monotherapy and prolonged follow-up confirmed PFS and overall- survival (OS) advantage in favour of ibrutinib. However, ibrutinib treatment must be continued long-term in order to improve or maintain clinical responses. The best combination therapy with ibrutinib is still unknown, warranting mechanistic studies in order to understand the biological changes in the CLL cell with BCR antagonists. Carefully designed studies based on better understanding of the biology of the disease will inform future studies and improve outcomes in CLL patients. It was easier to answer these questions in small investigator-initiated trial and ICI-CLL trial was an attempt to answer these questions in a phase-2 design for both TN and RR CLL patients.

This Chapter focusses on the trial design, clinical features and clinical responses in all CLL patients treated on the trial with ibrutinib. The ICI-CLL trial was a single-arm, multi-centre feasibility study of ibrutinib (BTK inhibitor) in two cohorts: (A) Treatment naïve (TN) CLL patients requiring therapy according to IWCLL criteria; and (B) relapsed refractory (RR) CLL patients. It investigated the dynamics of disease response in all patients requiring treatment with continuous ibrutinib monotherapy. We hypothesized that ibrutinib would be an effective treatment for TN and RR CLL. We expected that continuous ibrutinib therapy will result in improved haematological, clinical and radiological response in both cohorts of the trial. The responses were assessed at various time points with frequent blood test monitoring, bone marrow testing and CT scans. It was hypothesized that patients confirmed to achieve minimal residual disease (MRD) negative remission will not receive further ibrutinib therapy.

3.2 TRIAL DESIGN

3.2.1 Patients

40 patients were recruited to the study, and all gave written informed consent prior to entry; cohort A comprised 20 TN patients, cohort B 20 RR patients. Eligible patients were ≥ 18 years, had progressive CLL requiring treatment as per IWCLL criteria (66, 246), an ECOG performance status (247, 248) of 0 to 2, and life expectancy ≥ 6 months. Patients with persisting severe pancytopenia due to bone marrow infiltration could enter the trial even with low platelet counts. Patients previously treated with a B-cell receptor inhibitor (BCRi) were excluded from the trial.

3.2.2 Assessments

3.2.2.1 Efficacy assessments

Response to treatment was assessed according to the updated 2008 IWCLL guidelines (66, 246). MRD was assessed by highly sensitive multiparameter flow cytometry with a level of detection below 1 CLL cell in 10000 leukocytes. Peripheral blood (PB) and bone marrow (BM) were taken at screening, 1 and 6 months, with additional peripheral blood at 0h (baseline), 4h, 24h, 7 and 14 days, and 2, 9, and 12 months(134). Levels of phosphorylated BTK pY551, SYK pY348, AKT pS473, and ERK1/2 pT204/pY204 were analysed *ex vivo* via phosflow at these time-points. Clinical assessments were performed at the protocol-specified time-points above and 6-monthly thereafter. Overall Survival (OS) and Progression-free survival (PFS) were estimated using the Kaplan-Meier method.

3.2.2.2 Outcomes

The objective of IclCLLe was to investigate the mechanism of action of ibrutinib and the biological response to ibrutinib. The primary outcome was the proportion of patients achieving MRD-negative remission by IWCLL criteria (depletion of CLL below 0.01% in the PB and BM) within 6 months of trial treatment. The clinical secondary outcomes included overall response rate (ORR), PFS at 1- and 2-years, OS at 1- and 5-years, and safety of ibrutinib. The biological secondary endpoints included CLL cell levels in PB and BM, proliferation index (Ki67) of CLL cells in PB and BM, and changes in expression of protocol specified CLL cell surface markers including CD20, CD23, CD200 and CXCR4 during treatment.

The primary outcome measures in the initial protocol (v1.0 to v4.0) were biological in nature, seeking to assess the impact of ibrutinib on CLL cells in PB and BM. From protocol v5.0, an extension study combining ibrutinib with the anti-CD20 monoclonal antibody obinutuzumab was added to the relapsed refractory cohort and the primary outcome was changed to rate of MRD-negative remission to provide a common, objective, and standardised outcome for the two trial stages as well as determining how this response differs in the TN and RR cohort of the trial.

3.2.3 Results

3.2.3.1 Clinical features

Baseline clinical features of two cohorts of patients are presented below in the following Table 3.1. The average age in TN group was 59 years whereas it was 62.5 years for RR cohort. The median age for all patients was 61.5 years; Median white cell count and lymphocytes were higher in the TN group. Median bone marrow infiltration and sum of diameter of product of lymph nodes (SDP) were higher in the TN group. However, median spleen size was 16 cm in RR cohort as compared to 14 cm in TN cohort. Most participants had Binet stage B or C and unmutated IGHV status in both cohorts. A variety of cytogenetic aberrations were prevalent in both cohorts.

Table 3.1 Baseline characteristics of TN and RR cohort of IcliLLe trial

<i>Parameters</i>	<i>Treatment naive</i>	<i>Relapsed refractory</i>	<i>All patients</i>
Median Age (range)	59 (42.3-71.2)	62.5 (50.6-82.8)	61.5 (42.3-82.8)
Median haemoglobin in g/dl (range)	10.5 (8.5-14.6)	12.1 (8.7-15.3)	10.9 (8.5-15.3)
Median Platelet in 10⁹/L (range)	125 (33-637)	127 (18-283)	126 (18-637)
Median WBC in 10⁹/L (range)	87.1 (9.1-738.2)	47.2 (3.2-222.2)	63.1 (3.2-738.2)
Median Neutrophil baseline in 10⁹/L (range)	4.1 (0.1-28.2)	4.3 (0.4-14.9)	4.2 (0.1-28.2)
Median lymphocytes in 10⁹/L (range)	82.75 (4-738.2)	32.3 (1.6-219.3)	55 (1.6-738.2)

β2 microglobulin	4.3 (1.8-9.3)	4.4 (2.2-9.1)	4.4 (1.8-9.3)
Median percentage Bone marrow infiltration (range)	90 (65-97)	84.5 (10.9-96)	88 (10.9-97)
Median SDP in cms (range)	43.5 (17.9-66.87)	30.68 (0-115.9)	35.1 (0-115.9)
Median spleen size in cms (range)	14 (10-23)	16.6 (11.1-27)	14 (10-27)
Binet staging n (%)			
stage A progressive	0 (0%)	1 (5%)	1 (2.6%)
Stage B	8 (42.1%)	9 (45%)	17 (43.6%)
Stage C	11 (57.9%)	10 (50%)	21 (53.8%)
unknown	1 (5%)		1 (2.5%)
17del	4 (20%)	2 (10%)	6 (15%)
ATM	4 (20%)	3 (15%)	7 (17.5%)
trisomy 12 not tested	1 (5.3%)	2 (10%)	3 (7.7%) 1
13q not tested	2 (10.5%)	8 (40%)	10 (25.6%) 1 (2.5%)
IgHV			
Mutated	6 (33.3%)	2 (10.5%)	8 (21.6%)
Unmutated	12 (66.7%)	17 (89.5%)	29 (78.4%)
not tested			3 (7.5%)

3.2.3.2 Assessment of baseline characteristics in TN and RR cohorts

Statistical significance of the difference in median of baseline parameters was compared between two groups using nonparametric independent sample test (Figure 3.1). The median of both groups was similar for all parameters except for bone marrow infiltration, which has shown that baseline infiltration is more in TN cohort compared to RR cohort. To conclude, there were no major differences in clinical features for both cohorts except for the level of bone marrow infiltration which was statistically significant in the TN cohort.

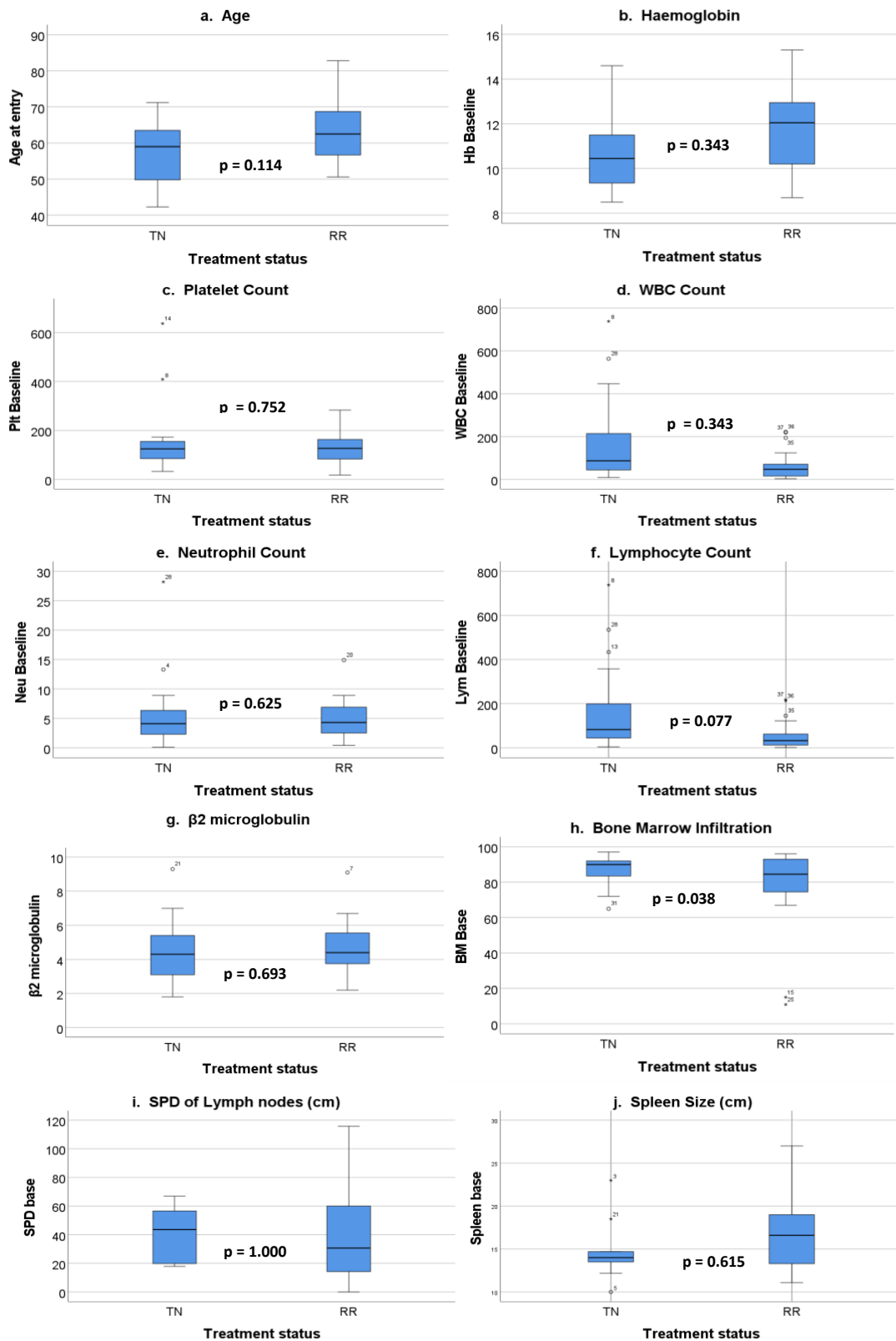


Figure 3.1 Baseline characteristics of treatment naïve (TN) and relapsed refractory (RR) cohorts: a) Age b) Haemoglobin c) Platelet count d) WBC count e) Neutrophil count f) Lymphocyte count g) $\beta 2$ microglobulin h) Bone marrow infiltration i) SPD of lymph nodes in cm j) Spleen size in cm. Median (central line), range (top and bottom bar) and interquartile range (top and bottom end of box) of various baseline clinical parameters separated into treatment naïve and relapsed refractory group are shown in the plots.

3.2.3.3 Assessment of baseline staging and biological characteristics in TN and RR cohorts

Baseline characteristics based on the clinical staging, cytogenetics and IGHV status were assessed across the two cohorts. Figure 3.2 shows the features across the two cohorts of the trial. Fisher Exact test was used to compare categorical variables. There was no statistically significant difference between the TN and RR groups.

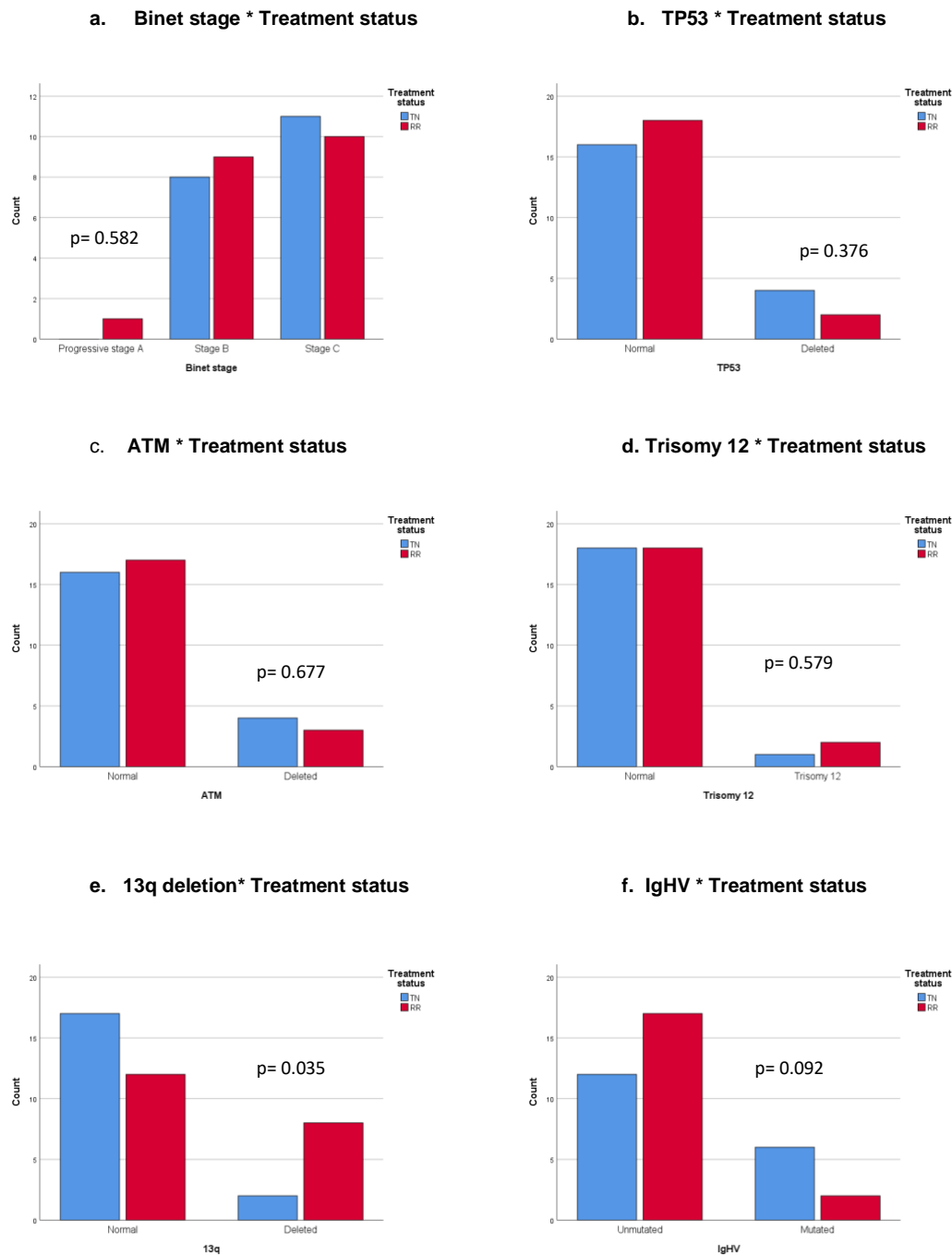


Figure 3.2 Baseline clinical staging, cytogenetics and IGHV status of TN and RR cohorts: a) Binet stage b) TP53 c) ATM d) Trisomy 12 e) 13 deletion f) IGHV mutation.

There was an expectation that there will be more patients with cytogenetically adverse disease in the RR group. However, there was no stratification adopted for the study and the small number of patients in both cohorts may explain the lack of difference between the two groups. To conclude, the baseline staging, cytogenetic features and IGHV mutation status were consistent across the two groups.

3.2.3.4 Clinical responses at various time points in all patients

Response to the treatment with ibrutinib for various clinical parameters were compared at multiple time points. For peripheral blood parameters, the time points compared were day 0, day 1, day 2, week 1, week 2, month 1, month 2, month 6, month 9 and month 12. Baseline, month 1 and month 6 were the time points analysed for bone marrow and radiological parameters. These time points were chosen to obtain in-depth analysis of the responses to ibrutinib. Statistical significance for the difference between various time points for the whole group were calculated using ANOVA with repeated measures (Figure 3.3).

a. Haemoglobin

The baseline haemoglobin (Hb) mean level was 11 g/L, which was maintained until 2 months post-treatment, at which time the levels began to increase (Figure 3.3a). Hb levels rose to 13 g/L by month 9 post-treatment and then stabilised out to 12 months. A repeated measures ANOVA with a Greenhouse-Geisser correction determined that the mean haemoglobin level differed statistically significantly between time points ($P=0.000$). This has shown that there is a consistent statistically significant improvement in haemoglobin. The consistent improvement in haemoglobin suggests clinical efficacy of ibrutinib and improvement in bone marrow function.

b. Platelet count

As shown in Figure 3.3b, the mean platelet count differed statistically significantly between time points ($P=0.004$). Details of post hoc tests using the Bonferroni correction has shown that there is a consistent statistically significant improvement in platelet count. This again reflects continued improvement with ibrutinib therapy in both cohorts.

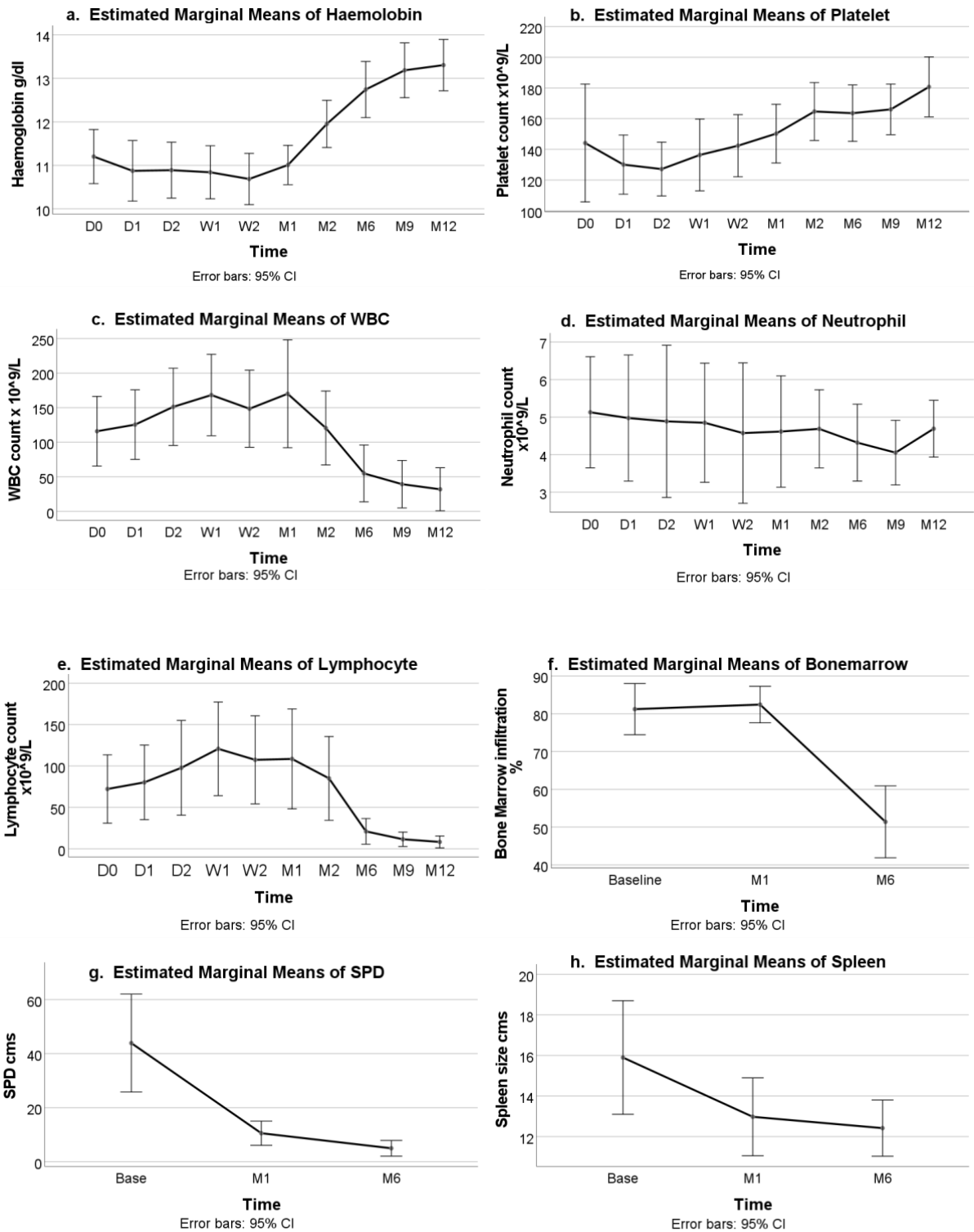


Figure 3.3 Estimated marginal means for all patients (n=40) of (a) Haemoglobin levels (b) Platelet count (c) WBC count (d) Neutrophil count (e) Lymphocyte count (f) Degree of bone marrow infiltration (g) SPD of lymph nodes and (h) Spleen size. Error bars represent the 95% confidence interval.

c. WBC count

A repeated measures ANOVA with a Greenhouse-Geisser correction determined that the mean WBC count differed statistically significantly between time points ($P=0.000$) (Figure 3.3c). There is a consistent statistically significant fall in WBC count in later measurements. This is consistent with initial rise in white cell count followed by a fall in the count over time.

d. Neutrophil count

In contrast to the platelets and WBCs, the mean neutrophil count did not differ statistically significantly between time points ($P=0.801$) (Figure 3.3d). The neutrophil count continues to be stable with continuous ibrutinib therapy in both cohorts.

e. Lymphocyte count

A repeated measures ANOVA with a Greenhouse-Geisser correction determined that mean lymphocyte count differed statistically significantly between time points ($P=0.000$) (Figure 3.3e). There is a statistically significant increase in lymphocyte count towards week 1 and the fall observed towards month 6. This is entirely consistent with the response expected with ibrutinib.

f. Bone marrow infiltration

The mean level of bone marrow infiltration in percentage differed statistically significantly between time points ($P=0.000$) (Figure 3.3f). Details of post hoc tests using the Bonferroni correction has shown that there is a statistically significant decrease in level of bone marrow infiltration towards month 6 compared to baseline and month 1. This suggests that the bone marrow clearance happens slowly with ibrutinib, but substantial improvement can be expected with continued therapy.

g. Sum of product of diameters (SDP) of lymph nodes

Moreover, the mean level of SDP in cms differed statistically significantly between time points ($P=0.000$) (Figure 3.3g) and that there is a statistically significant decrease in SDP towards month 1 which continued to month 6 when compared to baseline. This suggests a consistently improved radiological and clinical response to therapy in both cohorts.

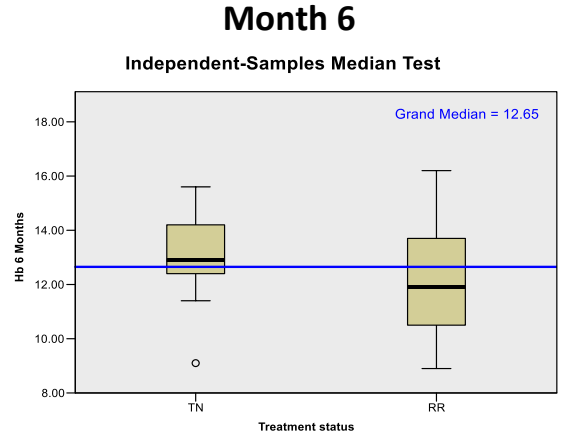
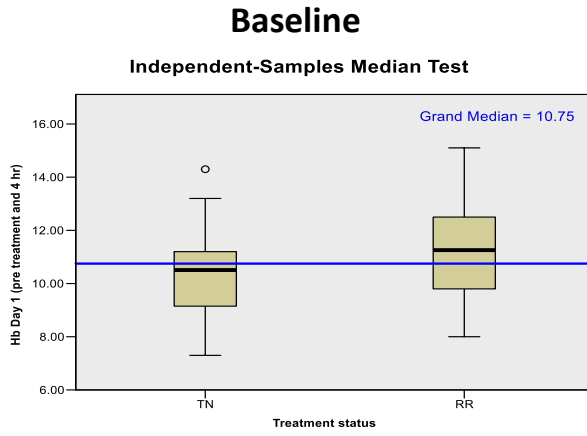
h. Spleen size

Consistent with the results for other secondary lymphoid structures, the mean level of spleen size in cms differed statistically significantly between time points ($P=0.000$) (Figure 3.3h). The post hoc tests have shown that there is a statistically significant decrease in spleen size towards month 1 which continued to month 6 when compared to baseline. This is like the clinical and radiological improvement in SPD with ibrutinib monotherapy.

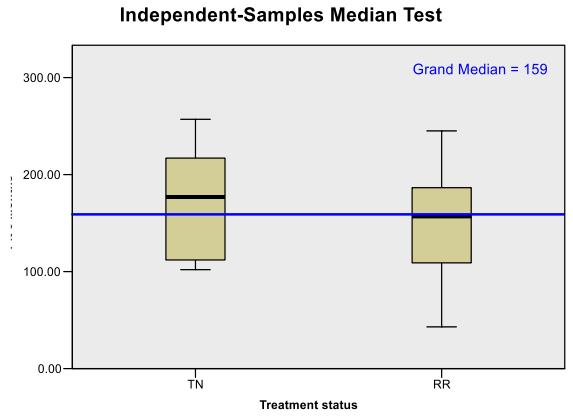
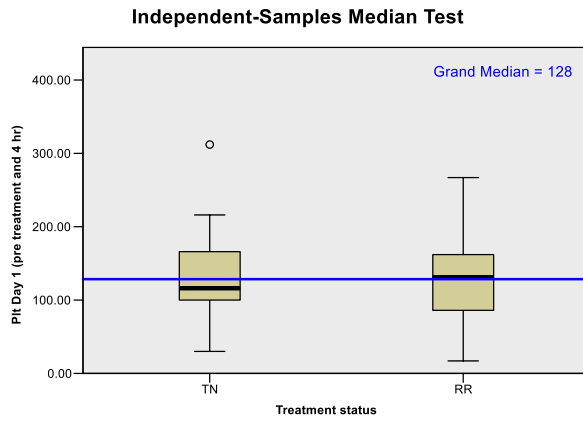
3.2.3.5 Difference in parameters between TN and RR groups at various time points

When evaluated as a single entity, both TN and RR groups exhibited a relatively uniform response to treatment with ibrutinib. To establish whether there were any discernible differences between TN and RR groups, a non-parametric independent sample test comparing medians between the two was used to assess the clinical parameters described above. A summary analysis of comparison of these variables between the TN and RR cohorts is presented below. For the variables presented in Figure 3.4, there was no statistically significant difference between TN and RR groups at any of the times measured suggesting a largely equivalent response between the two cohorts. The comparisons made at baseline and month 6 are shown as examples.

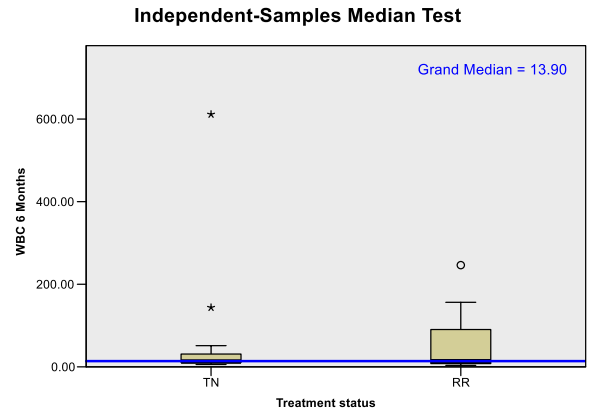
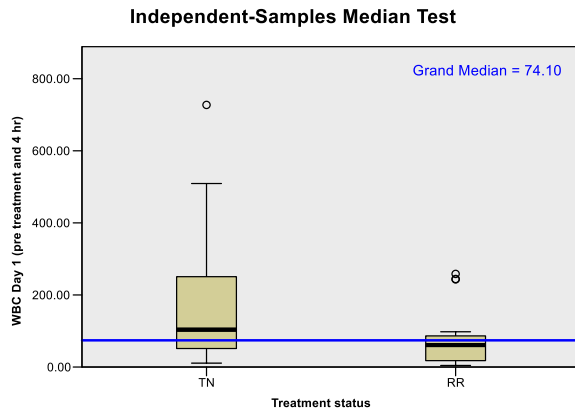
Haemoglobin



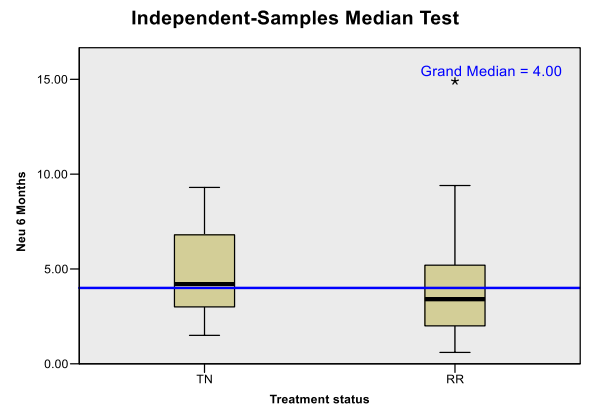
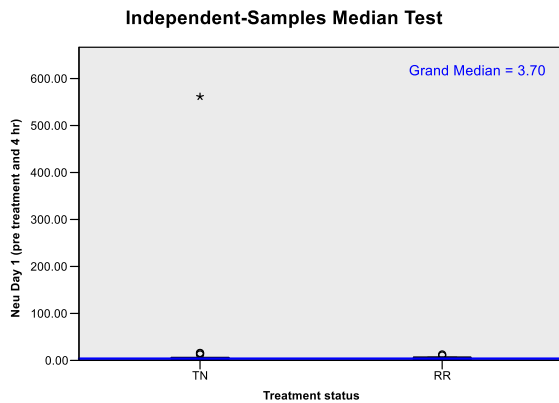
Platelets



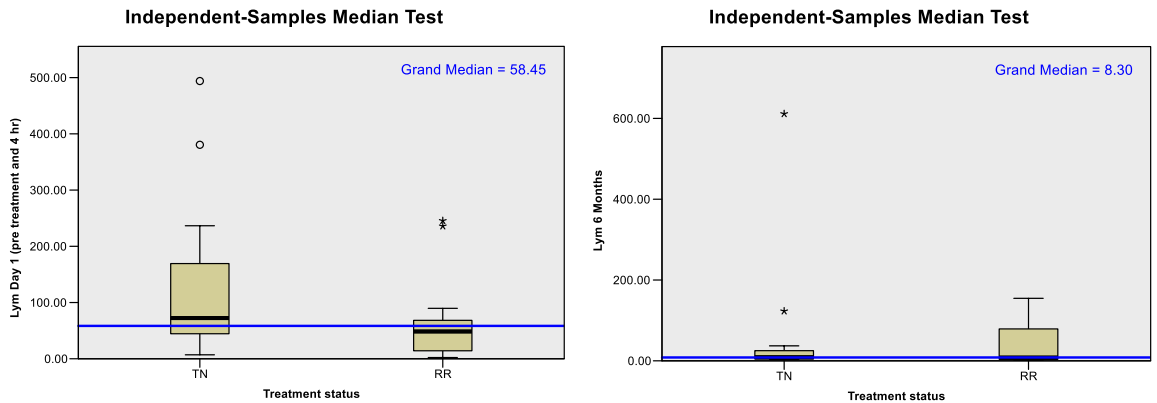
White blood cells (WBC)



Neutrophils



Lymphocytes



Spleen size

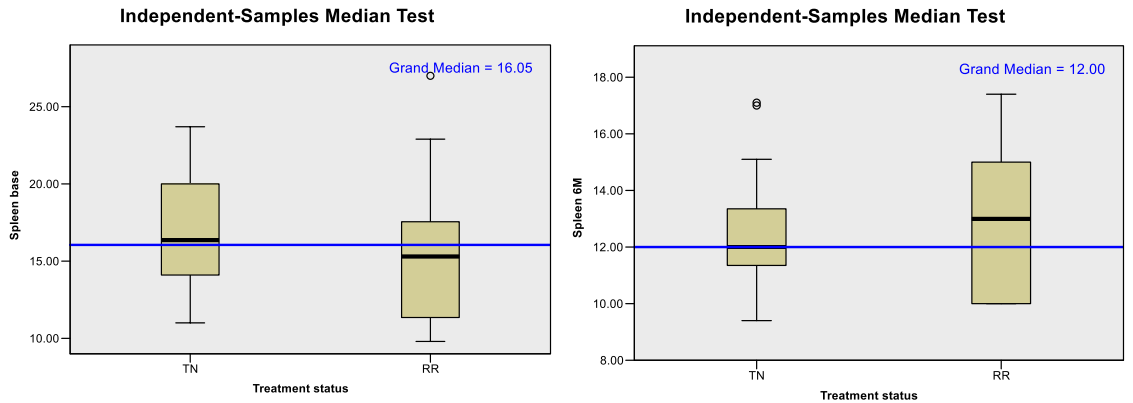


Figure 3.4 Independent sample median test for the indicated parameters in TN (n=20) and RR cohort (n=20). The median (central line), range (top and bottom bar) and interquartile range (top and bottom end of box) separated into TN and RR groups are shown in the plots.

In contrast, assessment of the bone marrow infiltration and SDP of the lymph nodes suggested that there were some observable differences between the two groups (Figure 3.5). The results suggest that there was a statistically significant difference in the degree of bone marrow infiltration at baseline. However, the difference was not prevalent at the month 6 time point. Moreover, there was no statistically significant difference in the degree of SDP at baseline and month 1. However, a statistically significant reduction in SDP was noted in TN cohort at month 6.

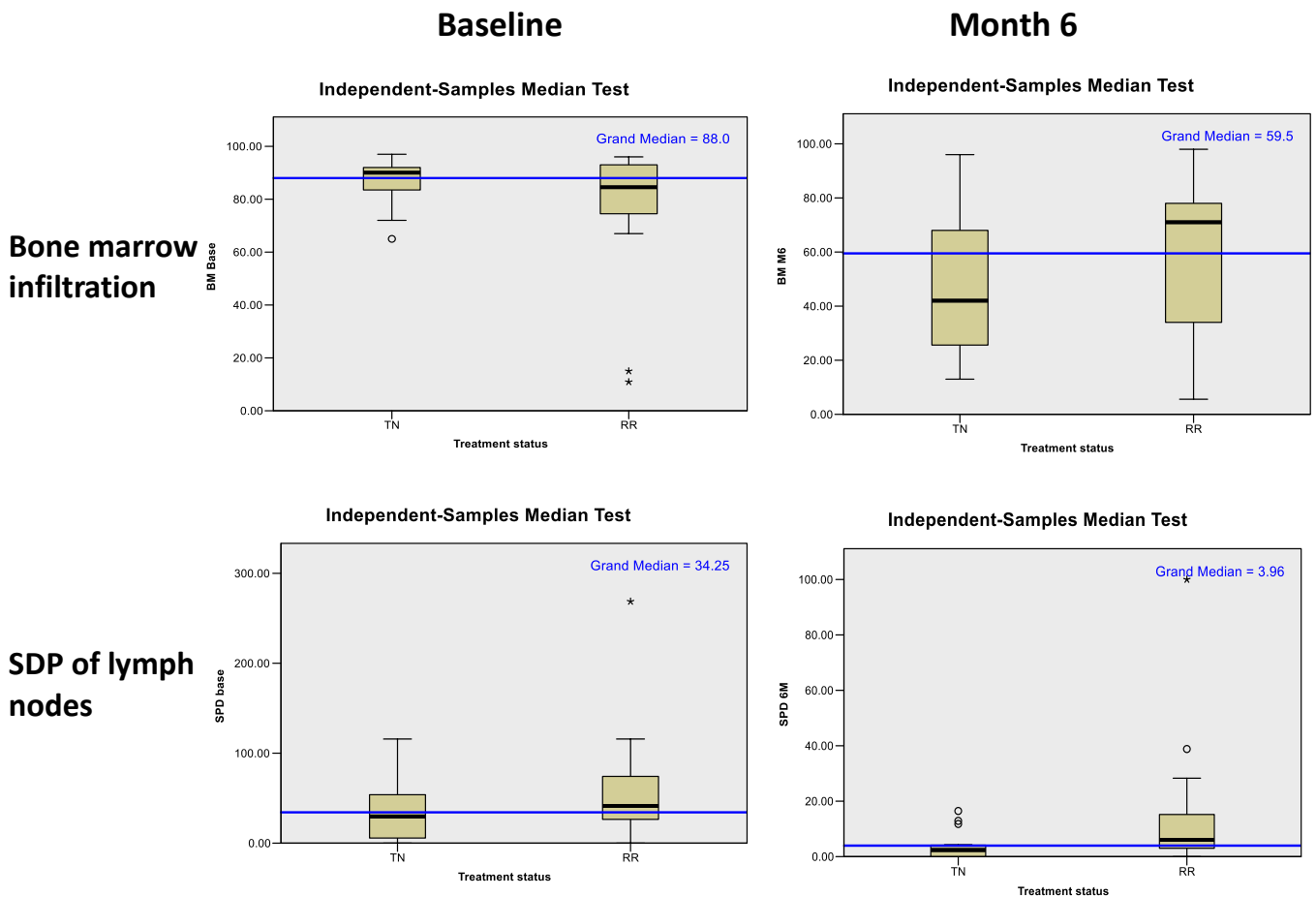


Figure 3.5 Independent sample median test for bone marrow infiltration and SDP of LN in TN (n=20) and RR cohort (n=20). The median (central line), range (top and bottom bar) and interquartile range (top and bottom end of box) separated into TN and RR groups are shown in the plots.

3.2.3.6 Comparison of means between TN and RR group

Analysis of differences between means of TN and RR group for various parameters were compared for statistical significance using independent sample t test. Group statistics were performed for comparison and statistically significant difference between both groups were identified with calculated mean, standard deviation and standard error of mean. Table 3.2 shows the independent sample tests for comparison of means between TN and RR cohorts. The variables with significant difference are shown in the table. Statistically significant difference was found in terms of age, WBC count on day 1, day 2, week 1 and lymphocyte

count on baseline and day 2 between the two cohorts. In short, the difference between the two groups were minimal in terms of the variables assessed.

Table 3.2 Independent Samples test for comparisons of means between TN and RR group (Only statistically significant variables are shown in the table).

		t-test for Equality of Means						
		t	df	Sig. (2-tailed)	Mean Difference	Std. Error Difference	95% Confidence Interval of the Difference	
							Lower	Upper
Age at entry	Equal variances assumed	-2.316	38	.026	-6.375	2.752	-11.947	-.802
WBC Baseline	Equal variances assumed	2.271	38	.029	110.280	48.551	11.992	208.567
WBC Day 1 (pre-treatment and 4 hr)	Equal variances assumed	2.182	38	.035	105.110	48.178	7.578	202.641
WBC Day 2 (24 hr)	Equal variances assumed	2.442	38	.019	122.065	49.992	20.861	223.268
WBC Week 1	Equal variances assumed	2.122	36	.041	101.659	47.908	4.495	198.823
Lym Baseline	Equal variances assumed	2.233	37	.032	107.471	48.125	9.961	204.982
Lym Day 2 (24 hr)	Equal variances assumed	2.378	31	.024	100.816	42.389	14.362	187.270

3.2.3.7 Clinical response assessment

Minimal residual disease in CLL is defined as when the patient has blood or marrow with fewer than one CLL cell per 10,000 leukocytes. Both 4-colour flow cytometry (MRD flow) and allele-specific oligonucleotide PCR are reliably sensitive down to a level of approximately one CLL cell in 10,000 leukocytes (0.01%). The detection of minimal residual disease (MRD) above a 0.01% (10^{-4}) threshold is an independent predictor of PFS and OS in patients with CLL treated with chemoimmunotherapy.

Analysis of the primary endpoint, depletion of MRD below 0.01% in the peripheral blood (PB) and bone marrow (BM) after 6 months of ibrutinib treatment, was carried out for all 40 patients. Analysis of the secondary endpoints was carried out for evaluable patients at the protocol-specified time points.

Absolute CLL counts in peripheral blood increased immediately after the first dose and peaked after two weeks to one month (Figure 3.6). In the TN group, absolute CLL counts returned to baseline by month 2 and were significantly reduced from baseline levels at 6 months (median 12%, range <1 to 64%). In the RR group, CLL counts remained approximately two-fold higher than baseline during the first 1-2 months of treatment and returned to baseline levels at month 6 (median 84%, range 1 to 786%). Bone marrow responses were not evident in either group after 1 month of treatment, but significant reductions occurred after 6 months of treatment in some patients, with at least 50% reduction evident in 8/16 (50%) TN patients and 3/18 (17%) RR patients.

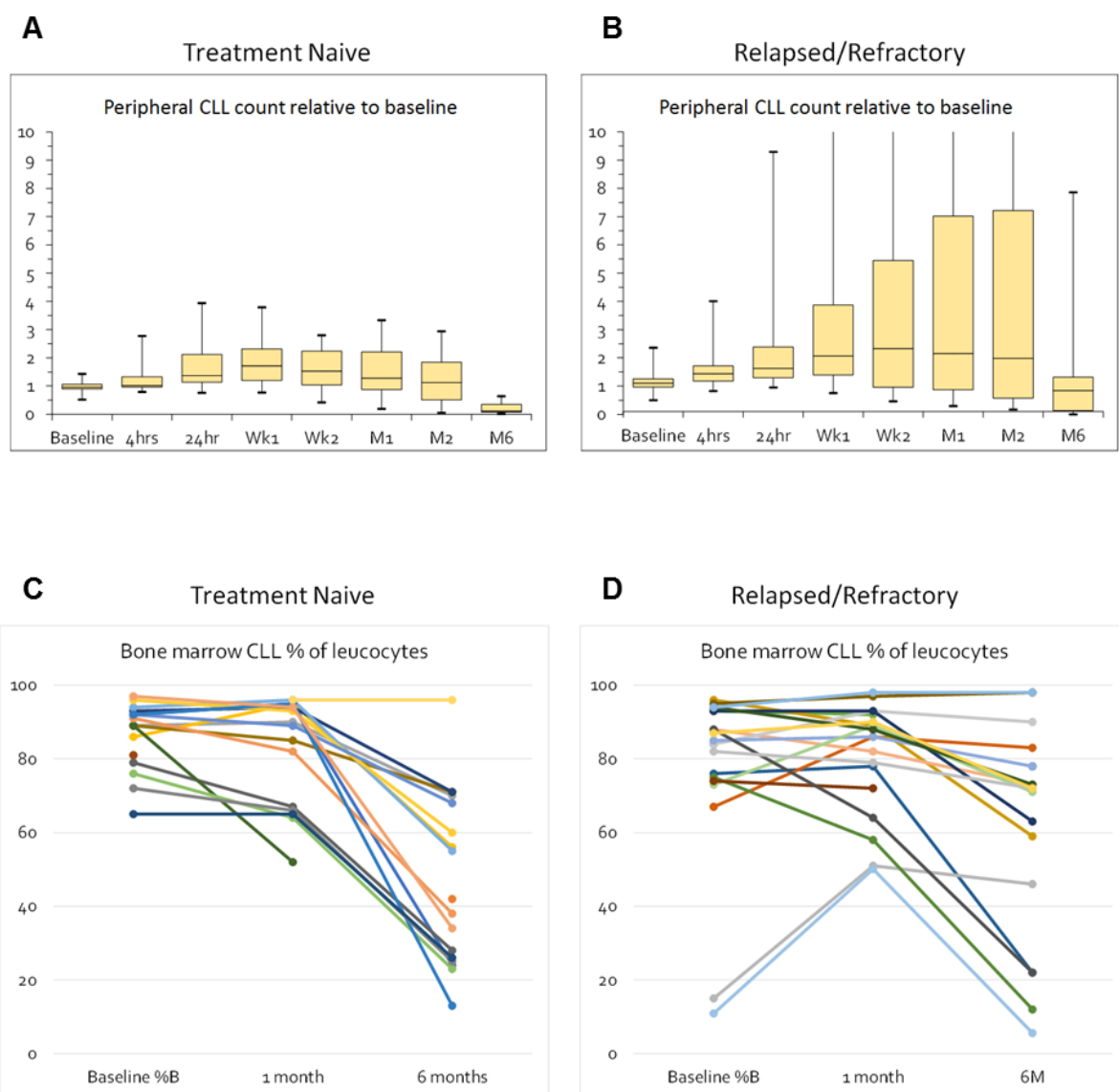


Figure 3.6(a) Peripheral blood CLL count from baseline to 6 months of treatment in TN cohort (b) Peripheral blood CLL count from baseline to 6 months of treatment in RR cohort (c) Bone marrow response from baseline to 6 months of treatment in TN cohort (d) Bone marrow response from baseline to 6 months of treatment in RR cohort.

Table 3.3 summarises best disease response by IWCLL criteria within 6 months of ibrutinib treatment. One TN patient died before the first disease assessment at 1 month. Three patients (n = 2, TN; n = 1, RR) were assessed at 1 month but not at 6 months. 16/20 (80%) TN patients and 18/20 (90%) RR patients experienced at least partial remission with lymphocytosis. The overall response rate was 85% of patients experiencing at least a partial

remission with lymphocytosis (PR-L). Two TN patients achieved an MRD-positive clinical complete remission (CR) with incomplete marrow recovery.

Table 3.3 Best IWCLL response within first six months of therapy.

	TN Cohort (N=20)		RR Cohort (N=20)	
	N	% (95% CI)	N	% (95% CI)
Complete Remission with incomplete marrow recovery	2	10.0 (2.8, 30.1)	0	
Partial Remission	8	40.0 (21.9, 61.3)	7	35.0 (18.1, 56.7)
Partial Remission with lymphocytosis	6	30.0 (14.5, 51.9)	11	55.0 (34.2, 74.2)
Stable Disease	3	15.0 (5.2, 36.0)	2	10.0 (2.8, 30.1)
Died before assessment	1	5 (.9, 23.6)	0	

Ibrutinib-monotherapy in TN patients was well tolerated with 18/20 patients alive and 13/20 remaining on IBR after median 4.9 years follow-up (range 0-5.9) with 7/20 stopping due to toxicity (3), progression/relapse (2) or other causes (2). Two patients achieved an IWCLL CR/CRi and MRD was >0.01% in PB/BM in all patients at all time points. Progression-free and overall survival at 3 years was 90% (Figure 3.7).

In the R/R group initially receiving Ibrutinib-monotherapy, 11/20 patients remain alive and 3/20 remain on IBR after a median 3.9 year follow-up (range 0.3-5.3). In this heavily pre-treated group, 10 did not enroll on the Obinutuzumab Extension study (1 died, 1 progression/relapse, 4 not eligible/other causes, 4 patient preference). The remaining 10/20 from the initial R/R group did enroll on the Extension and received Obinutuzumab at median 16.2 months (range 13-19) after starting Ibrutinib-monotherapy, of which all evaluable patients (9/10) had resolved any lymphadenopathy pre-OBI. Of this group, 2/10 achieved MRD-negative remission and stopped treatment, while 6/10 have since stopped ibrutinib due to death (2/6), progression/relapse (3/6) or other causes (1/6). Progression-free and

overall survival at 3 years was 60% and 69% respectively for the ten patients receiving the combination (Fig 3.7).

Median OS have not yet been reached in both arms. 5-year PFS and OS are trial outcomes which have not been reported.

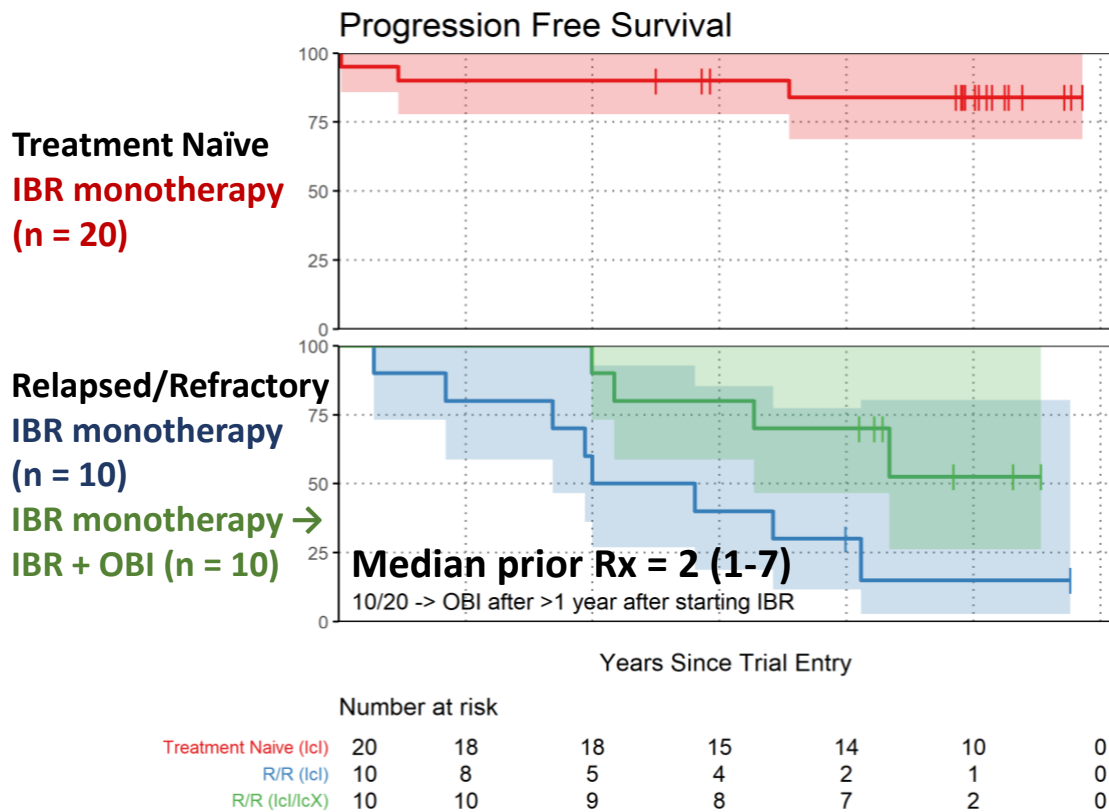


Figure 3.7 Kaplan Meier Curve for Progression-Free Survival in TN and RR cohorts.

3.3 CONCLUSIONS

IciCLLe trial was designed to assess the effectiveness of ibrutinib monotherapy and understand the effect of the drug on B-cell receptor pathways in real time. The effectiveness of the drug was established in this trial in two cohorts: Treatment naïve (TN) and relapsed refractory (RR) CLL. The clinical effectiveness of the drug was assessed using the IWCLL criteria: Overall response rates (ORR), Progression-free survival, Overall survival at various time points. However, the primary end point of the trial was assessment of MRD-negativity in patients receiving continuous therapy. It is well established now that ibrutinib on its own cannot achieve MRD-negativity and this is confirmed in this study (249).

However, assessment of MRD dynamics with ibrutinib is interesting and helped to design

future trials where combination of ibrutinib is assessed with other molecules such as anti-CD20 antibody and BCL-2 inhibitors.

This Chapter focussed on the design of the trial, clinical and biological characteristics of patients in the two cohorts of the trial, differences in the cohorts and the clinical outcomes.

Analysis of the baseline characteristics revealed that the participants represent a typical small phase 2 CLL trial population (250, 251). The average age for TN cohort was younger than average age of diagnosis of CLL which is 70 (65-74) years old (67, 68, 252). However, this is well established that the trials usually enrol younger participants (253, 254). The clinical parameters in both cohorts were consistent for participants entering the trial, hence the majority were classed as Binet Stage B and C. The haematological parameters were also as expected in both cohorts and there was no major difference in the baseline parameters. The degree of bone marrow infiltration was higher in the TN cohort, but this may just reflect the baseline disease bulk prior to initiation of therapy. In this trial, 66% and 90% of TN and RR participant had IGHV unmutated status, respectively. The cytogenetic aberrations in both cohorts are similar.

Clinical effectiveness was then analysed initially in individual variables in terms of response. Improvement in bone marrow function was evident as there was consistent improvement in haemoglobin and platelet count between baseline and month 12. This was accompanied by improvement in white cell count and lymphocytes reflective of improving clearance of disease systemically. This was confirmed as the degree of bone marrow infiltration between baseline and 6 months of therapy declined substantially. The total bulk of disease decreased with continuous ibrutinib therapy as manifested by reduction of sum of product of diameter of lymph nodes and spleen. In short, all clinical parameters confirmed the effectiveness of continuous ibrutinib.

Comparison of clinical response in the two cohorts was also assessed. The response at various time points was consistent, as there was no difference in response in terms of haemoglobin and platelet improvement. The fall in white cell count and lymphocyte were consistent in both groups. The degree of bone marrow infiltration was higher in the TN cohort, but the extent of infiltration was not statistically significant at month 6 in both cohorts suggesting that the clearance of bone marrow happened substantially in both

cohorts but significantly in TN cohort. There was improvement in sum of product of diameter of lymph nodes (SDP) and spleen in both cohorts. However, the SDP clearance was statistically significant at Month 6 in the TN cohort suggestive of sensitivity of response to ibrutinib. The comparisons of mean between two cohorts revealed minimal differences at various time points.

The primary endpoint of the trial was assessment of MRD negativity at a level of $< 0.01\%$ as per IWCLL criteria. Ibrutinib is unlikely to achieve MRD negativity and this was seen in all participants. However, analysis of MRD consistently shown an improvement in the CLL count in peripheral blood and bone marrow at various time points. Though achievement of MRD negativity is not possible with continuous ibrutinib therapy, this insight into the dynamics of disease clearance is important in understanding the logical combinations to achieve the goal of deeper remissions in CLL. Responses as per IWCLL criteria varied in two cohorts: In TN cohort, majority of participant achieved either partial response (PR) or partial response with lymphocytosis (PR-L). However, there were two patients who achieved complete response with incomplete marrow recovery (CRi). Majority of response in RR cohort were partial response (PR) or partial response with lymphocytosis (PR-L). Though there was higher disease bulk in the TN cohort than RR cohort at baseline, the response suggests accelerated and deeper responses in TN cohort. These results are consistent with prolonged follow-up studies for ibrutinib in both TN and RR CLL, where overall response rate (ORR) improved with continuous ibrutinib therapy. The CR rate in Resonate study for RR CLL patients was 11% with an overall follow-up- of 74 months, whereas the CR rate in Resonate-2 for TN patients was 30% with median follow-up of 5 years. No patient achieved MRD-negativity in these trials, but MRD was not formally assessed at various time points in these pivotal studies (118, 245). Other trials have reported similar results with single agent ibrutinib but combination with other agents such as Obinutuzumab, CIT and Venetoclax has resulted in deeper clinical and MRD responses in both TN and RR CLL (110, 111, 255, 256). In iLLUMINATE trial, addition of Obinutuzumab to ibrutinib resulted in higher PB MRD-negativity (35%) as compared to Chlormbucil-Obinutuzumab (25%) assessed flow cytometry (110). On the contrary, ibrutinib in combination with rituximab induced few MRD-negative results (4% Ibrutinib + Rituximab vs 1% Ibrutinib vs 8% Bendamustine-Rituximab) in A041202 trial (111). Similar results have been reported in R/R CLL where addition of

rituximab has not improved MRD responses (257) but combination with CIT has yielded better MRD response in HELIOS study (256). Addition of Venetoclax to ibrutinib does results in deeper MRD responses in RR CLL (255, 258). Hence, PFS and OS in both cohorts of ICI-CLL trial were as expected and consistent with the reported literature.

In summary, the clinical responses in ICI-CLL trial were seen in both TN and RR cohorts with subtle differences at various time points. The information collected from the initial data informed the design of ICI-CLL extension trial and CLARITY study.

CHAPTER 4:

Results of IciCLLe trial Cellular Kinases; TN VS RR Patients

4.1 ASSESSMENT OF RESIDUAL KINASE ACTIVITY IN ICICLLe TRIAL

Signals transmitted through the BCR are essential for the development, function and survival of normal B cells as well their malignant counterparts. As detailed in the previous chapters, CLL is reliant on proximal BCR signalling events transmitted through a cascade of cytosolic kinases whose activity can be effectively monitored through the detection of phosphorylated residues using specific antibodies and a flow cytometric assay. It is well established that ibrutinib blocks the phosphorylation of BTK on tyrosine 551 on the catalytic domain as well as tyrosine 223 on the SH2 domain, thus rendering the kinase inactive. However, whether the effect is sustained in all patients or whether blocking one pathway in CLL cells may alter the activation of other downstream pathways remains an open question. This is particularly important for patients that are refractory to treatment.

Various intracellular kinases are involved in the signalling from the BCR and there is a close link between the pathways regulated by these enzymes (259). SYK was assessed as this kinase is required to activate BTK and ERK1/2 is downstream of BTK (260-262). AKT is an important kinase in the PI3K pathway that is also a direct target of BTK (263). Real-time phospho-flow was incorporated in the trial protocol to analyse the effect of continuous ibrutinib therapy on these key kinases that control the behaviour of CLL cells.

We therefore reasoned that the assessment of kinase activity levels during the ICICLLe trial would allow us to formally test the following hypotheses:

Hypothesis 1:

In vivo ibrutinib exposure will result in decreased steady-state phosphorylation in all of the major BCR associated pathways downstream of BTK over time in responding patients.

Hypothesis 2:

In vivo ibrutinib exposure will result in failure of ex vivo IgM/IgD-mediated stimulation of pathways downstream of BTK over time in responding patients.

Hypothesis 3:

Continuing in vivo exposure to ibrutinib should result in diminished efficacy when cells are re-exposed to the drug ex vivo.

4.2 GENERAL METHODOLOGY

The analysis initially included all eleven time points (D-14, D0, D1Hr4, D1Hr24, D7, D14, M1, M2, M6, M9 and M12) analysed by ANOVA with repeated measures with a Greenhouse-Geisser correction. A major limitation of using this method here is the absence of data at all time points in all patients. The missing data was the result of several issues, which included missed sampling, insufficient sample or delayed delivery of the samples from the sites. This considerably reduced the numbers for this analysis. Therefore, later calculations were performed using the 3 major time points where most patients have provided samples for the tests. This includes D0, M1 and M6 data.

4.3 EFFECT OF IBRUTINIB TREATMENT ON STEADY-STATE KINASE PHOSPHORYLATION

There is a wealth of evidence that signalling through the BCR plays an important role in driving and maintaining CLL and that interfering with signals propagated through the BTK effectively halts CLL growth, although some patients may show prolonged lymphocytosis(240). Previous work has shown that despite inhibition of BTK activity, persistent CLL cells in patients exhibiting extended lymphocytosis maintain activation of other BCR signalling pathways when evaluated at 1- and 6-months post-treatment (240). To determine whether ibrutinib treatment effectively muted BCR signalling pathways in CLL, peripheral blood samples were evaluated at 11 time points by intracellular staining for phosphorylated BTK, SYK, ERK and AKT (Figure 4.1).

The mean MFI for phospho-BTK did not differ statistically significantly between time points ($p=0.353$) and remained relatively constant throughout the time course. In contrast, the mean MFI of phospho-SYK began to decrease after two weeks of treatment and reached a statistically significant difference between week 1 and Month 12 ($p=0.001$). The phosphorylation of ERK1/2 and AKT displayed small initial increases followed by more pronounced differences that reached significance ($p < 0.005$) between D0 and M9.

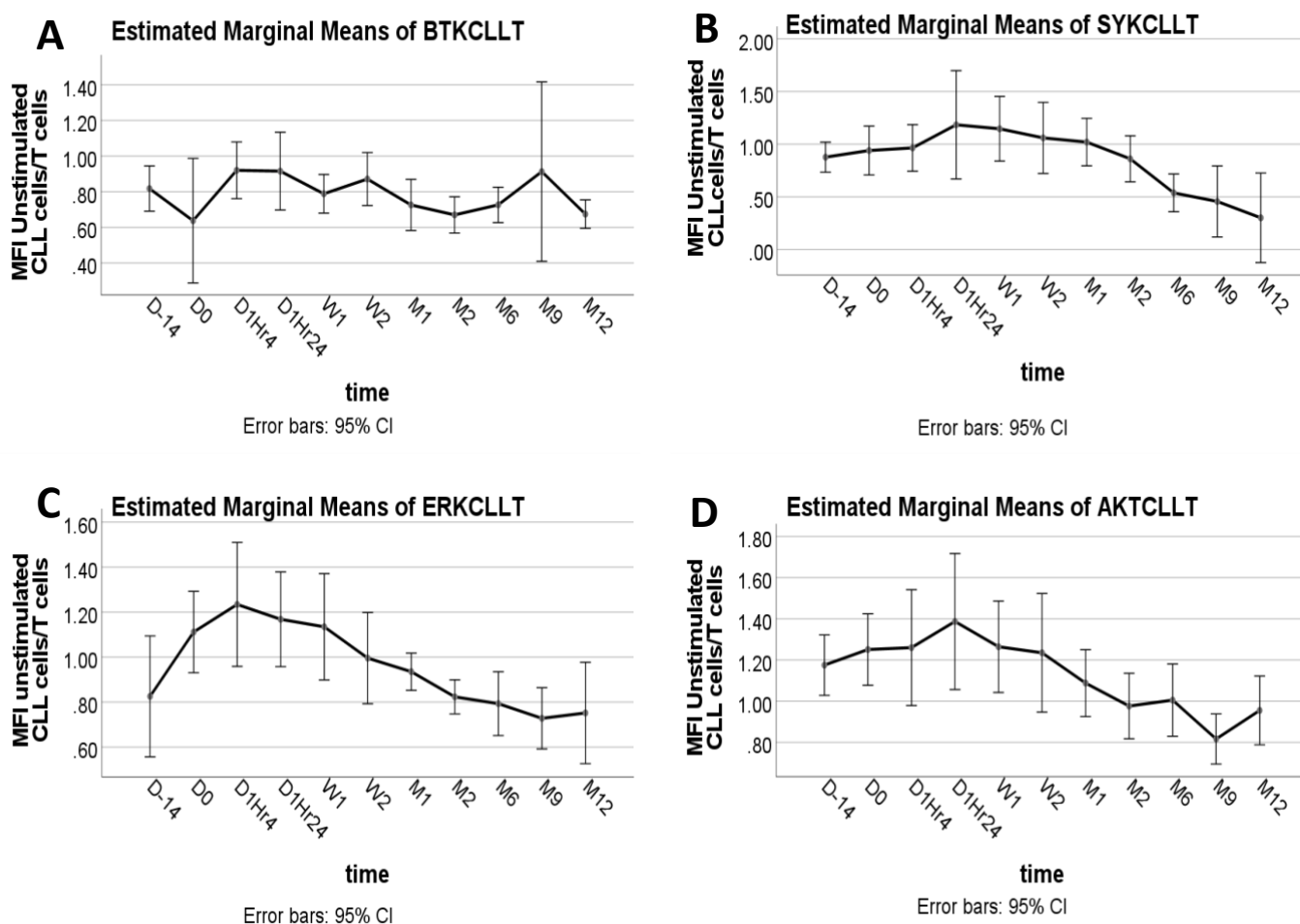


Figure 4.1 Estimated marginal means of kinase phosphorylation in peripheral blood samples during full course of ibrutinib treatment. MFI of phosphorylated versions of (A) BTK (B) SYK (C) ERK and (D) AKT in unstimulated CLL cells/T cells.

Although the patterns of kinase phosphorylation reached statistical significance, there was a large spread of data at each of the time points, which in part may be due to missing samples or may reflect differences in the responses of patients with particular features. To ascertain whether there were any differences between treatment naïve patients or relapsed refractory patients, additional analyses were performed, treating the groups separately. Moreover, samples from bone marrow were additionally evaluated to assess the impact of microenvironment.

As shown in Figure 4.2A, there is no statistically significant difference in the MFI for BTK pY551 between D0 and M6, regardless of patient group. However, in bone marrow samples there is a statistically significant difference in MFI between Day 0 and Month 6 ($p=0.003$) (Figure 4.2B). The fall in MFI is similar in both group of patients suggesting that there is a progressive decline in phosphorylation in BTK pY551 with continuous ibrutinib therapy. This is different to the pattern seen in the peripheral blood.

Figure 4.2C shows the means of SYK pY348 in TN and RR patients. The fall in MFI is similar in both group of patients suggesting that there is a progressive decline in phosphorylation in SYK pY348 with continuous ibrutinib therapy. However, there is no statistical difference in both cohorts ($p=0.754$). Similarly, there is a statistically significant difference in the MFI of SYK pY348 in bone marrow of TN and RR patients between Day 0 and Month 6 ($p=0.001$) (Figure 4.2D). The fall in MFI is similar in both group of patients. There was no statistical difference between TN and RR cohort ($p= 0.386$).

The fall in MFI for ERK1/2 in peripheral blood samples is similar in both cohorts of patients, suggesting that there is a progressive decline in phosphorylation in ERK with continuous ibrutinib therapy (Figure 4.2E). There was no statistical difference between cohorts ($p=0.325$). The pattern for ERK1/2 phosphorylation in the bone marrow is similar to the pattern seen in the peripheral blood (Figure 4.2F). There is a statistically significant difference in MFI between Day 0 and Month 6 ($p=0.001$). The fall in MFI is similar in both group of patients.

Figure 4.2G shows the means of AKT pS473 in peripheral blood samples from TN and RR patients, which reached significance between D0 and M6 ($p=0.0030$). The fall in MFI is similar in both groups. Figure 4.2H shows the means of AKT pS473 in bone marrow of TN and RR patients. The pattern is similar in both groups of patients with no statistical difference between two cohorts ($p=0.113$).

In summary, BTK phosphorylation levels appeared to be less impacted by ibrutinib therapy, with a decline only observed in the bone marrow. In contrast, patterns of phosphorylation for SYK, ERK1/2 and AKT displayed a progressive decline in phosphorylation with continuous ibrutinib therapy in both the peripheral blood and bone marrow with no difference between TN and RR patients.

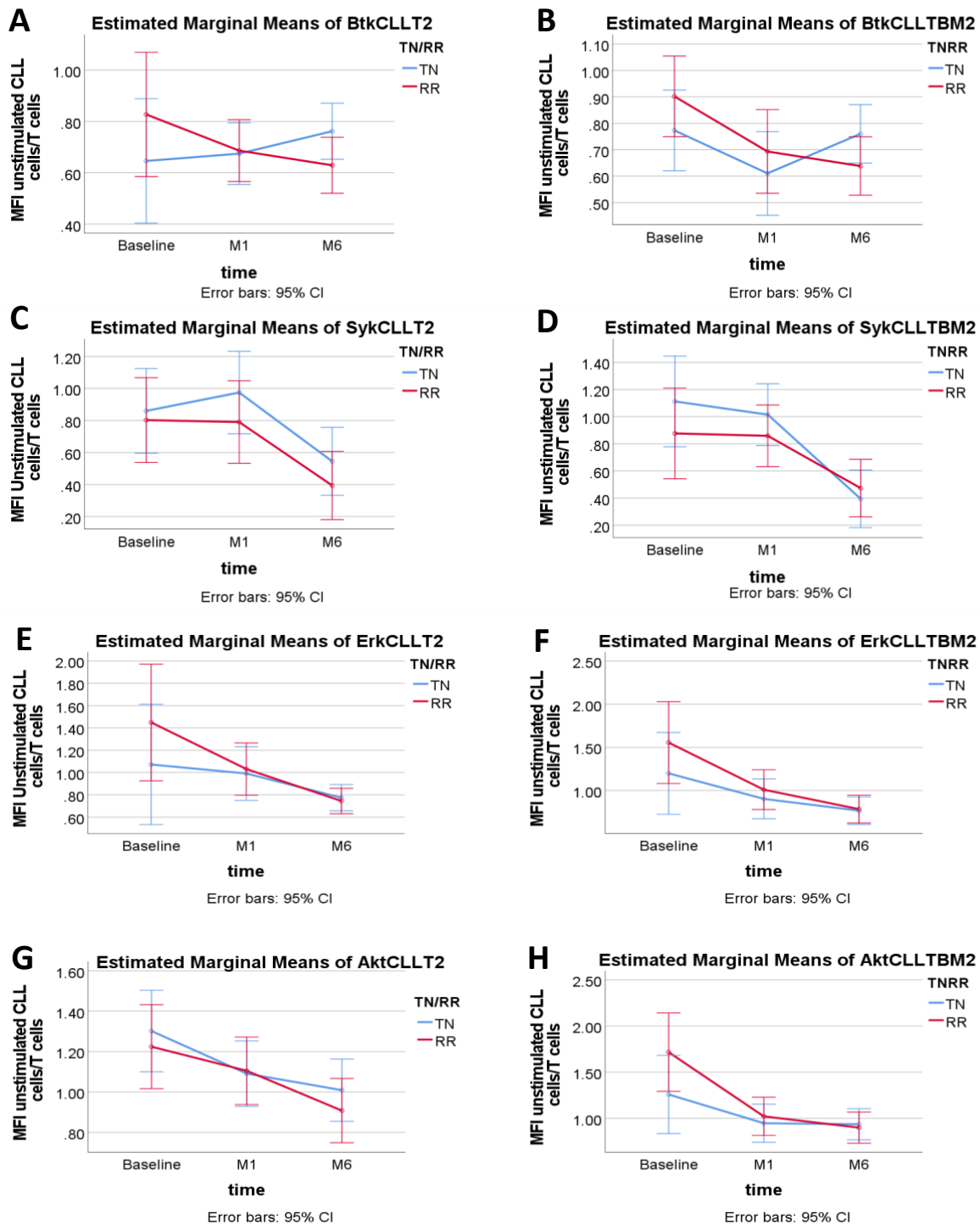


Figure 4.2 Estimated marginal means of kinase phosphorylation during ibrutinib treatment. (A) MFI of pBTK (pY551) in unstimulated CLL cells/ T cells from treatment naïve patients (TN) vs relapsed refractory (RR) in peripheral blood or (B) bone marrow; (C) MFI of pSYK in peripheral blood or (D) bone marrow; (E)MFI of pERK1/2 in peripheral blood or (F) bone marrow; and (G) MFI of pAKT in peripheral blood or (H) bone marrow.

4.4: EFFECT OF IBRUTINIB TREATMENT ON IGM/IGD STIMULATED KINASE PHOSPHORYLATION

The B-cell receptor (BCR) repertoire is highly restricted in CLL suggesting a role for antigenic selection in the initiation or progression of the disease (196, 200). Antigens binding to CLL BCRs include self-antigens, such as non-muscle myosin IIA, vimentin, apoptotic cells and oxidized low-density lipoprotein, as well as foreign antigens (bacterial polysaccharides and β -(1,6)-glucan, a major antigenic determinant on fungi) (210, 215, 264-268). Interestingly, evidence was provided in mice that pathogens may drive CLL pathogenesis by selecting and expanding pathogen-specific B cells that cross-react with self-antigens (209). CLL cells were reported to display cell-autonomous Ca^{2+} mobilisation in the absence of exogenous ligands, by virtue of recognising a single conserved BCR-internal epitope in the IGHV second framework region (88). Recently, it was found that the internal epitopes recognized by CLL BCRs from distinct subgroups are different (269).

In line with chronic BCR-mediated signalling, CLL cells show constitutive activation of various BCR pathway associated kinases. CLL cells are thought to interact with the tissue microenvironment and lymph node resident CLL cells show gene expression signatures indicative of BCR activation (270, 271). Moreover, BTK is critical for BCR- and chemokine-controlled integrin-mediated retention and/or homing of CLL B cells in their microenvironment (272).

IgM and IgD receptor isotypes are co-expressed on mature B cells and their function in B-cell development and maturation is widely interchangeable, as demonstrated in IgM and IgD knock-out mouse models (273, 274). Most CLL cells express both IgMs and IgDs, and several studies characterised the importance of IgM BCRs for CLL cell survival, cell-cycle entry, and proliferation (216, 275-279). The function of IgD in CLL has also been studied, with controversial results, mostly related to the effects of IgD stimulation on either inducing cell survival, or rather apoptosis (280, 281). IgM responsiveness typically increases in U-CLL cases, while such differential responses are generally not seen after IgD stimulation (216, 275, 276, 280, 281). The differential response in terms of HS1 phosphorylation, F-actin

polymerisation, ERK activation and chemokine secretion to IgM and IgD stimulation has also been evaluated (282).

Whether the stimulated phosphorylation of the key BCR-controlled kinases declines with continuous ibrutinib therapy was therefore tested by following analyses:

- a. IgM/IgD stimulated kinase phosphorylation in CLL cells as compared to T-cells for TN and RR cohorts
- b. IgM/IgD stimulated kinase phosphorylation in CLL cells as compared to unstimulated CLL cells for TN and RR cohorts
- c. IgM/IgD stimulated kinase phosphorylation in CLL cells as to baseline IgM/IgD stimulated kinase phosphorylation for TN and RR cohorts

4.4.1. IgM/IgD stimulated kinase phosphorylation in CLL cells as compared to T-cells for TN and RR cohorts should fall

The evidence presented thus far in this chapter suggests that BCR-associated signalling in vivo is dampened in the face of continuous exposure to ibrutinib. However, these results do not indicate whether the cells remain refractory to signalling after acute triggering through the BCR. To test this, peripheral blood samples were obtained at multiple intervals during treatment and cells exposed to an F(ab')₂ antibody capable of cross-linking both IgM and IgD. The extent of signalling was monitored by intracellular staining for phosphorylated BTK, SYK, ERK and AKT, initially in comparison to T cells as a control population where no increase is expected (Figure 4.3).

The mean MFI for stimulated BTK did not differ statistically significantly between time points ($p=0.262$) and remained relatively constant throughout the time course in the peripheral blood. In contrast, the mean MFI of stimulated SYK began to decrease after month 6 of treatment and reached a statistically significant difference between early time points and M9-12 ($p=0.002$). The phosphorylation of stimulated ERK1/2 started to decline at M2 and continued to decline till M12 but did not reach statistical significance ($p=0.114$)

Stimulated AKT displayed small initial increases in early time points followed by decline at week 2 and more pronounced differences that reached significance ($p < 0.005$) between D0 and M6 to M12.

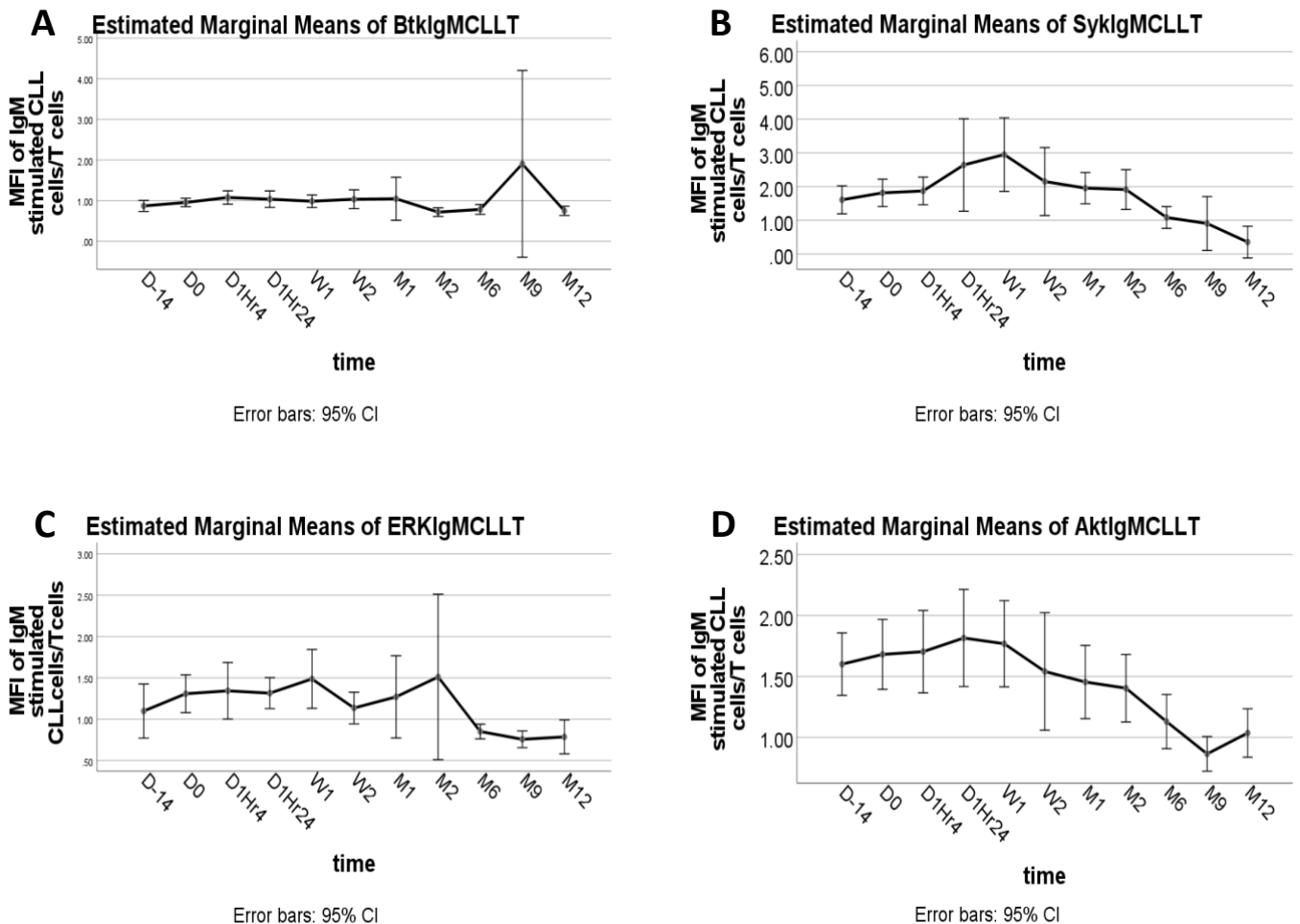


Figure 4.3 Estimated marginal means of kinase phosphorylation in peripheral blood samples following stimulation with anti-IgM/IgD for 2 min during full course of ibrutinib treatment. MFI of (A) pBTK (B) pSYK (C) pERK and (D) pAKT in stimulated CLL cells/ T cells.

The data were then further divided into treatment naïve patients or relapsed refractory patients and samples from bone marrow were additionally evaluated.

As shown in Figure 4.4A, there is no statistically significant difference in the MFI for stimulated BTK pY551 between D0 and M6, regardless of patient group in the peripheral blood ($p=0.267$). There was a similar pattern observed in the bone marrow at similar time

points ($p=0.151$) (Figure 4.4B). The stable stimulated MFI is similar in both group of patients suggesting that there is a no change in stimulated phosphorylation in BTK pY551 with continuous ibrutinib therapy. This pattern was similar in in the peripheral blood and bone marrow and there were no statistically significant differences between the TN and RR cohorts in peripheral blood ($p=0.139$) and bone marrow ($p=0.110$).

Figure 4.4C shows the means of stimulated SYK pY348 in TN and RR patients. The fall in MFI is similar in both group of patients at baseline and M6 suggesting that there is a progressive decline in stimulated phosphorylation in SYK pY348 with continuous ibrutinib therapy ($p=0.002$). However, there is no statistical difference in both cohorts ($p=0.660$). Similarly, there is a statistically significant difference in the MFI of SYK pY348 in bone marrow of TN and RR patients between Day 0 and Month 6 ($p=0.002$) (Figure 4.4D). However, the fall in phosphorylation is more evident in TN cohort as compared to RR cohort in bone marrow which is dissimilar to peripheral blood ($p=0.037$).

The fall in MFI for stimulated ERK1/2 in peripheral blood samples is similar in both cohorts of patients, suggesting that there is a progressive decline in stimulated phosphorylation in ERK with continuous ibrutinib therapy ($p=0.008$) (Figure 4.4E). There was no statistical difference between both cohorts ($p=0.587$). The pattern for stimulated ERK1/2 phosphorylation in the bone marrow is like the pattern seen in the peripheral blood (Figure 4.4F). There is a statistically significant difference in MFI between Day 0 and Month 6 ($p=0.032$). The fall in MFI is similar in both group of patients ($p=0.589$).

Figure 4.4G shows the means of stimulated AKT pS473 in peripheral blood samples from TN and RR patients, which reached significance between D0 and M6 ($p=0.000$). The fall in MFI is similar in both group of patients ($p=0.624$). Figure 4.4H shows the means of AKT pS473 in bone marrow of TN and RR patients ($p=0.000$). The pattern is similar in both group of patients with no statistical difference between two cohorts ($p=0.816$).

In summary, stimulated BTK phosphorylation levels appeared to be stable with ibrutinib therapy, both in peripheral blood and bone marrow. In contrast, patterns of stimulated phosphorylation for SYK, ERK1/2 and AKT displayed a progressive decline in phosphorylation with continuous ibrutinib therapy in both the peripheral blood and bone marrow with no

difference between TN and RR patients. The decline in stimulated phosphorylation for SYK was more pronounced in TN patients as compared to RR patients.

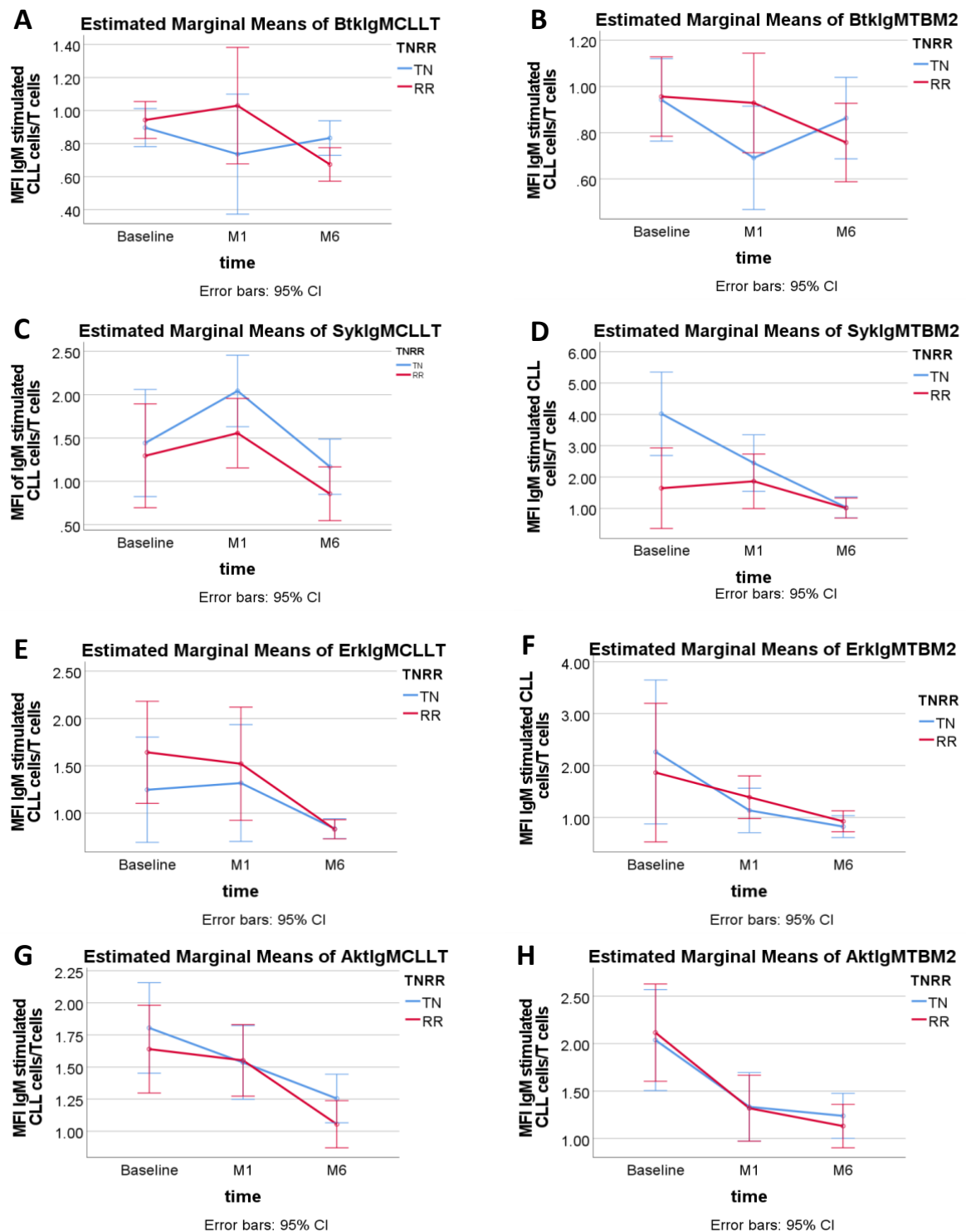


Figure 4.4 Estimated marginal means of kinase phosphorylation following stimulation with anti-IgM/IgD for 2 min. (A) MFI of pBTK (pY551) in stimulated CLL cells/ unstimulated CLL cells from treatment naïve patients (TN) vs relapsed refractory (RR) in peripheral blood or

(B) bone marrow; (C) MFI of pSYK in peripheral blood or (D) bone marrow; (E)MFI of pERK1/2 in peripheral blood or (F) bone marrow; and (G) MFI of pAKT in peripheral blood or (H) bone marrow.

4.4.2 IgM/IgD stimulated kinase phosphorylation in CLL cells as compared to unstimulated CLL cells for TN and RR cohorts should fall

The above data using T cells as a comparator suggest that BCR signalling can still occur, albeit at a reduced level, after prolonged exposure to ibrutinib. However, kinases such as SYK and BTK are not expressed in T cells, so the background levels in the flow cytometry assay may not be representative of the change in B cells. To address this issue, comparisons were made instead between anti-IgM/D stimulated versus unstimulated CLL cells (Figure 4.5). Only three-point comparisons are done, as 11-points comparison is not more informative and due to reduced number of available samples there is more possibility for error.

As shown in Figure 4.5A, there is no statistically significant difference in the MFI for stimulated BTK pY551 between D0 and M6, regardless of patient group in the peripheral blood ($p=0.406$). There was a similar pattern observed in the bone marrow at similar time points ($p=0.705$) (Figure 4.5B). The stable stimulated MFI is similar in both group of patients suggesting that there is a no change in stimulated phosphorylation in BTK pY551 as compared to unstimulated CLL cells with continuous ibrutinib therapy. This pattern was similar in in the peripheral blood and bone marrow and there was a statistically significant difference between the TN and RR cohorts in peripheral blood ($p=0.04$) but no difference in bone marrow ($p=0.640$).

Figure 4.5C shows the means of stimulated SYK pY348 in TN and RR patients. The decline in stimulated SYK phosphorylation as compared to unstimulated SYK phosphorylation was not statistically different in peripheral blood ($p=0.559$) and there is no statistical difference in both cohorts ($p=0.757$). Similarly, there was no statistically significant difference in the bone marrow of TN and RR patients between Day 0 and Month 6 ($p=0.440$) (Figure 4.5D), nor was there a statistical difference between both cohorts in the bone marrow ($p=0.144$).

The stimulated ERK1/2 in peripheral blood samples as compared to unstimulated CLL cells is similar in both cohort of patients ($p=0.109$) (Figure 4.5E). There was no statistical difference between both cohorts ($p=0.062$). The pattern for stimulated ERK1/2 phosphorylation in the bone marrow is like the pattern seen in the peripheral blood (Figure 4.5F). There was no statistically significant difference in MFI between Day 0 and Month 6 ($p=0.141$). The fall in MFI is similar in both group of patients ($p=0.195$).

Figure 4.5G shows the means of stimulated AKT pS473 in peripheral blood samples from TN and RR patients, which did not reach significance between D0 and M6 ($p=0.373$). The fall in MFI is similar in both group of patients ($p=0.501$). Figure 4.5H shows the means of AKT pS473 in bone marrow of TN and RR patients ($p=0.601$). The pattern is similar in both group of patients with no statistical difference between two cohorts ($p=0.246$).

Thus, the overall picture of anti-BCR triggered signalling when assessed by comparison to unstimulated CLL cells is consistent with the results using T cells.

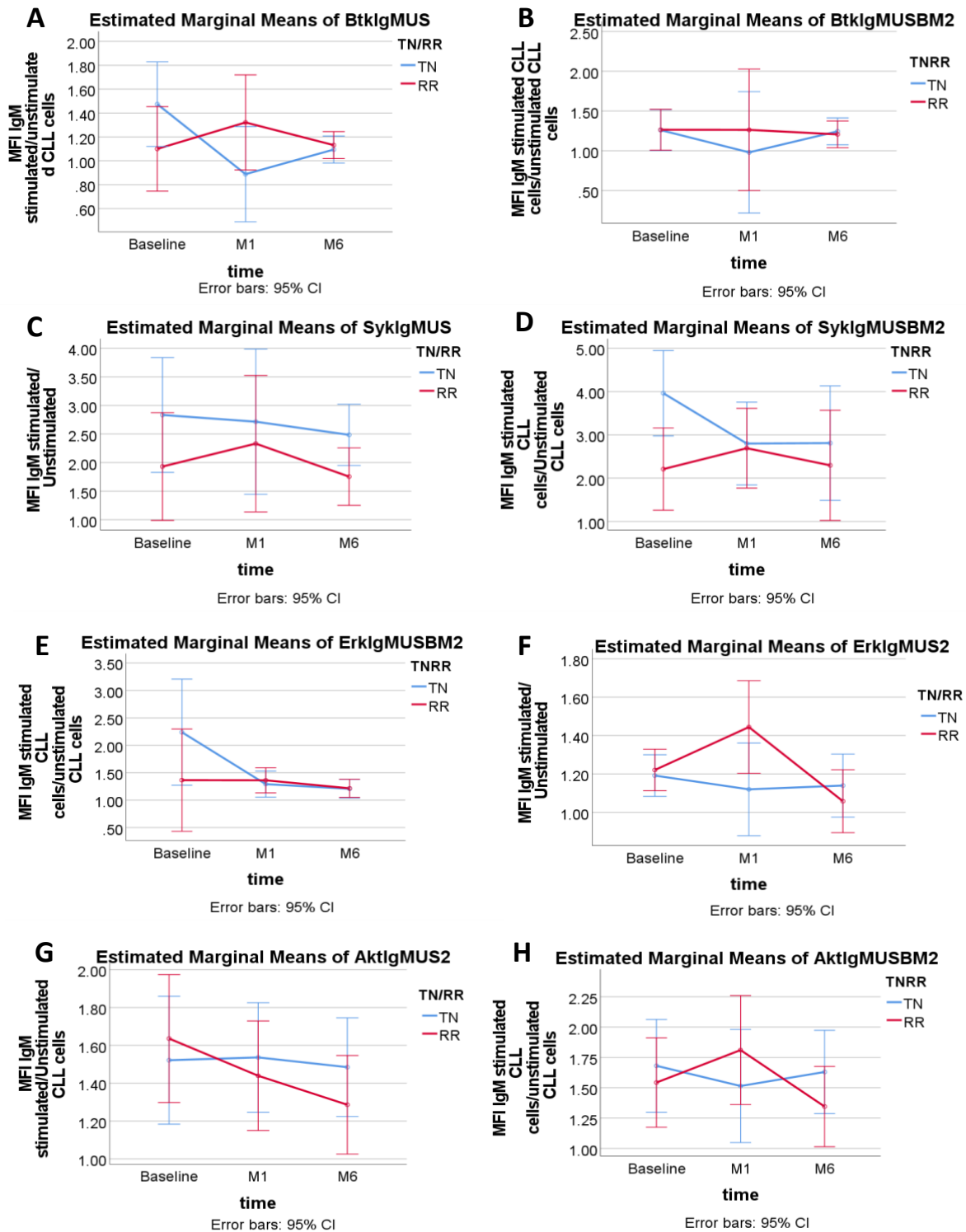


Figure 4.5 Estimated marginal means of kinase phosphorylation following stimulation with anti-IgM/D for 2 min. (A) MFI of pBTK (pY551) in stimulated CLL cells/ unstimulated CLL cells from treatment naïve patients (TN) vs relapsed refractory (RR) in peripheral blood or (B) bone marrow; (C) MFI of pSYK in peripheral blood or (D) bone marrow; (E) MFI of pERK1/2 in peripheral blood or (F) bone marrow; and (G) MFI of pAKT in peripheral blood or (H) bone marrow.

4.4.3. IgM/IgD stimulated kinase phosphorylation in CLL cells as compared to baseline IgM/IgD stimulated kinase phosphorylation for TN and RR cohorts should fall

To ascertain whether the strength of stimulated phosphorylation in CLL cells as compared to unstimulated phosphorylation in CLL cells declines with continuous ibrutinib therapy at various time points, additional analyses were performed.

As shown in Figure 4.6A, there is no statistically significant difference in the MFI for stimulated BTK pY551 between D0 and M6, regardless of patient group in the peripheral blood ($p=0.944$). There was a similar pattern observed in the bone marrow at similar time points ($p=0.066$) (Figure 4.6B). The stable stimulated MFI is similar in both group of patients suggesting that there is a no change in stimulated phosphorylation in BTK pY551 as compared to unstimulated CLL cells with continuous ibrutinib therapy. This pattern was similar in in the peripheral blood and bone marrow and there was a statistically significant difference between the TN and RR cohorts in peripheral blood ($p=0.405$) but no difference in bone marrow ($p=0.300$).

Figure 4.6C shows the means of stimulated SYK pY348 in TN and RR patients. The strength of increment in stimulated SYK phosphorylation did not fall as compared to unstimulated SYK phosphorylation and this was not statistically different in peripheral blood ($p=0.843$); There was no statistical difference in both cohorts ($p=0.152$). Similarly, there was no statistically significant difference in the bone marrow of TN and RR patients between Day 0 and Month 6 ($p=0.685$) (Figure 4.6D).

The increment in the stimulated ERK1/2 in peripheral blood samples as compared to unstimulated CLL cells is similar in both cohort of patients ($p=0.113$) (Figure 4.6E). There was no statistical difference between both cohorts ($p=0.06$). The pattern for stimulated ERK1/2 phosphorylation in the bone marrow is similar to the pattern seen in the peripheral blood (Figure 4.6F). There was no statistically significant difference in MFI between Day 0 and Month 6 ($p=0.173$) and the pattern was similar in both cohorts ($p=0.499$).

Figure 4.6G shows the increments in the means of stimulated AKT pS473 in peripheral blood samples from TN and RR patients, which did not reach significance between D0 and M6

($p=0.706$). The fall in MFI is similar in both group of patients ($p=0.452$). Figure 4.6H shows the means of AKT pS473 in bone marrow of TN and RR patients ($p=0.956$). The pattern is similar in both group of patients with no statistical difference between two cohorts ($p=0.089$).

In summary, the lack of increments in stimulated BTK, SYK, ERK 1/2, AKT phosphorylation levels as compared to unstimulated state appeared to be stable with ibrutinib therapy, both in peripheral blood and bone marrow. The pattern was similar in both cohorts.

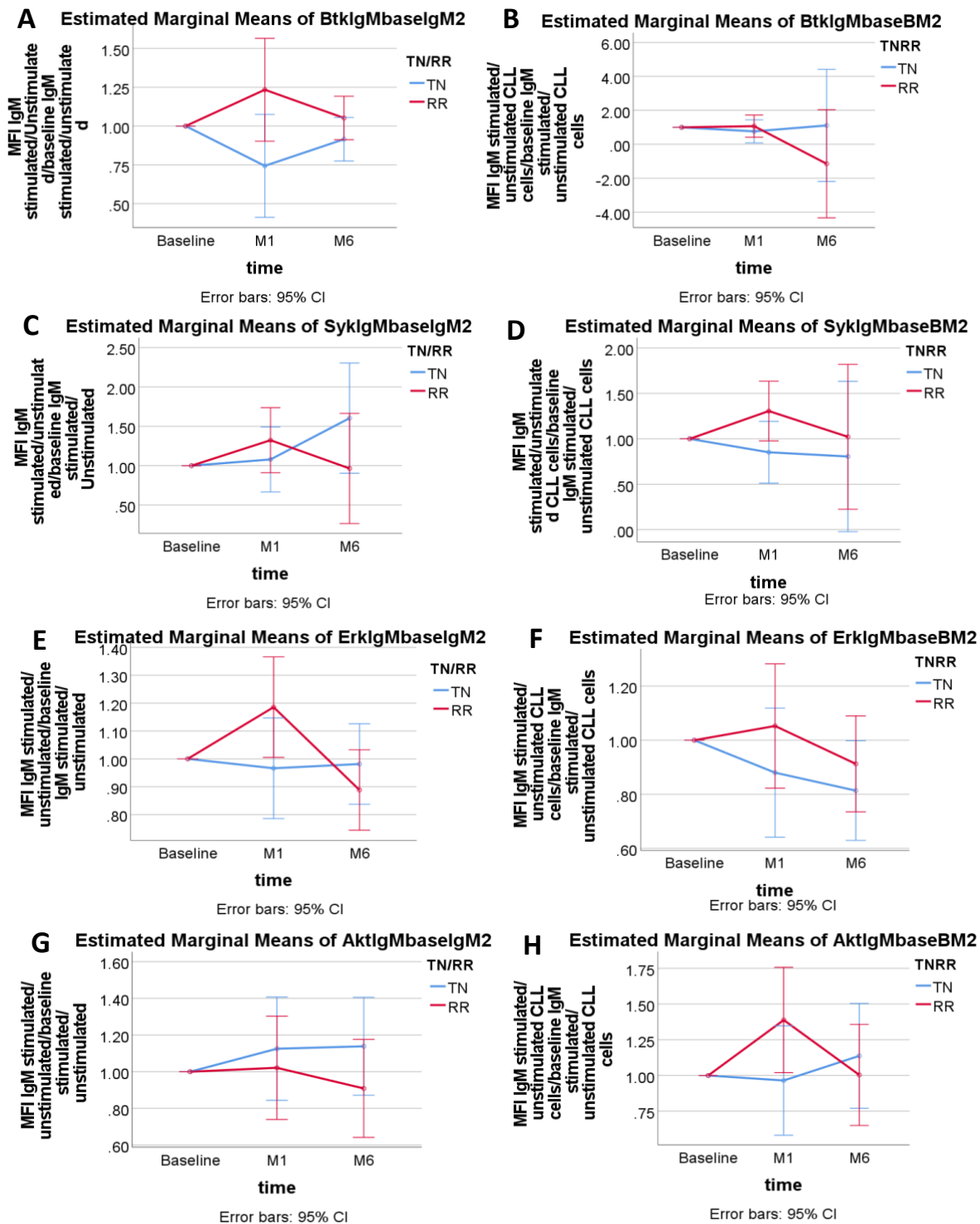


Figure 4.6 Estimated marginal means of kinase phosphorylation following stimulation with anti-IgM/D for x min. (A) MFI of pBTK (pY551) in stimulated CLL cells/ baseline unstimulated from treatment naïve patients (TN) vs relapsed refractory (RR) in peripheral blood or (B) bone marrow; (C) MFI of pSYK in peripheral blood or (D) bone marrow; (E) MFI of pERK1/2 in peripheral blood or (F) bone marrow; and (G) MFI of pAKT in peripheral blood or (H) bone marrow.

4.5 EFFECT OF IBRUTINIB TREATMENT ON EX VIVO EXPOSURE TO REPEATED DOSAGE

A final prediction is that continued in vivo exposure to ibrutinib should result in diminished efficacy when cells are re-exposed to the drug ex vivo. The irreversible binding of ibrutinib to BTK should render the kinase inactive and refractory to both inducible stimulation as well as further inhibition after additional application. To test this, samples were evaluated for kinase activation status at the 3 major points, D0, M1 and M6 during therapy.

Figure 4.7A shows the estimated marginal means of MFI of BTK-pY551 in vitro ibrutinib treated CLL cell/Unstimulated CLL cells at baseline, Month 1 and Month 6 in peripheral blood. This shows stable levels as expected, with no statistical differences over time. This pattern was additionally observed in bone marrow samples (Figure 4.7B). There was a gradual increase in the detected level of SYK phosphorylation over time in the blood, but this was not significant and was not mirrored in the pattern for bone marrow where the levels were lower at M6 (Figure 4.7C and D). In both instances the changes were non-significant ($P = 0.466$ and $P = 0.084$). The pattern for ERK1/2 phosphorylation was essentially the same for both blood and bone marrow samples and remained stable throughout ($P = 0.629$ and $P = 0.173$) (Figure 4.7E and F). Moreover, the MFI for phosphorylated AKT was also relatively static over the entire course of treatment, regardless of whether the samples were obtained from blood (difference in MFI $p = 0.188$) or bone marrow ($p = 0.393$) (Figure 4.7G and H).

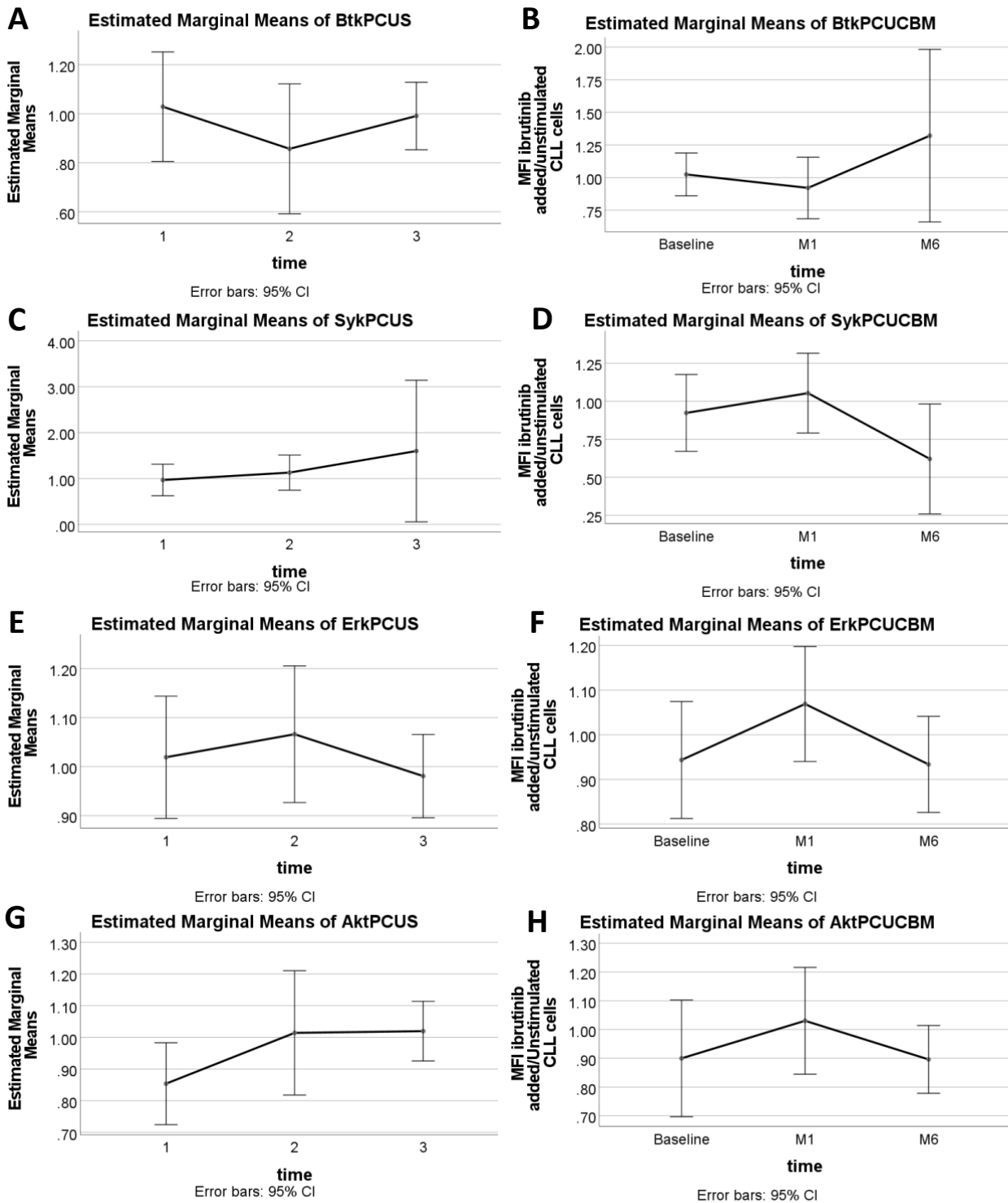


Figure 4.7 Estimated marginal means of kinase phosphorylation following treatment with ibrutinib for 2 min. (A) MFI of pBTK (pY551) in stimulated CLL cells/ unstimulated CLL cells in peripheral blood or (B) bone marrow; (C) MFI of pSYK in peripheral blood or (D) bone marrow; (E) MFI of pERK1/2 in peripheral blood or (F) bone marrow; and (G) MFI of pAKT in peripheral blood or (H) bone marrow.

Although the patterns above were generally stable for each of the kinases assessed, subtle differences may emerge when considering TN and RR cohorts separately. However, evaluation of the two groups did not generate any statistically significant differences in either blood or bone marrow samples for any of the kinases (Figure 4.8), thus confirming the effect on the patients as a whole.

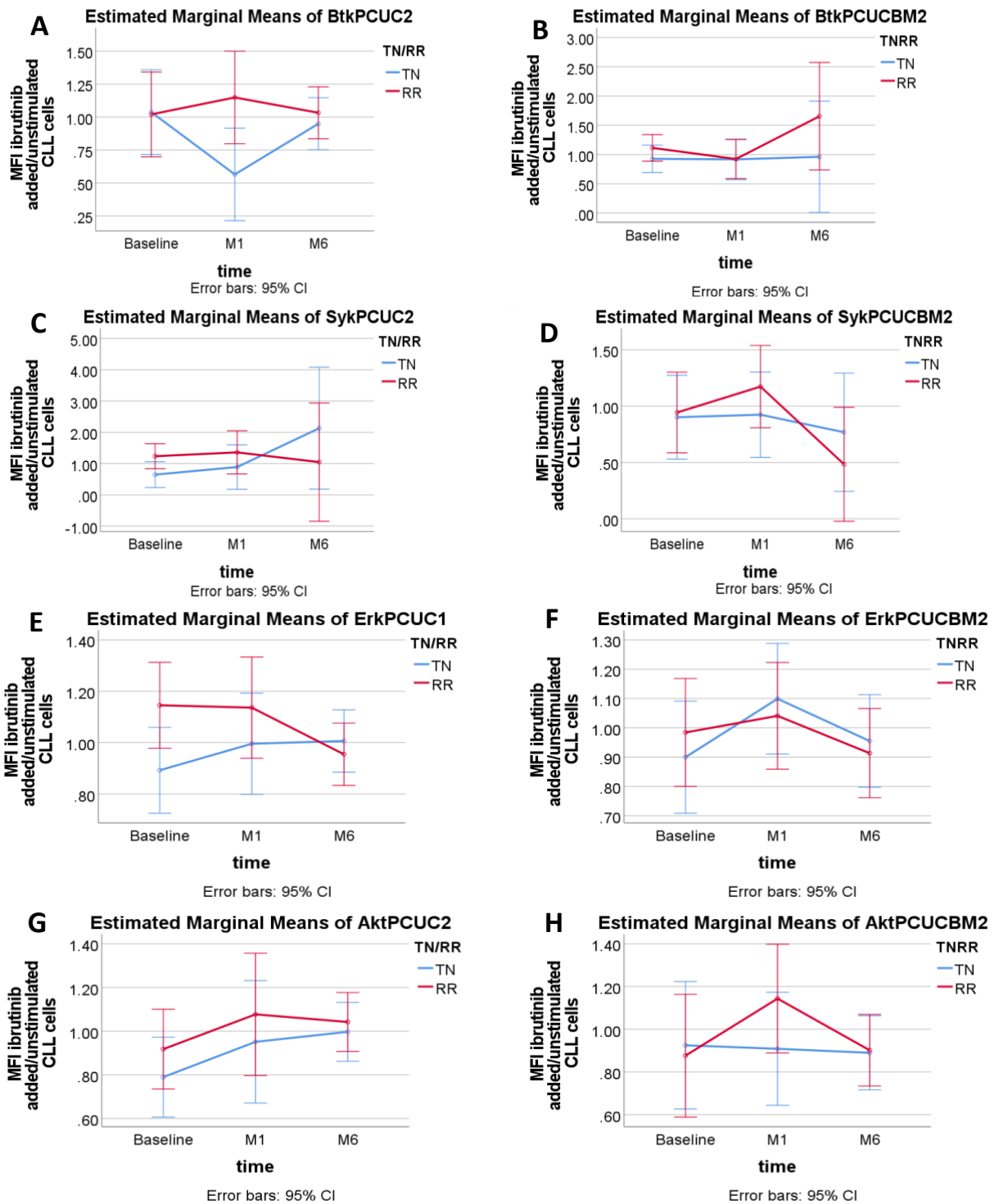


Figure 4.8 Estimated marginal means of kinase phosphorylation following treatment with ibrutinib for 2 min. (A) MFI of pBTK (pY551) in stimulated CLL cells/ baseline unstimulated from treatment naïve patients (TN) vs relapsed refractory (RR) in peripheral blood or (B) bone marrow; (C) MFI of pSYK in peripheral blood or (D) bone marrow; (E) MFI of pERK1/2 in peripheral blood or (F) bone marrow; and (G) MFI of pAKT in peripheral blood or (H) bone marrow.

The result from the above data suggests that the CLL cells exposed to long-term ibrutinib are indeed resistant to further dosage. To provide additional evidence, the CLL samples from blood and bone marrow were also subjected to ex vivo IgM/IgD stimulation in the presence of fresh ibrutinib and compared to the IgM/IgD stimulated CLL cells at the same time points. The prediction is that over time, the ratio will fall.

Figure 4.9 shows the estimated marginal means of phosphorylation patterns for the 4 kinases at baseline, Month 1 and Month 6 in peripheral blood and bone marrow. The MFI of BTK-pY551 in vitro IgM/IgD treated CLL cell/Ibrutinib treated IgM/IgD stimulated CLL cells is stable in both blood (Figure 4.9A) and bone marrow (Figure 4.9B) with no statistical differences over time. The pattern for SYK phosphorylation was similar to BTK (Figure 4.9C and D) with non-significant changes over time in blood and bone marrow ($p = 0.659$ and $p = 0.302$). ERK1/2 (Figure 7.9C and D) and AKT (Figure 4.9E and F) phosphorylation looked highly similar. In both cases, the MFIs showed a slight downward trend with continued treatment, but the changes were not significant (ERK blood $p = 0.267$ and bone marrow $p = 0.592$; AKT blood $p = 0.054$ and bone marrow $p = 0.080$) (Figure 4.9G and H).

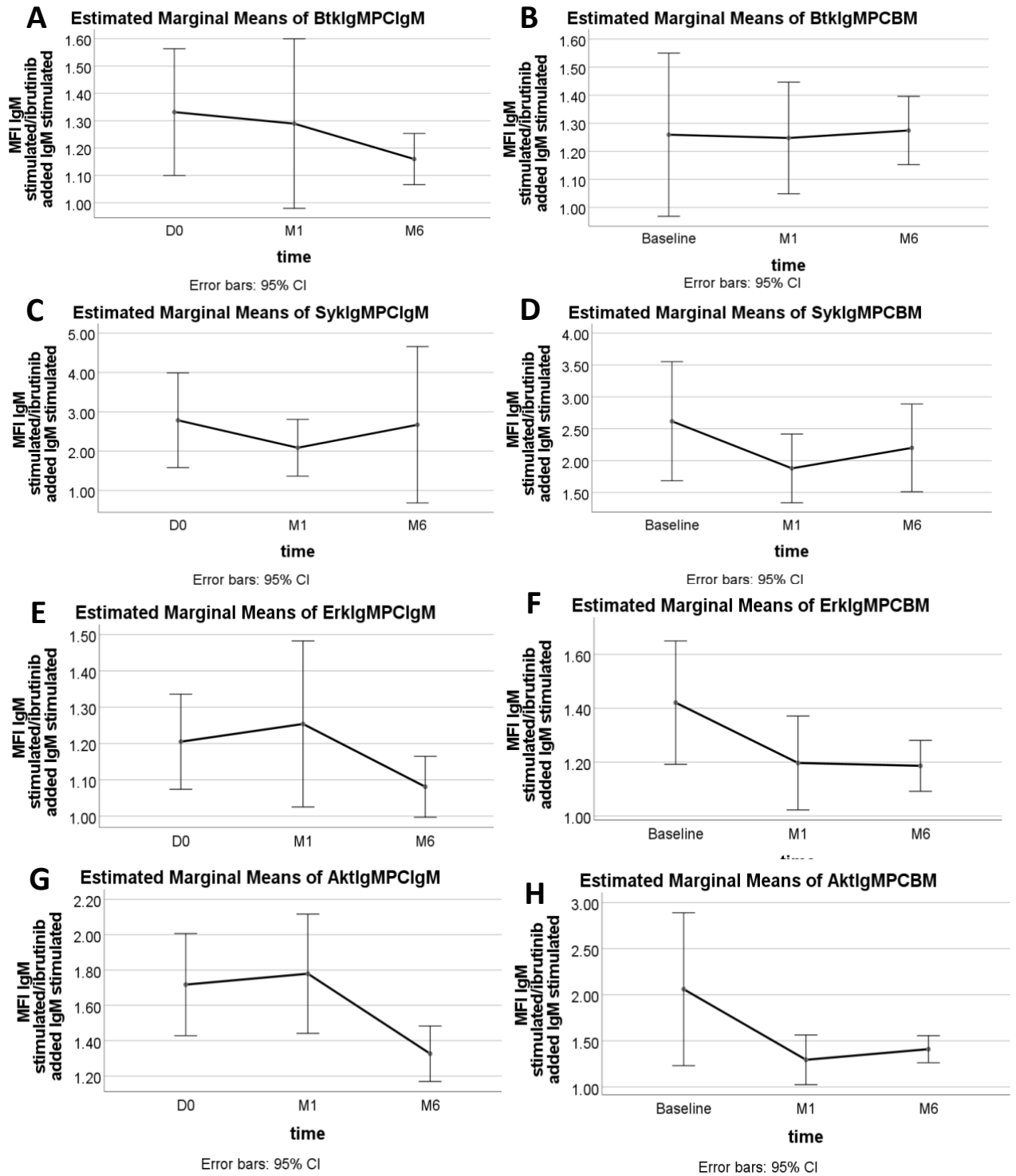


Figure 4.9 Estimated marginal means of kinase phosphorylation following a 30 min pre-treatment with 1 uM Ibrutinib or media followed by stimulation with anti-IgM/D for 2 min. (A) MFI of pBTK (pY551) in stimulated CLL cells/ ibrutinib treated stimulated CLL cells in peripheral blood or (B) bone marrow; (C) MFI of pSYK in peripheral blood or (D) bone marrow; (E)MFI of pERK1/2 in peripheral blood or (F) bone marrow; and (G) MFI of pAKT in peripheral blood or (H) bone marrow.

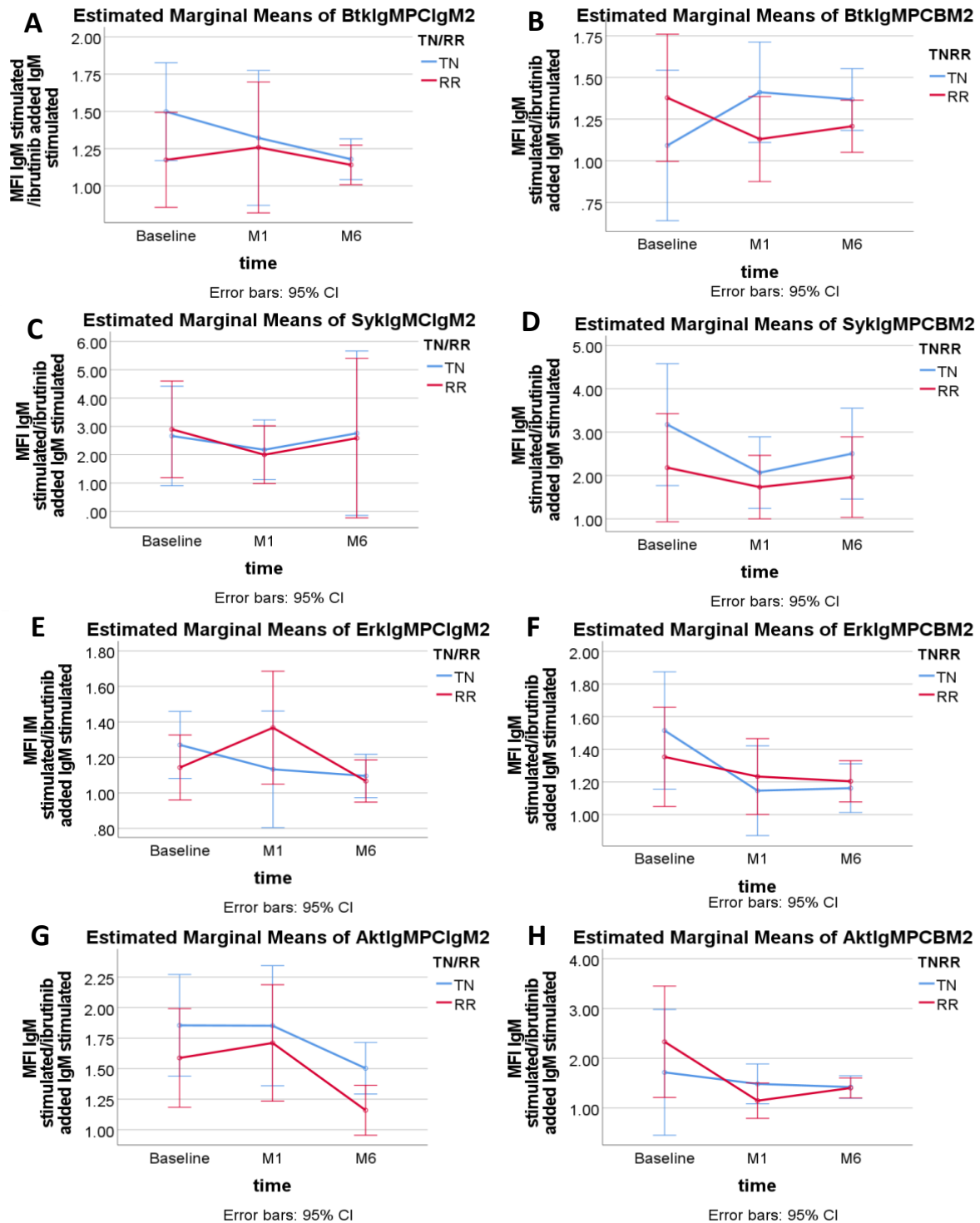


Figure 4.10 Estimated marginal means of kinase phosphorylation following a 30 min pre-treatment with 1 μ M Ibrutinib or media followed by stimulation with anti-IgM/D for 2 min. (A) MFI of pBTK (pY551) in stimulated CLL cells/ ibrutinib treated stimulated CLL cells from treatment naïve patients (TN) vs relapsed refractory (RR) in peripheral blood or (B) bone marrow; (C) MFI of pSYK in peripheral blood or (D) bone marrow; (E) MFI of pERK1/2 in peripheral blood or (F) bone marrow; and (G) MFI of pAKT in peripheral blood or (H) bone marrow.

The overall patterns for each of the kinases appeared to be stable and suggests that fresh ibrutinib has no further effect on stimulated phosphorylation. Evaluation of the two cohorts treated separately did not generate any statistically significant differences in either blood or bone marrow samples for any of the kinases (Figure 4.10).

In short, the addition of *in vitro* exposure to ibrutinib did not impact the IgM/IgD stimulation of various kinases and the results for both cohorts were not statistically significant. This is consistent with the idea that *in vitro* exposure to ibrutinib has minimal impact once the ongoing therapy with ibrutinib ensures an inhibitory effect on intracellular kinases. However, the results did not convincingly show the anticipated fall in ratio between BCR-stimulated /ibrutinib treated stimulated CLL cells.

4.6 CONCLUSIONS

In the ICI-CLL trial, the phosphorylation of key BCR associated kinases were assessed in real-time, along with other parameters. We tested three hypotheses based on phosflow analysis for following kinases including BTK, SYK, ERK1/2 and AKT in both peripheral blood and bone marrow compartments. Based on the data presented here, the following conclusions can be reached:

1. Reduction in steady state phosphorylation of BCR associated kinases with *in vivo* continuous ibrutinib exposure: The data from both TN and RR cohorts suggest that this is true and there is a decline in phosphorylation of kinases with prolonged ibrutinib exposure.
2. Reduction in stimulated state phosphorylation of BCR associated kinases with *in vivo* continuous ibrutinib exposure. There was a consistent decline of stimulated kinases in CLL cells with continued treatment. However, we could not prove the hypothesis when comparing the stimulated kinases vs, the unstimulated kinases in CLL as it did not reach statistical significance in both cohorts and both compartments.
3. Reduction in phosphorylation of kinases in steady-state and stimulated-state with *in vitro* exposure to ibrutinib. There was minimal impact on the kinases with secondary ibrutinib exposure but there was not a significant decline in the ratio of stimulated samples therefore the hypothesis could not be conclusively proven.

4.7 DISCUSSION

There is ample data on the dysregulation of BCR signalling pathway in CLL. SYK has been shown to be overexpressed at mRNA and protein levels(283). Baseline phosphorylation of SYK is higher in CLL cells than in normal B-cells but the response to antigen stimulation via BCR has been shown to be variable (283, 284). The SYK inhibitor R406 abrogates survival after IgM stimulation and reduces downstream targets of BCR signalling, including calcium mobilisation and phosphorylation of ERK and AKT (285).

Aberrant activation of the PI3K/AKT pathway has been shown in CLL and is implicated in cell survival (286). The BTK pathway has also been shown to be amplified in CLL and leads to pro-survival signals through its effects on PI3K, PLC- γ 2, and NF- κ B. BTK expression at the gene level is elevated in CLL compared with normal B cells(233, 238). Inhibition of BTK by ibrutinib induces apoptosis in a caspase-dependent manner and inhibits both phosphorylation of BTK after IgM ligation as well as downstream targets of BTK activation, including ERK, NF- κ B, and AKT (233). Phosphorylation of BTK pY223 and PLC γ 2 was shown to be downregulated with ibrutinib therapy but the gene expression did not change. Also, phosphorylation of ERK, MEK 1/2 and AKT was up regulated with ibrutinib therapy (240).

Finally, ERK1/2 is dysregulated in CLL (204). A subset of CLL patients have constitutive phosphorylation of ERK, which is associated with decreased responsiveness to BCR stimulation like anergic B cells CLL cells, which lack constitutive phosphorylation but show inducible phosphorylation and cell survival in the presence of phorbol ester (287).

Expression of the transcription factor Myc has been found to be dependent on ERK1/2 activation after BCR stimulation, suggesting that this pathway is important to CLL survival and proliferation (276).

The phosflow data from the IciCLLe trial confirms the impact of ibrutinib on phosphorylation of BCR associated kinases but has not provided a definitive answer. Phosphorylation of kinases is a transient event, and the regulation of this process is also complex process. There is an intricate balance between activation and inhibitory kinases as well as the effect of intracellular phosphatases. The utilisation of particular phosflow protocols can also impact the analysis such as addition of H₂O₂ to inhibit phosphatases. In the IciCLLe trial, established protocols were followed to limit any bias or variations in analysis of phosphorylation. Lastly,

the samples were analysed in real-time but there was a variation in the time between blood or bone marrow draw and analysis depending on the means of delivery of the samples to the laboratory. None of the samples were cryopreserved.

The longer follow-up analysis of the phosphorylation of the kinases with continuous ibrutinib in ICI-CLL trial suggests that there is decline in steady state phosphorylation in all kinases. This would be expected as ibrutinib would likely to inhibit signalling downstream of BTK. However, the decline in steady state phosphorylation of SYK is difficult to explain as the kinase is upstream of BTK. One explanation could be the anergic state of CLL cells and the unresponsiveness state of the CLL cells. The unresponsiveness state of CLL cells in peripheral circulation may be enhanced by ibrutinib (288). Phosphorylation of ERK1/2 and AKT S473, downstream of BTK was effectively downregulated by ibrutinib.

The data also shows that the IgM/IgD stimulation of the kinases were reduced with continuous ibrutinib therapy. This was consistent in both compartments and at various assessed time points. However, there was not a consistent difference of phosphorylation in kinases between stimulated and unstimulated state. This may suggest decreased responsiveness to the external stimulus as seen in other studies as well (238, 288, 289). However, the surface expression of surface IgM has been shown to increase in CLL patients receiving ibrutinib with minimal impact on surface IgD expression (290). This may well suggest an inhibitory milieu in the CLL cells with continuous ibrutinib therapy.

Lastly, assessment of *ex vivo* addition of ibrutinib at all time points suggested that there was minimal impact of addition of ibrutinib on the kinase activation in this scenario. While this data generally fits with the hypothesis that *in vivo* exposure is sufficient to terminate subsequent signalling, the experiments with added stimulation failed to show a significant drop. This was unexpected, but it is conceivable that persistent cells are exhibiting a variable response in phosphorylation of kinases as shown in other studies where the effect of ibrutinib has been assessed with continuous therapy (240).

CHAPTER 5:

**Does phosphorylation of kinases
inform the degree of clinical response
in patients treated with ibrutinib?**

5.1 INTRODUCTION

This Chapter focuses on the hypothesis that the degree of phosphorylation of intracellular kinases should correlate with the clinical responses observed in the clinical trial. This exploratory analysis was performed based on phosflow responses achieved at various time points of the study and compared to responses in the treatment naïve (TN) and relapsed refractory (RR) cohorts. Assessment of phosflow correlation was made with following clinical parameters:

- Phosflow response in TN and RR cohorts
- Correlation with radiological responses
- Correlation with haematological responses
- Correlation with peripheral blood lymphocytosis responses

It was hypothesised that a significant drop in kinase phosflow MFI in the unstimulated and IgM/IgD-stimulated state in CLL cells will result in better clinical responses. The fall in MFI was assessed in kinases including:

- Phospho-ERK 1/2
- SYK pY348
- BTK pY551
- AKT S473

The phosflow response was considered as a complete response if there was a drop in phosphorylation in three or more out of four kinases in unstimulated and stimulated states. It was considered as a partial response if there was a drop in phosphorylation in two of four kinases. Finally, it was considered as an insignificant response if there was no drop in phosphorylation of kinases at various time points.

Clinical data was collected as per trial protocol, which has been detailed in Chapter 3. The responses are assessed as per IWCLL criteria in terms of response assessments.

5.2 CORRELATION OF PHOSFLOW RESPONSE WITH TREATMENT STATUS

Table 5.1 shows the correlation of treatment status with phosflow response. The responses shown in the table are presented for TN and RR cohorts. All patients showed a reduction in phosphorylation of the 4 intracellular kinases being evaluated. In TN cohort, 9/19 participants demonstrated complete phosflow response, whereas only 4/20 participants in the RR cohort showed a complete phosflow response as manifested by reduction in phosphorylation of at least three out of four kinases. Most responses in RR cohorts manifested partial phosflow responses comprising 16/20 participants, whereas 10/19 participants in TN cohort also manifested partial phosflow responses. This suggests that reduction in phosphorylation of intracellular kinases is more prominent in TN cohort.

Table 5.1 Correlation of Phosflow response in treatment naïve and relapsed refractory cohorts.

Treatment status with phosflow Crosstabulation					
			Phosflow		Total
			CR-Ph*	PR-Ph^	
Treatment status	TN	Count	9	10	19
		% within Treatment status	47.4%	52.6%	100.0%
		% within Phosflow	69.2%	38.5%	48.7%
		% of Total	23.1%	25.6%	48.7%
	RR	Count	4	16	20
		% within Treatment status	20.0%	80.0%	100.0%
		% within Phosflow	30.8%	61.5%	51.3%
		% of Total	10.3%	41.0%	51.3%
Total		Count	13	26	39

	% within Treatment status	33.3%	66.7%	100.0%
	% within Phosflow	100.0%	100.0%	100.0%
	% of Total	33.3%	66.7%	100.0%

*CR-Ph- Complete response- Phosflow

^PR-Ph- Partial response- Phosflow

Figure 5.1 show the bar chart of phosflow responses in the TN and RR cohorts. There were more complete phosflow responses in the TN cohort as compared to RR cohort, though partial responses were observed in majority of participants in both cohorts.

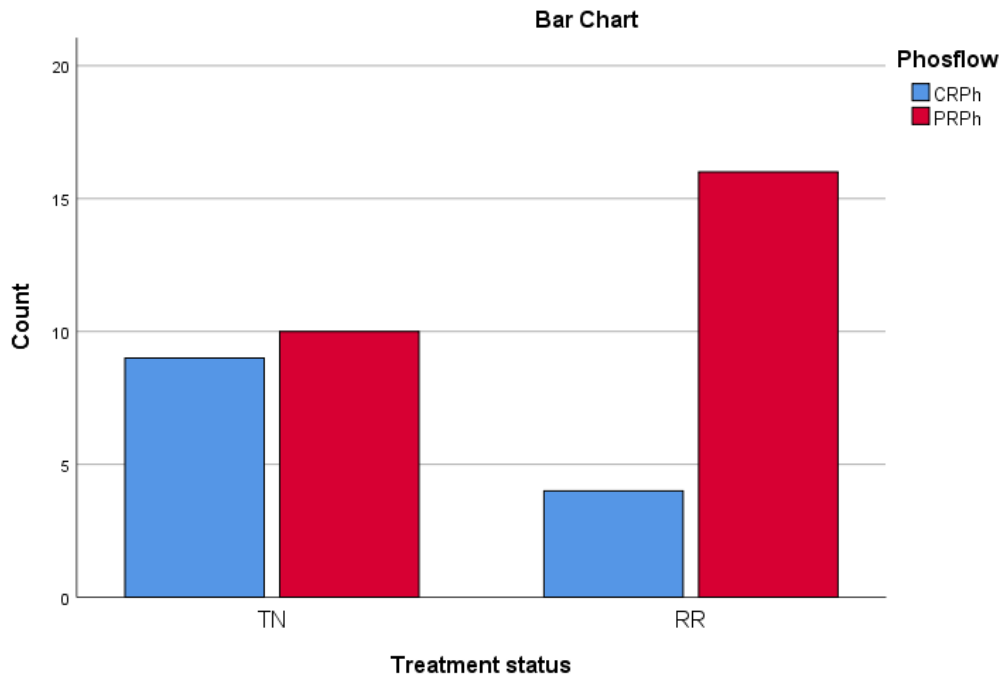


Figure 5.1 Bar charts showing the correlation of cohorts with phosflow response. The number of cases with complete phosflow response (CRPh) are shown in blue and partial phosflow response (PRPh) in red.

Table 5.2 exhibits the Chi-Square tests analysis of significance of treatment status with the respective phosflow analysis. Even though not statistically significant, RR patients are less likely to have complete phosflow response than TN patients (Pearson Chi-Square $p=0.070$).

The numbers are too small to reach definite conclusions, but the data is suggestive of deeper reduction in phosphorylation of kinases in the TN cohort as compared to RR cohort.

Table 5.2 Chi-Square tests analysis of significance of treatment status with phosflow analysis.

Chi-Square Tests					
	Value	df	Asymptotic Significance (2- sided)	Exact Sig. (2- sided)	Exact Sig. (1- sided)
Pearson Chi-Square	3.284 ^a	1	.070		
Fisher's Exact Test				.096	.070
N of Valid Cases	39				
a. 0 cells (0.0%) have expected count less than 5. The minimum expected count is 6.33.					

5.3 CORRELATION OF PHOSFLOW WITH RADIOLOGICAL RESPONSE

Assessment of the correlation of phosflow response with radiological response on the clinical trial showed that participants achieving complete radiological response are more likely to also achieve complete phosflow response. As shown in the Table 5.3, 8 participants achieved complete radiological response and a complete phosflow response; 19 participants achieving a partial radiological response also achieved a partial or stable phosflow response. The concordance is not complete but deeper radiological responses correlated with deeper phosflow responses.

Table 5.3 Correlation of Radiological response with phosflow response.

Combined CT data with phosflow Crosstabulation					
			Phosflow		Total
			CRPh	PRPh	
Combined CT data	CTCR	Count	8	7	15
		% within Combined CT data	53.3%	46.7%	100.0%
		% within Phosflow	61.5%	26.9%	38.5%
		% of Total	20.5%	17.9%	38.5%
	CTPR	Count	5	19	24
		% within Combined CT data	20.8%	79.2%	100.0%
		% within Phosflow	38.5%	73.1%	61.5%
		% of Total	12.8%	48.7%	61.5%
Total	Count	13	26	39	
	% within Combined CT data	33.3%	66.7%	100.0%	
	% within Phosflow	100.0%	100.0%	100.0%	
	% of Total	33.3%	66.7%	100.0%	

Figure 5.2 shows the bar chart for the correlative data between radiological responses and phosflow responses. This again reflects that most participants achieved partial radiological and phosflow responses. However, improvement in depth of radiological response correlated with higher number of participants achieving deeper phosflow response.

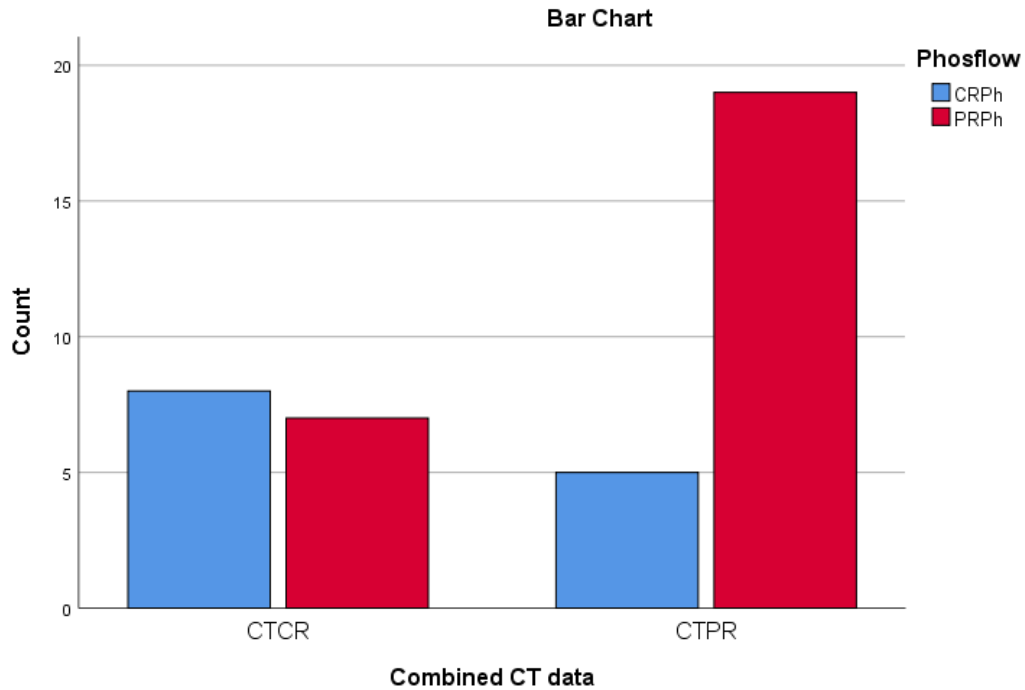


Figure 5.2 Bar charts showing the correlation of radiological response with phosflow response. The number of cases with complete phosflow response (CRPh) are shown in blue and partial phosflow response (PRPh) in red.

Table 5.4 illustrates the Chi-Square tests analysis of significance between radiological and phosflow response. Participants who had excellent phosflow response are more likely to have complete radiological response compared to participants who had partial or stable phosflow response (Pearson Chi-Square $p=0.036$). The difference is statistically significant between the two groups.

Table 5.4 Chi-Square tests analysis of significance of radiological response with phosflow response

Chi-Square Tests					
	Value	df	Asymptotic Significance (2- sided)	Exact Sig. (2- sided)	Exact Sig. (1- sided)
Pearson Chi-Square	4.387 ^a	1	.036		
Fisher's Exact Test				.079	.041
N of Valid Cases	39				

a. 0 cells (0.0%) have expected count less than 5. The minimum expected count is 5.00.

5.4 CORRELATION OF PHOSFLOW WITH HAEMATOLOGICAL RESPONSE

Assessment of the correlation of phosflow response with haematological response showed that participants achieving complete haematological response, which is defined by normal Haemoglobin levels, Neutrophil count, and platelet count are more likely to also achieve complete phosflow response. Table 5.5 illustrates that 9 participants achieved complete haematological response and achieved a complete phosflow response; 21 participants achieving a partial haematological response also achieved a partial or stable phosflow response. The concordance is not complete but deeper haematological responses correlated with deeper phosflow responses.

Table 5.5 Correlation of Haematological response with phosflow response.

Haem data with phosflow Crosstabulation					
			Phosflow		Total
			CRPh	PRPh	
Haem data	CRhaem	Count	9	5	14
		% within Haem data	64.3%	35.7%	100.0%
		% within Phosflow	69.2%	19.2%	35.9%
		% of Total	23.1%	12.8%	35.9%
	PRhaem	Count	4	21	25
		% within Haem data	16.0%	84.0%	100.0%
		% within Phosflow	30.8%	80.8%	64.1%
		% of Total	10.3%	53.8%	64.1%
Total	Count	13	26	39	
	% within Haem data	33.3%	66.7%	100.0%	
	% within Phosflow	100.0%	100.0%	100.0%	
	% of Total	33.3%	66.7%	100.0%	

Figure 5.3 shows the bar chart for the correlative data between haematological and phosflow responses. Most participants achieved partial haematological and phosflow responses. However, improvement in depth of haematological responses correlated with higher number of participants achieving deeper phosflow response. Only a small number of participants achieving partial haematological response had concomitant complete phosflow response.

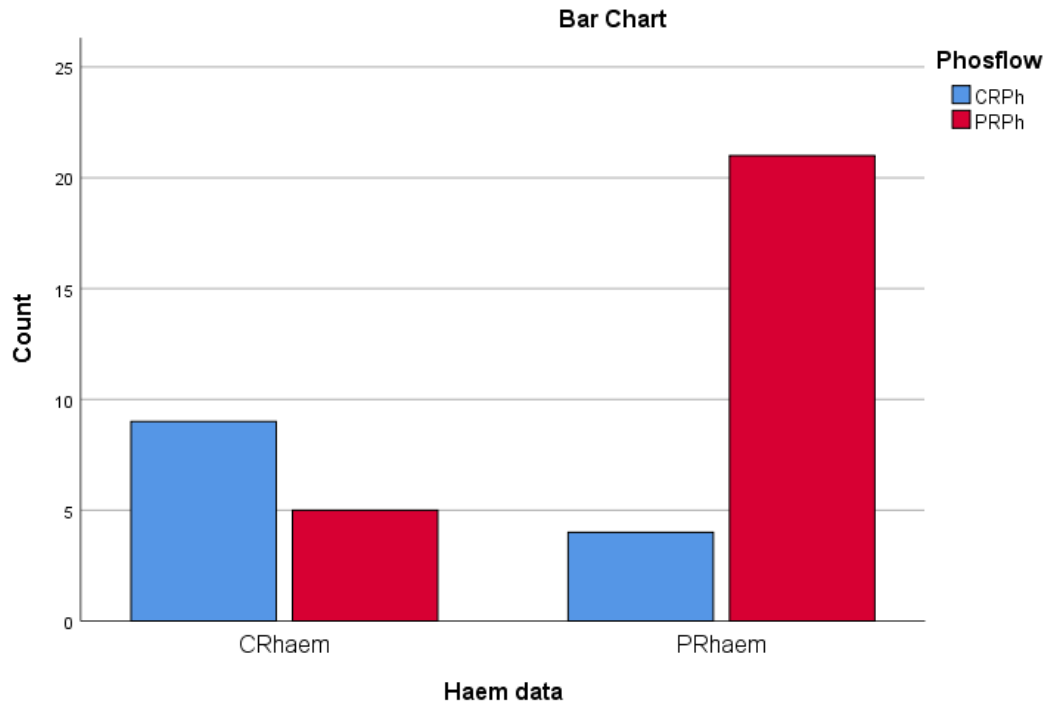


Figure 5.3 Bar charts showing the correlation of haematological response with phosflow response. The number of cases with complete phosflow response (CRPh) are shown in blue and partial phosflow response (PRPh) in red.

Table 5.6 illustrate that participants who had an excellent phosflow response are more likely to have complete haematological response compared to patients who had partial or stable phosflow response (Pearson Chi-Square $p=.002$). The analysis showed statistically significant deeper phosflow response correlating with complete haematological response.

Table 5.6 Chi-Square tests analysis of significance of Haematological response with phosflow response.

Chi-Square Tests					
	Value	df	Asymptotic Significance (2-sided)	Exact Sig. (2-sided)	Exact Sig. (1-sided)
Pearson Chi-Square	9.416 ^a	1	.002		
Fisher's Exact Test				.004	.003
N of Valid Cases	39				
a. 1 cells (25.0%) have expected count less than 5. The minimum expected count is 4.67.					

5.5 CORRELATION OF PHOSFLOW WITH PERIPHERAL BLOOD LYMPHOCYTOSIS

Assessment of the correlation of phosflow response with peripheral blood lymphocytosis, as defined by absolute lymphocyte count less than $4 \times 10^9/L$, showed that participants achieving normalisation of lymphocytes are likely to also achieve complete phosflow response. Table 5.7 illustrates that 13 participants achieved normal lymphocyte count and a complete phosflow response; 25 Participants achieved partial phosflow response

Table 5.7 Correlation of peripheral blood lymphocytosis with phosflow response.

Peripheral blood * phosflow Crosstabulation					
			Phosflow		Total
			CRPh	PRPh	
Peripheral blood	CRPB	Count	8	14	22
		% within Peripheral blood	36.4%	63.6%	100.0%
		% within Phosflow	61.5%	56.0%	57.9%
		% of Total	21.1%	36.8%	57.9%
	PRPB	Count	5	11	16
		% within Peripheral blood	31.3%	68.8%	100.0%
		% within Phosflow	38.5%	44.0%	42.1%
		% of Total	13.2%	28.9%	42.1%
Total	Count	13	25	38	
	% within Peripheral blood	34.2%	65.8%	100.0%	
	% within Phosflow	100.0%	100.0%	100.0%	
	% of Total	34.2%	65.8%	100.0%	

Figure 5.4 shows the bar chart for the correlative data between peripheral blood lymphocytosis and phosflow responses. The response data is heterogenous and the peripheral blood lymphocytosis does not correlate with the phosflow data.

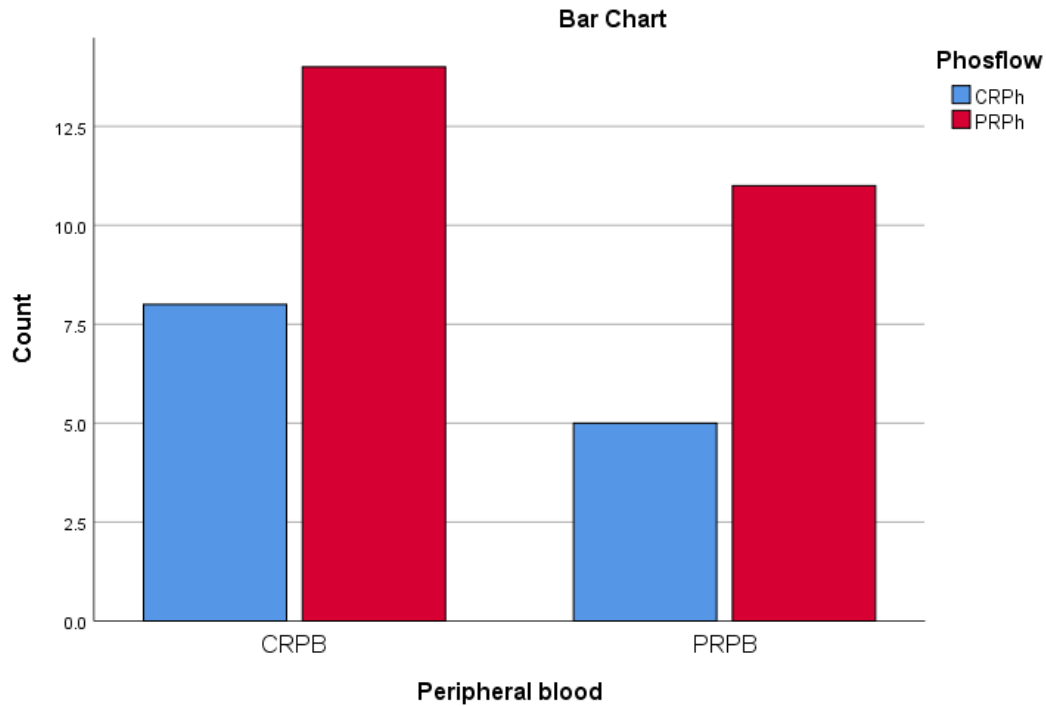


Figure 5.4 Bar charts showing the correlation of peripheral blood lymphocytosis with phosflow response. The number of cases with complete phosflow response (CRPh) are shown in blue and partial phosflow response (PRPh) in red.

Table 5.8 illustrates that there is no statistically significant correlation between phosflow response and peripheral blood lymphocytosis in response to ibrutinib.

Table 5.8 Chi-Square tests analysis of significance of peripheral blood lymphocytosis with phosflow response.

Chi-Square Tests					
	Value	df	Asymptotic Significance (2-sided)	Exact Sig. (2-sided)	Exact Sig. (1-sided)
Pearson Chi-Square	.108 ^a	1	.743		
Fisher's Exact Test				1.000	.510
N of Valid Cases	38				

a. 0 cells (0.0%) have expected count less than 5. The minimum expected count is 5.47.

5.6 CONCLUSIONS

This Chapter tests the hypothesis that the phosflow data will predict clinical responses observed in the ICI-CLL trial. In the trial, the clinical responses were assessed as per 2008 IWCLL response criteria. These criteria include haematological and radiological responses. The complete haematological response is characterised by normalisation of Haemoglobin, neutrophil count and platelet count. Complete radiological response is defined as absence of any measurable lymph nodes and normalisation of liver and spleen size. Lymphocytosis is a feature typical of BTK inhibitor therapies which is caused by shifting of CLL cells from the lymph nodes and bone marrow into the peripheral blood (238, 291).

The analysis of phosflow data suggests that it is possible to correlate the response. We hypothesized that a decline in phosphorylation in kinases downstream of the BCR in both stimulated and unstimulated states with continuous ibrutinib may correlate with clinical responses. The assessment of phosflow responses in TN suggested deeper responses which is understandable, as the TN patients have no previous exposure to therapies such as chemo-immunotherapy and the disease is likely to be more responsive to BTK inhibitor therapy in this setting. There were more participants in the TN cohort who achieved a deeper phosflow response as compared to RR cohort where response was less apparent in all kinases assessed. The phosflow data also suggests that the responses are again observable in all kinases with participants achieving complete haematological and radiological responses. This finding may also suggest the varied sensitivity of the kinases to the continuous ibrutinib therapy resulted in the varied clinical responses. Moreover, the data lend support to the idea that the degree of phosflow responses could be used to identify the best responders.

The assessment of phosflow has been done in a variety of previous studies (292). The inhibition of phosphorylation of BTK, PLC γ 2 and ERK correlated with clinical responses in phase 1/2 study looking the efficacy of ibrutinib and suggested that full inhibition would

require more than a single dose, potentially due to secondary effects of the microenvironment (289). Another study explored the degree of phosphorylation at baseline and at 28 days into treatment. The activities of BTK and PLC γ 2 as well as downstream signalling molecules, AKT and ERK, were all co-ordinately downregulated over time in ibrutinib-treated patients and this correlated with clinical responses (293). The data presented within this chapter agree with these earlier findings. The increased number of longitudinal samples and additional clinical parameters in this study strengthen the idea that successful outcome after continuous ibrutinib therapy is directly linked to the degree of signalling inhibition.

However, there are caveats to the interpretation of phosflow data. Firstly, the criteria used to assess a complete or partial phosflow responder is not well defined and this was an exploratory analysis performed as part of the trial. However, it is assumed that the ability to downregulate the phosphorylation of major kinases in the B-cell receptor pathway with continuous ibrutinib monotherapy should be considered as a marker of decent response; Hence, this hypothesis could be preliminarily assessed in the context of this trial. Secondly, there are other confounding factors such as phosphorylation of other kinases in the B cell receptor pathway which cannot be assessed due to limitation of number of kinases being assessed on the flow cytometer and the need to perform this analysis in real time. For example, phosphorylation of alternative kinases or other target residues on BTK, SYK, AKT was not done but all these experiments were performed prior to the trial and the most relevant kinases were assessed. Lastly, the depth of phosflow responses correlated well with clinical responses but there were outliers in the analysis and there are other factors which could not be assessed as part of the clinical trial.

In short, the ability of ibrutinib to downregulate phosphorylation of various kinases forms an intriguing concept of correlation with clinical response and this should be assessed in the context of larger clinical trials.

CHAPTER 6:

CONCLUSION AND DISCUSSION

IciCLLe trial was conducted to assess the response to ibrutinib with in-depth analysis of clinical, immunophenotypic, biological response. It was a small phase-2 study incorporating 20 TN and RR patients each and recruitment started in 2014. It is fair to say that the treatment landscape of CLL has changed beyond recognition over the last 5 years. Three classes of drugs have made a major impact on management of CLL which include BTK inhibitors, anti-CD20 monoclonal antibodies and BCL-2 inhibitors. Ibrutinib has now been licensed by FDA and EMA for use alone or in combination with chemo-immunotherapy or anti-CD20 such as Obinutuzumab in both TN and RR CLL (294, 295). Ibrutinib in combination with the BCL-2 inhibitor, Venetoclax has also been assessed in NCRI trial “CLARITY study” for relapsed refractory CLL and this combination is now being assessed in frontline phase 3 studies including “FLAIR” and “GLOW”(255, 296, 297). In short, the changing landscape of CLL management has improved outcomes for CLL patients by improving efficacy and making treatments more tolerable even with combinations.

However, there are unanswered questions as CLL is still an incurable disease despite the advances made in the last decade. Our understanding of biology of CLL has been enhanced by the development of these classes of drugs but the impact of these drugs on various subtypes of CLL has been heterogeneous. For example, ECOG 1912 study suggested that the impact of combining ibrutinib and rituximab is most profound on UM-IGHV CLL and this resulted in improved outcomes as compared to patients receiving CIT (113). This finding can be explained by some biological reasoning that the proliferation of the UM-IGHV clone happens in context of a microenvironment where the clone can be responsive to multiple antigenic stimuli (218). It is also intriguing that BTKi cannot completely clear the disease despite extensive clearance of nodal compartment and bone marrow (BM) with continuous therapy. This is supported by the evidence that cell death happens with BTKi therapy, but the process is slow (239). Another unclear question in terms of continuous therapy is the differential response achieved in TN and RR CLL patients. The duration responses are shorter with each line of therapy in RR CLL, and this has been a consistent feature in all the ibrutinib trials (110, 112, 118). The median PFS for trials involving TN CLL patients have not

reached despite some trials now reporting up to 6 years follow-up (112). However, the median PFS for ibrutinib monotherapy was 44.1 months in RESONATE trial and was 65.1 months for ibrutinib in combination with BR in HELIOS study (118, 256). What the biological features are that distinguish the response in TN and RR cohorts are not clear. It is thought that genomic instability acquired with multiple lines of therapies in RR CLL results in shortened responses, such as acquisition of TP53 aberrations in relapsed refractory CLL, are more common (271). However, TN patients harbouring TP53 aberrations continue to show a decent response to ibrutinib monotherapy which is different to the RR patients harbouring TP53 aberrations (298).

In ICI-CLE trial, the clinical responses were assessed as per IWCLL criteria in both TN and RR cohorts. In a small study like this with 20 patients in each cohort, no stratification was performed though there were some baseline differences in the two cohorts. The degree of bone marrow infiltration was higher in TN cohort, whereas RR cohort had more adverse genetic parameters. This is in line with other reported studies. There was an improvement in all haematological parameters and there was more pronounced clearance of BM in the TN group over time. The PFS after a median follow-up of 5 years in both arms of the study is consistent with what has been reported in literature (112, 118, 256). The data is constantly being updated, and patients will continue to be followed up in the study to get the maximum information on the long-term outcomes.

One of the primary endpoints of the study was achievement of MRD-negativity at the IWCLL criteria of 1×10^{-4} and it was clear that no patient achieved MRD-negativity in both cohorts. This is understandable and consistent with reported literature. However, the assessment of MRD and subsequent analysis of immunophenotypic changes in the CLL cells with continuous ibrutinib monotherapy has helped to understand the pattern of surface expression of various antigens along with the changes in proliferation markers. These results have helped to inform the development of next set of phase 2 trials in CLL. For example, in ICI-CLE extension trial, anti-CD20 antibody Obinutuzumab was added in 10 patients from ICI-CLE trial who had been taking ibrutinib for more than 1 year. This was compared to concomitant use of ibrutinib and Obinutuzumab together. This was based on the finding that the CD20 expression on CLL cells initially declines with ibrutinib and regained after more than 6 months of continuous therapy (299). Hence, the biological findings in the trial

helped to inform the next set of trials. Other trials where anti-CD20 antibodies have been combined with BTKi in relapsed refractory CLL have reported outcomes as per IWCLL criteria but have not reported the biological changes resulting in surface expression changes of various antigens in CLL (257, 300-304).

In ICI-CLL trial, assessment of phosphorylation of BCR associated kinases were assessed with a flow cytometry-based assay "Phosflow". The assessments were performed in peripheral blood (PB) and bone marrow (BM) at various time points up to a year and thereafter. The assessments were performed in real-time along assessment of MRD and cell surface expression markers. Rigid protocols were followed, and the samples were run on the flow cytometer in parallel. Hence, every effort was taken to reduce the bias in the performance of the assay. Optimisation of assay was performed before the initiation of trial and a single BD Fortessa machine was used to acquire as well as analyse the samples.

There were benefits and disadvantages to this approach. The benefits were the uniformity of acquisition of samples and applying same protocol to each sample ran on the machine. As a result, the protocol was followed by other team members for using this assay in other clinical trials and in the extension of this study. The assay was incorporated as a routine assay performed in HMDS, Leeds. There were clear disadvantages with this approach. As the trial was conducted in multiple UK centres, the delivery time from withdrawal of blood sample from the patient and receipt in HMDS, Leeds varied significantly. Every effort was taken to proceed with analysis after receipt of sample but the delays in transit may have induce some variability into the analysis. This issue was partly mitigated by the experiments performed prior to trial where same sample from a patient was analysed at day 1, 2 and day 3. The phosflow results were consistent at these but there was more loss of cells along with debris and noise if the sample was analysed after 4 days. This issue could not have been resolved even if we cryopreserved the samples as cryopreservation was not available at various sites and there was no funding available.

The data from phosflow in both compartments including PB and BM suggested that the phosphorylation of the assessed kinases in the steady state whether upstream or downstream of target of ibrutinib i.e., BTK decline with continuous therapy. The effect was consistent across both TN and RR cohorts with no major differences which reached

statistical significance. Explanation of the downregulation of assessed kinases can be based on the hypothesis that blocking the main signalling pathway via the BCR induces a state of anergy. This can be partially overcome with stimulation via other signalling pathways but ibrutinib may be able to induce an inhibitory effect on the kinome of CLL cells in both compartments. There were very few CLL patients with M-IGHV in ICI-CLL trial and no comparison could be made to UM-IGHV patients. It is known that M-IGHV CLL cells are in state of anergy, and it was interesting to note the analysis that majority of analysed samples had downregulation of phosphorylated kinases with continuous ibrutinib despite more CLL cases with UM-IGHV state in this trial (204). It is also clear from other studies with longer follow-up that the response deepens with on-going therapy with ibrutinib, but eradication of disease is not possible. This may suggest that signalling via BCR pathway is downregulated but not completely abrogated with continuous ibrutinib.

The next step was the analysis of the effect of stimulation of BCR pathway with induction with IgM/IgD. As CLL cells have reduced sIgM expression but retained IgD expression, the use of IgM and IgD together ensured induction of the pathway at all time points. The differential effect of stimulation via IgM or IgD is well known but the essence in this trial here was to ensure effective stimulation whilst covering all basis. As the main signalling pathway in B cells and CLL cells is through the BCR pathway, analysis via stimulation of TLR signalling or CD40-L was not performed. This analysis supplemented the early finding that stimulation with IgM/IgD consistently declined in both compartments and in both cohorts. There were variations in individual responses, but the overall picture was consistent with inhibitory state.

Ex vivo addition of ibrutinib in CLL cells results in inhibition of BTK and it has been shown various studies that addition of ibrutinib induces a state of inhibitory milieu in the CLL kinome especially ibrutinib. These studies have used different protocols and different antibodies to assess the phosphorylation of tyrosine kinases at different sites especially BTK such as BTK pY223. One difference in protocols was that analysis of the steady state phosphorylation and stimulated state was performed without addition of any phosphatase inhibitors. This ensured that there was minimal impact on the baseline phosphorylation state as there is a balance of stimulated kinases and inhibitory phosphatases in CLL cells. This could partly explain why we did not see a major impact on *ex vivo* addition of ibrutinib.

Another explanation could be the irreversible inhibition of BTK with continuous ibrutinib and minimal impact of *ex vivo* addition of ibrutinib.

There are caveats to generalised interpretation of phosphorylation of BCR related kinases. It was not possible to analyse all cellular kinases in this trial, but we did analyse limited samples for phosphorylation of other kinases such MAPK-p38 and AKT pT308. It was not possible to run all the antibodies at the same time due to number of tests being performed and the availability of antibodies on different fluorochromes. Hence, it was decided to use the most relevant kinases for this analysis. Whether ibrutinib impacted other kinases which are directly or indirectly related to BCR pathway cannot be interpreted based on this analysis. However, the hypothesis can be generated, and it would be interesting to analyse this in future trials as the options to analyse multiple antibodies for various cellular kinases simultaneously has improved with the advent of 10-16 coloured flow cytometers. Though we did not analyse the impact of addition of phosphatases in a similar context of the clinical trial, this would be an interesting analysis to be performed in future trials.

The other limitation of this was the lack the comparison of phosphorylated kinase and total kinase. Though phosphorylation is the major step in the stimulation or inhibition of kinase activity, it would have been a useful adjunct to the data to establish whether the inhibitory effect of the drug results in steady or increased production of total kinase as compared to phosphorylated kinase. The limiting factor again was the difficulty in performing multiple analysis in a single experiment for multiple samples at various time points.

In Chapter 5, the intriguing question of whether one can infer any more information from the phosphorylation data and correlate it with the clinical response is presented. The trial gave a unique opportunity as the sampling was done frequently and analysis was performed at various time points. The hypothesis was that the deeper phosphorylation responses resulted in better clinical response. First, the phosflow data correlated with clinical, haematological and radiological response. Secondly, there was correlation with peripheral blood lymphocytosis and patients achieving reduction in lymphocytes also achieved a better phosflow response. Lastly, the phosflow response in TN group was better than RR group and this finding is consistent with what has been described in term of clinical response as above.

The interpretation of this analysis was based on the hypothesis that steady-state decline in phosphorylation in the kinases will result in better responses. This approach has not been verified in larger studies, but it is an intriguing concept and may help to ascertain another way to assess functional biological response in CLL. What is lacking is the change in the phosphorylation pattern of the kinases at relapse. The trial did not incorporate this endpoint as an essential assessment in terms of biological changes. Also, there have been very few relapses and the samples were not available for analysis. Some relapses were due to Richter's syndrome, and it was not possible to get an appropriate sample due to the clinical need to start chemo-immunotherapy for treatment of Richter's syndrome.

In short, IciCLLe trial was one of the first NCI trials to assess the effectiveness of ibrutinib in treatment of TN and RR CLL. The trial tried to incorporate clinical responses with biological responses and provided interesting insights into the phosphorylation marks in CLL kinome with continuous ibrutinib therapy. The data of the trial informed the next set of trials including IciCLLe extension and CLARITY (255, 299). These small phase 2 designed trials conducted in TN and RR CLL have enabled the larger phase 3 NCI trial FLAIR which has been amended to incorporate the findings of above-mentioned trials.

The future direction for this work will likely incorporate similar phase 2 studies that combine clinical and biological work together. The data from the trial has informed us about the need for assessment at fewer time points which should reduce the workload but will allow the incorporation of other important biological endpoints. At present, efforts are being made to use reversible BTKi, Pirtobrutinib in patients relapsing on irreversible BTKi (305). The plan is to analyse the same aspects as assessed in the IciCLLe trial but also incorporate transcriptome and genomic data in collaboration with other centres. Analysis of phosphorylation marks on various BCR related kinases will be one of the assessments planned in the trial. This will help to ascertain phosphorylation patterns at baseline on patients relapsing on irreversible BTKi and subsequent impact of reversible BTKi on phosphorylation of cellular kinases associated with BCRi.

Acknowledgements:

I would like to thank Professor Peter Hillmen, Dr Gina Doody for their constant support and help. This work would not have been possible without their help. I would also like to pay my

special thanks to Dr Abraham Varghese and Dr Andy Rawstron for their encouragement and helping through the whole process of this work.

References:

1. Montecino-Rodriguez E, Dorshkind K. B-1 B cell development in the fetus and adult. *Immunity*. 2012;36(1):13-21.
2. Pillai S, Cariappa A. The follicular versus marginal zone B lymphocyte cell fate decision. *Nature reviews Immunology*. 2009;9(11):767-77.
3. Baumgarth N. The double life of a B-1 cell: self-reactivity selects for protective effector functions. *Nature reviews Immunology*. 2011;11(1):34-46.
4. Cerutti A, Cols M, Puga I. Marginal zone B cells: virtues of innate-like antibody-producing lymphocytes. *Nature reviews Immunology*. 2013;13(2):118-32.
5. Springer GF, Horton RE. Blood group isoantibody stimulation in man by feeding blood group-active bacteria. *The Journal of clinical investigation*. 1969;48(7):1280-91.
6. Wuttke NJ, Macardle PJ, Zola H. Blood group antibodies are made by CD5+ and by CD5- B cells. *Immunology and cell biology*. 1997;75(5):478-83.
7. Grönwall C, Vas J, Silverman GJ. Protective Roles of Natural IgM Antibodies. *Frontiers in immunology*. 2012;3:66.
8. Suzuki K, Maruya M, Kawamoto S, Fagarasan S. Roles of B-1 and B-2 cells in innate and acquired IgA-mediated immunity. *Immunological reviews*. 2010;237(1):180-90.
9. Arnon TI, Horton RM, Grigorova IL, Cyster JG. Visualization of splenic marginal zone B-cell shuttling and follicular B-cell egress. *Nature*. 2013;493(7434):684-8.
10. Murphy K, Weaver C. *Janeway's immunobiology*: Garland science; 2016.
11. Hoffman W, Lakkis FG, Chalasani G. B Cells, Antibodies, and More. *Clinical Journal of the American Society of Nephrology*. 2016;11(1):137-54.
12. Cobaleda C, Schebesta A, Delogu A, Busslinger M. Pax5: the guardian of B cell identity and function. *Nature immunology*. 2007;8(5):463-70.
13. Thomas MD, Srivastava B, Allman D. Regulation of peripheral B cell maturation. *Cellular immunology*. 2006;239(2):92-102.
14. Wardemann H, Yurasov S, Schaefer A, Young JW, Meffre E, Nussenzweig MC. Predominant autoantibody production by early human B cell precursors. *Science (New York, NY)*. 2003;301(5638):1374-7.
15. Cambier JC, Gauld SB, Merrell KT, Vilen BJ. B-cell anergy: from transgenic models to naturally occurring anergic B cells? *Nature reviews Immunology*. 2007;7(8):633-43.
16. Hervé M, Isnardi I, Ng YS, Bussel JB, Ochs HD, Cunningham-Rundles C, et al. CD40 ligand and MHC class II expression are essential for human peripheral B cell tolerance. *The Journal of experimental medicine*. 2007;204(7):1583-93.

17. Rathmell JC, Townsend SE, Xu JC, Flavell RA, Goodnow CC. Expansion or elimination of B cells in vivo: dual roles for CD40- and Fas (CD95)-ligands modulated by the B cell antigen receptor. *Cell*. 1996;87(2):319-29.
18. Nutt SL, Hodgkin PD, Tarlinton DM, Corcoran LM. The generation of antibody-secreting plasma cells. *Nature reviews Immunology*. 2015;15(3):160-71.
19. Cerutti A, Cols M, Puga I. Activation of B cells by non-canonical helper signals. *EMBO reports*. 2012;13(9):798-810.
20. Victora GD, Nussenzweig MC. Germinal centers. *Annual review of immunology*. 2012;30:429-57.
21. Cyster JG. Chemokines, sphingosine-1-phosphate, and cell migration in secondary lymphoid organs. *Annual review of immunology*. 2005;23:127-59.
22. Kerfoot SM, Yaari G, Patel JR, Johnson KL, Gonzalez DG, Kleinstein SH, et al. Germinal center B cell and T follicular helper cell development initiates in the interfollicular zone. *Immunity*. 2011;34(6):947-60.
23. Green JA, Cyster JG. S1PR2 links germinal center confinement and growth regulation. *Immunological reviews*. 2012;247(1):36-51.
24. Shlomchik MJ, Weisel F. Germinal center selection and the development of memory B and plasma cells. *Immunological reviews*. 2012;247(1):52-63.
25. Muramatsu M, Kinoshita K, Fagarasan S, Yamada S, Shinkai Y, Honjo T. Class switch recombination and hypermutation require activation-induced cytidine deaminase (AID), a potential RNA editing enzyme. *Cell*. 2000;102(5):553-63.
26. Papavasiliou FN, Schatz DG. Somatic hypermutation of immunoglobulin genes: merging mechanisms for genetic diversity. *Cell*. 2002;109 Suppl:S35-44.
27. Chaudhuri J, Alt FW. Class-switch recombination: interplay of transcription, DNA deamination and DNA repair. *Nature reviews Immunology*. 2004;4(7):541-52.
28. Allen CD, Ansel KM, Low C, Lesley R, Tamamura H, Fujii N, et al. Germinal center dark and light zone organization is mediated by CXCR4 and CXCR5. *Nature immunology*. 2004;5(9):943-52.
29. Nutt SL, Tarlinton DM. Germinal center B and follicular helper T cells: siblings, cousins or just good friends? *Nature immunology*. 2011;12(6):472-7.
30. Kurosaki T, Kometani K, Ise W. Memory B cells. *Nature reviews Immunology*. 2015;15(3):149-59.
31. Ochiai K, Maienschein-Cline M, Simonetti G, Chen J, Rosenthal R, Brink R, et al. Transcriptional regulation of germinal center B and plasma cell fates by dynamical control of IRF4. *Immunity*. 2013;38(5):918-29.
32. De Silva NS, Simonetti G, Heise N, Klein U. The diverse roles of IRF4 in late germinal center B-cell differentiation. *Immunological reviews*. 2012;247(1):73-92.
33. Pape KA, Taylor JJ, Maul RW, Gearhart PJ, Jenkins MK. Different B cell populations mediate early and late memory during an endogenous immune response. *Science (New York, NY)*. 2011;331(6021):1203-7.

34. Dogan I, Bertocci B, Vilmont V, Delbos F, Mégret J, Storck S, et al. Multiple layers of B cell memory with different effector functions. *Nature immunology*. 2009;10(12):1292-9.
35. Zuccarino-Catania GV, Sadanand S, Weisel FJ, Tomayko MM, Meng H, Kleinstein SH, et al. CD80 and PD-L2 define functionally distinct memory B cell subsets that are independent of antibody isotype. *Nature immunology*. 2014;15(7):631-7.
36. McHeyzer-Williams LJ, Milpied PJ, Okitsu SL, McHeyzer-Williams MG. Class-switched memory B cells remodel BCRs within secondary germinal centers. *Nature immunology*. 2015;16(3):296-305.
37. Vincent FB, Saulep-Easton D, Figgett WA, Fairfax KA, Mackay F. The BAFF/APRIL system: emerging functions beyond B cell biology and autoimmunity. *Cytokine & growth factor reviews*. 2013;24(3):203-15.
38. Gorelik L, Gilbride K, Dobles M, Kalled SL, Zandman D, Scott ML. Normal B cell homeostasis requires B cell activation factor production by radiation-resistant cells. *The Journal of experimental medicine*. 2003;198(6):937-45.
39. Rowland SL, Leahy KF, Halverson R, Torres RM, Pelanda R. BAFF receptor signaling aids the differentiation of immature B cells into transitional B cells following tonic BCR signaling. *Journal of immunology (Baltimore, Md : 1950)*. 2010;185(8):4570-81.
40. Campbell KS, Hager EJ, Friedrich RJ, Cambier JC. IgM antigen receptor complex contains phosphoprotein products of B29 and mb-1 genes. *Proceedings of the National Academy of Sciences of the United States of America*. 1991;88(9):3982-6.
41. Messina JP, Gilkeson GS, Pisetsky DS. Stimulation of in vitro murine lymphocyte proliferation by bacterial DNA. *Journal of immunology (Baltimore, Md : 1950)*. 1991;147(6):1759-64.
42. Stashenko P, Nadler LM, Hardy R, Schlossman SF. Characterization of a human B lymphocyte-specific antigen. *Journal of immunology (Baltimore, Md : 1950)*. 1980;125(4):1678-85.
43. Kiel MJ, Morrison SJ. Uncertainty in the niches that maintain haematopoietic stem cells. *Nat Rev Immunol*. 2008;8(4):290-301.
44. Medina KL, Pongubala JM, Reddy KL, Lancki DW, Dekoter R, Kieslinger M, et al. Assembling a gene regulatory network for specification of the B cell fate. *Developmental cell*. 2004;7(4):607-17.
45. Miller JP, Izon D, DeMuth W, Gerstein R, Bhandoola A, Allman D. The earliest step in B lineage differentiation from common lymphoid progenitors is critically dependent upon interleukin 7. *The Journal of experimental medicine*. 2002;196(5):705-11.
46. Sitnicka E, Brakebusch C, Martensson IL, Svensson M, Agace WW, Sigvardsson M, et al. Complementary signaling through flt3 and interleukin-7 receptor alpha is indispensable for fetal and adult B cell genesis. *The Journal of experimental medicine*. 2003;198(10):1495-506.
47. von Freeden-Jeffry U, Vieira P, Lucian LA, McNeil T, Burdach SE, Murray R. Lymphopenia in interleukin (IL)-7 gene-deleted mice identifies IL-7 as a nonredundant cytokine. *The Journal of experimental medicine*. 1995;181(4):1519-26.

48. Busslinger M. Transcriptional control of early B cell development. *Annu Rev Immunol.* 2004;22:55-79.
49. Kee BL, Murre C. Induction of early B cell factor (EBF) and multiple B lineage genes by the basic helix-loop-helix transcription factor E12. *The Journal of experimental medicine.* 1998;188(4):699-713.
50. Nutt SL, Heavey B, Rolink AG, Busslinger M. Commitment to the B-lymphoid lineage depends on the transcription factor Pax5. *Nature.* 1999;401(6753):556-62.
51. O'Riordan M, Grosschedl R. Coordinate regulation of B cell differentiation by the transcription factors EBF and E2A. *Immunity.* 1999;11(1):21-31.
52. Bankovich AJ, Raunser S, Joo ZS, Walz T, Davis MM, Garcia KC. Structural insight into pre-B cell receptor function. *Science.* 2007;316(5822):291-4.
53. DeFranco AL, Richards JD, Blum JH, Stevens TL, Law DA, Chan VW, et al. Signal transduction by the B-cell antigen receptor. *Ann N Y Acad Sci.* 1995;766:195-201.
54. Kurosaki T. Functional dissection of BCR signaling pathways. *Curr Opin Immunol.* 2000;12(3):276-81.
55. Pleiman CM, D'Ambrosio D, Cambier JC. The B-cell antigen receptor complex: structure and signal transduction. *Immunol Today.* 1994;15(9):393-9.
56. Hogan PG, Chen L, Nardone J, Rao A. Transcriptional regulation by calcium, calcineurin, and NFAT. *Genes Dev.* 2003;17(18):2205-32.
57. Leever SJ, Marshall CJ. Activation of extracellular signal-regulated kinase, ERK2, by p21ras oncoprotein. *EMBO J.* 1992;11(2):569-74.
58. Cambier JC, Pleiman CM, Clark MR. Signal transduction by the B cell antigen receptor and its coreceptors. *Annu Rev Immunol.* 1994;12:457-86.
59. Rueda D, Thome M. Phosphorylation of CARMA1: the link(er) to NF-kappaB activation. *Immunity.* 2005;23(6):551-3.
60. Sommer K, Guo B, Pomerantz JL, Bandaranayake AD, Moreno-Garcia ME, Ovechkina YL, et al. Phosphorylation of the CARMA1 linker controls NF-kappaB activation. *Immunity.* 2005;23(6):561-74.
61. Agathangelidis A, Ntoufa S, Stamatopoulos K. B cell receptor and antigens in CLL. *Adv Exp Med Biol.* 2013;792:1-24.
62. Schweighoffer E, Vanes L, Nys J, Cantrell D, McCleary S, Smithers N, et al. The BAFF receptor transduces survival signals by co-opting the B cell receptor signaling pathway. *Immunity.* 2013;38(3):475-88.
63. Cuni S, Perez-Aciego P, Perez-Chacon G, Vargas JA, Sanchez A, Martin-Saavedra FM, et al. A sustained activation of PI3K/NF-kappaB pathway is critical for the survival of chronic lymphocytic leukemia B cells. *Leukemia.* 2004;18(8):1391-400.
64. Arana E, Harwood NE, Batista FD. Regulation of integrin activation through the B-cell receptor. *J Cell Sci.* 2008;121(Pt 14):2279-86.

65. Baldini LG, Cro LM. Structure and function of VLA integrins: differential expression in B-cell leukemia/lymphoma. *Leuk Lymphoma*. 1994;12(3-4):197-203.
66. Hallek M, Cheson BD, Catovsky D, Caligaris-Cappio F, Dighiero G, Döhner H, et al. Guidelines for the diagnosis and treatment of chronic lymphocytic leukemia: a report from the International Workshop on Chronic Lymphocytic Leukemia updating the National Cancer Institute-Working Group 1996 guidelines. *Blood*. 2008;111(12):5446-56.
67. UK CR. Chronic lymphocytic leukaemia (CLL) statistics. 2021.
68. SEER NCICsfllc.
69. Gupta N, Kavuru S, Patel D, Janson D, Driscoll N, Ahmed S, et al. Rituximab-based chemotherapy for steroid-refractory autoimmune hemolytic anemia of chronic lymphocytic leukemia. *Leukemia*. 2002;16(10):2092-5.
70. Hamblin TJ. Autoimmune complications of chronic lymphocytic leukemia. *Seminars in oncology*. 2006;33(2):230-9.
71. Hodgson K, Ferrer G, Montserrat E, Moreno C. Chronic lymphocytic leukemia and autoimmunity: a systematic review. *Haematologica*. 2011;96(5):752-61.
72. Rodon P, Breton P, Courouble G. Treatment of pure red cell aplasia and autoimmune haemolytic anaemia in chronic lymphocytic leukaemia with Campath-1H. *European journal of haematology*. 2003;70(5):319-21.
73. Zaja F, Vianelli N, Sperotto A, Patriarca F, Tani M, Marin L, et al. Anti-CD20 therapy for chronic lymphocytic leukemia-associated autoimmune diseases. *Leukemia & lymphoma*. 2003;44(11):1951-5.
74. Eichhorst B, Robak T, Montserrat E, Ghia P, Niemann CU, Kater AP, et al. Chronic lymphocytic leukaemia: ESMO Clinical Practice Guidelines for diagnosis, treatment and follow-up. *Annals of Oncology*. 2021;32(1):23-33.
75. Seifert M, Sellmann L, Bloehdorn J, Wein F, Stilgenbauer S, Dürig J, et al. Cellular origin and pathophysiology of chronic lymphocytic leukemia. *The Journal of experimental medicine*. 2012;209(12):2183-98.
76. Chiorazzi N, Ferrarini M. Cellular origin(s) of chronic lymphocytic leukemia: cautionary notes and additional considerations and possibilities. *Blood*. 2011;117(6):1781-91.
77. Kikushige Y, Ishikawa F, Miyamoto T, Shima T, Urata S, Yoshimoto G, et al. Self-renewing hematopoietic stem cell is the primary target in pathogenesis of human chronic lymphocytic leukemia. *Cancer cell*. 2011;20(2):246-59.
78. Shi Y, Agematsu K, Ochs HD, Sugane K. Functional analysis of human memory B-cell subpopulations: IgD+ CD27+ B cells are crucial in secondary immune response by producing high affinity IgM. *Clinical immunology*. 2003;108(2):128-37.
79. Damle RN, Ghiotto F, Valetto A, Albesiano E, Fais F, Yan X-J, et al. B-cell chronic lymphocytic leukemia cells express a surface membrane phenotype of activated, antigen-experienced B lymphocytes: Presented in part at the 42nd Annual Meeting of the American Society of Hematology, December 1-5, 2000, San Francisco, CA. *Blood, The Journal of the American Society of Hematology*. 2002;99(11):4087-93.

80. Tangye SG, Liu Y-J, Aversa G, Phillips JH, De Vries JE. Identification of functional human splenic memory B cells by expression of CD148 and CD27. *Journal of Experimental Medicine*. 1998;188(9):1691-703.
81. Sindhava V, Bondada S. Multiple regulatory mechanisms control B-1 B cell activation. *Frontiers in immunology*. 2012;3:372.
82. Sims GP, Ettinger R, Shirota Y, Yarboro CH, Illei GG, Lipsky PE. Identification and characterization of circulating human transitional B cells. *Blood*. 2005;105(11):4390-8.
83. Schroeder Jr HW, Dighiero G. The pathogenesis of chronic lymphocytic leukemia: analysis of the antibody repertoire. *Immunology today*. 1994;15(6):288-94.
84. Klein U, Tu Y, Stolovitzky GA, Mattioli M, Cattoretto G, Husson H, et al. Gene expression profiling of B cell chronic lymphocytic leukemia reveals a homogeneous phenotype related to memory B cells. *The Journal of experimental medicine*. 2001;194(11):1625-38.
85. Negrini M, Cutrona G, Bassi C, Fabris S, Zagatti B, Colombo M, et al. microRNAome expression in chronic lymphocytic leukemia: comparison with normal B-cell subsets and correlations with prognostic and clinical parameters. *Clinical Cancer Research*. 2014;20(15):4141-53.
86. Kulis M, Heath S, Bibikova M, Queirós AC, Navarro A, Clot G, et al. Epigenomic analysis detects widespread gene-body DNA hypomethylation in chronic lymphocytic leukemia. *Nature genetics*. 2012;44(11):1236-42.
87. Oakes CC, Seifert M, Assenov Y, Gu L, Przekopowicz M, Ruppert AS, et al. DNA methylation dynamics during B cell maturation underlie a continuum of disease phenotypes in chronic lymphocytic leukemia. *Nature genetics*. 2016;48(3):253-64.
88. Dühren-von Minden M, Übelhart R, Schneider D, Wossning T, Bach MP, Buchner M, et al. Chronic lymphocytic leukaemia is driven by antigen-independent cell-autonomous signalling. *Nature*. 2012;489(7415):309-12.
89. Matutes E, Owusu-Ankomah K, Morilla R, Garcia Marco J, Houlihan A, Que TH, et al. The immunological profile of B-cell disorders and proposal of a scoring system for the diagnosis of CLL. *Leukemia*. 1994;8(10):1640-5.
90. Moreau EJ, Matutes E, A'Hern RP, Morilla AM, Morilla RM, Owusu-Ankomah KA, et al. Improvement of the chronic lymphocytic leukemia scoring system with the monoclonal antibody SN8 (CD79b). *American journal of clinical pathology*. 1997;108(4):378-82.
91. Ginaldi L, De Martinis M, Matutes E, Farahat N, Morilla R, Catovsky D. Levels of expression of CD19 and CD20 in chronic B cell leukaemias. *Journal of clinical pathology*. 1998;51(5):364-9.
92. Rawstron AC, Kreuzer KA, Soosapilla A, Spacek M, Stehlikova O, Gambell P, et al. Reproducible diagnosis of chronic lymphocytic leukemia by flow cytometry: An European Research Initiative on CLL (ERIC) & European Society for Clinical Cell Analysis (ESCCA) Harmonisation project. *Cytometry Part B, Clinical cytometry*. 2018;94(1):121-8.
93. Rai KR, Sawitsky A, Cronkite EP, Chanana AD, Levy RN, Pasternack BS. Clinical staging of chronic lymphocytic leukemia. *Blood*. 1975;46(2):219-34.

94. Binet JL, Leparrier M, Dighiero G, Charron D, D'Athis P, Vaugier G, et al. A clinical staging system for chronic lymphocytic leukemia: prognostic significance. *Cancer*. 1977;40(2):855-64.
95. Matutes E, Polliack A. Morphological and immunophenotypic features of chronic lymphocytic leukemia. *Rev Clin Exp Hematol*. 2000;4(1):22-47.
96. Damle RN, Wasil T, Fais F, Ghiotto F, Valetto A, Allen SL, et al. Ig V gene mutation status and CD38 expression as novel prognostic indicators in chronic lymphocytic leukemia. *Blood*. 1999;94(6):1840-7.
97. Geisler CH, Larsen JK, Hansen NE, Hansen MM, Christensen BE, Lund B, et al. Prognostic importance of flow cytometric immunophenotyping of 540 consecutive patients with B-cell chronic lymphocytic leukemia. *Blood*. 1991;78(7):1795-802.
98. Oscier DG, Gardiner AC, Mould SJ, Glide S, Davis ZA, Ibbotson RE, et al. Multivariate analysis of prognostic factors in CLL: clinical stage, IGVH gene mutational status, and loss or mutation of the p53 gene are independent prognostic factors. *Blood*. 2002;100(4):1177-84.
99. Döhner H, Stilgenbauer S, Benner A, Leupolt E, Kröber A, Bullinger L, et al. Genomic aberrations and survival in chronic lymphocytic leukemia. *The New England journal of medicine*. 2000;343(26):1910-6.
100. An international prognostic index for patients with chronic lymphocytic leukaemia (CLL-IPI): a meta-analysis of individual patient data. *The Lancet Oncology*. 2016;17(6):779-90.
101. Catovsky D, Richards S, Matutes E, Oscier D, Dyer MJ, Bezares RF, et al. Assessment of fludarabine plus cyclophosphamide for patients with chronic lymphocytic leukaemia (the LRF CLL4 Trial): a randomised controlled trial. *Lancet*. 2007;370(9583):230-9.
102. Eichhorst BF, Busch R, Hopfinger G, Pasold R, Hensel M, Steinbrecher C, et al. Fludarabine plus cyclophosphamide versus fludarabine alone in first-line therapy of younger patients with chronic lymphocytic leukemia. *Blood*. 2006;107(3):885-91.
103. Hallek M, Fischer K, Fingerle-Rowson G, Fink AM, Busch R, Mayer J, et al. Addition of rituximab to fludarabine and cyclophosphamide in patients with chronic lymphocytic leukaemia: a randomised, open-label, phase 3 trial. *Lancet*. 2010;376(9747):1164-74.
104. Flinn IW, Neuberg DS, Grever MR, Dewald GW, Bennett JM, Pajetta EM, et al. Phase III trial of fludarabine plus cyclophosphamide compared with fludarabine for patients with previously untreated chronic lymphocytic leukemia: US Intergroup Trial E2997. *J Clin Oncol*. 2007;25(7):793-8.
105. Fischer K, Bahlo J, Fink AM, Goede V, Herling CD, Cramer P, et al. Long-term remissions after FCR chemoimmunotherapy in previously untreated patients with CLL: updated results of the CLL8 trial. *Blood*. 2016;127(2):208-15.
106. Kovacs G, Robrecht S, Fink AM, Bahlo J, Cramer P, von Tresckow J, et al. Minimal Residual Disease Assessment Improves Prediction of Outcome in Patients With Chronic Lymphocytic Leukemia (CLL) Who Achieve Partial Response: Comprehensive Analysis of Two Phase III Studies of the German CLL Study Group. *Journal of clinical oncology : official journal of the American Society of Clinical Oncology*. 2016;34(31):3758-65.

107. Eichhorst B, Fink AM, Bahlo J, Busch R, Kovacs G, Maurer C, et al. First-line chemoimmunotherapy with bendamustine and rituximab versus fludarabine, cyclophosphamide, and rituximab in patients with advanced chronic lymphocytic leukaemia (CLL10): an international, open-label, randomised, phase 3, non-inferiority trial. *The Lancet Oncology*. 2016;17(7):928-42.
108. Goede V, Fischer K, Busch R, Engelke A, Eichhorst B, Wendtner CM, et al. Obinutuzumab plus chlorambucil in patients with CLL and coexisting conditions. *The New England journal of medicine*. 2014;370(12):1101-10.
109. Dreger P, Schetelig J, Andersen N, Corradini P, van Gelder M, Gribben J, et al. Managing high-risk CLL during transition to a new treatment era: stem cell transplantation or novel agents? *Blood*. 2014;124(26):3841-9.
110. Moreno C, Greil R, Demirkan F, Tedeschi A, Anz B, Larratt L, et al. Ibrutinib plus obinutuzumab versus chlorambucil plus obinutuzumab in first-line treatment of chronic lymphocytic leukaemia (iLLUMINATE): a multicentre, randomised, open-label, phase 3 trial. *The Lancet Oncology*. 2019;20(1):43-56.
111. Woyach JA, Ruppert AS, Heerema NA, Zhao W, Booth AM, Ding W, et al. Ibrutinib Regimens versus Chemoimmunotherapy in Older Patients with Untreated CLL. *The New England journal of medicine*. 2018;379(26):2517-28.
112. Burger JA, Tedeschi A, Barr PM, Robak T, Owen C, Ghia P, et al. Ibrutinib as Initial Therapy for Patients with Chronic Lymphocytic Leukemia. *The New England journal of medicine*. 2015;373(25):2425-37.
113. Shanafelt TD, Wang V, Kay NE, Hanson CA, O'Brien SM, Barrientos JC, et al. A randomized phase III study of ibrutinib (PCI-32765)-based therapy vs. standard fludarabine, cyclophosphamide, and rituximab (FCR) chemoimmunotherapy in untreated younger patients with chronic lymphocytic leukemia (CLL): a trial of the ECOG-ACRIN Cancer Research Group (E1912). *Blood*. 2018;132(Supplement 1):LBA-4-LBA-.
114. Sharman JP, Egyed M, Jurczak W, Skarbnik A, Pagel JM, Flinn IW, et al. Acalabrutinib with or without obinutuzumab versus chlorambucil and obinutuzumab for treatment-naive chronic lymphocytic leukaemia (ELEVATE TN): a randomised, controlled, phase 3 trial. *Lancet (London, England)*. 2020;395(10232):1278-91.
115. Fischer K, Al-Sawaf O, Bahlo J, Fink AM, Tandon M, Dixon M, et al. Venetoclax and Obinutuzumab in Patients with CLL and Coexisting Conditions. *The New England journal of medicine*. 2019;380(23):2225-36.
116. Fischer K, Cramer P, Busch R, Stilgenbauer S, Bahlo J, Schweighofer CD, et al. Bendamustine combined with rituximab in patients with relapsed and/or refractory chronic lymphocytic leukemia: a multicenter phase II trial of the German Chronic Lymphocytic Leukemia Study Group. *Journal of clinical oncology : official journal of the American Society of Clinical Oncology*. 2011;29(26):3559-66.
117. Awan FT, Hillmen P, Hellmann A, Robak T, Hughes SG, Trone D, et al. A randomized, open-label, multicentre, phase 2/3 study to evaluate the safety and efficacy of lumiliximab in combination with fludarabine, cyclophosphamide and rituximab versus fludarabine,

cyclophosphamide and rituximab alone in subjects with relapsed chronic lymphocytic leukaemia. *British journal of haematology*. 2014;167(4):466-77.

118. Munir T, Brown JR, O'Brien S, Barrientos JC, Barr PM, Reddy NM, et al. Final analysis from RESONATE: Up to six years of follow-up on ibrutinib in patients with previously treated chronic lymphocytic leukemia or small lymphocytic lymphoma. *American journal of hematology*. 2019;94(12):1353-63.

119. Fraser G, Cramer P, Demirkan F, Silva RS, Grosicki S, Pristupa A, et al. Updated results from the phase 3 HELIOS study of ibrutinib, bendamustine, and rituximab in relapsed chronic lymphocytic leukemia/small lymphocytic lymphoma. *Leukemia*. 2019;33(4):969-80.

120. Sharman JP, Coutre SE, Furman RR, Cheson BD, Pagel JM, Hillmen P, et al. Final Results of a Randomized, Phase III Study of Rituximab With or Without Idelalisib Followed by Open-Label Idelalisib in Patients With Relapsed Chronic Lymphocytic Leukemia. *Journal of clinical oncology : official journal of the American Society of Clinical Oncology*. 2019;37(16):1391-402.

121. Zelenetz AD, Barrientos JC, Brown JR, Coiffier B, Delgado J, Egyed M, et al. Idelalisib or placebo in combination with bendamustine and rituximab in patients with relapsed or refractory chronic lymphocytic leukaemia: interim results from a phase 3, randomised, double-blind, placebo-controlled trial. *The Lancet Oncology*. 2017;18(3):297-311.

122. Flinn IW, Hillmen P, Montillo M, Nagy Z, Illés Á, Etienne G, et al. The phase 3 DUO trial: duvelisib vs ofatumumab in relapsed and refractory CLL/SLL. *Blood*. 2018;132(23):2446-55.

123. Ghia P, Pluta A, Wach M, Lysak D, Kozak T, Simkovic M, et al. ASCEND: Phase III, Randomized Trial of Acalabrutinib Versus Idelalisib Plus Rituximab or Bendamustine Plus Rituximab in Relapsed or Refractory Chronic Lymphocytic Leukemia. *Journal of clinical oncology : official journal of the American Society of Clinical Oncology*. 2020;38(25):2849-61.

124. Seymour JF, Kipps TJ, Eichhorst B, Hillmen P, D'Rozario J, Assouline S, et al. Venetoclax–Rituximab in Relapsed or Refractory Chronic Lymphocytic Leukemia. *New England Journal of Medicine*. 2018;378(12):1107-20.

125. Stilgenbauer S, Eichhorst B, Schetelig J, Hillmen P, Seymour JF, Coutre S, et al. Venetoclax for Patients With Chronic Lymphocytic Leukemia With 17p Deletion: Results From the Full Population of a Phase II Pivotal Trial. *Journal of clinical oncology : official journal of the American Society of Clinical Oncology*. 2018;36(19):1973-80.

126. Mato AR, Roeker LE, Jacobs R, Hill BT, Lamanna N, Brander D, et al. Assessment of the Efficacy of Therapies Following Venetoclax Discontinuation in CLL Reveals BTK Inhibition as an Effective Strategy. *Clinical cancer research : an official journal of the American Association for Cancer Research*. 2020;26(14):3589-96.

127. Brion A, Mahé B, Kolb B, Audhuy B, Colombat P, Maisonneuve H, et al. Autologous transplantation in CLL patients with B and C Binet stages: final results of the prospective randomized GOELAMS LLC 98 trial. *Bone marrow transplantation*. 2012;47(4):542-8.

128. Balducci L, Extermann M. Management of cancer in the older person: a practical approach. *The oncologist*. 2000;5(3):224-37.

129. Kharfan-Dabaja MA, Kumar A, Hamadani M, Stilgenbauer S, Ghia P, Anasetti C, et al. Clinical Practice Recommendations for Use of Allogeneic Hematopoietic Cell Transplantation in Chronic Lymphocytic Leukemia on Behalf of the Guidelines Committee of the American Society for Blood and Marrow Transplantation. *Biology of blood and marrow transplantation : journal of the American Society for Blood and Marrow Transplantation*. 2016;22(12):2117-25.
130. Montserrat E, Dreger P. Treatment of Chronic Lymphocytic Leukemia With del(17p)/TP53 Mutation: Allogeneic Hematopoietic Stem Cell Transplantation or BCR-Signaling Inhibitors? *Clinical lymphoma, myeloma & leukemia*. 2016;16 Suppl:S74-81.
131. Roeker LE, Dreger P, Brown JR, Lahoud OB, Eyre TA, Brander DM, et al. Allogeneic stem cell transplantation for chronic lymphocytic leukemia in the era of novel agents. *Blood advances*. 2020;4(16):3977-89.
132. Sorror ML, Maris MB, Storb R, Baron F, Sandmaier BM, Maloney DG, et al. Hematopoietic cell transplantation (HCT)-specific comorbidity index: a new tool for risk assessment before allogeneic HCT. *Blood*. 2005;106(8):2912-9.
133. Ghia P. A look into the future: can minimal residual disease guide therapy and predict prognosis in chronic lymphocytic leukemia? *Hematology Am Soc Hematol Educ Program*. 2012;2012:97-104.
134. Rawstron AC, Villamor N, Ritgen M, Böttcher S, Ghia P, Zehnder JL, et al. International standardized approach for flow cytometric residual disease monitoring in chronic lymphocytic leukaemia. *Leukemia*. 2007;21(5):956-64.
135. Rawstron AC, Fazi C, Agathangelidis A, Villamor N, Letestu R, Nomdedeu J, et al. A complementary role of multiparameter flow cytometry and high-throughput sequencing for minimal residual disease detection in chronic lymphocytic leukemia: an European Research Initiative on CLL study. *Leukemia*. 2016;30(4):929-36.
136. Verhagen O, Willemsse M, Breunis W, Wijkhuijs A, Jacobs D, Joosten S, et al. Application of germline IGH probes in real-time quantitative PCR for the detection of minimal residual disease in acute lymphoblastic leukemia. *Leukemia*. 2000;14(8):1426-35.
137. Logan A, Zhang B, Narasimhan B, Carlton V, Zheng J, Moorhead M, et al. Minimal residual disease quantification using consensus primers and high-throughput IGH sequencing predicts post-transplant relapse in chronic lymphocytic leukemia. *Leukemia*. 2013;27(8):1659-65.
138. Tedder TF, Engel P. CD20: a regulator of cell-cycle progression of B lymphocytes. *Immunol Today*. 1994;15(9):450-4.
139. Tedder TF. CD19: a promising B cell target for rheumatoid arthritis. *Nat Rev Rheumatol*. 2009;5(10):572-7.
140. Carter RH, Doody GM, Bolen JB, Fearon DT. Membrane IgM-induced tyrosine phosphorylation of CD19 requires a CD19 domain that mediates association with components of the B cell antigen receptor complex. *J Immunol*. 1997;158(7):3062-9.
141. Cabezudo E, Carrara P, Morilla R, Matutes E. Quantitative analysis of CD79b, CD5 and CD19 in mature B-cell lymphoproliferative disorders. *Haematologica*. 1999;84(5):413-8.

142. Raman C. CD5, an important regulator of lymphocyte selection and immune tolerance. *Immunol Res.* 2002;26(1-3):255-63.
143. Dornan D, Bennett F, Chen Y, Dennis M, Eaton D, Elkins K, et al. Therapeutic potential of an anti-CD79b antibody-drug conjugate, anti-CD79b-vc-MMAE, for the treatment of non-Hodgkin lymphoma. *Blood.* 2009;114(13):2721-9.
144. Bazil V, Brandt J, Tsukamoto A, Hoffman R. Apoptosis of human hematopoietic progenitor cells induced by crosslinking of surface CD43, the major sialoglycoprotein of leukocytes. *Blood.* 1995;86(2):502-11.
145. Park JK, Rosenstein YJ, Remold-O'Donnell E, Bierer BE, Rosen FS, Burakoff SJ. Enhancement of T-cell activation by the CD43 molecule whose expression is defective in Wiskott-Aldrich syndrome. *Nature.* 1991;350(6320):706-9.
146. de Smet W, Walter H, van Hove L. A new CD43 monoclonal antibody induces homotypic aggregation of human leucocytes through a CD11a/CD18-dependent and -independent mechanism. *Immunology.* 1993;79(1):46-54.
147. Valentin H, Gelin C, Coulombel L, Zoccola D, Morizet J, Bernard A. The distribution of the CDW52 molecule on blood cells and characterization of its involvement in T cell activation. *Transplantation.* 1992;54(1):97-104.
148. Hoek RM, Ruuls SR, Murphy CA, Wright GJ, Goddard R, Zurawski SM, et al. Down-regulation of the macrophage lineage through interaction with OX2 (CD200). *Science.* 2000;290(5497):1768-71.
149. Kretz-Rommel A, Qin F, Dakappagari N, Ravey EP, McWhirter J, Oltean D, et al. CD200 expression on tumor cells suppresses antitumor immunity: new approaches to cancer immunotherapy. *J Immunol.* 2007;178(9):5595-605.
150. Ewart MA, Ozanne BW, Cushley W. The CD23a and CD23b proximal promoters display different sensitivities to exogenous stimuli in B lymphocytes. *Genes Immun.* 2002;3(3):158-64.
151. Goller ME, Kneitz C, Mehringer C, Muller K, Jelley-Gibbs DM, Gosselin EJ, et al. Regulation of CD23 isoforms on B-chronic lymphocytic leukemia. *Leuk Res.* 2002;26(9):795-802.
152. Cartwright RA, Bernard SM, Bird CC, Darwin CM, O'Brien C, Richards ID, et al. Chronic lymphocytic leukaemia: case control epidemiological study in Yorkshire. *Br J Cancer.* 1987;56(1):79-82.
153. Lampert IA, Wotherspoon A, Van Noorden S, Hasserjian RP. High expression of CD23 in the proliferation centers of chronic lymphocytic leukemia in lymph nodes and spleen. *Hum Pathol.* 1999;30(6):648-54.
154. Leonard JP, Coleman M, Ketas JC, Chadburn A, Ely S, Furman RR, et al. Phase I/II trial of epratuzumab (humanized anti-CD22 antibody) in indolent non-Hodgkin's lymphoma. *J Clin Oncol.* 2003;21(16):3051-9.
155. Pezzutto A, Dorken B, Moldenhauer G, Clark EA. Amplification of human B cell activation by a monoclonal antibody to the B cell-specific antigen CD22, Bp 130/140. *J Immunol.* 1987;138(1):98-103.

156. Pezzutto A, Rabinovitch PS, Dorken B, Moldenhauer G, Clark EA. Role of the CD22 human B cell antigen in B cell triggering by anti-immunoglobulin. *J Immunol.* 1988;140(6):1791-5.
157. Frankel AE, Surendranathan A, Black JH, White A, Ganjoo K, Cripe LD. Phase II clinical studies of denileukin diftotox diphtheria toxin fusion protein in patients with previously treated chronic lymphocytic leukemia. *Cancer.* 2006;106(10):2158-64.
158. Johnson AR, Ashton J, Schulz WW, Erdos EG. Neutral metalloendopeptidase in human lung tissue and cultured cells. *Am Rev Respir Dis.* 1985;132(3):564-8.
159. Deaglio S, Vaisitti T, Bergui L, Bonello L, Horenstein AL, Tamagnone L, et al. CD38 and CD100 lead a network of surface receptors relaying positive signals for B-CLL growth and survival. *Blood.* 2005;105(8):3042-50.
160. Krober A, Seiler T, Benner A, Bullinger L, Bruckle E, Lichter P, et al. V(H) mutation status, CD38 expression level, genomic aberrations, and survival in chronic lymphocytic leukemia. *Blood.* 2002;100(4):1410-6.
161. Mehta K, Shahid U, Malavasi F. Human CD38, a cell-surface protein with multiple functions. *FASEB J.* 1996;10(12):1408-17.
162. Agace WW, Higgins JM, Sadasivan B, Brenner MB, Parker CM. T-lymphocyte-epithelial-cell interactions: integrin alpha(E)(CD103)beta(7), LEEP-CAM and chemokines. *Curr Opin Cell Biol.* 2000;12(5):563-8.
163. Suffia I, Reckling SK, Salay G, Belkaid Y. A role for CD103 in the retention of CD4+CD25+ Treg and control of *Leishmania major* infection. *J Immunol.* 2005;174(9):5444-55.
164. Lucio PJ, Faria MT, Pinto AM, da Silva MR, Correia Junior ME, da Costa RJ, et al. Expression of adhesion molecules in chronic B-cell lymphoproliferative disorders. *Haematologica.* 1998;83(2):104-11.
165. Postigo AA, Corbi AL, Sanchez-Madrid F, de Landazuri MO. Regulated expression and function of CD11c/CD18 integrin on human B lymphocytes. Relation between attachment to fibrinogen and triggering of proliferation through CD11c/CD18. *J Exp Med.* 1991;174(6):1313-22.
166. Sembries S, Pahl H, Stilgenbauer S, Dohner H, Schriever F. Reduced expression of adhesion molecules and cell signaling receptors by chronic lymphocytic leukemia cells with 11q deletion. *Blood.* 1999;93(2):624-31.
167. Pao LI, Famiglietti SJ, Cambier JC. Asymmetrical phosphorylation and function of immunoreceptor tyrosine-based activation motif tyrosines in B cell antigen receptor signal transduction. *J Immunol.* 1998;160(7):3305-14.
168. Maloney DG, Smith B, Rose A. Rituximab: Mechanism of action and resistance. *Semin Oncol.* 2002;29(1S2):2-9.
169. Pedersen IM, Kitada S, Leoni LM, Zapata JM, Karras JG, Tsukada N, et al. Protection of CLL B cells by a follicular dendritic cell line is dependent on induction of Mcl-1. *Blood.* 2002;100(5):1795-801.

170. Thompson AA, Do HN, Saxon A, Wall R. Widespread B29 (CD79b) gene defects and loss of expression in chronic lymphocytic leukemia. *Leuk Lymphoma*. 1999;32(5-6):561-9.
171. Delespesse G, Suter U, Mossalayi D, Bettler B, Sarfati M, Hofstetter H, et al. Expression, structure, and function of the CD23 antigen. *Adv Immunol*. 1991;49:149-91.
172. Fournier S, Yang LP, Delespesse G, Rubio M, Biron G, Sarfati M. The two CD23 isoforms display differential regulation in chronic lymphocytic leukaemia. *Br J Haematol*. 1995;89(2):373-9.
173. Klein U, Rajewsky K, Küppers R. Human immunoglobulin (Ig)M+IgD+ peripheral blood B cells expressing the CD27 cell surface antigen carry somatically mutated variable region genes: CD27 as a general marker for somatically mutated (memory) B cells. *The Journal of experimental medicine*. 1998;188(9):1679-89.
174. Tangye SG, Good KL. Human IgM+CD27+ B cells: memory B cells or "memory" B cells? *J Immunol*. 2007;179(1):13-9.
175. Budeus B, Schweigle de Reynoso S, Przekopowicz M, Hoffmann D, Seifert M, Küppers R. Complexity of the human memory B-cell compartment is determined by the versatility of clonal diversification in germinal centers. *Proceedings of the National Academy of Sciences of the United States of America*. 2015;112(38):E5281-E9.
176. Lampert IA, Wotherspoon A, Van Noorden S, Hasserjian RP. High expression of CD23 in the proliferation centers of chronic lymphocytic leukemia in lymph nodes and spleen. *Human Pathology*. 1999;30(6):648-54.
177. Damle RN, Temburni S, Calissano C, Yancopoulos S, Banapour T, Sison C, et al. CD38 expression labels an activated subset within chronic lymphocytic leukemia clones enriched in proliferating B cells. *Blood*. 2007;110(9):3352-9.
178. Crespo M, Bosch F, Villamor N, Bellosillo B, Colomer D, Rozman M, et al. ZAP-70 expression as a surrogate for immunoglobulin-variable-region mutations in chronic lymphocytic leukemia. *The New England journal of medicine*. 2003;348(18):1764-75.
179. Durig J, Nuckel H, Cremer M, Fuhrer A, Halfmeyer K, Fandrey J, et al. ZAP-70 expression is a prognostic factor in chronic lymphocytic leukemia. *Leukemia*. 2003;17(12):2426-34.
180. Richardson SJ, Matthews C, Catherwood MA, Alexander HD, Carey BS, Farrugia J, et al. ZAP-70 expression is associated with enhanced ability to respond to migratory and survival signals in B-cell chronic lymphocytic leukemia (B-CLL). *Blood*. 2006;107(9):3584-92.
181. Wiestner A, Rosenwald A, Barry TS, Wright G, Davis RE, Henrickson SE, et al. ZAP-70 expression identifies a chronic lymphocytic leukemia subtype with unmutated immunoglobulin genes, inferior clinical outcome, and distinct gene expression profile. *Blood*. 2003;101(12):4944-51.
182. Bennett F, Rawstron A, Plummer M, de Tute R, Moreton P, Jack A, et al. B-cell chronic lymphocytic leukaemia cells show specific changes in membrane protein expression during different stages of cell cycle. *Br J Haematol*. 2007;139(4):600-4.

183. Burger JA, Tsukada N, Burger M, Zvaifler NJ, Dell'Aquila M, Kipps TJ. Blood-derived nurse-like cells protect chronic lymphocytic leukemia B cells from spontaneous apoptosis through stromal cell-derived factor-1. *Blood*. 2000;96(8):2655-63.
184. Kimby E, Rincon J, Patarroyo M, Mellstedt H. Expression of adhesion molecules CD11/CD18 (Leu-CAMs, beta 2-integrins), CD54 (ICAM-1) and CD58 (LFA-3) in B-chronic lymphocytic leukemia. *Leuk Lymphoma*. 1994;13(3-4):297-306.
185. Rutella S, Rumi C, Puggioni P, Barberi T, Di Mario A, Larocca LM, et al. Expression of thrombospondin receptor (CD36) in B-cell chronic lymphocytic leukemia as an indicator of tumor cell dissemination. *Haematologica*. 1999;84(5):419-24.
186. Nishio M, Endo T, Tsukada N, Ohata J, Kitada S, Reed JC, et al. Nurselike cells express BAFF and APRIL, which can promote survival of chronic lymphocytic leukemia cells via a paracrine pathway distinct from that of SDF-1alpha. *Blood*. 2005;106(3):1012-20.
187. Burger JA, Quiroga MP, Hartmann E, Burkle A, Wierda WG, Keating MJ, et al. High-level expression of the T-cell chemokines CCL3 and CCL4 by chronic lymphocytic leukemia B cells in nurselike cell cocultures and after BCR stimulation. *Blood*. 2009;113(13):3050-8.
188. Salvesen GS, Dixit VM. Caspase activation: the induced-proximity model. *Proc Natl Acad Sci U S A*. 1999;96(20):10964-7.
189. Siegel RM. Caspases at the crossroads of immune-cell life and death. *Nat Rev Immunol*. 2006;6(4):308-17.
190. Strasser A. The role of BH3-only proteins in the immune system. *Nat Rev Immunol*. 2005;5(3):189-200.
191. Calin GA, Pekarsky Y, Croce CM. The role of microRNA and other non-coding RNA in the pathogenesis of chronic lymphocytic leukemia. *Best Pract Res Clin Haematol*. 2007;20(3):425-37.
192. Dyer MJ, Zani VJ, Lu WZ, O'Byrne A, Mould S, Chapman R, et al. BCL2 translocations in leukemias of mature B cells. *Blood*. 1994;83(12):3682-8.
193. Johnston JB, Daeninck P, Verburg L, Lee K, Williams G, Israels LG, et al. P53, MDM-2, BAX and BCL-2 and drug resistance in chronic lymphocytic leukemia. *Leuk Lymphoma*. 1997;26(5-6):435-49.
194. Carter A, Lin K, Sherrington PD, Pettitt AR. Detection of p53 dysfunction by flow cytometry in chronic lymphocytic leukaemia. *Br J Haematol*. 2004;127(4):425-8.
195. Chang H, Jiang AM, Qi CX. Aberrant nuclear p53 expression predicts hemizygous 17p (TP53) deletion in chronic lymphocytic leukemia. *Am J Clin Pathol*. 2010;133(1):70-4.
196. Agathangelidis A, Darzentas N, Hadzidimitriou A, Brochet X, Murray F, Yan XJ, et al. Stereotyped B-cell receptors in one-third of chronic lymphocytic leukemia: a molecular classification with implications for targeted therapies. *Blood*. 2012;119(19):4467-75.
197. Hamblin TJ, Davis Z, Gardiner A, Oscier DG, Stevenson FK. Unmutated Ig V(H) genes are associated with a more aggressive form of chronic lymphocytic leukemia. *Blood*. 1999;94(6):1848-54.

198. D'Avola A, Drennan S, Tracy I, Henderson I, Chiecchio L, Larrayoz M, et al. Surface IgM expression and function are associated with clinical behavior, genetic abnormalities, and DNA methylation in CLL. *Blood*. 2016;128(6):816-26.
199. Baliakas P, Hadzidimitriou A, Sutton LA, Minga E, Agathangelidis A, Nichelatti M, et al. Clinical effect of stereotyped B-cell receptor immunoglobulins in chronic lymphocytic leukaemia: a retrospective multicentre study. *The Lancet Haematology*. 2014;1(2):e74-84.
200. Stamatopoulos K, Agathangelidis A, Rosenquist R, Ghia P. Antigen receptor stereotypy in chronic lymphocytic leukemia. *Leukemia*. 2017;31(2):282-91.
201. Stamatopoulos K, Belessi C, Moreno C, Boudjograh M, Guida G, Smilevska T, et al. Over 20% of patients with chronic lymphocytic leukemia carry stereotyped receptors: Pathogenetic implications and clinical correlations. *Blood*. 2007;109(1):259-70.
202. Herishanu Y, Pérez-Galán P, Liu D, Biancotto A, Pittaluga S, Vire B, et al. The lymph node microenvironment promotes B-cell receptor signaling, NF-kappaB activation, and tumor proliferation in chronic lymphocytic leukemia. *Blood*. 2011;117(2):563-74.
203. Koehrer S, Burger JA. B-cell receptor signaling in chronic lymphocytic leukemia and other B-cell malignancies. *Clin Adv Hematol Oncol*. 2016;14(1):55-65.
204. Muzio M, Apollonio B, Scielzo C, Frenquelli M, Vandoni I, Bousiotis V, et al. Constitutive activation of distinct BCR-signaling pathways in a subset of CLL patients: a molecular signature of anergy. *Blood*. 2008;112(1):188-95.
205. Murray F, Darzentas N, Hadzidimitriou A, Tobin G, Boudjogra M, Scielzo C, et al. Stereotyped patterns of somatic hypermutation in subsets of patients with chronic lymphocytic leukemia: implications for the role of antigen selection in leukemogenesis. *Blood*. 2008;111(3):1524-33.
206. Thorsélius M, Kröber A, Murray F, Thunberg U, Tobin G, Bühler A, et al. Strikingly homologous immunoglobulin gene rearrangements and poor outcome in VH3-21-using chronic lymphocytic leukemia patients independent of geographic origin and mutational status. *Blood*. 2006;107(7):2889-94.
207. Vardi A, Agathangelidis A, Sutton L-A, Ghia P, Rosenquist R, Stamatopoulos K. Immunogenetic studies of chronic lymphocytic leukemia: revelations and speculations about ontogeny and clinical evolution. *Cancer research*. 2014;74(16):4211-6.
208. Marcatili P, Ghiotto F, Tenca C, Chailyan A, Mazzarello AN, Yan X-J, et al. Igs expressed by chronic lymphocytic leukemia B cells show limited binding-site structure variability. *The Journal of Immunology*. 2013;190(11):5771-8.
209. Jiménez de Oya N, De Giovanni M, Fioravanti J, Übelhart R, Di Lucia P, Fiocchi A, et al. Pathogen-specific B-cell receptors drive chronic lymphocytic leukemia by light-chain-dependent cross-reaction with autoantigens. *EMBO molecular medicine*. 2017;9(11):1482-90.
210. Lanemo Myhrinder A, Hellqvist E, Sidorova E, Söderberg A, Baxendale H, Dahle C, et al. A new perspective: molecular motifs on oxidized LDL, apoptotic cells, and bacteria are targets for chronic lymphocytic leukemia antibodies. *Blood*. 2008;111(7):3838-48.

211. Chu CC, CATERA R, Zhang L, Didier S, Agagnina BM, Damle RN, et al. Many chronic lymphocytic leukemia antibodies recognize apoptotic cells with exposed nonmuscle myosin heavy chain IIA: implications for patient outcome and cell of origin. *Blood*. 2010;115(19):3907-15.
212. Gounari M, Ntoufa S, Apollonio B, Papakonstantinou N, Ponzoni M, Chu CC, et al. Excessive antigen reactivity may underlie the clinical aggressiveness of chronic lymphocytic leukemia stereotyped subset #8. *Blood*. 2015;125(23):3580-7.
213. Binder M, Müller F, Frick M, Wehr C, Simon F, Leistler B, et al. CLL B-cell receptors can recognize themselves: alternative epitopes and structural clues for autostimulatory mechanisms in CLL. *Blood, The Journal of the American Society of Hematology*. 2013;121(1):239-41.
214. Steininger C, Widhopf GF, 2nd, Ghia EM, Morello CS, Vanura K, Sanders R, et al. Recombinant antibodies encoded by IGHV1-69 react with pUL32, a phosphoprotein of cytomegalovirus and B-cell superantigen. *Blood*. 2012;119(10):2293-301.
215. Hoogeboom R, van Kessel KP, Hochstenbach F, Wormhoudt TA, Reinten RJ, Wagner K, et al. A mutated B cell chronic lymphocytic leukemia subset that recognizes and responds to fungi. *The Journal of experimental medicine*. 2013;210(1):59-70.
216. Mockridge CI, Potter KN, Wheatley I, Neville LA, Packham G, Stevenson FK. Reversible anergy of sIgM-mediated signaling in the two subsets of CLL defined by VH-gene mutational status. *Blood*. 2007;109(10):4424-31.
217. Graham P, Serge K, Alex A, Natalia S, Andrew JS, Francesco F, et al. The outcome of B-cell receptor signaling in chronic lymphocytic leukemia: proliferation or anergy. *Haematologica*. 2014;99(7):1138-48.
218. Forconi F, Potter KN, Wheatley I, Darzentas N, Sozzi E, Stamatopoulos K, et al. The normal IGHV1-69-derived B-cell repertoire contains stereotypic patterns characteristic of unmutated CLL. *Blood*. 2010;115(1):71-7.
219. Rawlings DJ, Witte ON. The Btk subfamily of cytoplasmic tyrosine kinases: structure, regulation and function. *Semin Immunol*. 1995;7(4):237-46.
220. Smith CI, Baskin B, Humire-Greiff P, Zhou JN, Olsson PG, Maniar HS, et al. Expression of Bruton's agammaglobulinemia tyrosine kinase gene, BTK, is selectively down-regulated in T lymphocytes and plasma cells. *J Immunol*. 1994;152(2):557-65.
221. Dye JR, Palvanov A, Guo B, Rothstein TL. B cell receptor cross-talk: exposure to lipopolysaccharide induces an alternate pathway for B cell receptor-induced ERK phosphorylation and NF-kappa B activation. *J Immunol*. 2007;179(1):229-35.
222. Gustafsson MO, Hussain A, Mohammad DK, Mohamed AJ, Nguyen V, Metalnikov P, et al. Regulation of nucleocytoplasmic shuttling of Bruton's tyrosine kinase (Btk) through a novel SH3-dependent interaction with ankyrin repeat domain 54 (ANKRD54). *Mol Cell Biol*. 2012;32(13):2440-53.
223. Moscat J, Diaz-Meco MT, Rennert P. NF-kappaB activation by protein kinase C isoforms and B-cell function. *EMBO Rep*. 2003;4(1):31-6.

224. Rajaiya J, Hatfield M, Nixon JC, Rawlings DJ, Webb CF. Bruton's tyrosine kinase regulates immunoglobulin promoter activation in association with the transcription factor Bright. *Mol Cell Biol.* 2005;25(6):2073-84.
225. Mahajan S, Vassilev A, Sun N, Ozer Z, Mao C, Uckun FM. Transcription factor STAT5A is a substrate of Bruton's tyrosine kinase in B cells. *J Biol Chem.* 2001;276(33):31216-28.
226. Chalhoub N, Baker SJ. PTEN and the PI3-kinase pathway in cancer. *Annu Rev Pathol.* 2009;4:127-50.
227. Okkenhaug K. Signaling by the phosphoinositide 3-kinase family in immune cells. *Annu Rev Immunol.* 2013;31:675-704.
228. Franke TF, Kaplan DR, Cantley LC, Toker A. Direct regulation of the Akt proto-oncogene product by phosphatidylinositol-3,4-bisphosphate. *Science.* 1997;275(5300):665-8.
229. Mocsai A, Ruland J, Tybulewicz VL. The SYK tyrosine kinase: a crucial player in diverse biological functions. *Nat Rev Immunol.* 2010;10(6):387-402.
230. Zi F, Yu L, Shi Q, Tang A, Cheng J. Ibrutinib in CLL/SLL: From bench to bedside (Review). *Oncology reports.* 2019;42(6):2213-27.
231. Burger JA, Buggy JJ. Bruton tyrosine kinase inhibitor ibrutinib (PCI-32765). *Leuk Lymphoma.* 2013;54(11):2385-91.
232. Idelalisib, ibrutinib show benefits in CLL. *Cancer Discov.* 2014;4(4):382.
233. Herman SE, Gordon AL, Hertlein E, Ramanunni A, Zhang X, Jaglowski S, et al. Bruton tyrosine kinase represents a promising therapeutic target for treatment of chronic lymphocytic leukemia and is effectively targeted by PCI-32765. *Blood.* 2011;117(23):6287-96.
234. Advani RH, Buggy JJ, Sharman JP, Smith SM, Boyd TE, Grant B, et al. Bruton Tyrosine Kinase Inhibitor Ibrutinib (PCI-32765) Has Significant Activity in Patients With Relapsed/Refractory B-Cell Malignancies. *Journal of Clinical Oncology.* 2013;31(1):88-94.
235. Ferrarini I, Rigo A, Montresor A, Laudanna C, Vinante F. Monocyte-to-macrophage switch reversibly impaired by Ibrutinib. *Oncotarget.* 2019;10(20):1943-56.
236. Bye AP, Unsworth AJ, Desborough MJ, Hildyard CAT, Appleby N, Bruce D, et al. Severe platelet dysfunction in NHL patients receiving ibrutinib is absent in patients receiving acalabrutinib. *Blood advances.* 2017;1(26):2610-23.
237. Dubovsky JA, Chappell DL, Harrington BK, Agrawal K, Andritsos LA, Flynn JM, et al. Lymphocyte cytosolic protein 1 is a chronic lymphocytic leukemia membrane-associated antigen critical to niche homing. *Blood.* 2013;122(19):3308-16.
238. Herman SE, Niemann CU, Farooqui M, Jones J, Mustafa RZ, Lipsky A, et al. Ibrutinib-induced lymphocytosis in patients with chronic lymphocytic leukemia: correlative analyses from a phase II study. *Leukemia.* 2014;28(11):2188-96.
239. Wodarz D, Garg N, Komarova NL, Benjamini O, Keating MJ, Wierda WG, et al. Kinetics of CLL cells in tissues and blood during therapy with the BTK inhibitor ibrutinib. *Blood.* 2014;123(26):4132-5.

240. Woyach JA, Smucker K, Smith LL, Lozanski A, Zhong Y, Ruppert AS, et al. Prolonged lymphocytosis during ibrutinib therapy is associated with distinct molecular characteristics and does not indicate a suboptimal response to therapy. *Blood*. 2014;123(12):1810-7.
241. Team RDC. R: A language and environment for statistical computing. v3.3.1 ed: R Foundation for Statistical Computing, Vienna, Austria; 2016.
242. Francois HWaR. dplyr: A Grammar of Data Manipulation. 0.5.0 ed2016.
243. Therneau TM. A Package for Survival Analysis in S. 2.38 ed2015.
244. Corp. I. IBM SPSS Statistics for Windows [Internet]. Armonk, NY: IBM Corp; 2017. . 2017.
245. Burger JA, Barr PM, Robak T, Owen C, Ghia P, Tedeschi A, et al. Long-term efficacy and safety of first-line ibrutinib treatment for patients with CLL/SLL: 5 years of follow-up from the phase 3 RESONATE-2 study. *Leukemia*. 2020;34(3):787-98.
246. Hallek M. Chronic lymphocytic leukemia: 2017 update on diagnosis, risk stratification, and treatment. *Am J Hematol*. 2017;92(9):946-65.
247. Oken MM, Creech RH, Tormey DC, Horton J, Davis TE, McFadden ET, et al. Toxicity and response criteria of the Eastern Cooperative Oncology Group. *American journal of clinical oncology*. 1982;5(6):649-55.
248. ECOG. [Available from: <https://ecog-acrin.org/resources/ecog-performance-status>.
249. Del Giudice I, Raponi S, Della Starza I, De Propriis MS, Cavalli M, De Novi LA, et al. Minimal Residual Disease in Chronic Lymphocytic Leukemia: A New Goal? *Frontiers in oncology*. 2019;9:689.
250. Forsat ND, Palmowski A, Palmowski Y, Boers M, Buttgereit F. Recruitment and Retention of Older People in Clinical Research: A Systematic Literature Review. *Journal of the American Geriatrics Society*. 2020;68(12):2955-63.
251. Isaksson E, Wester P, Laska AC, Näsman P, Lundström E. Identifying important barriers to recruitment of patients in randomised clinical studies using a questionnaire for study personnel. *Trials*. 2019;20(1):618.
252. Zenz T, Eichhorst B, Busch R, Denzel T, Häbe S, Winkler D, et al. TP53 mutation and survival in chronic lymphocytic leukemia. *Journal of clinical oncology : official journal of the American Society of Clinical Oncology*. 2010;28(29):4473-9.
253. Abel GA. The real world: CLL. *Blood*. 2011;117(13):3481-2.
254. Mato A, Nabhan C, Kay NE, Weiss MA, Lamanna N, Kipps TJ, et al. Real-world clinical experience in the Connect® chronic lymphocytic leukaemia registry: a prospective cohort study of 1494 patients across 199 US centres. *British journal of haematology*. 2016;175(5):892-903.
255. Hillmen P, Rawstron AC, Brock K, Muñoz-Vicente S, Yates FJ, Bishop R, et al. Ibrutinib Plus Venetoclax in Relapsed/Refractory Chronic Lymphocytic Leukemia: The CLARITY Study. *Journal of clinical oncology : official journal of the American Society of Clinical Oncology*. 2019;37(30):2722-9.

256. Fraser GAM, Chanan-Khan A, Demirkan F, Santucci Silva R, Grosicki S, Janssens A, et al. Final 5-year findings from the phase 3 HELIOS study of ibrutinib plus bendamustine and rituximab in patients with relapsed/refractory chronic lymphocytic leukemia/small lymphocytic lymphoma. *Leukemia & lymphoma*. 2020;61(13):3188-97.
257. Burger JA, Sivina M, Jain N, Kim E, Kadia T, Estrov Z, et al. Randomized trial of ibrutinib vs ibrutinib plus rituximab in patients with chronic lymphocytic leukemia. *Blood*. 2019;133(10):1011-9.
258. Jain N, Keating M, Thompson P, Ferrajoli A, Burger J, Borthakur G, et al. Ibrutinib and venetoclax for first-line treatment of CLL. *New England Journal of Medicine*. 2019;380(22):2095-103.
259. Craxton A, Jiang A, Kurosaki T, Clark EA. Syk and Bruton's tyrosine kinase are required for B cell antigen receptor-mediated activation of the kinase Akt. *The Journal of biological chemistry*. 1999;274(43):30644-50.
260. Rolli V, Gallwitz M, Wossning T, Flemming A, Schamel WW, Zürn C, et al. Amplification of B cell antigen receptor signaling by a Syk/ITAM positive feedback loop. *Molecular cell*. 2002;10(5):1057-69.
261. Liu C, Miller H, Hui KL, Grooman B, Bolland S, Upadhyaya A, et al. A balance of Bruton's tyrosine kinase and SHIP activation regulates B cell receptor cluster formation by controlling actin remodeling. *Journal of immunology (Baltimore, Md : 1950)*. 2011;187(1):230-9.
262. Johnson GL, Lapadat R. Mitogen-activated protein kinase pathways mediated by ERK, JNK, and p38 protein kinases. *Science (New York, NY)*. 2002;298(5600):1911-2.
263. Bellacosa A, Chan TO, Ahmed NN, Datta K, Malstrom S, Stokoe D, et al. Akt activation by growth factors is a multiple-step process: the role of the PH domain. *Oncogene*. 1998;17(3):313-25.
264. Hayakawa K, Formica AM, Colombo MJ, Shinton SA, Brill-Dashoff J, Morse lii HC, et al. Loss of a chromosomal region with synteny to human 13q14 occurs in mouse chronic lymphocytic leukemia that originates from early-generated B-1 B cells. *Leukemia*. 2016;30(7):1510-9.
265. Chen SS, Batliwalla F, Holodick NE, Yan XJ, Yancopoulos S, Croce CM, et al. Autoantigen can promote progression to a more aggressive TCL1 leukemia by selecting variants with enhanced B-cell receptor signaling. *Proceedings of the National Academy of Sciences of the United States of America*. 2013;110(16):E1500-7.
266. Singh SP, Pillai SY, de Bruijn MJ, Stadhouders R, Corneth OB, van den Ham HJ, et al. Cell lines generated from a chronic lymphocytic leukemia mouse model exhibit constitutive Btk and Akt signaling. *Oncotarget*. 2017;8(42):71981.
267. Messmer BT, Albesiano E, Efremov DG, Ghiotto F, Allen SL, Kolitz J, et al. Multiple distinct sets of stereotyped antigen receptors indicate a role for antigen in promoting chronic lymphocytic leukemia. *The Journal of experimental medicine*. 2004;200(4):519-25.
268. Hervé M, Xu K, Ng YS, Wardemann H, Albesiano E, Messmer BT, et al. Unmutated and mutated chronic lymphocytic leukemias derive from self-reactive B cell precursors

- despite expressing different antibody reactivity. *The Journal of clinical investigation*. 2005;115(6):1636-43.
269. Minici C, Gounari M, Übelhart R, Scarfò L, Dühren-von Minden M, Schneider D, et al. Distinct homotypic B-cell receptor interactions shape the outcome of chronic lymphocytic leukaemia. *Nature communications*. 2017;8:15746.
270. Ramsay AD, Rodriguez-Justo M. Chronic lymphocytic leukaemia--the role of the microenvironment pathogenesis and therapy. *British journal of haematology*. 2013;162(1):15-24.
271. Burger JA, Gribben JG. The microenvironment in chronic lymphocytic leukemia (CLL) and other B cell malignancies: insight into disease biology and new targeted therapies. *Seminars in cancer biology*. 2014;24:71-81.
272. de Rooij MF, Kuil A, Geest CR, Eldering E, Chang BY, Buggy JJ, et al. The clinically active BTK inhibitor PCI-32765 targets B-cell receptor- and chemokine-controlled adhesion and migration in chronic lymphocytic leukemia. *Blood*. 2012;119(11):2590-4.
273. Lutz C, Ledermann B, Kosco-Vilbois MH, Ochsenbein AF, Zinkernagel RM, Köhler G, et al. IgD can largely substitute for loss of IgM function in B cells. *Nature*. 1998;393(6687):797-801.
274. Roes J, Rajewsky K. Immunoglobulin D (IgD)-deficient mice reveal an auxiliary receptor function for IgD in antigen-mediated recruitment of B cells. *The Journal of experimental medicine*. 1993;177(1):45-55.
275. Lanham S, Hamblin T, Oscier D, Ibbotson R, Stevenson F, Packham G. Differential signaling via surface IgM is associated with VH gene mutational status and CD38 expression in chronic lymphocytic leukemia. *Blood*. 2003;101(3):1087-93.
276. Krysov S, Dias S, Paterson A, Mockridge CI, Potter KN, Smith KA, et al. Surface IgM stimulation induces MEK1/2-dependent MYC expression in chronic lymphocytic leukemia cells. *Blood*. 2012;119(1):170-9.
277. Bernal A, Pastore RD, Asgary Z, Keller SA, Cesarman E, Liou HC, et al. Survival of leukemic B cells promoted by engagement of the antigen receptor. *Blood*. 2001;98(10):3050-7.
278. Petlickovski A, Laurenti L, Li X, Marietti S, Chiusolo P, Sica S, et al. Sustained signaling through the B-cell receptor induces Mcl-1 and promotes survival of chronic lymphocytic leukemia B cells. *Blood*. 2005;105(12):4820-7.
279. Paterson A, Mockridge CI, Adams JE, Krysov S, Potter KN, Duncombe AS, et al. Mechanisms and clinical significance of BIM phosphorylation in chronic lymphocytic leukemia. *Blood*. 2012;119(7):1726-36.
280. Allsup DJ, Kamiguti AS, Lin K, Sherrington PD, Matrai Z, Slupsky JR, et al. B-cell receptor translocation to lipid rafts and associated signaling differ between prognostically important subgroups of chronic lymphocytic leukemia. *Cancer research*. 2005;65(16):7328-37.

281. Guarini A, Chiaretti S, Tavolaro S, Maggio R, Peragine N, Citarella F, et al. BCR ligation induced by IgM stimulation results in gene expression and functional changes only in IgVH unmutated chronic lymphocytic leukemia (CLL) cells. *Blood*. 2008;112(3):782-92.
282. Ten Hacken E, Sivina M, Kim E, O'Brien S, Wierda WG, Ferrajoli A, et al. Functional Differences between IgM and IgD Signaling in Chronic Lymphocytic Leukemia. *Journal of immunology (Baltimore, Md : 1950)*. 2016;197(6):2522-31.
283. Buchner M, Fuchs S, Prinz G, Pfeifer D, Bartholomé K, Burger M, et al. Spleen tyrosine kinase is overexpressed and represents a potential therapeutic target in chronic lymphocytic leukemia. *Cancer research*. 2009;69(13):5424-32.
284. Semichon M, Merle-Béral H, Lang V, Bismuth G. Normal Syk protein level but abnormal tyrosine phosphorylation in B-CLL cells. *Leukemia*. 1997;11(11):1921-8.
285. Quiroga MP, Balakrishnan K, Kurtova AV, Sivina M, Keating MJ, Wierda WG, et al. B-cell antigen receptor signaling enhances chronic lymphocytic leukemia cell migration and survival: specific targeting with a novel spleen tyrosine kinase inhibitor, R406. *Blood*. 2009;114(5):1029-37.
286. Zhuang J, Hawkins SF, Glenn MA, Lin K, Johnson GG, Carter A, et al. Akt is activated in chronic lymphocytic leukemia cells and delivers a pro-survival signal: the therapeutic potential of Akt inhibition. *Haematologica*. 2010;95(1):110-8.
287. Barragán M, Bellosillo B, Campàs C, Colomer D, Pons G, Gil J. Involvement of protein kinase C and phosphatidylinositol 3-kinase pathways in the survival of B-cell chronic lymphocytic leukemia cells. *Blood*. 2002;99(8):2969-76.
288. Coelho V, Krysov S, Steele A, Sanchez Hidalgo M, Johnson PW, Chana PS, et al. Identification in CLL of circulating intraclonal subgroups with varying B-cell receptor expression and function. *Blood*. 2013;122(15):2664-72.
289. Herman SE, Mustafa RZ, Gyamfi JA, Pittaluga S, Chang S, Chang B, et al. Ibrutinib inhibits BCR and NF- κ B signaling and reduces tumor proliferation in tissue-resident cells of patients with CLL. *Blood*. 2014;123(21):3286-95.
290. Drennan S, Chiodin G, D'Avola A, Tracy I, Johnson PW, Trentin L, et al. Ibrutinib Therapy Releases Leukemic Surface IgM from Antigen Drive in Chronic Lymphocytic Leukemia Patients. *Clinical cancer research : an official journal of the American Association for Cancer Research*. 2019;25(8):2503-12.
291. Cheson BD, Byrd JC, Rai KR, Kay NE, O'Brien SM, Flinn IW, et al. Novel targeted agents and the need to refine clinical end points in chronic lymphocytic leukemia. *Journal of clinical oncology : official journal of the American Society of Clinical Oncology*. 2012;30(23):2820-2.
292. Wiestner A. Emerging role of kinase-targeted strategies in chronic lymphocytic leukemia. *Blood*. 2012;120(24):4684-91.
293. Cheng S, Ma J, Guo A, Lu P, Leonard JP, Coleman M, et al. BTK inhibition targets in vivo CLL proliferation through its effects on B-cell receptor signaling activity. *Leukemia*. 2014;28(3):649-57.
294. (FDA). IF-ADUFaDA. Retrieved 19 June 2021.

295. 2021 IEEMAEJ. Retrieved 14th July 2021.
296. Howard DR, Hockaday A, Brown JM, Gregory WM, Todd S, Munir T, et al. A platform trial in practice: adding a new experimental research arm to the ongoing confirmatory FLAIR trial in chronic lymphocytic leukaemia. *Trials*. 2021;22(1):38.
297. Stretton O. EHA 2021 Virtual Congress. *The Lancet Haematology*.
298. Ahn IE, Tian X, Wiestner A. Ibrutinib for Chronic Lymphocytic Leukemia with TP53 Alterations. *New England Journal of Medicine*. 2020;383(5):498-500.
299. Rawstron A, Munir T, Brock K, Webster N, Munoz Vicente S, Yates F, et al. Ibrutinib and Obinutuzumab in CLL: Improved MRD Response Rates with Substantially Enhanced MRD Depletion for Patients with >1 Year Prior Ibrutinib Exposure. *Blood*. 2018;132(Supplement 1):181-.
300. Da Roit F, Engelberts PJ, Taylor RP, Breij EC, Gritti G, Rambaldi A, et al. Ibrutinib interferes with the cell-mediated anti-tumor activities of therapeutic CD20 antibodies: implications for combination therapy. *Haematologica*. 2015;100(1):77-86.
301. Michallet AS, Dilhuydy MS, Subtil F, Rouille V, Mahe B, Laribi K, et al. Obinutuzumab and ibrutinib induction therapy followed by a minimal residual disease-driven strategy in patients with chronic lymphocytic leukaemia (ICLL07 FILO): a single-arm, multicentre, phase 2 trial. *The Lancet Haematology*. 2019;6(9):e470-e9.
302. Jaglowski SM, Jones JA, Nagar V, Flynn JM, Andritsos LA, Maddocks KJ, et al. Safety and activity of BTK inhibitor ibrutinib combined with ofatumumab in chronic lymphocytic leukemia: a phase 1b/2 study. *Blood*. 2015;126(7):842-50.
303. Sharman JP, Farber CM, Mahadevan D, Schreeder MT, Brooks HD, Kolibaba KS, et al. Ublituximab (TG-1101), a novel glycoengineered anti-CD20 antibody, in combination with ibrutinib is safe and highly active in patients with relapsed and/or refractory chronic lymphocytic leukaemia: results of a phase 2 trial. *British journal of haematology*. 2017;176(3):412-20.
304. Sharman JP, Brander DM, Mato A, Kambhampati S, Burke JM, Lansigan F, et al. Ublituximab and ibrutinib for previously treated genetically high-risk chronic lymphocytic leukemia: results of the GENUINE phase 3 study. *Journal of clinical oncology : official journal of the American Society of Clinical Oncology*. 2017;35(Supplemental).
305. Puła B, Gołos A, Górniak P, Jamroziak K. Overcoming Ibrutinib Resistance in Chronic Lymphocytic Leukemia. *Cancers*. 2019;11(12).

